Compound Fault Diagnosis of Centrifugal Pumps Using Vibration Analysis Techniques

OSAMA HASAN INBAIA HAMOMD

A thesis submitted to the University of Huddersfield in partial fulfilment of requirements for the degree of Doctor of Philosophy

The University of Huddersfield

School of Computing and Engineering

Mechanical Engineering Department

March 2017

COPYRIGHT

ABSTRACT

Centrifugal pumps are widely used in many different industrial processes, such as power generation stations, chemical processing plants, and petroleum industries. The problem of failures in centrifugal pumps is a large concern due to its significant influence on such critical industries. Particularly, as the core, parts of a pump, bearings and the impellers are subject to different corrosions and their faults can cause major degradation of pump performances and lead to the breakdown of production. Therefore, an early detection of these types of faults would provide information to take timely preventive actions.

This research investigates more effective techniques for diagnosing common faults of impellers and bearings with advanced signal analysis of surface vibration. As overall vibration responses contain a high level of broadband noises due to fluid cavities and turbulences, noise reduction is critical to developing reliable and accurate features. However, considering the modulation effect between the rotating shaft, vane passing components and any structural resonances, a modulation signal bispectrum (MSB) method is mainly used to extract these deterministic characteristics of modulations, which differs from previous researches in that the broadband vibration is often characterised with statistical methods, high frequency demodulation along spectrum analysis. Both theoretical analysis and experimental evaluation show that the diagnostic features developed by MSB allow impellers with inlet vane damages and exit vane faults to be identified under different operating conditions.

It starts with an in-depth examination of the vibration excitation mechanisms associated with each type of common pump faults including impeller leakages, impeller blockages, bearing inner race defects and bearing outrace defects. Subsequently, fault diagnosis was carried out using popular spectrum and envelope analysis, and more advanced kurtogram and MSB analysis. These methods all can successfully provide correct detection and diagnosis of the faults, which are induced manually to the test pump.

Envelope analysis in a bands optimised with Kurtogram produces outstanding detection results for bearing faults but not the impeller faults in a frequency range as high as several thousand hertz (about 7.5kHz). In addition, it cannot provide satisfactory diagnostic results in separating the faults across different flow rates, especially when the compound faults were evaluated. This deficiency is because they do not have the capability of suppressing the random noises.

Meanwhile, it has found that the MSB analysis allows both impeller and bearing faults to be detected and diagnosed. Especially, when the pump operated with compound faults both the fault types and severity can be attained by the analysis with acceptable accuracy for different flow rates. This high performance of diagnosis is due to that MSB has the unique capability of noise reduction and nonlinearity demodulation. Moreover, MSB diagnosis can be a frequency range lower than 2 times of the blade pass frequency (<1kHz), meaning that it can be more cost-effective as it demands lower performance measurement systems.

In addition, the study also found that one accelerometer mounted on the pump housing is sufficient to monitor the faults on both the impeller and the bearing as it uses a lower frequency vibration which propagates far away from the bearing to the housing, rather than another accelerometer on the bearing pedestal directly.

ACKNOWLEDGEMENTS

Firstly, I wish to express the sincere gratitude to my advisors, Dr Fengshou Gu, Prof. Andrew Ball who supplied encouragement, guidance and technical support through this thesis. None of this work could have taken place without their engineering experience and insight. I would also like to thank my committee for their interests in my work and carefully reviewing this dissertation.

Secondly, I would like to convey my thanks and appreciation to all of the colleagues at the Centre for Efficiency and Performance Engineering and research fellows and staff members who have over the years made my time such a great experience on a professional and personal level, also my friends who always give me help and encouragement.

Finally, I would especially like to thank my wonderful family, my wife and son: Adam, for their continued support, encouragement and love. Special and grateful thanks to my mother, soul of my father and all my brothers and sisters for their high expectation and encouragement. An additional I am always indebted to my Mum for the love and patience she shows me.

DECLARATION

I hereby declare that I am the sole author of this thesis.

No portion of the work referred to in this thesis has been submitted, in support of an application for another degree or qualification at this or any other university or another institute of learning.

Osama Hamomd

DEDICATION

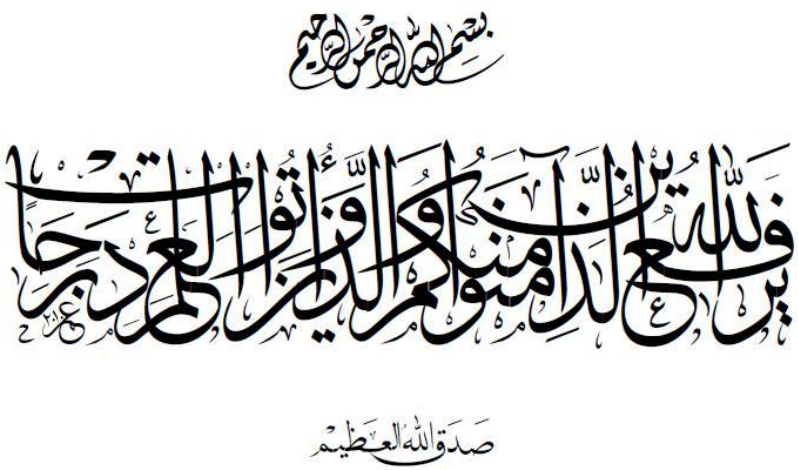

The road to success comes through hard work, determination, sacrifice and guidance of elders, especially those very close to the heart.

My humble effort I dedicate to my sweet and loving

Mother, Wife and Son,

whose affection, love, encouragement and prayers day and night enable me to achieve much success and honour.

LIST OF ABBREVIATIONS

AC	Alternating Current
API	American Petroleum Institute
AS	Angular Speed
BEP	Best Efficiency Point
BL	Base Line
BPF	Blade Passage Frequency
BPFIR	Ball Passing Frequency Inner Race
BPFOR	Ball Passing Frequency Outer Race
BSF	Ball Spin Frequency
CB	Conventional Bispectrum
CBM	Condition Based Maintenance
CF	Crest Factor
CM	Condition Monitoring
CHMM	Continuous Hidden Markov Model
CWT	Continuous Wavelet Transform
DAQ	Data Acquisition
DC	Direct Current
DFFT	Discrete Fast Fourier Transform
EA	Envelope Analysis
FDA	Frequency Domain Analysis
FFT	Fast Fourier Transform
FK	Fast Kurtogram
FTF	Fundamental Train Frequency
HOSA	Higher Order Spectra Analysis
Hz	Hertz
IRD	Inner Race Defect
ISO	International Organization for Standardization

K	Kurtosis
LIB	Large Impeller Blockage
MSB	Modulation Signal Analysis
MTTF	The Mean Time to Failure
NPSH	Net Positive Suction Head
NPSHA	Net Positive Suction Head Available
NPSHR	Net Positive Suction Head Required
ORD	Outer Race Defect
OEM	Original Equipment Manufacture
PD	Positive Displacement
PM	Predictive Maintenance
PS	Power Spectrum
PV	Peak Value
RF	Rotational Frequency
RMS	Root Mean Square
RPM	Revolution Per Minute
SC	Sideband Characteristics
SIB	Small Impeller Blockage
SK	Skewness
STFT	Short Time Fourier Transform
SVP	Saturated Vapour Pressure
TDA	Time Domain Analysis
TSA	Time Synchronous Averaging
WT	Wavelet Transform

LIST OF NOTATIONS

ATM	Atmospheric head (m)
BHP	Brake horsepower (kW)
D	Impeller diameter (m)
FFT	Fast Fourier Transformer
G	Gravitational acceleration (m/s2)
H	Total head developed (m)
Ha	Atmospheric head (m)
Hf	Friction head (m)
Hi	Pump inlet losses head (m)
Hs	Static head (m)
Hv	Velocity head (m)
Hvp	Vapour pressure head (m)
Jm	Moment of inertia of the mechanical system (kg-m2)
Ko	Moment of inertia of the water inside the impeller (kg-m2)
M	Modulation index (dimensionless)
MSB	Modulated signal bispectrum
N	Shaft speed (rpm)
Po	Hydraulic power (kW)
Q	Pump capacity (m3/hour)
Te	Active torque produced by the driving motor (Nm)
Tf	Torque due to the friction losses (Nm)
Th	Torque component for the of delivery head (Nm)
Tv	Torque due to viscosity of pumped liquid (Nm)
Tζ	Viscous torque (Nm)
V	Flow velocity (m/sec)
P	Fluid density (kg/m3)

Φ	Load angle (Electrical degree)
Ω	Angular speed (rad/s)

LIST OF PUBLICATIONS

1. Osama Hamomd, Xiange Tian, Zhi Chen, Abdulrahman Albraik, Fengshou Gu, Andrew Ball, A New Method of Vibration Analysis for the diagnosis of impeller in a centrifugal pump, University of Huddersfield, UK. Accepted for publication on ICSV 21 Beijing/China 2014.

2. Hamomd, Osama, Ball, Andrew, Gu, Fengshou and Thobiani, F. (2013) *Pump Rotor System Monitoring Based on Advanced Measurements and Analysis Techniques.* In: Proceedings of Computing and Engineering Annual Researchers' Conference 2013 : CEARC'13. University of Huddersfield, Huddersfield, p. 230. ISBN 9781862181212

3. Abdulrahman Al-braik, Osama Hamomd, F. Gu and A. D. Ball, Diagnosis of Impeller Faults in a Centrifugal Pump Based on Spectrum Analysis of Vibration Signals, University of Huddersfield, UK. Accepted for publication on CM 2014 and MFPT 2014, Manchester, UK

4. Osama Hamomd, Samir Alabied, Yuandong Xu, Alsadak Daraz, Fengshou Gu and Andrew Ball, vibration based centrifugal pump fault diagnosis based on modulation signal bispectrum analysis, University of Huddersfield, UK, accepted for publication on ICAC17 2017 Proceedings of the 23rd International Conference on Automation & Computing, Huddersfield, UK.

5. Samir Alabied, Osama Hamomd, Alsadak Daraz, Fengshou Gu, and Andrew D Ball, Fault Diagnosis of Centrifugal Pumps based on the Intrinsic Time-scale Decomposition of Motor Current Signals, University of Huddersfield, UK, accepted for publication on ICAC17 2017 Proceedings of the 23rd International Conference on Automation & Computing, Huddersfield, UK.

LIST OF CONTENTS

LIST OF FIGURES

LIST OF TABLES

CHAPTER ONE
INTRODUCTION

In this chapter, the general introduction and literature review regarding condition monitoring techniques are presented. These condition-monitoring techniques involve fault diagnostic and detection techniques, which have been used for centrifugal pumps. It describes also the importance of maintenance strategy and the life cycle of a centrifugal pump. Finally, it explains the research motivation, aim and objectives. In addition, the outline of the thesis is presented.

1.1 Background

One of the crucial parts of Predictive Maintenance (PM) is Machine Condition Controlling (CM). It is considered one of the most appropriate strategy to employ when carrying out machine maintenance in various industries. To operate the machine from maximum time until shutdowns repeatedly, that can occur breakdowns and catastrophic faults, occasionally, these consequences will affect strongly on repairing cost, reducing products and safety. Preventive maintenance is a first reaction, whereas the maintenance that carried out whilst approaching high efficiency also very small failures are expected during period of repairs. However, the maintenance activities are essential and as a result of that more spares are used [1].

In some cases, the maintenance department waits for the equipment or machine to fail before they carry out any maintenance and this form of reactive management method is referred to as Run-to-failure. In this technique, the department does not anticipate for any maintenance requirements, in order to predict and address all the possible failures that are likely to affect the plant. When this reactive technique is applied, the maintenance department is forced to maintain various inventories of spare parts that include spare equipment or at least all main components for the plant's important machine. The other option is to depend on the vendor's equipment that can be delivered immediately when need arises [2-4]. However, even if this alternative is possible, the amount of money charged for quick delivery significantly increases the repair parts' costs as well as the downtime needed to maintain the machine failures. Therefore, run-to –failure management approach is considered a very expensive maintenance management technique. Also, this approach results to limited availability of the process machinery. It is a few plants that apply the true philosophy of run-to-failure management approach [4].

The initial response was the preventive maintenance approach. In this approach, maintenance is conducted in intervals in order to minimize the likelihood of machine failure in between the repairs. The challenge of preventive maintenance is the scheduling guideline time. All preventive maintenance management programs assume that machines will degrade within a period. The mean-time-to-failure (MTTF) or bathtub curve, as shown in Figure 1-1, indicates that a new machine has a high probability of failure because of installation problems during early period of operation time. After this initial period, the probability of failure is relatively low and lowest for an extended period [2]. After this normal machine life period, the probability of failure increases sharply with elapsed operation time. In preventive maintenance

management, machine repairs or rebuilds are scheduled based on the MTTF statistic. However, different kinds of components have different failure distribution curves. Statistical result of failure distribution is often not an accurate guideline for a single machine or its components, which can operate under different conditions and undergo different deterioration speed. Thus preventive maintenance management can often be in over-maintenance or under-maintenance.

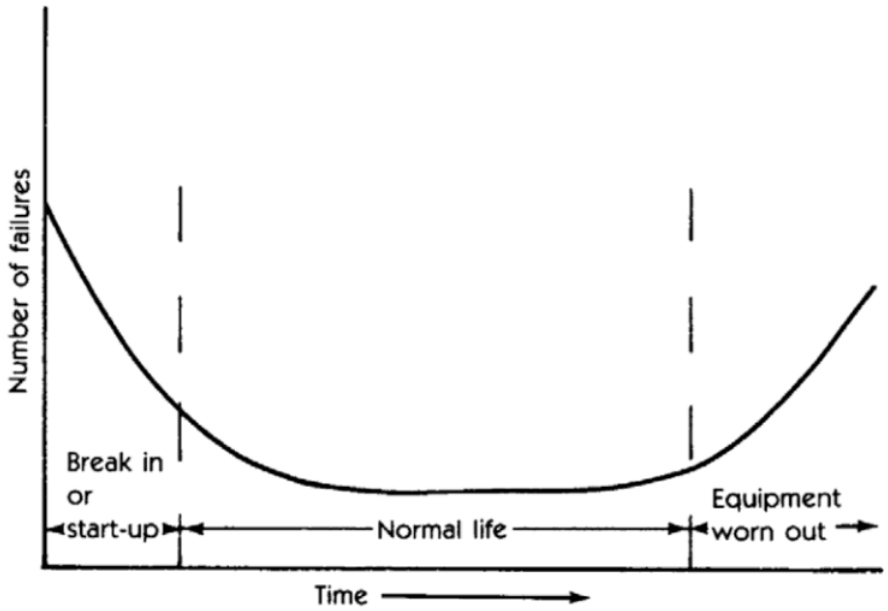

Figure 1-1 Bathtub curve of failure indications[3]

Predictive Maintenance (PM), also known as Condition-Based Maintenance (CBM), is a widely accepted maintenance philosophy [4]. As in predictive management philosophy, maintenance action is taken in time instead of on schedule, to avoid unexpected catastrophic failures as well as unnecessary maintenance costs. Taking pump as an example, it is very important to carry out maintenance at regular intervals, which are shorter than the expected time between failures. The preventive maintenance philosophy entails a strategy that prompts discussion, and it involves scheduling of the maintenance actions whenever the maintenance department detects potential functional failures. Such an earlier detection is conducted to avoid any unanticipated catastrophic failures [5]. This does mean that the vast majority could have run longer by the factor of two or more. The advantage of this method is that most maintenance can be planned and that disastrous failure is significantly reduced. On the other hand, with the advanced maintenance of pump condition monitoring and maintenance carried out at the optimum time, it has “obvious” advantages compared with either run to break or preventive

maintenance but does require reliable condition monitoring techniques, which not only are able to determine current condition but also give reasonable prediction of remaining useful life.

Various technologies can, and should be applied as part of the extensive predictive maintenance approach. This is due to the fact that machine or mechanical systems account for most of the plant equipment failure. Therefore, vibration monitoring is considered a crucial component of the predictive maintenance programs, although a few other techniques, such as acoustic emissions, eddy-current signal and thermography are also useful [3]. The problem of failures in centrifugal pumps is a large concern due to its significant influence over industrial production. Particularly, as the core, parts of the pump, bearings and the impellers are subject to different corrosions, undesirable noise/vibration, and their faults can cause major degradation of pump performances and lead to breakdown of production. Therefore, an early detection of such faults would provide information to take timely preventive actions.

1.2 Condition Monitoring Methods

The condition monitoring approach identifies the various problems affecting the plant early so that they can be addressed immediately before they escalate into a complex problem that can result in a complete breakdown. Most of the condition monitoring techniques consider vibration monitoring as a crucial element, which has a lot of information about the piece of machinery. In addition, the objective of machinery condition monitoring is to obtain the earliest possible warning of incipient damage or malfunction and to assist in the diagnosis of the subsequent cause. There are many books that focus on condition monitoring and fault diagnosis [6, 7]. Machine condition monitoring is concerned with obtaining data that would aid in evaluating machinery mechanical and electrical integrity. It is the measurement of various parameters related to the mechanical and electrical condition of the machinery such as vibration, acoustic emission, temperature, oil pressure, oil debris, voltage, current conductivity and corrosion, which make it possible to determine whether the machine is healthy. In addition machinery models can be established for simulating and predicting the trend of changing parameters [8]. These are parameters such as vibration, temperature, pressure, current and voltage that change as a result of differing operating condition, thus providing the maintenance engineer with prior knowledge that may be used for maintenance or improving the performance of the machine. It is generally accepted that condition monitoring offers many advantages, including:

1) Avoiding unexpected catastrophic breakdowns with expensive or dangerous consequences

2) Reducing the number of machine overhauls to a minimum and thereby reducing maintenance costs.

3) Eliminating unnecessary intervention and subsequent risk of introducing faults on previously healthy machines

4) Improving the manufacturing efficiency

5) Reducing the intervention time and thereby minimising production loss (as the fault to be repaired is known in advance and overhauls can be scheduled when most convenient)

Condition-based maintenance; is made based on collecting, processing and analysing data from the monitored machine in order to determine the actual operating condition of a system or component at any time. A replacement or repair decision is then taken based on the analysis of the data. This method is possible because of the great developments achieved in sensors, data acquisition, signal processing techniques and suitable software. Therefore, a CM system must have the ability of providing accurate information about the running machines with the presence of electrical interference, expecting the needs for maintenance prior severe deterioration, failure or breakdown happens, clearly detecting and locating the faults in detail, and even providing an approximation of the machines life. Vibration monitoring is generally the key component of most condition monitoring systems. The following is the most common CM techniques used.

Vibration Based Condition Monitoring: vibration based condition monitoring uses of non-destructive sensing and analysis of system characteristics in the time and frequency domains to detect changes, which may indicate damage or degradation. It picks up the vibration signals generated by machines and analyses these signals to determine the condition of the machine [9].

Whenever a machine is experiencing a particular problem, the vibration analysis sends warning signals to inform the maintenance department that there is an issue that requires to be addressed. Some of the problems that affect machines include misalignment, unbalance as well as mechanical looseness of the rotating machineries. The vibration analysis sends warning signals when such failure occurs. Also, condition monitoring track other process parameters and operating conditions such as temperature loads in order to give display a clear picture on how the systems are running. The main principle of the vibration-based damages detection approach

is that damage will highly alter the system's mass, stiffness or dissipation properties, which, in turn, change the systems' measured dynamic response. Although the key basis of vibration-based damage detection approach seems intuitive, its real uses poses various significant technical problems. One of the most significant challenges is because damage is a local condition and may not really affect the low-frequency global responses experienced by structures that is measured during the vibration tests. Also, the challenge is supported by various issues related to making repeatable and accurate measurements at a few location on the structures that operate in different settings [10].

Sohn and Farrar [11] came up with a process for damage detection as well as localization within a system. This procedure is solely based on time series analysis of the vibration data recorded. Lin et al. [12] assert that they have recorded excellent results in the detection of mechanical faults using the wavelet denoising method. This technique performs well when it is used to denoise the mechanical vibration signals of low signal-to-noise ratios. R Pandian, BVA Rao [13] assert that the application of vibration monitoring technique together with the debris analysis, one can diagnose about 98% of the key challenges affecting the mechanical system using these two methods. Moreover, Konruff, Mike [14] assert that using preventive maintenance technique will increase the uptime and life of the machine, reduce the costs of operation, enhance the quality of products, protect the environment as well as render a safe working environment.

Visual Inspection: Visual inspection typically means inspection using human senses or any non-specialized inspection equipment. Visual inspection is a simple method makes using either or all of human senses such as vision, hearing, touch and smell in maintenance of facilities. Visual inspection provides a flexible and immediate assessment of condition [15].

Temperature Monitoring: Defects of the bearings and impellers are likely to experience greater friction and as a result, the various rotating parts of the centrifugal pump will produce a lot of heat. The simplest technique to detect faults in the rotary machines id thus to track the temperature of the lubricant or bearing's housing as well as the impeller housing.

Acoustic Based Condition Monitoring: Acoustic technology has been developed to include the field of condition monitoring. Acoustic analysis is now a recognised technique of non-destructive testing. This approach concentrates on the analysis of acoustic or noise waveforms produced by machinery processes. Whenever solid objects vibrate, they generate sound. Also, sound can refer to vibration signals propagated on the air. Therefore, the sound produced is as

a result of the vibrating objects. Generally, a machine will generate acoustic and vibrations or sound signals while it is running or performing its processes. The acoustic signals from the running machine should be recorded by the microphones, and be used for both vibration and condition monitoring. Unlike the vibration sensors, it is easy to install microphones. Also, microphones have greater frequency response ranges [16].

Acoustic Emission Technology for Condition Monitoring: Acoustic emissions are defined as transient elastic waves generated from a rapid release of strain energy caused by a deformation or damage within or on the surface of a material. Sources of acoustic emission in rotating machinery include impacting, cyclic fatigue, friction, turbulence, material loss, cavitation, leakage, etc. The acoustic emission most commonly parameters for diagnosis are amplitude, RMS, energy, kurtosis and events [17].

1.3 Previous Research on the Centrifugal Pump Faults Diagnosis

Most industries like petroleum and chemical plants consider condition monitoring as one of the critical aspects of maintaining production safety as well as efficiency. In order to enhance monitoring performance, most of the studies conducted in the recent years used advanced data analysis techniques. These techniques are used on the surface vibrations of the pump. Various modelling approaches are being explored to enhance performance analysis of the centrifugal pumping machines. Anagnostopoulos [18] performed an investigation using a numerical methodology to simulate the turbulent flow in a 2-dimensional centrifugal pump impeller and to compute the features performance curves of the compact pump. The flow domain is discretized with a polar, Cartesian mesh and the Reynolds-averaged Navier–Stokes (RANS) equations are solved with the control volume approach of the turbulence model. By increasing the $k_e = \frac{m}{n'}$ the discrepancy with the design point increases as well; because with the increase of this parameter, the effect of the restriction applied by the head penalty to limit the optimization to the constant design point diminishes. Advanced numerical techniques for adaptive grid refinement and for treatment of grid cells that do not fit the irregular boundaries are implemented in order to achieve a fully automated grid construction for any impeller design. The conducting results show an evidence of an adequate precision and accuracy.
Experiments quote of flow rates were also conducted by Moore [19], whereas Howard and Kittmer used water as a working fluid and focused attention on the flow in shrouded and unshrouded impeller configurations, using a hot-film measurement technique. Visser et al. [20]

presented the outcomes of the experiments conducted for blade passage flow using a low speed model pump impeller. They reported that the flow within the rotating impeller passage can be described well by distribution flow which is postulated by the boundary-layer and potential flow considerations. Acosta et al. [21] established that by using static piezometer taps in the blade surfaces and simple impact probes in the impeller passages. The results show that the relative velocity profile near the suction side of the blade progressively deteriorates from the inner to the outer radial stations.

Use of vibration method in the condition monitoring of rotating machinery has been well established over the last few decades, many studies have shown the positive results of using vibration method for monitoring the condition of centrifugal pumps [22-24]. According to previous student the vibration method is effective for monitoring the bearing of centrifugal pumps. Several publications discussed that the main feature of the vibration signal of centrifugal pumps and turbines the interaction between the flowing fluid moving parts such as rotor and fan blades, also the interaction between rotor vanes with the nearby stationary parts such as the volute tongue and casing. [25, 26].

The vibration signals are normally processed and analysed using a number of different methods. These methods include overall reading, spike energy, kurtosis, spectrum, envelop and spectrum analysis. These methods include also advanced techniques such as wavelet, neural network and genetic algorithms [27, 28]. It is of great importance that the right techniques should be chosen for a particular application, if not faults will either go undetected or will be wrongly diagnosed. It is important to know that some publications indicate that the vibration alone is not sufficient to monitor the health of rotating machinery especially when large industrial machines are concerned [29, 30]

Signal processing methods are combined with pattern recognition methods to achieve fault diagnosis of centrifugal pumps. Zhou et al. [31] introduced a method for centrifugal pump fault diagnosis based on the continuous hidden markov model (CHMM). Later, the author [32] put forward a new method based on Empirical Mode Decomposition (EMD), and Least Square Support Vector Machine (LS-SVM) for vibration signals analysis of the centrifugal pump which has the non-stationary and non-linearity characteristics of misalignment faults. Application results showed that the proposed method is effective, which can better extract the nonlinear features of the fault and more exactly diagnosis faults. Zheng et al. [33] suggested

another fault feature extraction technique which is based on the Intrinsic Mode Function, together with envelope sample entropy that diagnoses faults in rolling bearings.

Farokhzad [34] proposed an adaptive networks fuzzy interference system (ANFIS). The technique will be used to diagnose the type of fault affecting the pump. Some of the pump conditions to be diagnosed include healthy, worn impeller, broken impeller, cavitation and leakages. The FFT technique is used to extract features from the vibration signals. To validate the system's performance, the testing data set was applied to a trained ANFIS model. Based the outcomes recorded, a total classification accuracy of 90.67% was reported. This implies that the system is able to act as an intelligent system for fault diagnosis in real applications.

Zhang et al. [35] presented another technique based on ANFIS model and multi-scale entropy performed on the electric motor bearings. These electric motor bearing had three various fault categories including inner race, outer race as well as ball faults.

Nasiri et al. [36] utilized vibration analysis in order to detect the rate of cavitation in centrifugal pumps with a neural network approach. This technique is considered an intelligent system to monitor the condition of the centrifugal pumps. Faisal et al. [37] also applied air-borne acoustic signals and the surface vibration's spectral entropy for cavitation monitoring in the centrifugal pump. They realised that spectral entropy is more accurate in monitoring cavitation.

Wang et al. [38] proposed an intelligent diagnosis technique for the centrifugal pumping system using various features resulting from vibration signals for unbalance and misalignment monitoring. These diagnosis methods were obtained using partially linearized neural networks, rough sets and wavelet transform. A reverse wavelet function was applied to record the fault features of the measured vibration signals as well as to record the hidden fault data across optimum frequency areas.

Muralidharan et al. [39] suggested that the diagnosis of vibration based faults of mono-block centrifugal pump should be conducted using the J48 algorithm and wavelet analysis. The researchers explored the mono-block centrifugal pump faults like bearing faults, cavitation, impeller fault, both bearing and impeller faults. All of them simulated five standard states. Various features of wavelet have been derived using continuous wavelet transform (CWT) for various wavelets as well classified with the J48 algorithm. Moreover, (J48) is an algorithm used to generate a decision tree developed by Ross Quinlan mentioned earlier.

Li et al. [40] carried out their experiments investigation on the failure of the trial impeller of centrifugal pump, they have been employed a zinc hydrometallurgy industrial process happened only after a service a round month of period. However, a composition analysis technique in their study has been introduced for inspection an impeller material by spectrum analyser, microstructure analysis by optical microscopes. The results of this research shows the high nitrogen addition in the duplex stainless steel (DSS) resulted in too low ferrite content, because of too short service life; he recommended nitrogen content value is 0.1–0.3%.

S. Perovic, et al. [41] presented current spectrum signatures which are used for detection of different faults like cavitation and damaged impeller condition. A fuzzy logic system is also developed to classify the three faults. The authors conclude that the probability of fault detection varies from 50% to 93%.

Saeid Farokhzad et al. [42] have achieved vibration analysis and investigation different operation condition of centrifugal pump, the pump conditions were considered to be normal pump, broken impeller and leakage faults. Moreover, the vibration data was collected from the inspected pump and compared with vibration spectra of healthy machine. Additionally, the results from this work have given more understanding on the dependent roles of vibration analysis in predicting and diagnosing machine faults.

Siegler [43] explained the development and use of signal processing procedures for detection of the eroded impeller faults of the centrifugal pump in the submarines. Various fault features were recorded from the power spectrum. Using the neural network system, approximately 90% of these test cases were classified correctly. Schmalz, et al. [44] realised that spectral energy within bands of 5-25Hz can be calculated and also used to detect low flow condition or cavitation in centrifugal pumps.

Rafik Zouari et al. [45] elaborated another diagnosis technique for centrifugal pumps. This approach was development in line with the pump maintenance framework using the neuro-fussy models. This system is based on signal pre-processing, vibration measurements and classification using pattern recognition methods for diagnosing faults such as cavitation, air injection, misalignment and partial flow.

As fault recognition accuracy depends on separability of features, novel signal processing methods are investigated to extract fault features from vibration signal with low signal-to-noise ratio (SNR). Y Lei et al. [46] presented an improved kurtogram method for fault diagnosis of

rolling element bearings, has been proved to be a very powerful and practical instrument in machinery fault diagnosis. Kurtogram, based on the short time Fourier transform (STFT) or FIR filters. however, limits the accuracy improvement of kurtogram in extracting transient characteristics from a noisy signal and identifying machinery fault.

The sources of noise and vibrations are well known. However, techniques to identify the exact source of vibration or noise are still in earlier developmental stages. Noise is considered one of the major challenges to diagnosis of vibrations in the centrifugal pump. Vibration and noise significantly affect the service life and performance of the centrifugal pump. When compared to other machine tools and utility equipment, diagnosis of sources of vibrations and noise in centrifugal pumps is more difficult. This is due to the fact that the components of machine tools are visible. On the other hand, the root cause of vibrations and noise in centrifugal pumps may lie deep in the hydraulic or mechanical aspects. Identifying the mechanical faults is easy but it is more difficult to identify hydraulic issues. Therefore, diagnosis of vibrations and noise in centrifugal pumps is very complex.

This work characterises vibration signals from a centrifugal pump to determine an effective and reliable feature sets for detecting and diagnosing faults from the bearings and impellers. As the vibration signals contain high-level background noises due to inevitable flow cavitation and turbulences, noise reduction and feature extraction are critical procedures in vibration signal analysis. Therefore, wavelet based fast Kurtogram, which enhance periodic impulses is used to select the optimal sub-band for further envelop analysis. It has shown that the improved envelope analysis produces correct detection for both inner-race and outer-race faults in bearings. In the meantime, this work presents a new method of fault diagnosis based on Modulation Signal Bispectrum (MSB) analysis of surface vibration is used to enhance the periodic blade-pass components, producing accurate diagnosis of the impeller and bearing faults. Moreover, MSB is used to capture the deterministic nonlinear feature of modulation components between fluid pulsations, rotating oscillations of the driving shaft and the impeller for reliable diagnosis. The diagnostics performances are also valid for different flow conditions.

1.4 Research Problem (Motivation)

The main objective of this research is to develop a condition monitoring and fault diagnosis system for the centrifugal pumps, based on vibration measurements. The total cost and maintenance of the centrifugal pumps seems to be the main concern of the researchers and industrial designers. Subsequently, condition monitoring of the centrifugal pumps significantly will improve maintenance schedule and also reduce the cost of unforeseen faults. Therefore, a proper maintenance program, significantly improve the profitability of the enterprise in the past few decades, a good understanding of the industry today. However, high cost, and maintenance of the pumps and other equipment are often regarded as a necessary expense that belongs to the operating budget. Figure 1-2 shows typical maintenance costs relative to rotating machinery, petrochemical plants. Therefore, any significant improvement in the maintenance of the pump to achieve significant savings in maintenance costs, as well as the development of productivity, which is the objective of this project to motivate.

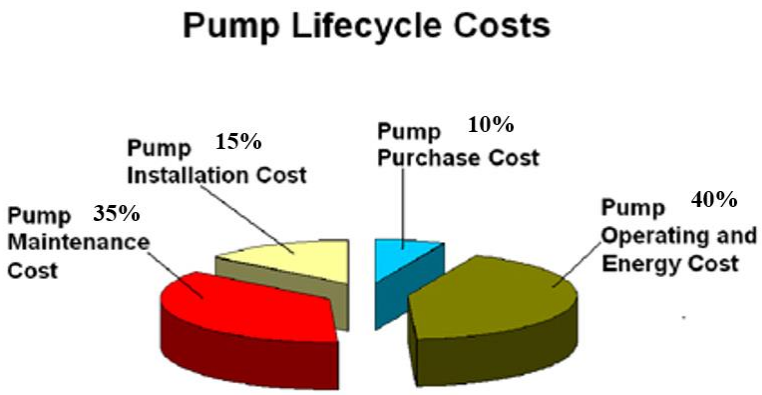

Figure 1-2 Typical maintenance costs [47].

Currently, various new technologies have made the automation of condition monitoring (CM) easier. This is the exact form of intervention that is required for these faults. The application of these technologies will ensure earlier diagnosis of faults, possible remedial action as well as deployment of the appropriate maintenance process before the centrifugal pump is damaged or fails to operate.

During signal processing of the practical signals, data collection processes, structural distortions, environmental disturbances as well as interferences generated from the other related components and machines inevitably induce a lot of noise. In order to implement reliable and efficient fault detection and fault diagnosis for the impeller and bearing faults, this

research greatly focuses on denoising as well as feature extraction from the vibration signals using the periodic, modulation and impulsive characteristics of the fault systems.

.

1.5 Overall Aim and Objectives

As centrifugal pumps are by far the most commonly used pumps in industry, they have been chosen for this project to develop condition monitoring techniques. Specifically, the research will investigate and monitor the key components: impeller and bearing in centrifugal pumps as they are relatively common defects in these pumps and can reduce performance, induce damages to the pump components and even catastrophic failures. Moreover, rising energy costs is causing manufacturing plants to focus their efforts on reducing the amount of energy used in rotating equipment's. Pumps of unsuitable size, poor condition and poor performance are causing companies to suffer reduced productivity and increased expenditure on maintenance and spare pumps. Moreover, such faults always accompany with addition noise and vibration, providing feasibility to diagnose them at early stages.

Therefore, this research aims at accurately characterizing the vibration responses and developing effective diagnostic features using the state of the art analytics techniques. Meanwhile, it also takes into account the minimization of the cost in monitoring a pump system by optimizing sensor placement and reducing data amount sizes while utilizing more advanced analysis techniques. Based on these considerations, the objectives of this research study are:

Objective 1: To review different condition monitoring techniques and especially vibration data analysis methods in developing effective vibration features for monitoring pump conditions. This is to include fault detection methods for pumps system.

Objective 2: To review the centrifugal pump fundamentals: operating process, types, pump selection, an overview of various applications where centrifugal pumps can be used, mechanical construction, mechanical and hydraulic faults including impellers and bearings.

Objective 3: To re-examine the influences of the centrifugal pump faults on the mechanical and hydraulic vibrations, which includes general assessments of vibration analysis methods that can be applied to the detection and diagnosis of pump faults.

Objective 4: To refine the existing pump test rig to be suitable for monitoring the centrifugal pump conditions by inducing different fault parts into the system and hence allowing a full evaluation of the vibration based condition monitoring techniques developed. In addition, right sensors and measurement systems are specified for adequately measuring vibrations along with speed encoder, suction and discharge pressures, flow rate hydraulic sound and airborne sound

Objective 5: To collect and analyse vibration signals under healthy/baseline pump conditions, and then perform experiments that reproduce common mechanical faults such as impellers and bearings at constant speed and under different flow rate/discharge conditions.

Objective 6: To analyse vibration signal data recorded from faulty and healthy condition using vibration spectrum for detecting and diagnosing the faults under different flow rates.

Objective 7: To apply higher order spectrum analysis techniques to the vibration signals for detecting and diagnosing impeller faults under different flow rates.

Objective 8: To analyse vibration signals recorded using the time domain, frequency domain and envelope analysis based on fast Kurtogram for bearing fault diagnosis under different flow rates.

Objective 9: To analyse vibration signals for developing methods being capable of the detection and diagnosis of combined faults using advanced signal processing methods.

1.6 Thesis Outline and Structure

This thesis is organised into Ten chapters to address the research objectives. The following gives a brief description of the contents of each chapter to show the basic interconnections between the chapters:

Chapter One

This chapter presents a general introduction and literature review of condition monitoring, which includes fault detection and diagnosis methods applied to centrifugal pumps. Also describes the importance of maintenance strategy and the life cycle of a centrifugal pump. Finally, it explains the research motivation, aim and objectives. In addition, the outline of the thesis is presented.

Chapter Two

This chapter provides a general introduction to centrifugal pumps and their importance in our lives. which includes an overview of various applications where centrifugal pumps can be used, mechanical construction of centrifugal pumps including the bearing, impeller, the pump casing. In additional mechanical and hydraulic faults are presented.

Chapter Three

This chapter provides a general introduction and overview of centrifugal pump vibration including an overview of mechanical and hydraulic sources of vibration in centrifugal pump in addition a review of vibration method.

Chapter Four

This chapter describes the methods for centrifugal pumps including details of the Higher Order Spectra Analysis (HOSA) measures (bispectrum) which are an extension of second order measures (e.g. power spectrum) to a higher order. Time and frequency domain methods are also presented.

Chapter Five

This chapter reviews the construction and design of a test rig suitable for measurements of the faults in centrifugal pumps. A complete description of all the components, equipment and sensors used in the construction of the test-rig, also reviews all test-rig configurations for monitoring faults in centrifugal pumps and instrumentation used to collect the vibration signals, finally the data which has been collected will be analysed by using Matlab software.

Chapter Six

This chapter review the sources of vibration in a centrifugal pump during operation with healthy compared with faulty conditions, also explains how defective impeller vanes affect the pump vibration level. In additional this chapter describes how the pump performance and vibration level is affected by the presence of the defective impeller. It then introduces the use

of vibration spectrum to detect the faults and finally, the experimental results are presented and discussed. In addition, the chapter focuses on the application of vibration method mainly based on the high frequency component of the vibration spectrum.

Chapter Seven

This chapter investigates the conditions of centrifugal pump impellers using surface vibration with advanced vibration signal analysis. Modulation signal bispectrum (MSB) is employed as the major tool to analyse vibration signals and hence diagnose the changes in impeller conditions. This chapter then describes how the pump performance and vibration level is affected by the presence of the defective impeller.

Chapter Eight

This chapter investigates the conditions of centrifugal pump, Bearings using surface vibration signal analysis, fast Kurtogram with advanced envelope analysis. This chapter then describes how the pump performance and vibration level is affected by the presence of the defective bearings. It then introduces the use of vibration spectrum to detect the faults and finally, the experimental results are presented and discussed.

Chapter Nine

This chapter investigates the conditions of centrifugal pump, diagnosis of combined faults bearings and impeller characteristics using surface vibration spectrum, envelope with advanced signal analysis: the modulation signal bispectrum. This chapter then describes how the pump performance and vibration level is affected by the presence of the defective faults.

Chapter Ten

This chapter draws conclusions from this research and proposes some aspects for future research in condition monitoring of centrifugal pump systems and for further improvements of some aspects for work.

CHAPTER TWO

CENTRIFUGAL PUMP FUNDAMENTALS AND FAULT MODES

This chapter provides a general introduction to centrifugal pumps and their importance in our lives, which includes an overview of various applications where centrifugal pumps can be used, mechanical construction of centrifugal pumps including the bearing, impeller, the pump casing. In addition, mechanical and hydraulic faults are presented.

2.1 Introduction

Centrifugal pump consists of a stationary pump casing and an impeller. The pump casing to guide the main function of the liquid from the suction nozzle in the centre of the impeller, the main function of the pump is to convert the energy delivered to a prime mover (electric motor) first into kinetic energy (velocity) and then into static pressure of the fluid that is being pumped. The purpose of the volute is to collect in the vicinity of the high speed of the impeller of the liquid out and lead to the gradual decline in the velocity of the fluid, by improving the flow of the region. Then, the liquid is discharged from the pump, through the most common problem with centrifugal pump vibration nozzle emissions [48, 49].

The centrifugal pump comprises of a stationary and rotating part. The stationary part comprises of a bearing, casing, electric motor as well as its cooling fan. On the other hand, the rotating part has a pump impeller and a shaft. Depending on the working processes, the sources of vibration in the pump can be categorised into two namely hydraulic and mechanical process. The mechanical sources of vibration include friction of seals or bearings and the vibrations from the unbalanced rotating objects. The hydraulic sources of vibration are fluid flow perturbation within the pump and contact between rotor blades and the stationary components like guide vanes and volute tongue [50].

2.2 The Centrifugal Pump

A device or machine used to transfer, raise or compress fluids is referred to as a pump. A Pump is a motor driven equipment and it one of the largest single user of power (31%) in the industry. Various process variables such as the flow of liquids and gases as well as pressure, have been regulated with mechanical clutches, adjustable in-let guide vanes and throttles. These pumps usually operate as variable torque loads. As the load increases, the speed increases and vice versa. All these mechanisms waste a lot of energy, provide inaccurate control, as well as require frequent maintenance [51, 52].

2.3 Working Mechanism of a Centrifugal Pump

A centrifugal pump refers to a machine which is able to transform an impeller’s electrical energy to rotational energy, and thus increasing the velocity of pumped fluid. The energy changes occur by virtue of two main parts of the pump, the impeller and the volute or diffuser.

The impeller is the rotating part that converts driver energy into the kinetic energy. The volute or diffuser is the stationary part that converts the kinetic energy into pressure energy. In addition, the presence of the stationary volute tongue which converts the kinetic energy of the fluid into fluid pressure as shown in Figure 2-1 [53].

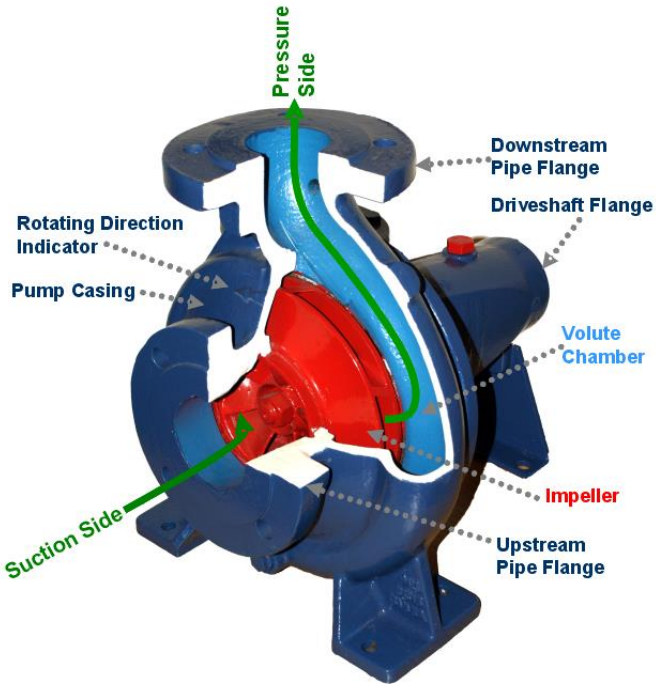

Figure 2-1 The liquid flow path inside a centrifugal pump [53].

2.4 Characteristic Curves of Centrifugal Pump

The performance of centrifugal pumps is usually described by various curves whereby the delivery head is plotted over the rate of flow. In addition, centrifugal pump performance can be demonstrated graphically using a characteristic pump. A characteristic curve exhibits the brake horsepower, total dynamic head, net positive suction head and efficiency plotted against the pump's capacity range [54]. There are three performance characteristics of pump:

- Head developed by the pump (H).
- Brake horse power (BHP).
- Efficiency of the pump.

Figure 2-2 shows that, the pump head decreases with increasing flow rate till the pump cannot deliver the fluid at Q= Q max. In addition, the horsepower shows slightly increase with increasing the flow rate. Moreover, the pump efficiency initially increases with increasing flow

rate, reaches a maximum up to at Q= Q*, and then decreases to zero at Q= Q max [54], where Q* is the best efficient point of the flow rate.

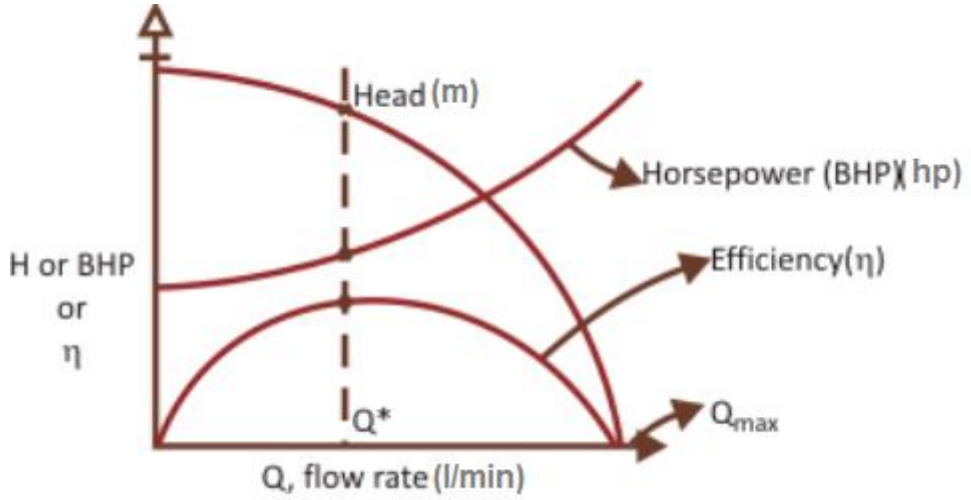

Figure 2-2 Performance characteristics of a pump [54].

2.5 Head Developed by the Pump (HDP)

Head refers to a total work done per unit weight of the water by a pump impeller. Also, it is the energy water acquires between the pump's suction and discharge sides. The pressure difference measured between the suction and discharge sides of a pump is referred to as pump head. Pressure in liquid is as a result of the liquid's column, because the weight of the liquids exerts some pressure on the surface. The column of water whose weigh exerts pressure is known as head. Head is normally expressed in meters (m) or feet (ft) of a liquid. Head and pressure are two distinct ways of expressing a similar value [55].

2.6 Brake Horse Power (BHP)

There are various losses that should be accounted for in any physical process. As a result, the pump shaft should be offered more power in order to provide the water with more power. This type of power is referred to as brake power or brake horse power. The pump's efficiency (discussed below) determined the amount of power needed at the pump shaft [55].

BP = WP/E

WP = water power in horsepower units
E = energy

2.7 Pump Efficiency

Pump efficiency is the present of power input to the pump shaft (the brake power) that is defined as a ratio of energy output to the energy input applied to the pump rotor. The pump often experiences losses; thus the pump's efficiency is less than 100 percent. As a result, the total amount of energy needed to operate the pump is more compared to the actual energy which is transferred to water. The brake power (BP) and water power (WP) are used to compute the pump's efficiency as follows:

E% = (BP /WP) x 100

Also, various tests are conducted to determine the pump's efficiency. They include the design, type and size of the pump. Generally, larger pumps are more efficient. The materials that are used in the construction of the pumps also affect its efficiency. For instance, smoother impeller finishes enhances the pump's [55].

Also, pump curves indicate the type and size of the pump, its operating speeds (revolutions/minute), as well as the size of the impeller (in inches). Moreover, it shows the best efficiency point (BEP) of the pump. When pump's operating point is very close to the best efficiency point, it is said to be operating cost effectively [55].

2.8 Pump Selection

Selection of pump based on total head (not discharge pressure) and flow rate. The flow rate will depend on the maximum requirement. Total head is the amount of energy that the pump needs to deliver to account for the elevation difference and friction loss in the system [56].

Before selection of pump model one should evaluate its performance curve. The performance curve is demonstrated by its operating curve or rate of head-flow. The curve exhibits the capacity of the pump (in gallons/minute) plotted against the cumulative developed head (in feet). Also, it demonstrates the required power input (brake horse power), efficiency (percentage), as well as suction head requirements (the net positive suctions head requirements in feet) over various flow rates. [57]. Pump manufacturers do not use discharge pressure as the criteria for pump selection.

2.8.1 Hydraulic Aspects

All the information needed to select the pump size such as the head H and the flow rate Q of the required operating points are presumed to be known. The data is acquired from a system

characteristic curve. Also, the frequency of the electric mains is given. It is possible to select the pump size and the rotation speed using the aforementioned values [57]. ISO 3555 indicates that the predicted characteristics experienced between the Positive Suction Head Required (NPSHR) and Net Positive Suction Head Available (NPSHA) for the system are highlighted in the Figure 2-3. More details regarding the pump selected such as the input power P, efficiency, E reduced impeller diameter Dr and the required (NPSHr) can be determined from a single characteristic curve as demonstrated in the figure below. Provided that there is no any other reasons to act otherwise, the selected pump's operating point should be close to its best efficiency point (BEP) Q^* =(rate of flow when the efficiency is highest)[57].

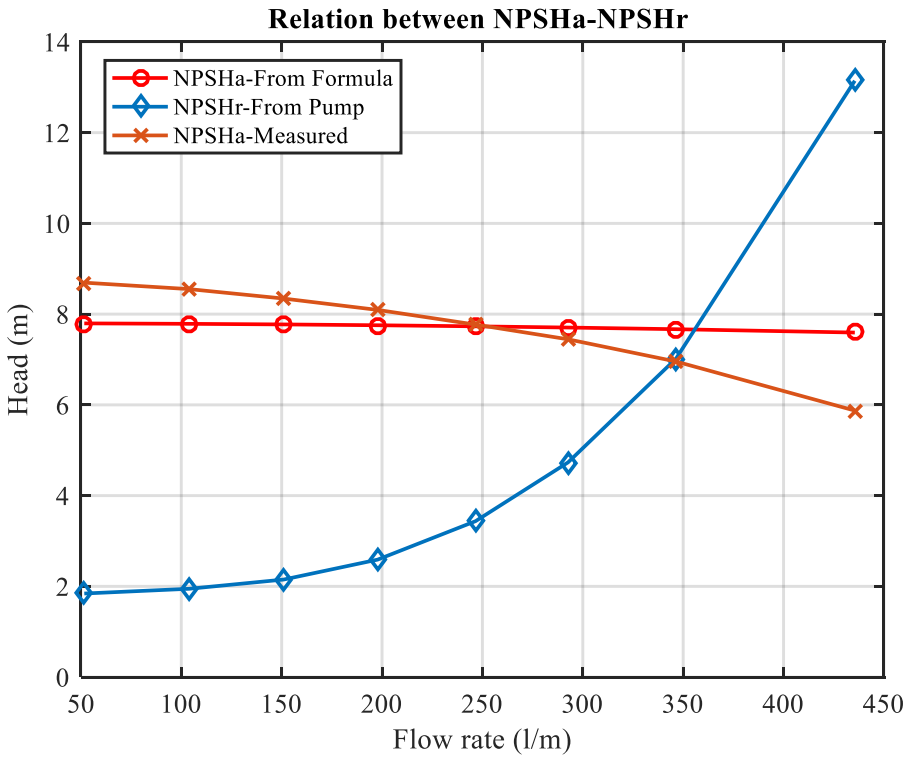

Figure 2-3 Pump performance curve

2.9 Pump Applications

All industrial processes that underpin our modern civilization and the need to transfer fluid pressure level from one to another, from one place to another. Pumps are, therefore, an important part of an industrial process an integral parts of all modern economic and social development [58].

Centrifugal pumps, as compared to axial compressors, are commonly used because of their simplicity and ability to generate relatively high-pressure ratio in a short axial distance. In

general, centrifugal pumps are used wherever any quantity of liquid is required to move from one place to another. This applies to a large number of applications and services including electric power plants, water supply plants (i.e. sewage, drainage or irrigation etc.), oil refineries, chemical plants, steel mills, food processing, mines, dredging and jetting operations, hydraulic power services and almost all ships whether propelled by steam or diesel engine [56, 58, 59] . Figure 2-4 show how the pump market is split between different industrial sectors.

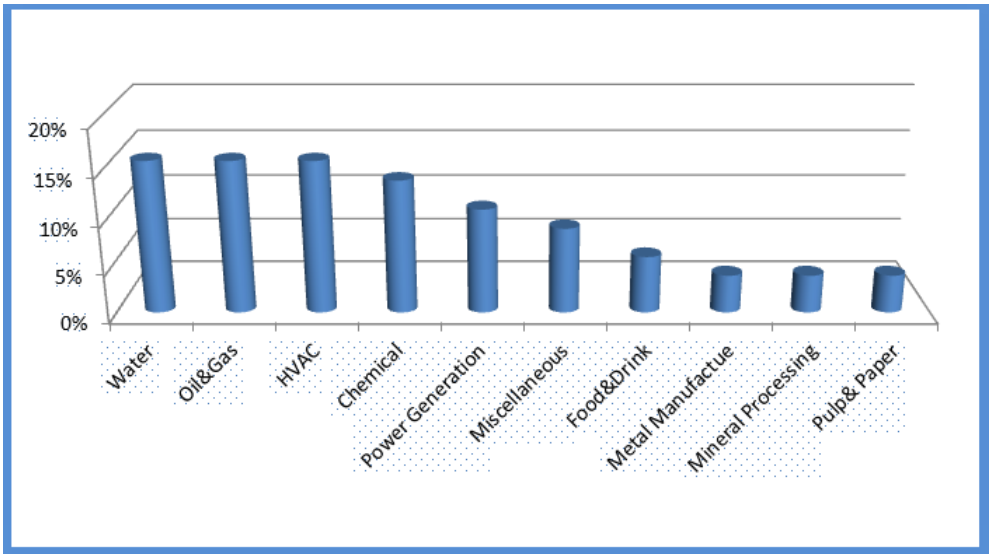

Figure 2-4 Overview of the pump application [58].

Furthermore, centrifugal pumps are found in services such as air-conditioning, refrigeration, pulp and paper mills and textiles. Although these pumps have much in common, they vary in design and construction to meet specific requirements of each service of various different categories of pumps used in different applications, the centrifugal pumps are the most commonly used. According to the business plan of ISO issued in January 2004, centrifugal pumps represent around 64% of the pump market as shown in Figure 2-5 below:

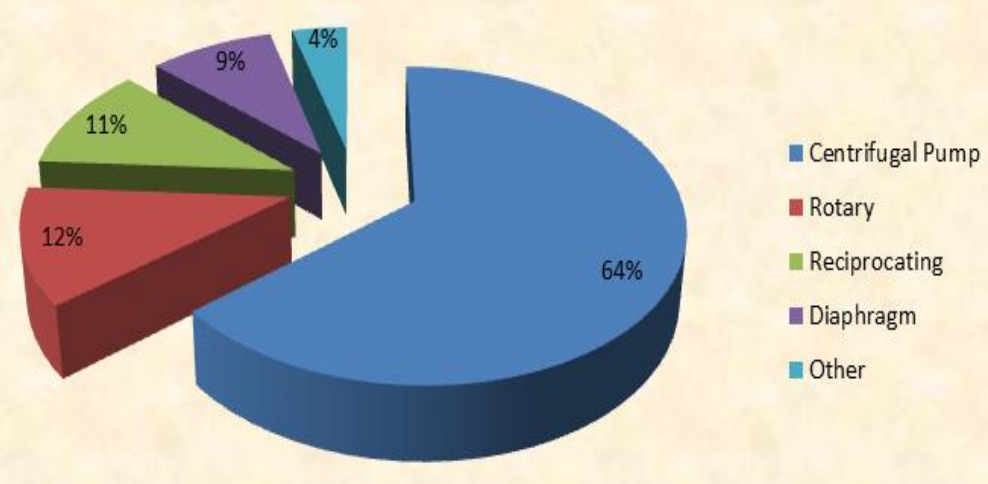

Figure 2-5 The pump market [60].

The right choice of pump in some applications such as nuclear power plant, does not affect only the industry production but other domestic and social developments as well. It is also strongly related to the people and environment safety as the pumps play a major role in the design and operation of nuclear power plants and nuclear facilities. Two typical industrial applications, (e.g. water treatment plant and water pumping station) where the centrifugal pump is extensively used, are illustrated in Figure 2-6 and Figure 2-7.

Figure 2-6 Centrifugal pump in a water treatment plants [61].

Figure 2-7 Centrifugal pump in water pumping station [62].

2.10 Pump in Industries

A pump is machinery that transfers mechanical energy from an external source to the liquid flowing through a machine, in order to move the liquid from one point to another. To put it more simple, energy is expanded to increase the pressure of a fluid (liquid or gas) and move it from one place to another [63, 64].

Broadly, pumps are classified into two main groups: *Kinetic Energy* pumps and *Displacement* pumps. These two groups are further divided into smaller groups for specific services [56, 64] both types of pumps add energy to the liquid, moving it through a pipeline and increasing the pressure, but they do it differently. Centrifugal pumps generate the pressure by accelerating and then decelerating the movement of the fluid through the pump. The positive displacement pumps, however, generate the pressure by expanding and then compressing a cavity space or moveable boundary within the pump.

The global pump industry is worth $18 billion of which, $13 billion is spent on new pumps [65]. The average growth of this market is around 3% per year. Apart from the pump users, the people, who are working in the industries where the pumps manufactured, are estimated to be 250 to 300000. Figure 2-8 shows the overview of the pump makers.

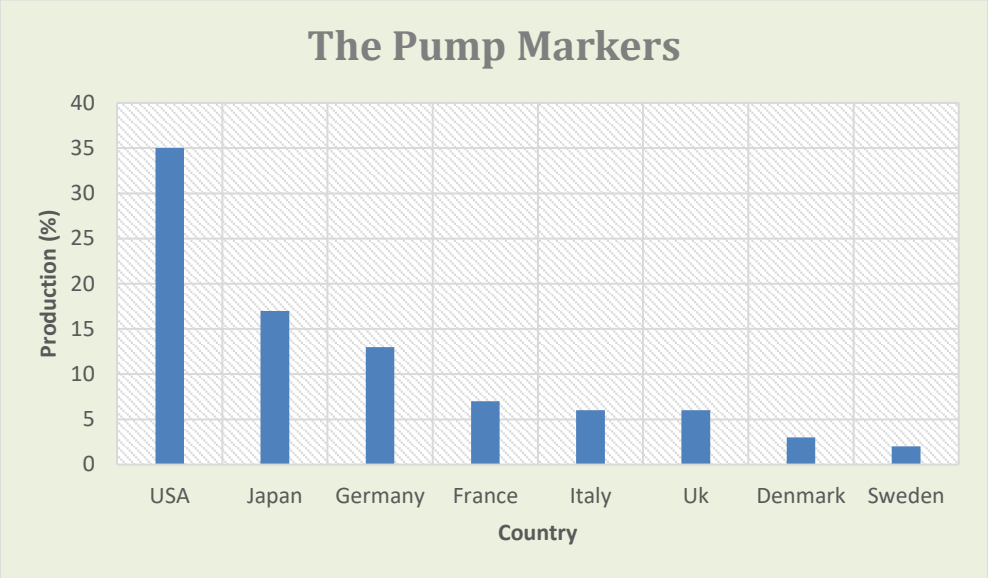

Figure 2-8 Overview of pump markers

There are various types of pumps of different sizes and specifications in the market, and therefore, the most important question is how to select the right pump for a specific application. It is not easy even for the skilled pump user to make an optimal selection. In many cases, a given plant simply utilises the past practice in selecting, purchasing and repairing a pump. The requirement of different departments within the plant may also differ at times, causing more complicity in decisions on the pump application strategy.

2.11 Construction of Centrifugal Pump

A centrifugal pump refers to a rotating device in which pressure and flow are dynamically generated. Similar to positive displacement pumps, the inlet is not enclosed from the outlet, irrespective of the fact that they are rotary or reciprocating in the configuration. The centrifugal pump gives the fluid energy through the velocity changes that are experienced as the fluid is conveyed through the impeller as well as the other related fixed pathways of the pump. All impeller pumps are rotor-dynamic including those with radial-flow, mixed-flow and axial-flow impellers. The term ‘centrifugal pump’ tends to encompass all rotor-dynamic pumps [66].

A centrifugal pump has two main parts: rotating parts that include an impeller and shaft and stationary parts comprising a casing, casing cover and bearings [67]. The components of a centrifugal pump are illustrated in Figure 2-9 below.

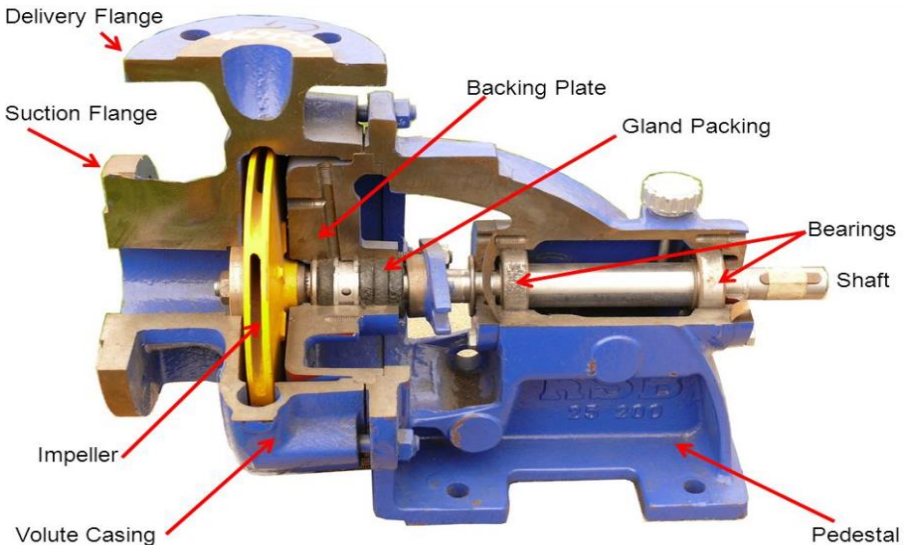

Figure 2-9 Centrifugal pump components [68]

2.11.1 The Impeller

The impeller is the main rotating part that provides the centrifugal acceleration to the fluid. The impeller is the fundamental component of a centrifugal pump. It is responsible for converting the torque applied to the pump shaft into pressure and kinetic energy in the pumped liquid. It does this by the action of its blades on the liquid. The other components, even those that convert kinetic energy to pressure, absorb some energy from the liquid [69].Mechanical construction also determines impeller classification. Accordingly, impellers can be classified as:

2.11.1.1 The Open Impeller

An open impeller consists of vanes attached to a central hub for mounting on the shaft without any form of shroud as shown in Figure 2-10. The main advantage of open impellers is that they are suitable for pumping liquids containing stringy materials. It is also claimed sometimes that they are better suited for handling liquids containing suspended matter because the solids in such matter are more likely to be clogged in the space between the rotating shrouds of a closed impeller. The disadvantage of these impellers is structural weakness. If the vanes are long, they must be strengthened by ribs or a partial shroud. Generally, open impellers are mainly used in small, low energy pumps. Furthermore, the open impeller is much more sensitive to wear than any other types [69, 70].

Figure 2-10 Open impeller [71].

2.11.1.2 Semi-Open Impeller

The semi-open impeller incorporates a single shroud as shown in Figure 2-11, usually at the back of the impeller. This shroud may or may not have pump out vanes, which are vanes located at the back of the impeller shroud. This function reduces the pressure at the backrub of the impeller and prevents foreign matter from lodging-in from back of the impeller that would interfere with the proper operation of the pump and the seal chamber [69].

Figure 2-11 A Semi-open impeller

2.11.1.3 The Closed Impeller

The closed impeller, which is almost commonly used in centrifugal pumps handling clear liquids, includes shrouds that totally enclose the impeller waterways from the suction eye to the periphery Figure 2-12. Although, the design of closed impellers prevents liquid slippage,

which occurs in an open or semi-open impeller, there should be a running joint between the casing and the impeller in order to separate the suction and discharge chambers of a pump. The running joint comprises of a short cylindrical surface mounted on an impeller shroud which rotates on a slightly larger static cylindrical surface [70].

Figure 2-12 Closed impeller

2.11.2 The Casing

The component that contains the pump impeller is generally referred as the pump casing. A pump comprises of a suction as well as a discharge penetration for the pump's main flow path. The pump normally has vent fittings and small drain to eliminate gases confined in the casing of the pump or to drain the pump's casing to perform maintenance as shown in Figure 2-13. In addition to all of these functions of the pump casing, it also performs five other important functions [59, 64]

- Provides pressure containment.
- Incorporates the collector.
- Allows rotor installation and removal.
- Supports the pump.
- Maintains the alignment of the pump and its rotor under the action of pressure and reasonable piping loads.

The required type of the collector classifies the centrifugal pump. The purpose of the collector is to collect and diffuse the high velocity liquid discharged by the impeller. This process is necessary to slow the liquid to a usable velocity and convert the kinetic energy into pressure energy, thereby recovering most of the pump's energy input. The selection of the pump casing type depends on the application of the pump [64].

Figure 2-13 Pump casing

2.11.3 The Shaft

The device that transmits the required torques for the rotation of an impeller of a centrifugal pump is referred to as shaft. The shaft also supports the impeller and rotating parts as demonstrated in Figure 2-14. shown below. The shape of the shaft and materials are designed in a way that the deflection is maintained to less than the allowance between the stationary and rotating parts. The pump shafts are normally protected from corrosion, wear and erosion at the leakage joints, seal chambers as well as internal bearings [64].

Figure 2-14 The Shaft.

2.11.4 The Bearings and Bearing Housing

The shaft bearings are enclosed within the bearing housing. These bearings maintain the rotor and shaft in the appropriate alignment with the other stationary components, despite the action of transverse and radial loads. Moreover, the bearing housing comprises of oil reservoir that facilitates lubrication, as well as cooling jacket with circulating water. Also, the bearings help to support both axial and radial loads that are imposed on a centrifugal pump, especially because of the weight and hydraulic loads which are enforced on the impeller as demonstrated in Figure 2-15. The shrouds of an impeller experiences high pressure which is exerted by the high pressure liquid that flows continuously over the impeller's circumference. This pressure produces forces in both longitudinal and lateral directions [72].

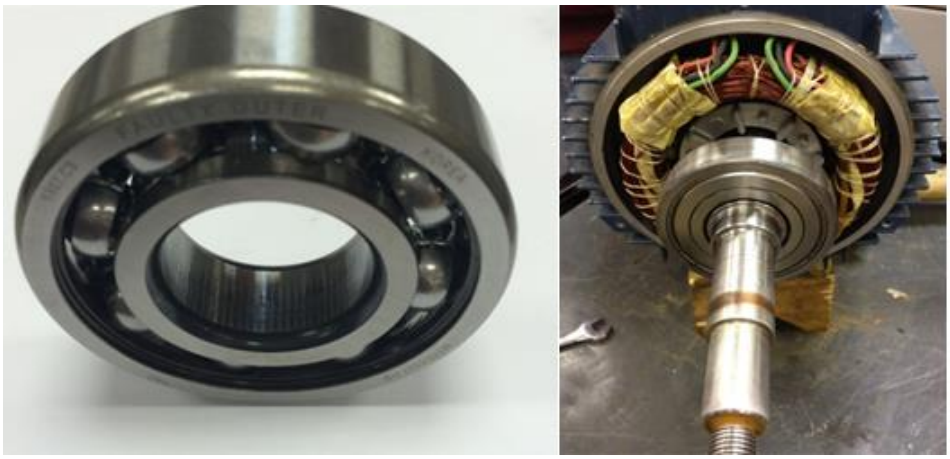

Figure 2-15 The bearing

2.11.5 The Mechanical Seal

A chamber is also known as a stuffing box or a seal chamber. The chamber is either part of or separate from the pump's casing house which is the region between the casing and the shaft where the sealing media is located. The chamber is usually called a seal chamber when a mechanical seal is used to achieve the seal. On the other hand, a chamber will be known as a stuffing box when the sealing is realized through packing. Both the stuffing box and seal chamber protect against leakage, especially when the shaft penetrates through the casing of the pump. The sub-ambient pressure experienced at the chamber's bottom level prevent all air leakages into a pump. The chambers eliminate liquid leakages out of a pump, when the pressure is above the atmospheric pressure. The heating or cooling arrangement of the stuffing boxes and seal chambers ensure that there is proper control of temperature. The main challenge that affects centrifugal pumps in delivering highly toxic, ultra-pure, delicate or sterile fluids is a shaft seal that seals a rotating shaft drive over the casing as demonstrated in Figure 2-16. Exxon

asserts that about 80% of the pumps used in chemical plants are removed from the service due to mechanical seal failure. Also, the other 20% are removed from service due to failure of couplings, bearing as well as other related items [73]. In most cases, the costs of maintenance are about twice the value of the pump its first five years [74].

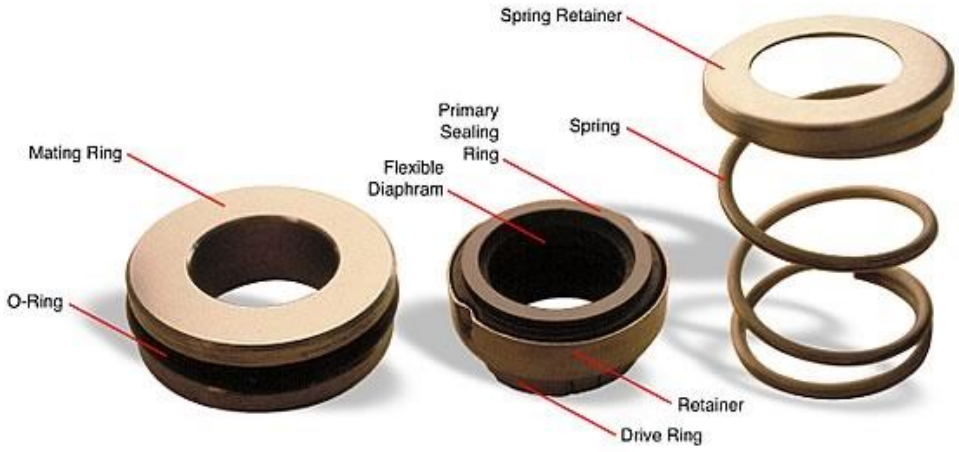

Figure 2-16 Mechanical seal [14].

2.12 Centrifugal Pump Faults

A centrifugal pump is composed of two main parts: the pump and the motor. Faults in the pump originate in the impeller, casing, seal, shaft or bearing [75]. In case of motor faults, they may occur in the stator, rotor shaft or bearing in general, faults in a centrifugal pump are categorized as follows:

2.12.1 Mechanical Faults

All faults relating to the pump components (i.e. the casing, impeller, shaft, bearing, and sealing) are considered as mechanical faults. Mechanical faults may cause physical damage to pump components and in some cases affect its hydraulic efficiency [75]. There is a strong connection between mechanical faults and other faults such as hydraulic faults. The most common mechanical faults of a centrifugal pump are:

2.12.1.1 Impeller Faults

The impeller is the heart of a centrifugal pump. Any fault occurring here, therefore, will affect the performance and efficiency of the pump. Both cavitation in the centrifugal pump and chemical reactions between the pumped liquid and the impeller material can cause corrosion and erosion, which result in pitting on the impeller. Sometimes it is the shaft material that is

more rapidly attacked [76]. Wearing of the keyway may occur if the impeller fits loosely on the shaft or the key is not fitted properly. In small pumps, wearing is best corrected by replacement of the impeller.

2.12.1.2 Bearing Faults

Pumps are very demanding applications for bearings. Many factors such as flow, temperature, pressure and others have to be considered prior to the selection of the right bearing for specific applications [76]. Two main causes of the failure of centrifugal pumps are excessive leakage and bearing problems. There are many reasons for the failure of the bearing rolling element; these include excessive heating of the bearing due to improper dissipation of heat, excessive radial load caused by low flow operation, misalignment of the unit, bent shaft or severe vibration within the installation [77]. Bearing problems are best corrected by replacing the defected bearing and by correcting the problem behind the fault.

2.12.1.3 Failure of Mechanical Seals

Although shaft-sealing techniques have made significant advances, shaft-sealing problems are still one of the most common causes of the pump failure. The reliability of mechanical seals is dependent on the design of the seal itself, its suitability for the pump and the manner in which the pump is being used, which is not always the situation pump was designed for [78].

2.12.1.4 Failure due to Foreign Matter

Foreign matter in the impeller or casing of centrifugal pumps may cause serious problems including the reduction of pump capacity, imbalances in the rotor and the imposition of excessive load on the bearings. Pumps can be protected from foreign matter using strainers and screens; this protection is particularly important for pumps not designed to handle suspensions of any kind [79].

2.12.2 Hydraulic Faults

During the working and operation of the centrifugal pump, aforementioned, the flowing liquid's kinetic energy is converted to pressure energy. The high pressure liquid continuously flows on the impeller's circumference. Also, it gets confined within the clearance between the casing and the impeller, resulting to cover. The high pressure liquid exerts a lot of pressure on the shrouds and outlet passages of the impeller leading to the creation of two forces, one in a longitudinal and another in a lateral direction in line with the pump shaft axis [72].

The hydraulic performance of the pump is very important. Any degradation in hydraulic performance will affect pump efficiency and may cause damage to the pump components. The hydraulic faults which causes damage to the impeller, casing and bearings[80]. In order to assess the hydraulic performance of a centrifugal pump, it is necessary to analyse the measurements of the differential pump head, flow rate and power consumption [78]. The specific gravity and temperature of the fluid too, must be known. When the hydraulic performance of a centrifugal pump declines, the symptoms normally include one of the followings:

- More power is required to produce the normal flow rate.
- A sudden trip of the electrical motor drive.
- A reduction of the maximum flow rate.
- The control valve needs opening to obtain the normal flow rate.

The most common hydraulic fault in centrifugal pump is cavitation. Cavitation is a phenomenon that takes place when the pressure inside the pump reaches the vapour pressure of the pumped fluid. This forms cavities in the low-pressure field, these cavities collapse when they reach a place of higher pressure in the pump.

2.13 Summary

This chapter has introduced the centrifugal pumps and their importance in the industrial filled applications. It is summarised the pumps mechanism, pump characteristic curves, pump efficiency, pump applications and pump selection. In addition, this chapter is over viewed mechanical configuration and components, which is including the impeller, bearing, and the stationary casing of the pump. Moreover, it is summarised the concept of the mechanical and hydraulic common faults which explored in association their causes and effects. Therefore, the following chapter will be present the centrifugal pump vibration overview.

CHAPTER THREE

CENTRIFUGAL PUMP VIBRATIONS

This chapter provides a general introduction and overview of centrifugal pump vibration. which includes an overview of mechanical and hydraulic sources of vibration in centrifugal pump. In addition, the dynamic responses of various pump arisen from local defects. Including the description of the hydraulic vibration and pressure pulsation in centrifugal pump (Van Passing Frequency).

3.1 Introduction

Centrifugal pump consists of a stationary pump casing and an impeller. The pump casing to guide the main function of the liquid from the suction nozzle in the centre of the impeller, the impeller radial conferred recommendations and dizziness liquid, resulting in increased pressure on the two kinetic energy, and force it to form a spiral. The purpose of the volute is to collect in the vicinity of the high speed of the impeller of the liquid out and lead to the gradual decline in the velocity of the fluid, by improving the flow of the region. Then, the liquid is discharged from the pump, through the most common problem with centrifugal pump vibration nozzle emissions [48, 49].

3.2 Vibration Characteristics of Centrifugal Pump

The centrifugal pump consists of two major parts: the stationary component that comprises of the bearings and casing box, as well as am electric motor that has a cooling fan and the rotating component that comprises of an impeller and a shaft. Based on the pump working process, vibration is generated by both hydrodynamic and mechanical sources. Mechanical sources are usually cause friction in the seals and bearings as well as the vibration of the unbalanced rotating masses. On the other hand, hydrodynamic sources cause perturbation of the fluid flow in the pump and they enable interaction of motor blades with the adjacent objects, like guide vanes or volute tongue. Both mechanisms produce vibrations that cause the pump's structure to vibrate. Moreover, general vibration responses to faults periodic with impeller and bearing characteristic frequency usually masked by random noises due to unsteady flows. From this perspective, the basic generating mechanisms for both structure-borne vibration and airborne noise are the same for a sealed pump system [81, 82].

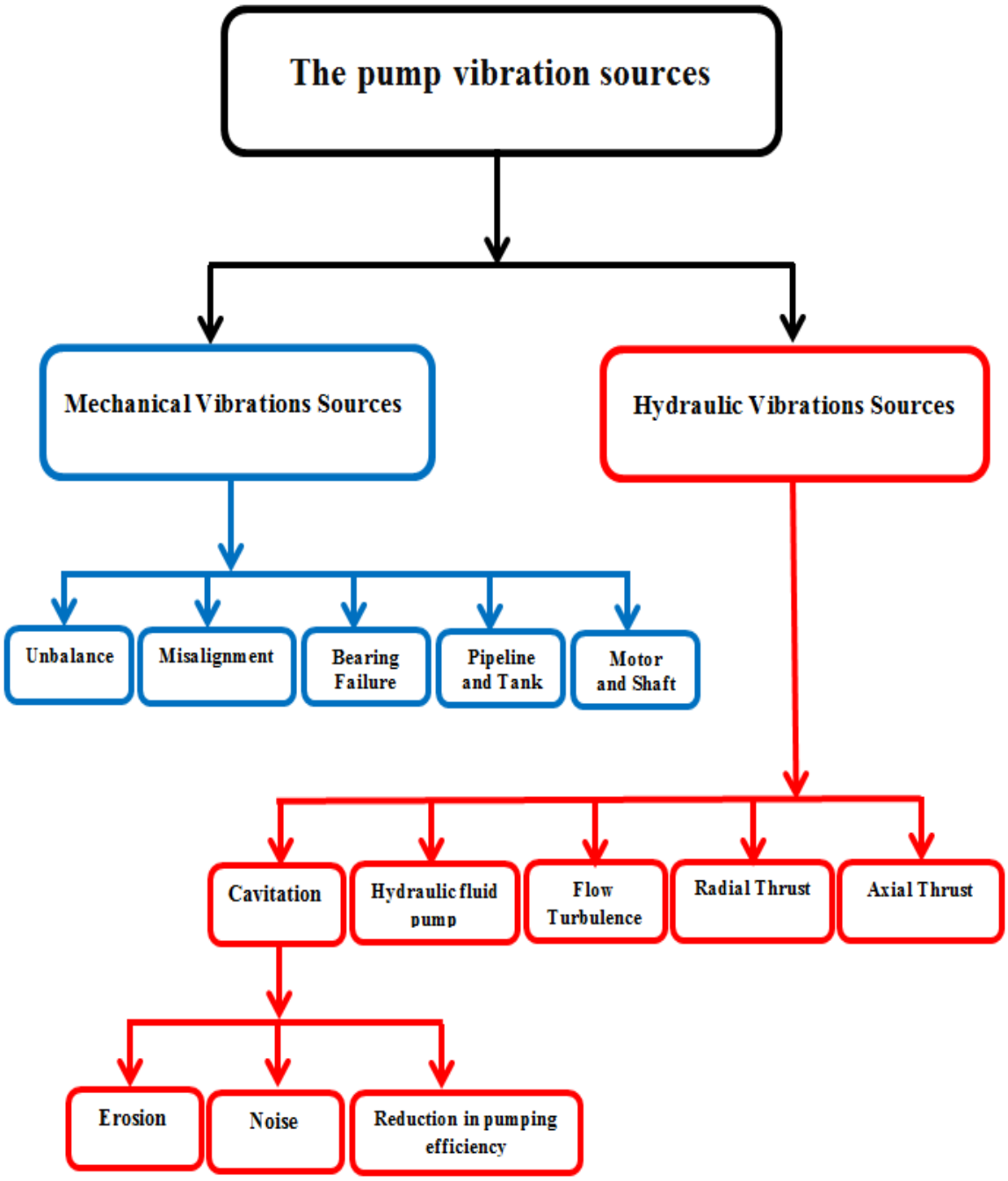

Figure 3-1 The vibration sources of centrifugal pumps

The pump vibration is consisting of two main sources the mechanical vibration sources such as the shaft and impeller that are rotating parts, and Hydraulic vibration sources such cavitation and flow turbulence. Moreover, sources of pump vibrations can be grouped into two as shown in Figure 3-1. The hydraulic sources result from the fluid flow perturbation within the pump as well as interaction of rotor blades with stationary elements like guide vanes or volute tongue.

The mechanical sources of vibration result due to friction in seals and bearings as well as vibration of the unbalanced rotating mass [50]

3.3 Mechanical Vibration Sources

3.3.1.1 Bearing Failure

There are many bearing types used in centrifugal pumps, their advantages, limitations, and other factors impacting bearing life. The function of the bearings in a centrifugal pump is to keep the shaft or rotor in correct alignment with the stationary parts under the action of radial and transverse (axial) loads. In addition, bearings that give radial positioning to the rotor are known as line bearings, and those that locate the rotor axially are called thrust bearings [83].

Bearing problems due to high heat or the contamination of bearing lubricants with solid particles or other liquids, occur as a result of overloads on the bearings. Once the bearing becomes faulty, then vibrations may display other components at frictional frequencies, $x \times f_r$ for the shaft frequency. Rolling element bearings can frailer in different ways such as spalls, as the result of fatigue on the shape of spalls on the outer race, inner race or rolling components. A race with a spall will almost occasionally collide with the rolling components. A fault signature is characterised with sequential impulses with repetition rates based on the geographical dimensions, rotational speed and the faulty components. The period between the successive impacts is distinct for all the aforementioned elements depending on the rotational speed, load angle and the bearing's geometry. For the case of fixed outer race bearings, theoretical characteristic fault frequencies are computed with the equations shown in section 8.3 [84].

3.3.1.2 Impeller Failure

The impeller is the heart of a centrifugal pump. Any fault occurring here, therefore, will affect the performance and efficiency of the pump. Both cavitation in the centrifugal pump and chemical reactions between the pumped liquid and the impeller material can cause corrosion and erosion, which result in pitting on the impeller. Sometimes it is the shaft material that is more rapidly attacked [76]. Wearing of the keyway may occur if the impeller fits loosely on the shaft or the key is not fitted properly. In small pumps, wearing is best corrected by replacement of the impeller.

3.3.1.3 Motor and Shaft

The hydraulic system has a motor that rotates at high speeds when working. As the motor rotates, the rotating element imbalance causes incentive mechanical vibration and periodic unbalanced force. The shaft vibrations are as a result of displacement of the shaft from its normal position because of external forces produced as the shaft rotates. In this case, the frequency of shaft vibration equals the motor rotation frequency.

3.3.1.4 Coupling

Flexible couplings are devices used to mechanically connect two shafts to transmit power from one shaft to the other. They are also able to compensate for shaft misalignment in a torsion ally rigid way. Misalignment can be angular, parallel or skew, this is particularly important for applications where misalignment could affect the velocity and acceleration of the driven shaft. and a prime mover driven shaft coaxial degree. If this value is out of tolerance, vibration will be generated.

3.3.1.5 Pipeline and Tank

The tank and pipeline do not generate vibrations. Vibrations are generated by other elements such as mechanical vibration, pressure, and flow pulsation. When the vibration frequency and natural frequencies of the tank and pipe are equal, resonance occurs, causing a strong vibration. Particularly when the pipeline is meticulous or too slender and the direction changes to a greater extent causing vibrations [85].

3.3.1.6 Unbalance

When the rotational axis is not parallel to the central axis, unbalance occurs. Because of the unbalance of the impeller, vibration occurs and this reduces the local pressure and velocity of the fluid which may lead to undesirable turbulence. Therefore, there is necessary to eliminate unbalance in the rotor [72]. Unbalance usually generates vibrations during the shaft frequency or first harmonic running speed $1xf_r$.

3.3.1.7 Misalignment

Another common cause of vibrations in the pump is misalignments. There are two main categories of misalignments: angular and offset. Offset refers to extent of offset between the two centerlines (i.e. motor and pump). Angular refers to a differential crossing angle between two shaft centerlines when they are projected to one another. Misalignments usually induces

vibrations twice the running speed $2 \times f_r$. Sometimes, the misalignment load can cause greater harmonics [85].

3.4 Hydraulic Vibration Sources

The interactions between the rotating impeller and stationary components of the pump like diffuser vanes and volute causes the pump to vibrate. Moreover, vibrations come as a result of interaction between the pumped fluid and impeller vanes.

3.4.1.1 Hydraulic Fluid Pump

One of the main source of noise in a hydraulic system is the hydraulic pump. Also, flow pulsation which is an inherent characteristic pump generates pump pressure generation together with piping and spreading to the entire system. Flow pulsation also generates vibrations. Moreover, other significant factors of vibration include pump hysteresis and hydraulic pump leakages.

3.4.1.2 Turbulent Flow and Vortex

Because of the high velocity of liquid flow, the liquid flow remains at a turbulent state and induces a local eddy as they flow cross the section mutation. Besides vortex and turbulent flow, mutual impact, fluid particle motion, and interaction with the pipeline, pump, valve body wall or various interactions will generate vibrations [85].

3.4.1.3 Cavitation

In the hydraulic system, cavitation is common at the hydraulic pump suction port as well as the narrow gap or orifice. During cavitation, fluids with bubbles are generated and forced to high pressure zones. This results to pressure fluctuations and greater local instantaneous burst that makes the system to generate vibrations. Also, cavitation causes a normal volume drop leading to poor performances of the slow motion elements [85].

3.4.1.4 Erosion

As the cavities collapse in areas experiencing high pressure, they exert massive local stress on the various surfaces onto which they collapse, thus damaging the pump surfaces. Because of the water hammering activities of collapsing vapor bubbles, various erosion signs will appear in form of pitting. Damage comes as a result of collapsing cavities, as the released liquid jet hits the pump's surface at local speeds of sound. This results to local high surface pressures

which may be higher compared to the material's ultimate strength [86]. It is also reported that as the volume of the liquid increases, the rate of cavitation damage increases. The rates of erosion increases four times when the fluid's capacity is increased from 100 to 120 percent of shock less flow.

3.4.1.5 Noise

When the cavities are subjected to high pressure, they collapse producing sharp crackling sounds. This sharp crackling sound is also referred to the pumping stones. The amount of noise generated from cavitation depends on the cavitation's severity. The pump suction also generates noise when it is working. If the sharp crackling noise appears to be random, together with high intensity knocks, it shows that cavitation within the suction is recirculating. However, this does not demonstrate a reduction in the pump's performance if the NPSHR is lower than NPSHA as shown in section 2.8.1 [86].

- **Reduction in pumping efficiency**

Vapour bubbles produced in the passages surrounding the impeller hinder the smooth flow of pumped fluid, thus causing a decrease in the output. In addition, a decrease in the efficiency of a pump is a reliable sign demonstrating the occurrence of cavitation, because noise is not generated until cavitation has advanced to levels where the pump's efficiency is poor. In some cases, it has been reported that the efficiency of the pump increases slightly moments before cavitation commences. This may be as a result of the decrease in friction during the commencement of separation of the flow, especially before the cavities begin to collapse [86].

3.4.1.6 Radial Thrust

Hydraulic radial load results from unequal velocity of fluid passing through the casing. This unequal fluid velocity causes non-uniform pressure to be exerted on the impeller's circumference. The design of the pump casing significantly influences the radial load. The pump casing has been designed in a way to guide fluid flow from the pump impeller into a discharge piping. In the theoretical incidence at Best Efficiency Point, a volute casing experiences uniform distribution of pressure and velocity around the periphery of the impeller. There are various formulas that are able to accurately predict the rate of hydraulic radial thrust. As demonstrated in Figure 3-2 radial thrust can be reduced by creating a double volute casing. Also, radial thrust can be reduced by offering a diffuser casing type [72].]. Moreover, radial thrust is subjected to the pump rotor, which is directed towards centre of rotation. Forces

exerted on the rotor typically comprises of a dynamic cyclic element, which is covered into a stable state load. This dynamic part increases swiftly when the pump is working on its recirculation state, when there is low flow within the system. Static load increases both high and low flow operations, with its minimum value near or at the best efficiency points of the flow rate [86]. Pumps with single volute designs commonly experience this effect. However, the effect is less in pumps with double volute designs, and rare in pumps having diffuser designs. The quantity of radial thrust in a system also depends on the geometry of a volute.

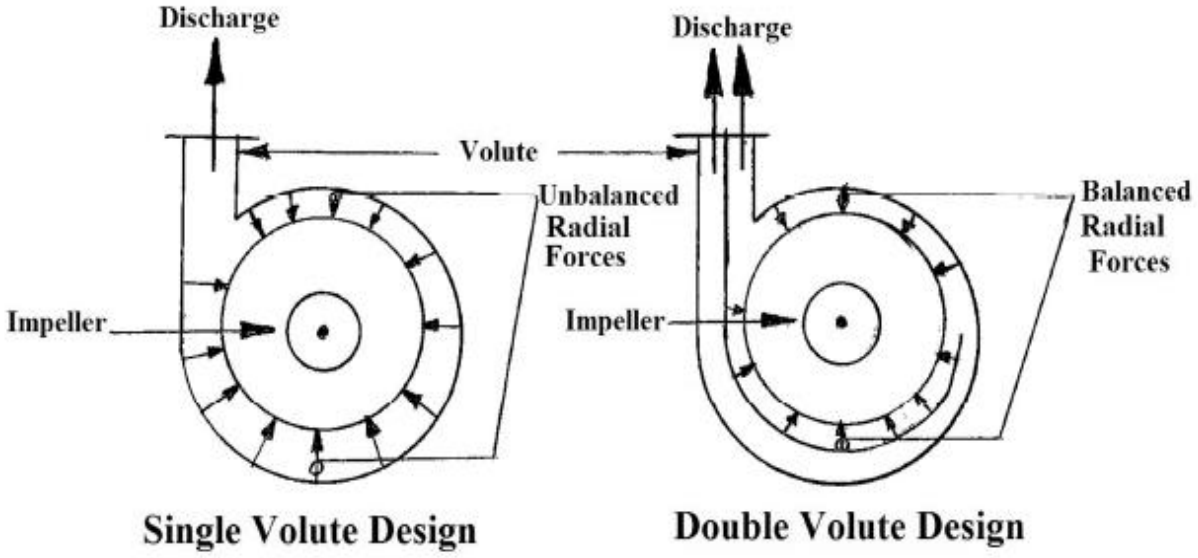

Figure 3-2 Single volute and double volute [72].

3.4.1.7 Axial Thrust

Axial thrust is exerted along the shaft axis in the outboard or onboard direction. The impeller back shroud and casing cover, casing as well as the impeller front shroud are usually filled with fluid on high pressure. The impeller shrouds are subjected to high pressure. Since the back shroud has a large surface area as compared to the front shroud, the net thrust is imposed to the impeller in a direction that is opposite to the one of the incoming flow as presented in Figure 3-3 . Also, the force resulting from change in the velocity of the incoming flow is taken into consideration [72].The axial thrust occurs due to a dynamic cyclic element that is superimposed in a stable state load from either directions. When the dynamic load on a shaft increases, it may exert excessive stress, which ultimately results to metal fatigue. The static, stable-state load is likely to impose more load on the bearings. This may raise the temperate to unacceptable levels, thus shortening the life of the bearings. Most of the thrust bearing failures are as a result of

fatigue failures because of dynamic cyclic-axial load experienced on the components of the bearing [86].

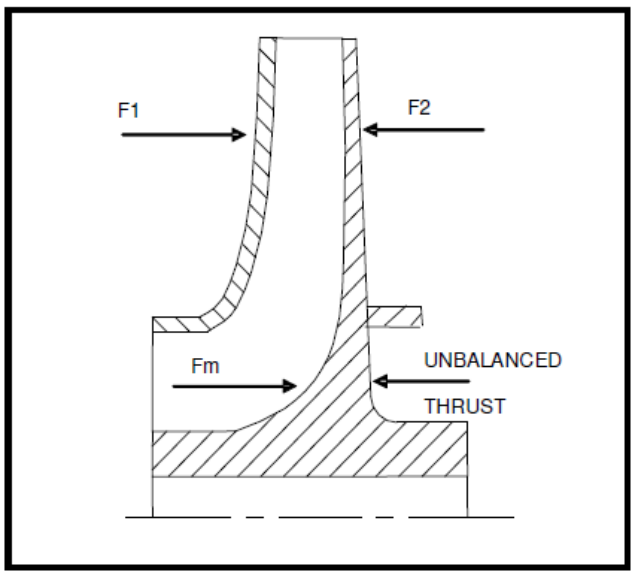

Figure 3-3 Axial thrust components [72].

3.5 Vibration based on Fluid Dynamics

In centrifugal pumps, certain amount of vibration and noise is expected due to dynamic forces of mechanical and hydraulic. There are many mechanical and hydraulic problems which causes vibration in centrifugal pumps. Major mechanical problems are mechanical unbalance, component run-out and bent shaft where main hydraulic problems are excitation due to cavitation, hydraulic unbalance and blade passage forces [87]. Hydraulic instability also sometimes effected from recirculation phenomena, where the liquid travels and recirculates between the casing channel and impeller blade in order to strike the impeller blade may times before final discharge, therefore recirculation must be considered as it can be much more critical than cavitation. Most of the fluid gets circulated but some quantity after striking the diffuser/casing moves back and collides with the incoming blade discharge. This causes pressure fluctuations and hence a wave of pressure pulse is generated as a result, inducing noise and vibration in the pump [88]. The dimensions of the cavity that affect the clearances between housing and the impellers are important factors in the development and level of the vibration, where the major concern in pumps is the cavitation. Cavitation results from the rapid implosion of the vapour bubble formed in low pressure zones as they are transmitted to high pressure regions of the pump causing hydraulic instability.

3.5.1 Description of the Hydraulic Vibration in Centrifugal Pumps

The vibration of hydrodynamic nature is related to features of the fluid flow in the working cavity of a pump. The non-stationary interaction of the pump casing with flow leaving the impeller gives rise to churning (vortex-type flow generation), consisting of small-scale turbulence and large-scale rotational structures (backward flows). In addition, cavitation can develop in the working cavity of the pump. These oscillations can be especially when they coincide with the structural components' resonance frequencies. Describing a pump with bladed diffuser as a rigid body, one can assume that vibration at blade-passing frequencies (BPF) acts as a transfer of non-stationary loads to the pump casing through the diffuser vanes [89].

The pressure pulsation generated in a working pump cavity is closely related to its vibration and its vibration and noise level, due to a current trend in increasing rotation speed and power; it can be subdivided to non-stationary hydrodynamic phenomenon in the pump's working cavity as delineated below:

3.5.1.1 The hydrodynamic interactions between a volute casing and impeller flow

Hydrodynamics, which literally means 'water motion', is the science of forces acting on or exerted by fluids, including piping, and to spread to the whole system, at the same time to generate vibration. In addition, hydraulic pump leakage and pump hysteresis are also important factors of vibration.

3.5.1.2 Vortex flow

Due to high flow velocity, the liquid flow will be in the turbulent state and generates a local eddy when flow cross section mutation. While turbulent flow and vortex appear, fluid particle motion, mutual impact, and interaction with the pump, pipeline, valve body wall or other interactions will produce vibration [85].

3.6 Vibration, Noise and Pressure Pulsation Spectra

The noise, vibration as well as pressure pulsation spectra for centrifugal pumps are characterized by broadband noise onto which clearly distinct components can be superimposed (commonly, blade passing frequencies). The level of tone elements determines the pump's noise as well as the vibrations characteristics. Moreover, if there is coincidence with resonance of a pump's working cavity, the oscillations are very harmful. The final phenomena is possible for complex high speed pumps [89].

- Small scale vortices produce turbulent noise. The noise provides of low-intensity broadband components in a frequency range of spectra of noise, pulsation, as well as vibration.
- Large scale vortices generate higher levels of the related pressure impulses. In the spectra of noise, vibration as well as pressure pulsation, this is demonstrated as an increase of the components of broadband in areas of medium and low frequencies also known as the pedestal.

In a pump, vibration is caused by the interaction between the rotating pump impeller and the stationary parts of the pump such as the volute and the diffuser vanes. Also, vibration is caused by the interaction between the impeller vanes and the fluid being pumped. The hydraulic part of the centrifugal pump consists of the inlet and outlet of the pump, and the impeller and the diffuser inside the pump. The impeller is the rotating part of the pump, which induces a rotational speed into the liquid. This speed is transformed into a static pressure in the diffuser and volute.

3.6.1 Vane Passing Frequency

Similar to the definition of the gear mesh frequency, which entails the rate with which the gear teeth combine together inside a gearbox, as well as equivalent to number of teeth time of the gear's rotational velocity. The impeller mesh frequency calculated via Equation (3-1)

$$f_{vp} = N_{vp} \times f_r \tag{3-1}$$

where, f_{vp} impeller mesh frequency, N_{vp} is number of vane in impeller, and f_r is rotational frequency of impeller in Hertz.

Hydraulic forces generate significant amount of vibrations in the centrifugal pumps [90]. Hydraulic forces are generated from pulsations as a result of flow interactions with flow turbulences, impeller vanes, hydraulic instability and cavitation. The separation of non-stationary pump processes is conditional on three types. Therefore, the formation of curls and cavitation in vane channels of the impeller strengthens the pitch non-uniformity of flow and promotes amplification of BPF pulsation. The recirculation of flow on the impeller outlet also strengthens the unsteadiness of the first type; because it is known that the same design measures reduce BPF pressure pulsation and recirculation of the flow at the impeller outlet. Flow separation and cavitation in pump casing can be in turn periodically initiated by the passage of impeller vanes [91].

3.6.2 Interaction between Impeller Flow and Volute Casing

Centrifugal pumps transmit fluids through conversion of kinetic energy into hydrodynamic energy of fluid flow. Once the fluid gets into the pump impeller near or along the rotating axis, it is accelerated and flows outwardly into a volute chamber or the diffuser and it exits. Since the fluid flow interacts with the impeller vanes as well as stationary volute chambers, the fluid's pressure pulsates largely with the impeller's structure. Particularly, the rate of pulsation will be related with the vane number. This characteristic frequency is also referred to as the vane-passing frequency equation Equation (3-2) shown below.

$$f_{vp} = k z f_r \tag{3-2}$$

where z represents the vane number and k represents the harmonics number. Also, when the centrifugal pump runs at the best efficiency point (BEP), the amplitude of pressure pulsation is maintained at a minimum. At this point, the flow velocity equals the vane angle, making the flow to have less interaction with the impeller. On the other hand, any BEP operations will result in a disparity between the angles of fluid velocity and the vane angle of the impeller. As a result, more pressure and vibrations will be experienced. Using these characteristics, appropriate features can be established to facilitate fault diagnosis of the impeller.

3.6.3 Flow Turbulence

Another inevitable phenomenon that occurs in centrifugal pumps is flow turbulence. Flow turbulence induces vortices. It also wakes the clearance spaces between the pump impeller vane tips and the volute lips or diffuser. This in turn generates pulsations or pressure fluctuations

resulting to vibration. The frequency of vibrations induced due to turbulence can be predicated using the Equation (3-3) below.

$$f_w = S_n V / D \tag{3-3}$$

whereby, v denotes the turbulence flow's velocity, s represents a non-dimensional Strouhl number whose values range between 0.2 and 0.5. Finally, D represents the characteristic obstruction dimension. Since the flow velocities are different, this form of pulsation can generate vibrations with higher frequencies. Also, the circulation flows near the discharge tip or suction of the vane impeller generates substantial turbulences. Vortices are created due to high velocity flows. As the vortices collapse, they produce noise as well as cavitation on the discharge and suction of the pump. Operating the centrifugal pump at low flow rates trigger recirculation in the impeller. This makes it to surge when the natural frequency of a system is reached [92].

3.7 Summary

This chapter has discussed a centrifugal pump vibration, including an overview of mechanical and hydraulic vibration sources. Along with pump fluid dynamic responses. It is explained a description of the hydraulic vibration and pressure pulsation in centrifugal pump. In addition, understanding the mechanical and hydraulic common faults which explored in association their causes and effects. Therefore, the following chapter will be reveal signal processing techniques overview.

CHAPTER FOUR

SIGNAL PROCESSING TECHNIQUES

This chapter presents an overview of the methods of centrifugal pump vibration analysis and vibration measurement techniques that are applied for condition monitoring (CM) as well as defect detection of the pump. Moreover, the chapter explores the techniques for centrifugal pumps such as HOSA (Higher Order Spectra Analysis) measures (spectra) which are typically an extension of 2nd order measures (i.e. power spectrum) to higher orders. Finally, the chapter presents the frequency and time domain techniques.

4.1 INTRODACTION

Vibration based condition monitoring uses of non-destructive sensing and analysis of system characteristics in the time, frequency or modal domains to detect changes, which may indicate damage or degradation. Vibration monitoring is one of the most commonly used condition monitoring techniques. It picks up the vibration signals generated by machines and analyses these signals to determine the condition of the machine [9].

Through vibration analysis, the maintenance department is able to receive signals pointing out to a specific fault within the system like misalignment, unbalance, as well as mechanical looseness of various rotating components. Moreover, condition monitoring detects the other process and condition parameters such as temperature loads in order to get a clear picture on how the entire system runs. The basic principle behind vibration-induced damage detection techniques is that any fault or damage may greatly affect the mass, stiffness or energy dissipation properties for the system. This may in turn affect the systems' measured dynamic response. Although vibration-based fault detection techniques seem intuitive, their actual use poses a number of significant challenges. One of the most significant challenge is that damage is a local phenomenon, thus it may not significantly affect the low frequency global response of the various structures that are usually measured using the vibration tests. In addition, this challenge is complemented with various practical issues related with making repeatable and accurate vibration measurements at few locations on structures that often open in different settings [10].

Mechanical vibrations are caused by various factors including looseness and distortion, critical speeds, misalignment, bad drive belts, unbalance, coupling and gearing inaccuracies, defective bearings, different forms of resonance, hydrodynamic or aerodynamic forces, reciprocating forces, friction whirl, oil whirl, bent rotor shafts, stator or rotor misalignments, defective rotor bars, among many more. Vibration analysis can detect most of these common faults [12].

A Davies. [93] Asserts that vibration analysis can contribute significantly to the demand of improving uptime on the machinery. The author states also that constant record data is considered so significant since it ensures that the machinery is kept operating in good working conditions. Many techniques are applied to record and process vibration signals of rotating machine faults detection and diagnosis, the most popular ones include frequency-domain and time-domain.

4.1.1 Time-Domain Analysis

Time-domain analysis entails an analysis or display of vibration data signal as a function of time as it is presented in Figure 4-1. One of the key advantages of this format is that no or little data gets lost before inspection. As a result, it is easy to conduct a detailed analysis using the data obtained. However, the format also has its own disadvantages. The format presents too much data for clear and easy diagnosis of faults. The time domain analysis for the vibration signals can be classified to various categories including time-waveform indices, negative averaging, time-synchronous averaging, time-waveform analysis, orbits as well as probability density moment [94].

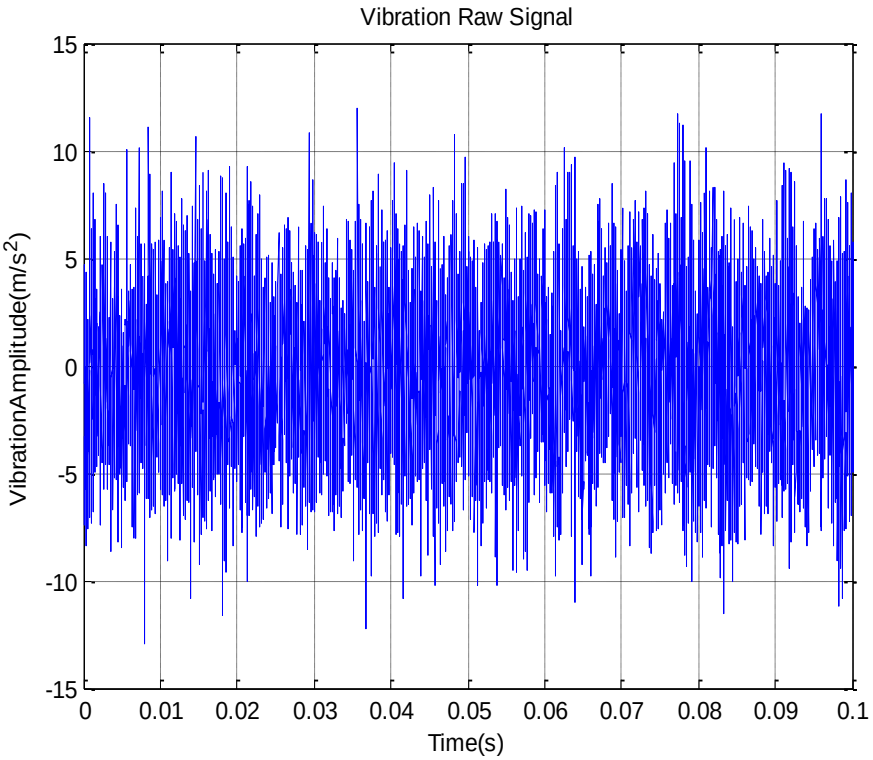

Figure 4-1 Raw data in the time domain

4.1.1.1 Peak Value (PV)

Peak value refers to the signal's highest value. Also, it is the maximum amplitude reached by a signal, and it can either be positive or negative as presented below in in Figure 4-2.

$$Peak = E(\max[x(t)]) \tag{4-1}$$

Where x (t) is random vibration signal and E represents the expected value.

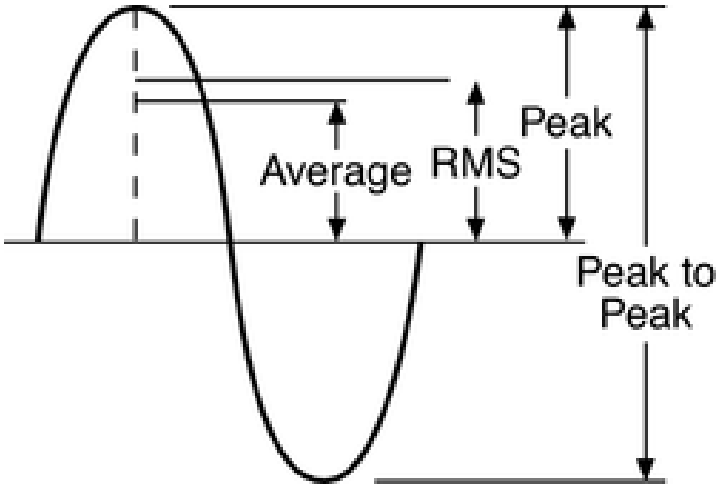

Figure 4-2 RMS, peak and peak to peak

4.1.1.2 Root Mean Square (RMS)

Root mean square refers to time–analysis features of vibration signals. Also, RMS refers to measure of the vibration signals' power content. Moreover, the RMS feature can be applied to detect noise. However, the data generated form RMS cannot be sufficient enough to give accurate information to identify the fault component. RMS can be applied for fault detection, especially the imbalances in the rotating components. The RMS values of data series (x_n over the length N) can be calculated using the equation presented in Figure 4-2

$$RMS = \sqrt{\frac{1}{N}\sum_{i}^{N} = 1(\chi_i)^2} \tag{4-2}$$

where, N represents total number of the samples and *xi* represents the time signal.

In time-domain analysis, the most common technique for defect detection is RMS approach. There is a likelihood of a fault within the system if the root mean square signal exceeds or increases suddenly to a set value, however it is not sensitive enough at detecting incipient faults in particular [95].

4.1.1.3 Crest Factor (CF)

Crest factor refers to the ratio of a waveform's peak value to the Root Mean Square (RMS) for a whole revolution. Moreover, it refers to the ratio between maximum absolute value attained by a signal in period of time to the signal's RMS value as shown in Figure 4-3 presented blow.

$$C_f = \frac{peak.value}{RMS.value} \tag{4-3}$$

The values of the signal's crest factor whose amplitude Gaussian ranges from 3 to 6 [95].

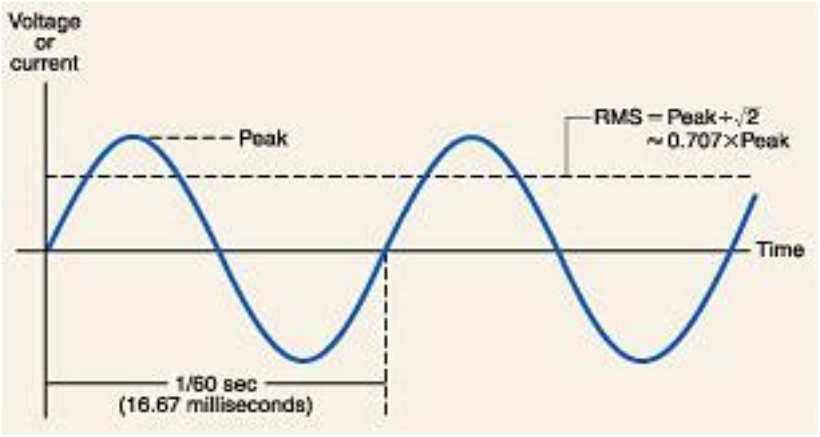

Figure 4-3 Peak and RMS [96].

4.1.1.4 Kurtosis (K)

Kurtosis refers to the fourth order statistic moments of a distribution. The relative flatness or peakedness of the distribution to that of a normal distribution indicates the existence of the major peaks of a data set [97]

$$K = \frac{\sum_{i=1}^{N}(x_i - \bar{x})^4}{N\sigma^4} \tag{4-4}$$

Kurtosis refers to the parameter that is sensitive to the signal's shape. It is adapted well to the nature of impulse of simulating forces produced by the damaged component. Signals with high kurtosis appears to have peaks exceeding 3 and this indicate a faulty component. These peaks record a value thrice to the signal's RMS value [98].

Based on distribution, kurtosis can be subdivided into three various categories as presented in Figure 4-4

- Mesokurtic: The Normal Distribution
- Platyurtic - has lighter trails and lower peaks compared to a normal
- Lepotokurtic: has heavier trails and higher peaks compared to the normal distribution

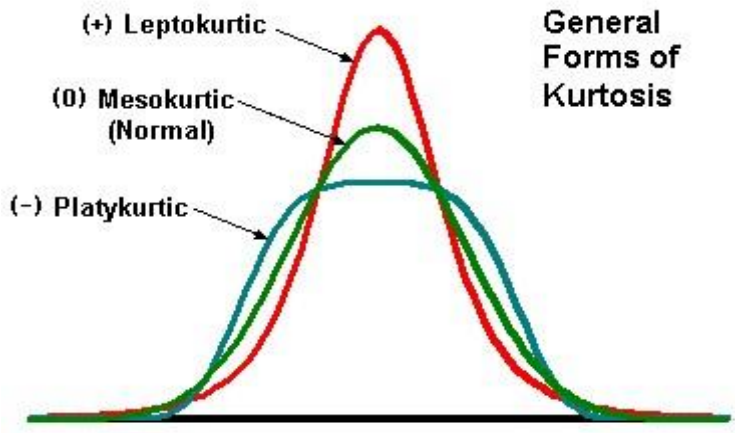

Figure 4-4 General forms of kurtosis [99]

4.1.1.5 Time Synchronous Averaging (TSA)

The time synchronous averaging technique is regarded as a powerful tool for the detection and diagnosis of epicyclic gear faults, and is sometimes referred to first-order cyclostationarity analysis. In vibration cyclostationarity analysis, TSA can potentially extract a deterministic signal and enhance the synchronous vibration components related to the frequency of interest (the reference frequency), while reducing non-synchronous components and noise. It has been shown that TSA is well suited to gearbox analysis, where it can isolate and separate a vibration signal generated by a specific gear from other vibration sources such as bearings. Damage can often be detected in its early stages by direct inspection of the time-averaged data. Generally speaking, rotating machines are characterized by cyclical phenomena directly related to the speed, which explains why cyclostationary analysis is particularly suitable for diagnosing these machines. However, in a practical environment, the shaft speed varies slightly with each cycle during normal operation. This variation will result in a smearing of amplitude energy in the frequency domain. To reduce the effect of smearing and to reinforce cyclostationarity, it is very important to resample the time domain signal into the angular domain [100].

4.1.2 Frequency-Domain Analysis

Frequency domain is an analysis or display of signal vibration data presented as function of frequency. Time- domain vibration signals are processed into frequency-domains by using a Fourier transform. The Fourier transform is typically in form of an FFT (Fast Fourier

Transform) algorithm. This key advantage of this technique is the repetitive nature of vibration signals which are easily and clearly exhibited as peaks within the frequency spectra at which the repetitive frequencies occur. This promotes faults, which typically produce certain characteristic frequency responses, which can be detected earlier, accurately diagnosed, as well as trended with time as the condition worsens. However, one of the disadvantages of frequency domain analysis is the substantial amount of data (transients and non-repetitive signal elements) is likely to be lost during the process of transformation. Unless a permanent record of raw vibration signals is made, this data remains non-retrievable. Some of the various techniques of frequency-domain vibrations signatures analyses include band pass analysis, enveloped spectrum, spike energy (shock pulse), signature spectrum, as well as waterfall plots (cascades) [94].

One of the most common technique of getting frequency-domain signals is by employing a digital fast Fourier analysis in respect to the waveform. By use of a signature spectrum, significant information can be obtained in regard to the machine's conditions. The signals to be analysed are presented in Figure 4-5. The original signal distribution in the frequency-domain analysis is described and offers significant information which is clearer as compared to the time domain.

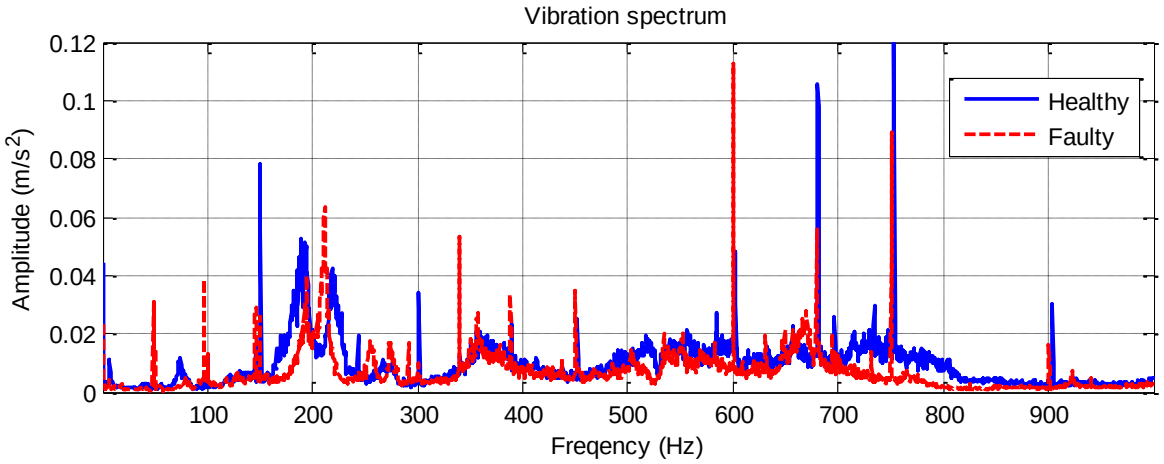

Figure 4-5 Raw data for frequency spectrum

4.1.2.1 Fast Fourier Transform (FFT)

Waveforms of a function or a signal can be broken down into an alternate representation characterised by sine and cosines using the Fourier transfer tool as presented in Figure 4-6.

This analysing method is able to show that any waveform can be re-written as the sum on the sinusoidal functions [101].

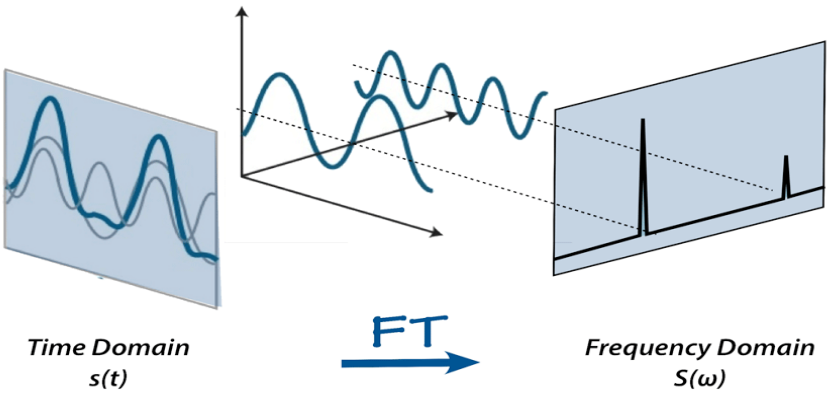

Figure 4-6 Relation between time and frequency domains [102]

4.1.2.2 Sideband Characteristics (SC)

It is very significant to analyse the sideband phenomenon of a machine. Also, sidebands are caused by amplitude modulations between two signals. Sidebands exist in machines with gearbox, rolling component bearings as well as other faulty conditions. One can recognize sidebands by examining carefully by examining the evenly spaced peaks within the spectrum (frequency-domain), which is centred on a single peak. The centre peak is referred to as a carrier frequency. Also, sidebands represent modulation frequency [103].

4.1.2.3 Envelope Analysis

Another suitable technique to diagnose machinery is envelope analysis. In envelope analysis, the faults have amplitude modulation effects on the machinery's characteristic frequencies [104]. With this algorithm, the modulating signal's power spectrum can be calculated and the implementation steps are presented in Figure 4-7 presented blow:

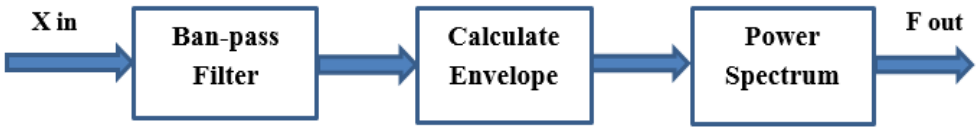

Figure 4-7 Procedures of envelope analysis

On the first step, use a band-pass filter to remove any low-frequency contents within high amplitude signals because of misalignment or imbalance as well as high-frequency noises from the system. This enable a good noise-to-signal ratio to be attained [104]. Also, in order to filter

vibration signals, 80 order finite impulse response band pass filter that has a pass-band of between 1000 and 2000 Hz should be used.

Second, the envelope of signal is calculated using the Hilbert transformation (HT). In such a case, the signal calculated can be regarded as a complex signal with the real part [105]. Equations (4-5), (4-6) and (4-7) demonstrate the procedures used in computing the Hilbert transformation. The real part of an analytical signal, x_a for the x_{in} entails original data x_{in}, while the imaginary part entails Hilbert transformation for x_{in}. It is also linked to an original signal by an angle of 90^o phase shift. Vibration signal's envelope is expressed by the Equation (4-8) shown below. The Equation (4-9) demonstrates the envelope's amplitude spectrum. Using the algorithm of Hilbert transformation, the computed data can be re-used and this is very critical for a processor that has limited storage.

$$\mathrm{X} = fft(\chi_{in}) \tag{4-5}$$

$$\mathrm{X}_a(n) = \begin{cases} x(n) & n = 0, \frac{N}{2} \\ 2 * \mathrm{X}(n), & 1 < \mathrm{n} < \mathrm{N}/2 - 1 \\ 0 & \mathrm{N}/2 + 1 < \mathrm{n} < \mathrm{N} - 1 \end{cases} \tag{4-6}$$

$$\chi_a = ifft(\chi_h) \tag{4-7}$$

$$(\chi_{env} = \sqrt{\chi_a * conj(\chi_a)} \tag{4-8}$$

$$\mathrm{X}_{env} = \left| fft(\chi_{env}) \right| \tag{4-9}$$

where x_{in} represents the signal of the vibration; X_a represents FFT of the analytic signal ofx_{in}; X represents FFT forx_{in}; $\mathrm{x}_a$represents an analytic signal ofx_{in}; X_{env} represents the envelope spectrum and x_{env} represents an analysed envelope signal. Envelope detection technique uses the high amplitudes existing in the defect signals of specific frequency bands, to realize the high signal-to-noise ratio present in low frequency noise from the mechanical system. Thus, envelope spectrum can generate clear peaks in the characteristic defect frequencies' harmonics.

4.1.2.4 Short-Time Fourier Transform (STFT)

The Fourier transform does not provide simultaneous frequency and time localisation. Fourier transform cannot be considered the most suitable technique of analysing time varying and non-stationary signals. To address this problem, a short-time Fourier transform (STFT) is applied [106].

The short-time Fourier transform (STFT) refers to a signal processing method which analyses non-stationary signals whose static properties vary with time. As a window moves over time, the STFT records a number of signal frames which are analysed as presented in Figure 4-8. Each frame can have been seen as stationary provided that the time window is adequately narrow. In this case a Fourier transform can be used. As the window is moved along the axis, it allows the correlation between time and variance of frequency to be established [107].

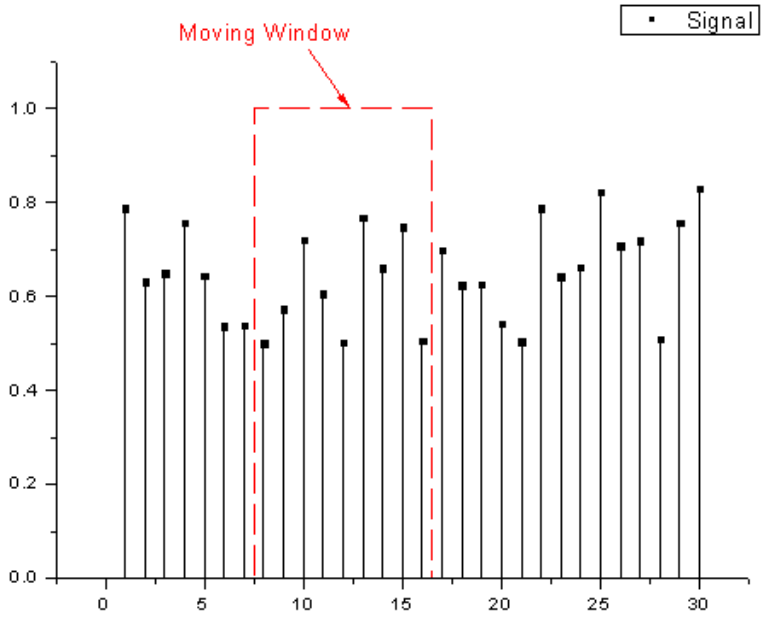

Figure 4-8 STFT showing moving window

4.1.2.5 Wavelet Transforms (WT)

The theory of Wavelet Transform (WT) is based on signal analysis by the use of varying scales in time of the frequency domain. The traditional Fourier analysis has challenges with high frequency and non-periodic oscillations since it assumes the periodical signals. In low frequencies, the wide-band signals require longer time periods and denser sampling in order to maintain a good resolution. Since it has a higher ability to derive information simultaneously

from the transient signals in both frequency domain and time, it is more preferred in many applications compared to the Fourier analysis [108].

Wavelet transforms permits variable window sizes when analysing various frequency elements in the signal. On the other hand, STFT has a fixed window size. This can be demonstrated by comparing a signal with various template functions acquired from shift and scaling of the base wavelet $\varphi(t)$ as well as analysing their similarities as presented on figure Figure 4-9 [109].

Using the notation as inner product, the wavelet transform of a signal $x(t)$ can be shown as Equation (4-10) [109]:

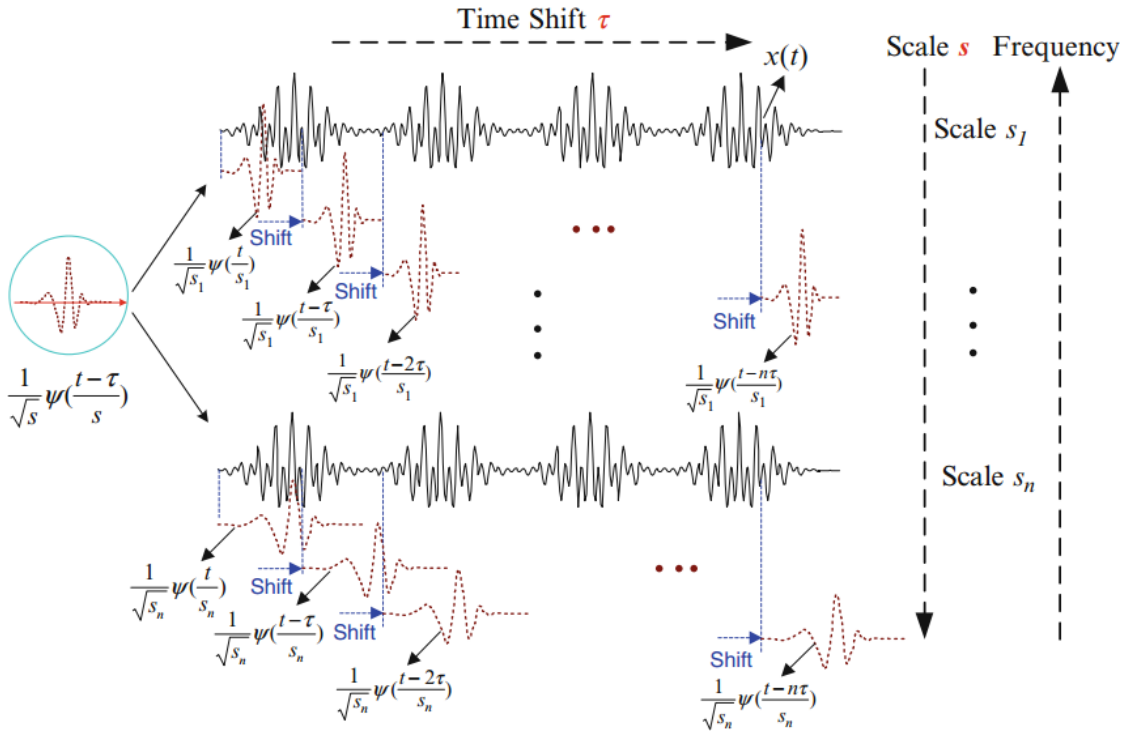

Figure 4-9 Illustration of wavelet transform [110].

$$wt(S,\tau) = x, \varphi_{S,\tau} \geq \frac{1}{\sqrt{S}} \int_{-\infty}^{\infty} x(t)\varphi \times \left(\frac{1-\tau}{s}\right) dt \qquad (4\text{-}10)$$

where the symbol $s > 0$ represents the scaling parameter, which determines the time and frequency resoloutions of the scaled base wavelet $\varphi \times \left(\frac{1-\tau}{s}\right)$. The shifting parameter is τ, this translates the scaled wavelet along the time axis. The complex conjugation of the base wavelet $\varphi(t)$ is denoted by $\varphi \times (.)$. The Figure 4-10 below shows the time and frequency resolutions of the wavelet transform ($s_2=2s_1$)[109, 110]:

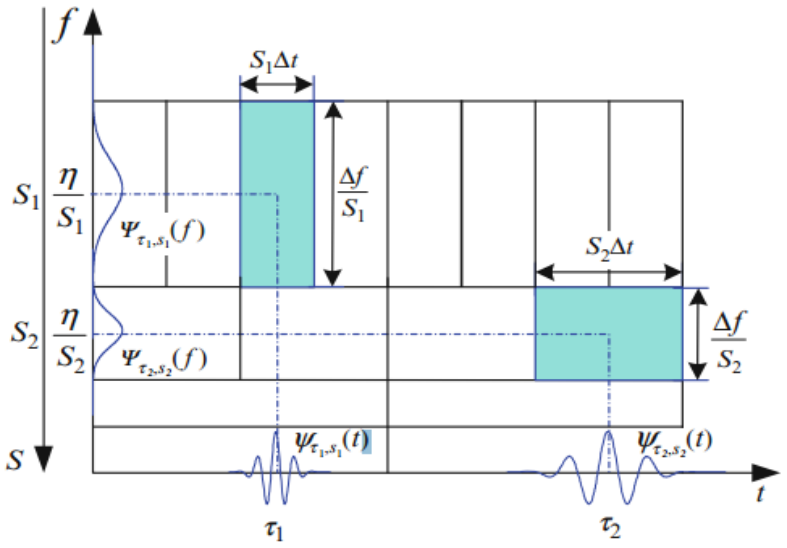

Figure 4-10 Time and frequency resolutions of the wavelet transform [110].

4.1.3 The Kurtogram

In spectral kurtosis, the optimal filter obtained from this process critically depends on the STFT window length selected or the band-width of band pass filter which output a complex envelope X (t, f). In order to address this challenge, spectral kurtosis as a function of a latter parameter, therefore generating a 2-dimensional representation referred to as ‘‘Kurtogram’’[111].

Spectral kurtosis is an advanced version of the kurtosis concept. It is of high significance to that of the frequency’s function, which shows how an impulsive signal is spread in a frequency domain. This principle is analogous in various respects to PSD that decomposes the signal’s power verses the frequency, provided that 4th order statistics are applied instead of the 2nd order statistics. This renders spectral kurtosis a popular technique of detecting transients within the signals even if they are in very strong addictive noises, by typically indicating the frequency bands in which they occurred [98].

Spectral kurtosis of the signal c (t) can be computed using the STFT X (t, f), which is a local Fourier transform over time, t.

This might be easy detected by computing the kurtosis of the complex envelope X (t,f) as follows Equation (4-11):

$$k(f)=\frac{\left\langle |X(tf)|^4 \right\rangle}{\left\langle |X(tf)|^2 \right\rangle^2}-2 \qquad (4\text{-}11)$$

As the time-averaging operator and where $K(f)=0$ is enforced by subtracting with 2 (instead of using 3 for the real signals) in the case of $X(t, f)$ which is *complex* Gaussian. Then, the equation for the Kurtogram of the signal which is centred on STFT is shown in Equation (4-12), [112].

$$K_y(f) = \frac{K_x(f)}{[1+p(f)]^2} \tag{4-12}$$

where $K_x(f)$ is the spectral kurtosis of $x(t)$ and $p(f) = S_n(f)/S_x(f)$ the noise-to-signal ratio. This suggests that the optimal filter that maximises the similarity between the filtered component and the true noise-free signal. The Wiener filter is the square root of the spectral kurtosis [98].

4.1.4 Fast-Kurtogram (FK)

The calculation of Kurtogram for various combinations of band widths and centre frequencies is both costly and inconvenient for practical purposes. However, sub-optimal solutions are applicable by subdividing the band widths into more rational ratios that allow the application of a fast multi-rate processing technique. In this respect, the simplest division is the dyadic one. It allows band widths to be iteratively halved right the largest bandwidth that covers the entire signal spectrum equivalent to a one sample window length as used in the computation of the convention al kurtosis.

Spectral kurtosis' possible window widths which are based on STFT are required to be tested by the kurtogram in order to accurately generate the proper band width and central frequency which is expensive to compute. Thus, Antoni in [68] came up with a fast kurtogram in order to quickly calculate and comprehend the outcomes of spectral kurtosis depending on the quasi-analytic filters and multi-rate filter bank structures [113].

Kurtogram is considered a practical and powerful tool in the diagnosis of machinery faults owing to its superiority in detecting as well as characterizing transients in the signals. FIR filters or short time Fourier transform-based kurtogram, however, minimizes kurtogram's accuracy improvements in detecting the transient characteristics of noisy signals as well as identifying the machinery faults. Therefore, there is need to develop more precise filters and incorporate them to the kurtogram technique in order to address its challenges and also improve on its accuracy of identifying characteristics and detecting the machinery faults.

In respect to this concept, Figure 4-11 demonstrates the steps followed in computing the largest bandwidths, which covers the entire spectra and stops at narrow bandwidth that considers independent time samples, $X(t,f)$ in order to compute the time averages as presented in Equation (4-11). The equation has been simplified based on 'a 1/3 binary-tree' and each halved bandwidth is subdivided into three more other bandwidths. This generates frequency resolutions in the following sequence 1/2, 1/3, 1/4, 1/6, 1/8, 1/12…, 2^{-k-1} and they all correspond to scale levels of k= 0, 1, 1.6, 2, 2.6,… [98]. In Figure 4-11 can be note the difficulty to choosing the step and the limits of the window lengths. The kurtogram overcomes this problem by proposing to decompose the signal into several frequency bands in several levels based on an arborescent multirate filter-bank structure. The solution is an even decomposition based on a 1/3-binary tree [68].

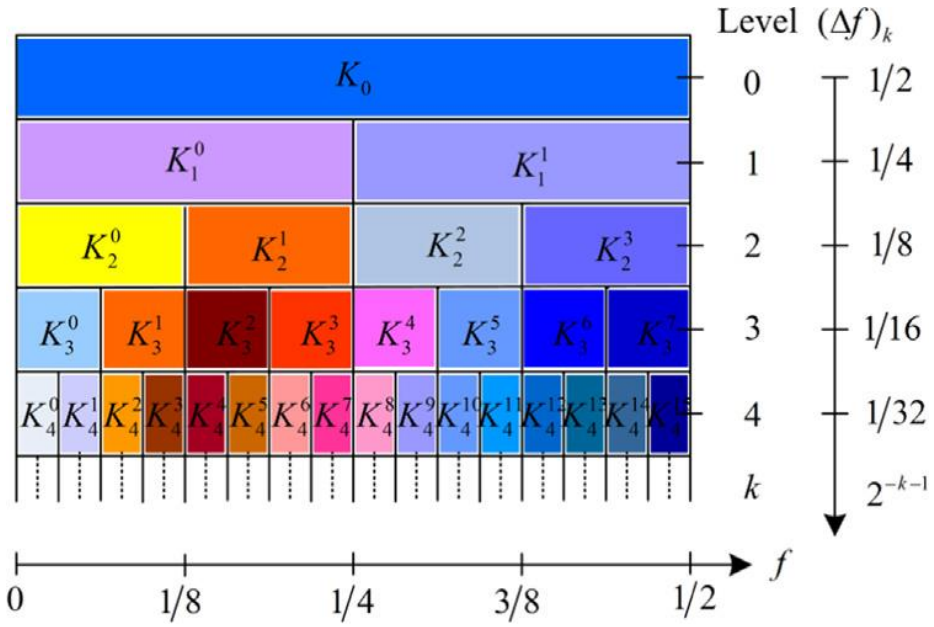

Figure 4-11 Centre frequency and Bandwidth for 1/3binary- tree Kurtogram [98].

4.1.5 Higher Order Spectra Analysis (HOSA)

Both the first as well as the second-order statistics (i.e. power spectrum, variance, mean, and autocorrelation) are considered common signal processing tools. They are extensively used to analyse processed data. However, second order statistics are commonly preferred in describing Gaussian and linear processes. It is quite unfortunate since in real life situations, various processes being explored are neither Gaussian nor linear but they display non-linear behaviours [114]. Most of these processes can only be explored using the Higher Order Statistics Analysis (HOSA) technique [115]. There is various situation in real life when these processes deviate from linearity and Gaussisnity, for instance, when they display non-linear bahaviours. In such

cases, High Order Statistic (HOS) can be applied to explore them. The three major reasons of using HOS include, extracting information because of deviations from linearity or Gaussianity, recovering a signal's true phase character, and detecting and quantifying any nonlinearities in the time series [114].

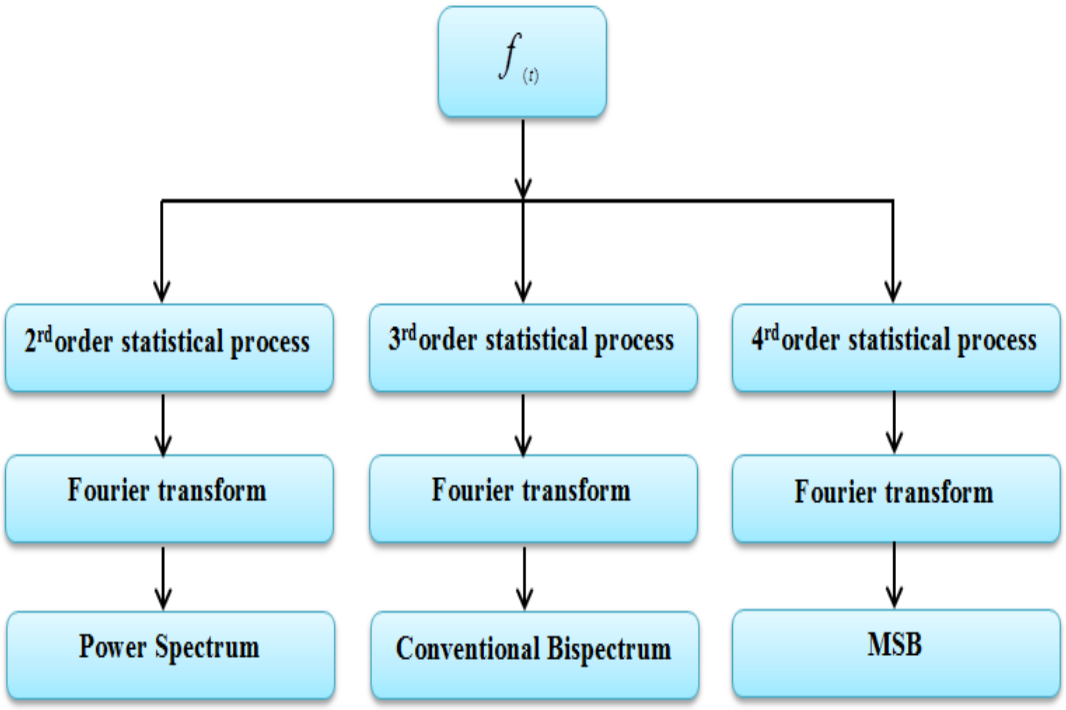

Figure 4-12 Classification of higher order spectra

4.1.5.1 Power Spectrum

The power spectrum of a time domain signal $x(t)$ is calculated by the discrete Fourier transform (DFT) of the signal as follows;

$$s_{xx}(f_k) = E[X(f_k)X^*(f_k)] \quad , \qquad k = 1,2,3, \qquad N \qquad (4\text{-}13)$$

where $S_{xx}(f_k)$ represents power density; N represents the total number of the frequency points $X(f_k)$ and $X^*(f_k)$ represent DFT and its extensive conjugate at the frequency (f_k) for time domain signal, $x(t)$ considered respectively, and $E($ mathematical operator) represents the mean. Also, the power spectrum computes the harmonic power in real-valued or discrete-time sequences. Power spectrum entails a representation of non-occurrences or occurrences of the recurring as well as correlated patterns in a signal. These patterns displayed by the power spectrum may be utilized in fault detection, signal detection, pattern recognition as well as data forecasting [116].

4.1.5.2 Conventional Bispectrum

Most of the researchers have been using the bispectrum analysis since the 1980s. Bispectrum is a high order spectrum [117]. In a practical setting, the detected signals have low signal-to-noise ratio and they may not be stable. Fourier transform as an analysis tool assumes that signal generated from vibrations are stationery. This traditional correlation approach and spectral analysis technique is unable to collect sufficient information from non-linear and non-stable signals. Under such circumstances, bispectrum analysis is considered effective since it is able to record characteristic frequencies, capture phasic information as well as express the non-linear advantages [117].

When given a discrete time signal $x(n)$, its discrete Fourier transform (DFT0) can be defined as:

$$\mathrm{X}(f) = \sum_{k=-\infty}^{\infty} x(n) e^{-j2\pi fn} \tag{4-14}$$

The conventional bispectrum can be defined as[118]**:**

$$B\left(f_1, f\right) = E\left\{\mathrm{X}\left(f_1\right)\mathrm{X}\left(f_2\right)\mathrm{X}\times\left(f_1 + f_2\right\}\right. \tag{4-15}$$

f_1, f_2 and $f_1 + f_2$ specify the separate frequency components achieved from Fourier series integral. Expression of the bispectrum $X(f)$ displayed decomposes the signal's skewness in a frequency domain. As a result, bispectrum of the zero mesan Gauss signals equal to zero. This theory then allows the bispectrum to entirely restrain any noise and capture only crucial information that is needed [117].

4.1.5.3 Modulation Signal Bispectrum

The third-order cumulant's bispectrum Fourier transform refers to a statistic approach used to detect non-linear interactions or minimize Gaussian noise. However, modulation signals cannot be adequately described using the conventional bispectrum. To address this challenge, the MSB was introduced [119, 120]. This technique considers a constant phase between both sidebands of the modulated signals as presented in Equation (4-16):

$$B_{MS}(f_1, f_2) = E\left\langle X(f_2 + f_1)X(f_2 - f_1)X^*(f_2)X^*(f_2)\right\rangle \tag{4-16}$$

Where f_2 is the frequency of carrier signal and f_1 is of modulated signal, $X(f_2)$ is Fourier transform of the carrier and $X^*(f_2)$ is conjugate of $X(f_2)$. The magnitude and phase of MSB can be expressed as Equation (4-17) and (4-18).

$$A_{MS}(f_1, f_2) = E\left\langle \left| X(f_2 + f_1) \right\| X(f_2 - f_1) \left\| X^*(f_2) \right\| X^*(f_2) \right| \right\rangle \quad (4\text{-}17)$$

$$\phi_{MS}(f_1, f_2) = \phi(f_2 + f_1) + \phi(f_2 - f_1) - \left|\phi(f_2)\right| - \left|\phi(f_2)\right| \quad (4\text{-}18)$$

It takes into account both $(f_2 - f_1)$ and $(f_2 + f_1)$ simultaneously in Eq. (4-16) for measuring the nonlinear effects of modulation signals. If $(f_2 - f_1)$ and $(f_2 + f_1)$ are both due to the nonlinear effect between $(f_2 - f_1)$ and $(f_2 + f_1)$, there will be a bispectral peak at bifrequency $B_{MS}(f_1, f_2)$ [121, 122]. Whereas, if these components have a random distribution but not coupled, then MSB magnitude will be almost zero. By doing so, the wide-band noise in the vibration signals can be suppressed effectively in order to obtain discrete components accurately. A modulation bicoherence signal can be used to measure the rate of coupling among three components. The degree of coupling among three components is computed as presented in Equation (4-19).

$$b^2_{MS}(f_1, f_2) = \frac{\left|B_{MS}(f_1, f_2)\right|^2}{E\left\langle \left| X(f_2)X(f_2)X^*(f_2)X^*(f_2) \right|^2 \right\rangle E\left\langle \left| X(f_2 + f_1)X(f_2 - f_1) \right|^2 \right\rangle} \quad (4\text{-}19)$$

In addition it can be also seen that for the case of $f_1 = 0$, the power spectrum can be obtained by Equation (4-20).

$$PS(f_2) = \sqrt{B_{MS}(0, f_2)} = \sqrt{E\left\langle X(f_2)X^*(f_2)X(f_2)X^*(f_2) \right\rangle} \quad (4\text{-}20)$$

As shown in Eq. (11), the phase of power spectrum for any components is nil and thus it is not possible to suppress random noise by averaging operation.

4.1.5.4 Bispectrum Performance

It has been mentioned in that bispectrum analysis has a number of distinctive properties such as phase information preservation, non-linear system recognition and Gaussian noise elimination as compared to traditional power spectrum analysis. In particular, the bispectrum method can be used to detect quadratic phase coupling (QPC) that arises when two signals interact non-linearly with each other and produce a third signal with a frequency and phase

equal to the sum or difference of the first two signals. Moreover, the current signal is produced by a non-linear interaction between only two components: the supply frequency and the shaft speed components. So it is expected that the bispectrum can provide a more precise diagnosis of the current signal for fault conditions [122].

Moreover, MSB can eliminate all components that are not as a result of modulation effects. In the MSB, a component at 10Hz displays a small peak of about 40Hz because of the limited numerical calculation accuracy. However, since the amplitude of a MSB coherence is relatively low, one can easily identify that it is not the real modulating component.

From this simulation study, it is evident that MSB produces a more effective representation of a modulation process that enhances reliable detection as well as accurate estimation of the modulating signals.

4.2 Summary

The chapter has reviewed a signal processing fundamentals of methods which is study in depth in this thesis including envelope analysis, time domain and frequency domain. Also, the chapter explores the Kurtogram-based short time Fourier transform (STFT), and advanced signal processing approaches like the higher order spectrum analysis (HOSA) measures (spectrum) which are an extension of second order measures (e.g. power spectrum) to a higher order. Bispectrum analysis such as MSB and CB facilitates noise reduction using signal phase alignments with no need for the reference signals. Moreover, bi-spectrum promotes non-linear characterisation. Also, it allows for sparse representation of the complex signals for a more effective feature extraction. Therefore, the next chapter will be present an overview of the construction and the design process of a test-rig.

CHAPTER FIVE

DESIGN AND CONSTRUCTION OF PUMP TEST-RIG

This chapter reviews the construction and the design process of a test-rig suitable for measuring the faults that affect performance of centrifugal pumps. Also, the chapter presents a description of various equipment, components, as well as sensors applied in the development of a test-rig. The design and construction of the test-rig, a review of all test-rig configurations possible for monitoring faults in centrifugal pumps, and instruments used to collect the vibration signals. In addition, this chapter describes the procedures used to investigate the vibration signals collecting from the centrifugal pump under healthy and faulty conditions. Moreover, the equipment, experimental procedures as well as instrumentations applied to record vibration signals are explored in this section. Finally, the Matlab software was used to analyse the data which had been collected.

5.1 Motivation

The central aim of this study is to optimise new technique for detecting and diagnosing centrifugal pump faults. In addition, mainly involves the condition monitoring of centrifugal pump test system and fault detection by vibration measurements and also develop more advanced measurement and analysis systems for pump condition monitoring.

In order to achieve this objective, it was necessary to improve the previous test-rig that was available in the lab. It includes some improvements both in design and configuration which has been added to test-rig (the second tank as discharge tank also changed the plastic pipes into still pipes upgrading the date Acquisition and the pump) as presented in Figure 5-2. There were two critical factors to be considered as discussed firstly the cost of the test-rig motivation secondly the test-rig suitability.

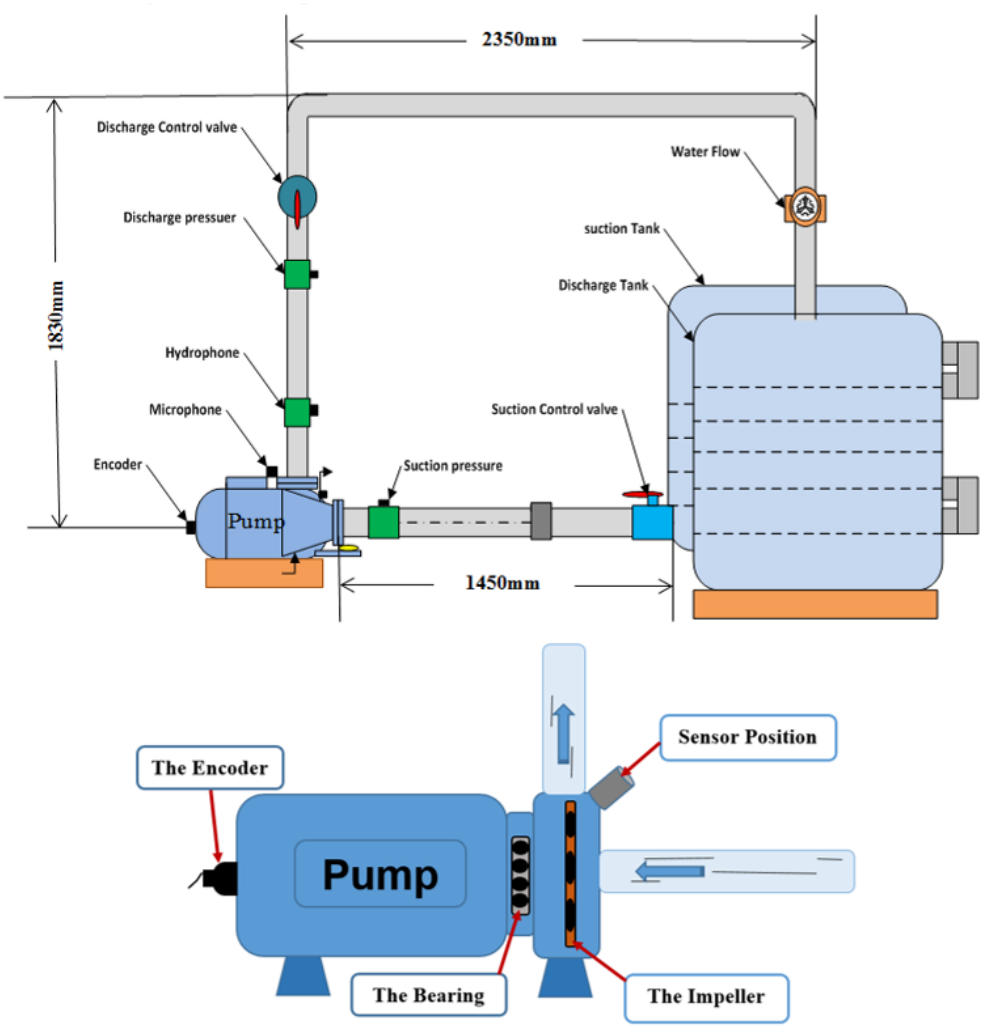

Figure 5-1 Schematic diagram of the pumping system and pump components

Figure 5-1 shows a schematic diagram of the test-rig which was used in this experiment and a photo was taken of the test-rig which can be seen in Figure 5-2. The centrifugal pump which was used in this work model was F32/200A series with a maximum pressure limit of about 10 bars. The pump can supply water to the tank. The system was re-circulatory and included a plastic water tank which was connected to the pump via steel pipes and steel components. All transducers were mounted on the test-rig as shown in Table 5-1 and Table 5-2. The pump which was used in this system is a single stage pump with a closed impeller which could deliver the water at a rate up to 450 l/min also at the head of 55 m. It is connected by a three-phase electric motor running at 2900 rpm at 9.5 A and in the 380-400 V range.

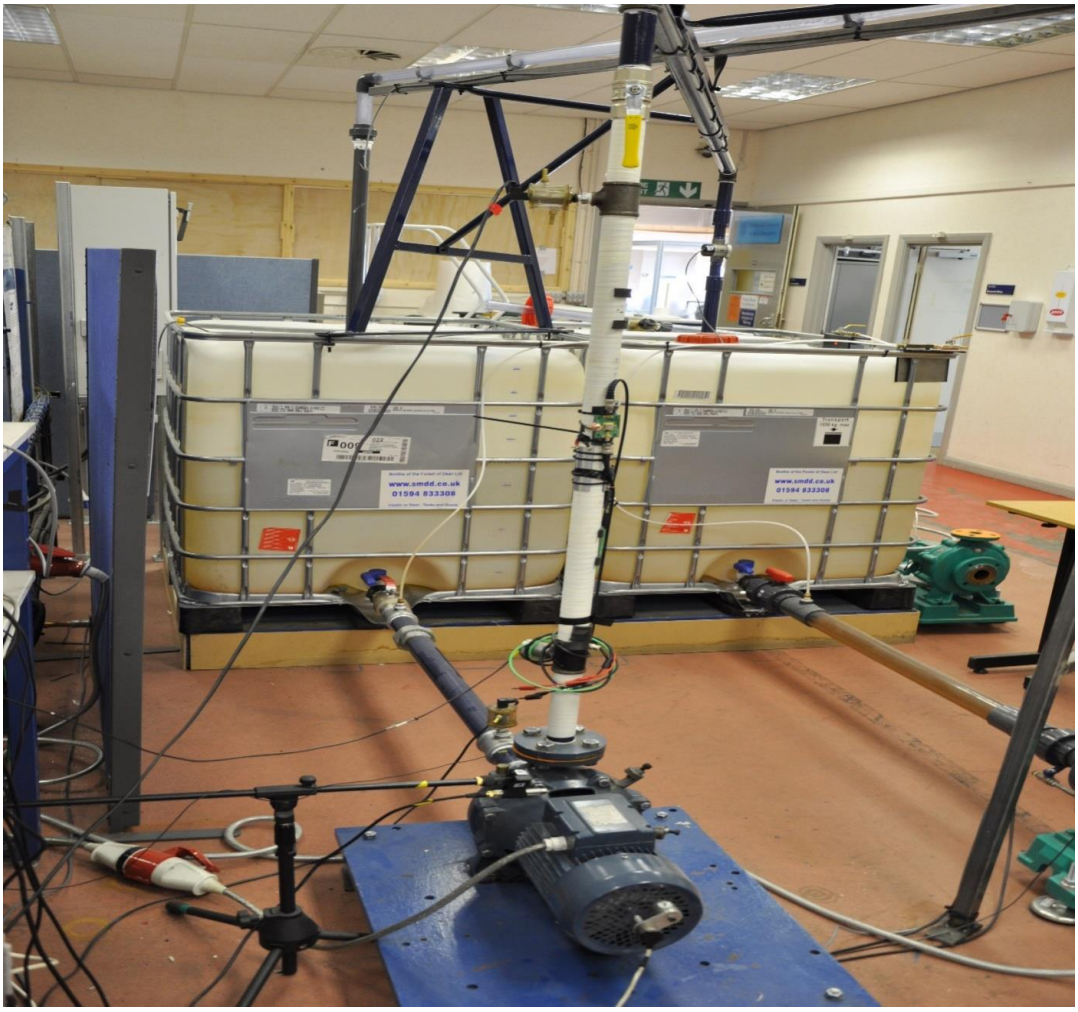

Figure 5-2 The pump test-rig

Table 5-1 Piping system components

System Item	Specification	Quantity	Remark
Water tank (plastic)	Volume = 0.911 m^3 Dimensions 870×1080×970 mm	1	
Steel valve 1½" BSP		1	Suction line
Steel reducing bush 2" to 1½"		1	Suction line
Steel valve 2" BSP		1	Suction line
Steel transparent pipe 2"	ID = 50.8 mm; OD = 60 mm Length between the tank and pump 1690 mm	1	Discharge and Suction line
Equal tee 2" BSP		3	Suction line
Steel coupling 2" BSP		1	Suction line
Steel socket 2" BSP		1	Suction line
Steel reducing screwed socket 1½ -1¼" BSP		1	Suction line
Steel transparent pipe 1¼	ID = 31.75 mm OD = 42 mm Height 1970 mm; Length 1770mm Drop = 1070 mm	1	Discharge line
Equal tee 1¼" BSP		2	Discharge line
Steel valve 1¼" BSP		1	Discharge line
Steel elbow 1¼" BSP		2	Discharge line
coupling 1¼‖ BSP		1	Discharge line
Steel reducing coupling 1¼'' to 1''		2	Discharge line

Table 5-2 Test-rig components.

Components	Type	Quantity	Remarks
Centrifugal pump	Pedrollo F32/200AH	1	
Water flow rate	Gems Rotor flow RFO	1	End of discharge line
High pressure transducer	Sinocera CY-YB-025-1 MPa	1	Discharge line 0-10 bar
Low pressure transducer	Sinocera CY-YB-025- 0.5 MPa	1	Suction line 0-5 bar
Accelerometers	Sinocera YD3 8131	1	Pump outlet
Shaft encoder	Hengstler R1 32	1	
Microphone	Sinocera type 4130	1	50 mm to pump casing
Hydrophone	Sinocera precision hydrophone	1	Discharge line
Speed controller	Omron 3G3MV	1	
Spectrum analyser	Type R4131D	1	
Data acquisition	Sinocera, YE6232B	1	(16CH channel 16bit)
Data acquisition	CED 1401 Plus	1	DAQ

The table above demonstrates how transducers were attached on a test-rig.

5.2 Measurement System

The test-rig should be able to simulate and monitor various centrifugal pump faults using various techniques. Therefore, a number of sensors were in the test-rig in order to measure various parameters like acoustics, vibrations, flow rate, pressure, speed and the power supply current. This plays a significant role in the diagnosis and detection of the pump faults. Moreover, more system parameters were measured using the following techniques:

- The rate of water flow was measured using a paddle wheel type.
- A sinocera was mounted on the suction and the discharge lines (the pressure transducers) of the pump to measure the water pressure.
- The pump vibrations were measured using a Sinocera (accelerometer) mounted at the pump’s casing adjacent to the bearing side and outlet.

- The air-bone noise produced by the pump was measures with a Sinocera (microphone) positioned 50 mm away from the pump.
- The hydro-acoustic noise was measured using Simocera (hydrophone) with a one-inch precision put along the pump's discharge line.
- A commercial (encoder) mounted on the anterior of a pump motor shaft was used to measure the speed of the pump shaft rotations.

All voltage measurements were regularly recorded from the transducer. It was observed that in each case, parameters measured from the converter's output voltage corresponded to the amplitude. All the measurements were then linked to the data acquisition system through BNC coaxial cable in order to prevent noise entering the system and utilize the data acquisition system in storage and computer signal conditioning. All sensors were connected to sufficient power supply (i.e. Farnell Instruments Ltd L30 / 2), the computer's USB port and the data acquisition system (YE6232B and CED 1401) [123].

5.2.1 Pressure Transducer

The pressure transducer used was the Sinocera (type CY-YB-025). It is a general-purpose pressure transducer used in the industries, with a maximum limit of approximately 10 bar gauge as presented in Figure 5-3. This type of transducers works behind the principle that the measured pressure acts on the diaphragm which is attached to a strain gauge. As the diaphragm moves, it induces strain on the gauge, which also triggers change in the electrical resistance proportional to pressure applied. It accuracy is high and it is estimated at ±0.2%. The two sensors mentioned above were used during the test-rig. One was mounted on the suction line near the pump's inlet as shown in Figure 5-4, and another on the discharge flow as presented in Figure 5-6. The specifications for both pressure transducers were used in this investigation and were placed on the test rig, clearly are listed in Table 5-3 and Table 5-4. The online raw data was obtained and presented as typical samples on the Figure 5-5 which is from the pressure transducer in the suction line. Figure 5-7 shows the data that was gathered from the pressure transducer and the fluctuation of the amount of discharge pressure provided in the discharge line.

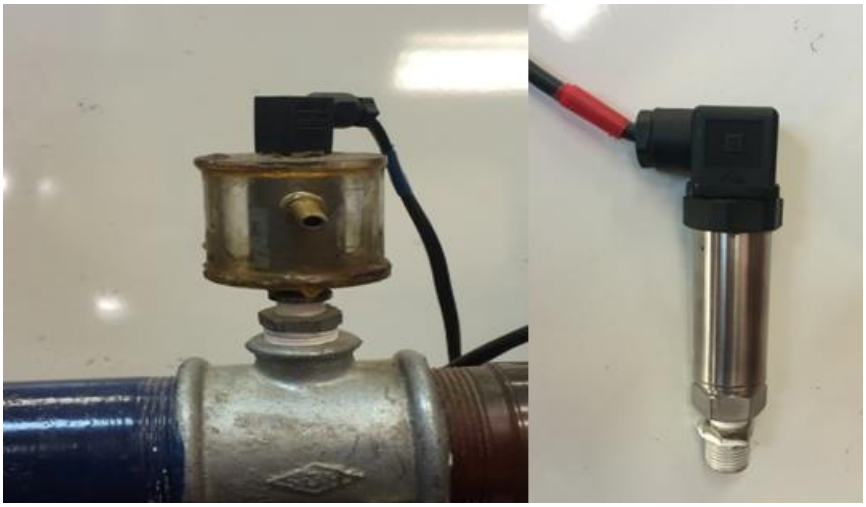

Figure 5-3 Pressure transducer in suction line

Table 5-3 Specifications of pressure transducer in suction line

Pressure transducer manufacturer	**Sinocera**
Product	Strain gauge pressure transducer
Type	Y084602
Measurement range	6 bar G
Operating voltage	10_15 VDC
Output mode	4-20 mA
Static precision	< 0.3% FS
Screw joint	1/ 4 - NPT external
Operating temperature range	-20 ºC to +125 ºC

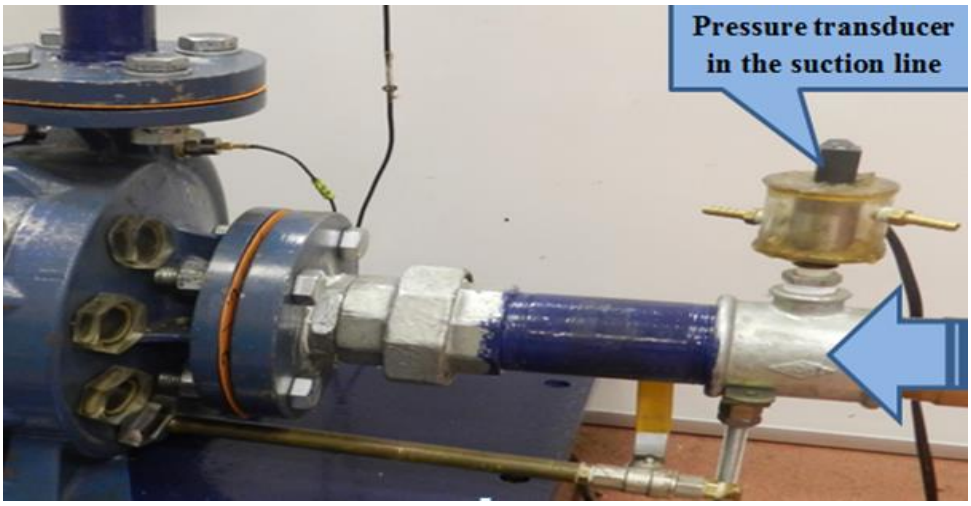

Figure 5-4 Pressure transducer in suction line at the pump inlet

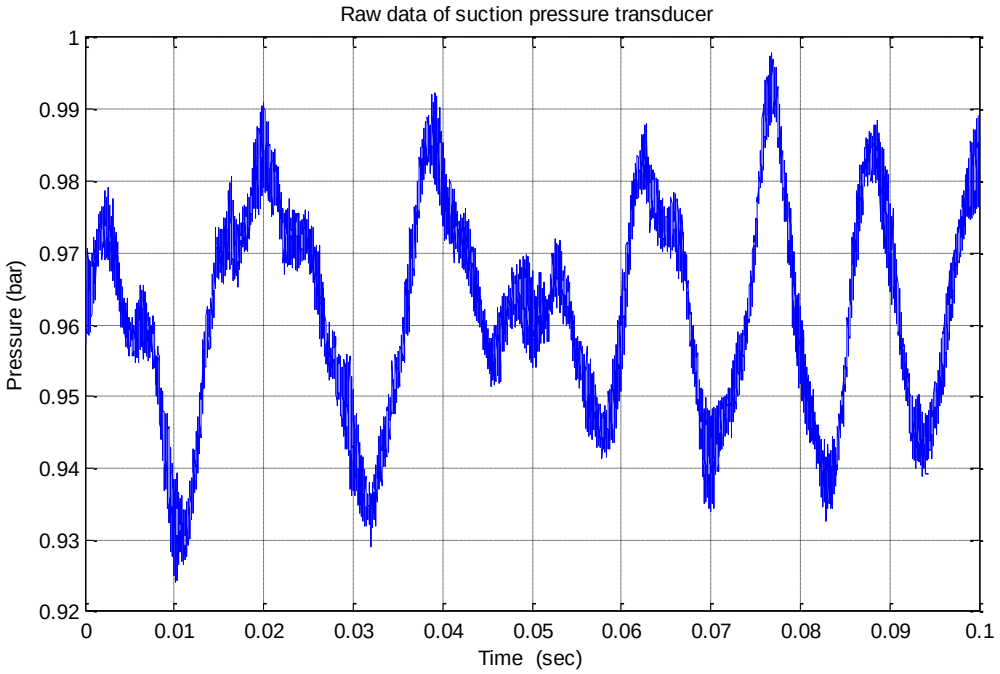

Figure 5-5 Online raw data recorded from the pressure transducer in the suction line

Figure 5-6 Pressure transducer in discharge line at the pump outlet

Table 5-4 Specifications of the pressure transducer in discharge

Pressure Transducer Manufacturer	**Sinocera**
Product	Strain gauge pressure transducer
Type	Y084602
Measurement range	6 bar G
Operating voltage	10_15 VDC
Output mode	4-20 mA
Static precision	< 0.3% FS
Screw joint	1/ 4 - NPT external
Operating temperature range	-20 ºC to +125 ºC

In a pumping system, the water pressure usually ranges between 0 and 5 bars. Based on the guidelines from the manufacturer, the maximum pressure that a sensor can measure in the discharge and for the transducer in the inlet line are 10 and 5 bars respectively. The pressure transducers were each connected to a power supply (Farnell Instruments Ltd L30/2) as well as the data acquisition system and a PC system.

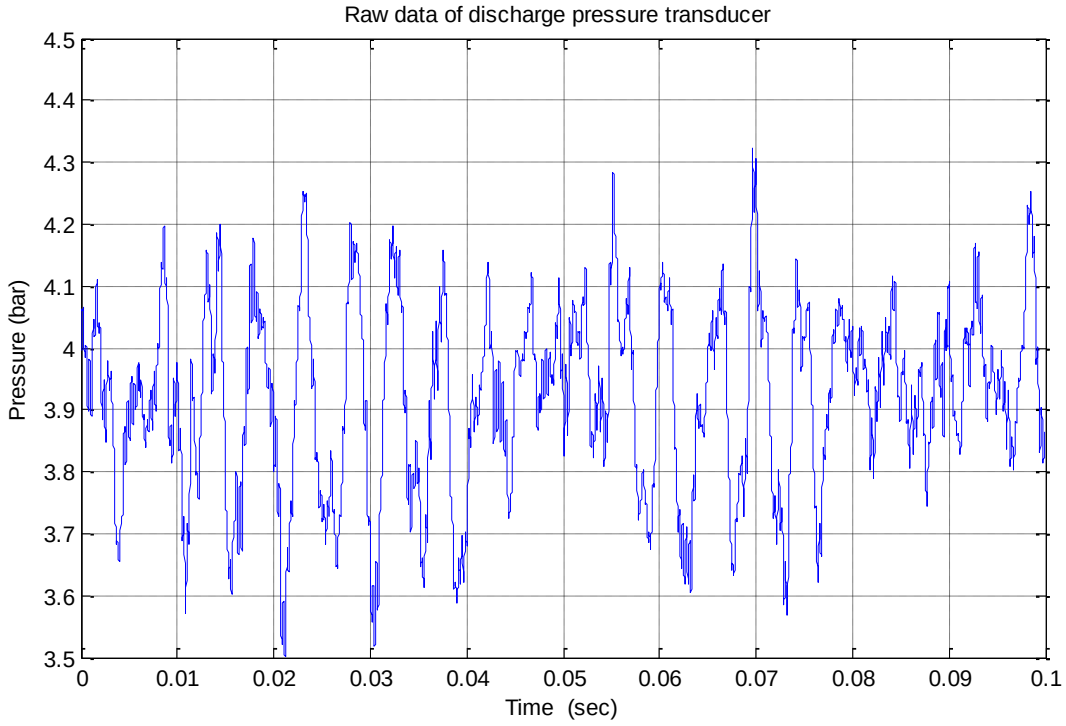

Figure 5-7 The online raw recorded from a pressure transducer in the discharge line.

5.2.2 The Flow Rate Transducer

A flow rate transducer is a crucial rotating vane machine commonly used to make measurements. Figure 5-8 shows the flow rate transducer. In this case, the model used was carefully selected to match the capacity of the pump. A transducer comprises of a single cylindrical rotor that has six vanes. The rotor is forced to rotate by fluid flow forces. The total amount of fluid flowing through the meter can be measured by counting the number of revolutions made by the rotor. The claimed accuracy of flow rate transducer is high, at approximately 0.1 %. A flow meter was placed along the pumps' outlet, which is the down flow that empties the fluid to the reservoir [123].

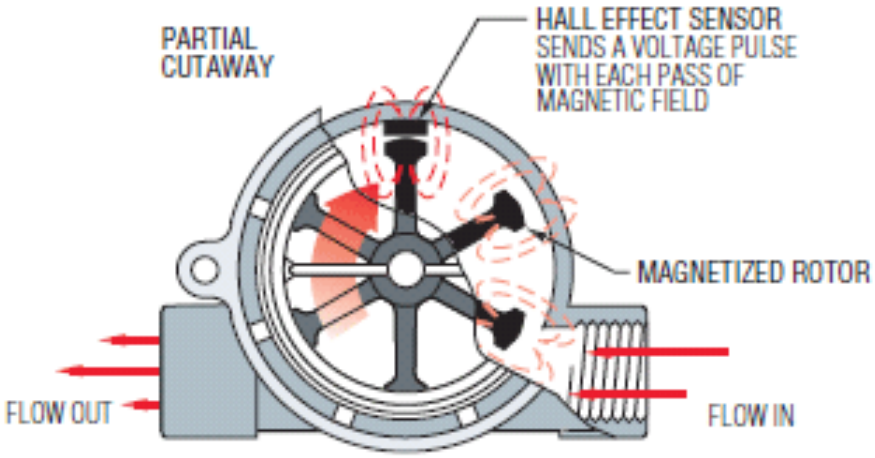

Figure 5-8 Gems rotor flow type RFO [124]

The on/off DC pulses observed occur at a frequency that is directly proportional to the rate of flow. The frequency range of the meter is between 24Hz and 225Hz. This translates into a flow rate range of 100 to 400 lit/min. The flow meter was placed at the end of the discharge pipe line as shown in Figure 5-9, also the flow rate meter signal as shown in the Figure 5-10 from the discharge line. The Table 5-5 presented the sensor which was used and its specifications.

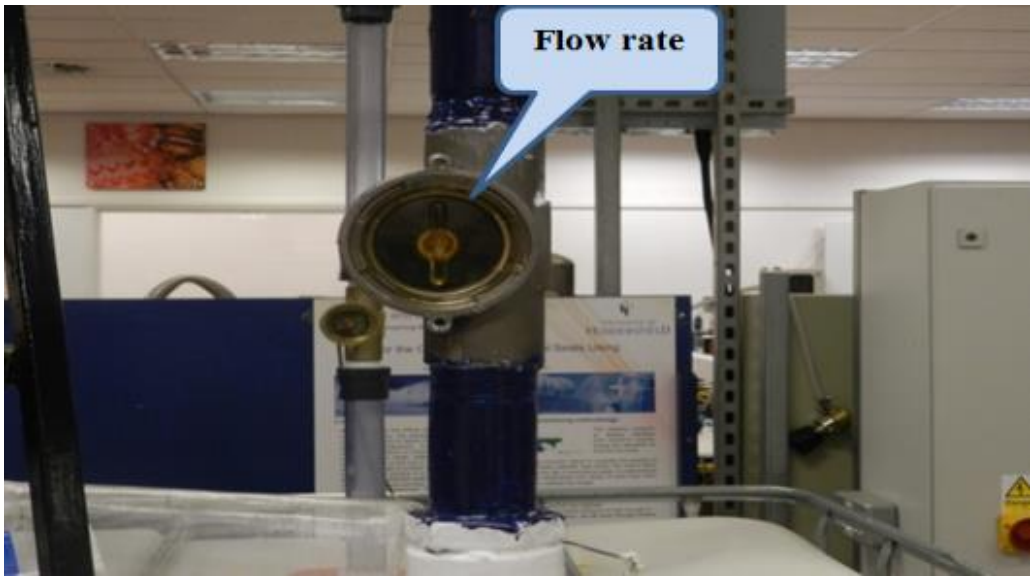

Figure 5-9 Gems water flow meter in discharge line

Table 5-5 Specifications of the gems RFO flow rate sensor

Flow Meter Manufacturer	**Gems**
Type	Rotor flow RFO
Operating pressure, maximum Polypropylene body	6.7 bar at 21 ºC, 2.8 bar max at 80 ºC
Max. operating temperature	80 °C
Electronics (both bodies)	65 °C Ambient
Max. viscosity	45 cSt
Input power	4.5 to 24 Vdc, (24 Vdc regulated supply)
Output signal	4.5 to 24 Vdc pulse. Pulse rate dependent on flow rate, port size and range
RFO type	0-10 VDC Analogy signal @1 mA max.
Current consumption	8 mA,no load
RFO type	25 mA max.
Max. current source output	70 mA
Frequency output range	15 Hz (low flow) to 225 Hz (high flow)

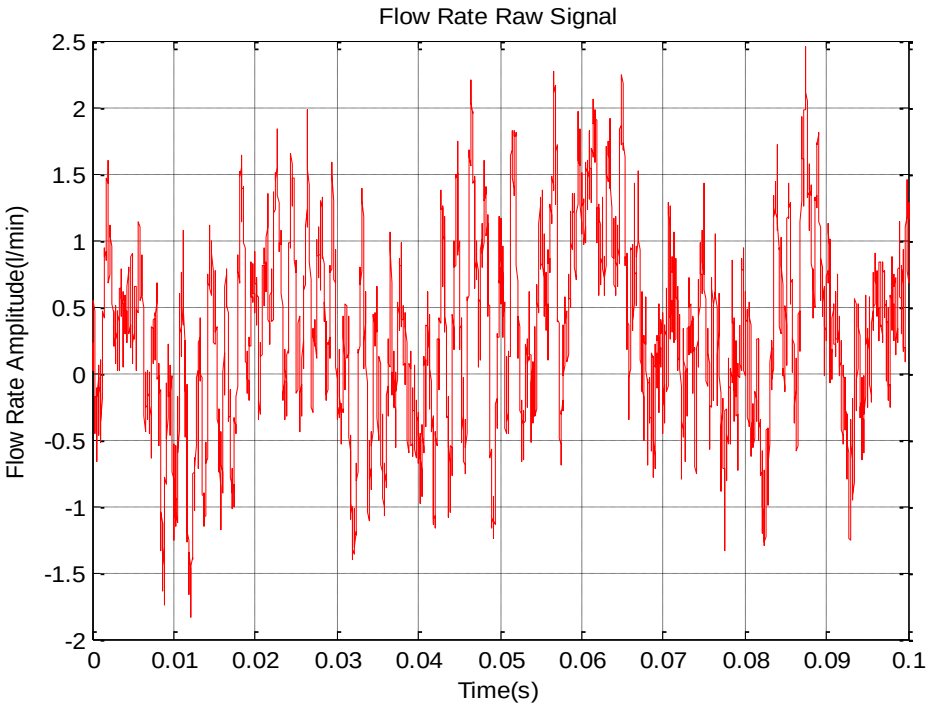

Figure 5-10 The flow rate signal from the meter on discharge line

5.2.3 Vibration Accelerometer

The accelerometer was Sinocera type YD38180 piezoelectric devices which were installed onto the outlet of the centrifugal pump as presented in Figure 5-11.The piezoelectric material responds to mechanical deformations by developing an electrical charge with a magnitude which is directly proportional to the applied mechanical stress (force) that runs across surfaces. The Table 5-6 shows the accelerometer specifications.

Table 5-6 Specifications of the Accelerometers

Maker	**Sinocera**
Type	Accelerometer (piezoelectric)
Model	YD38180
Frequency range	10 Hz – 10 KHz
Sensitive	1.56 mv/m.s^{-2}
Range accretion	<2000 ms^{-2}
Temperature range	To 250 °C

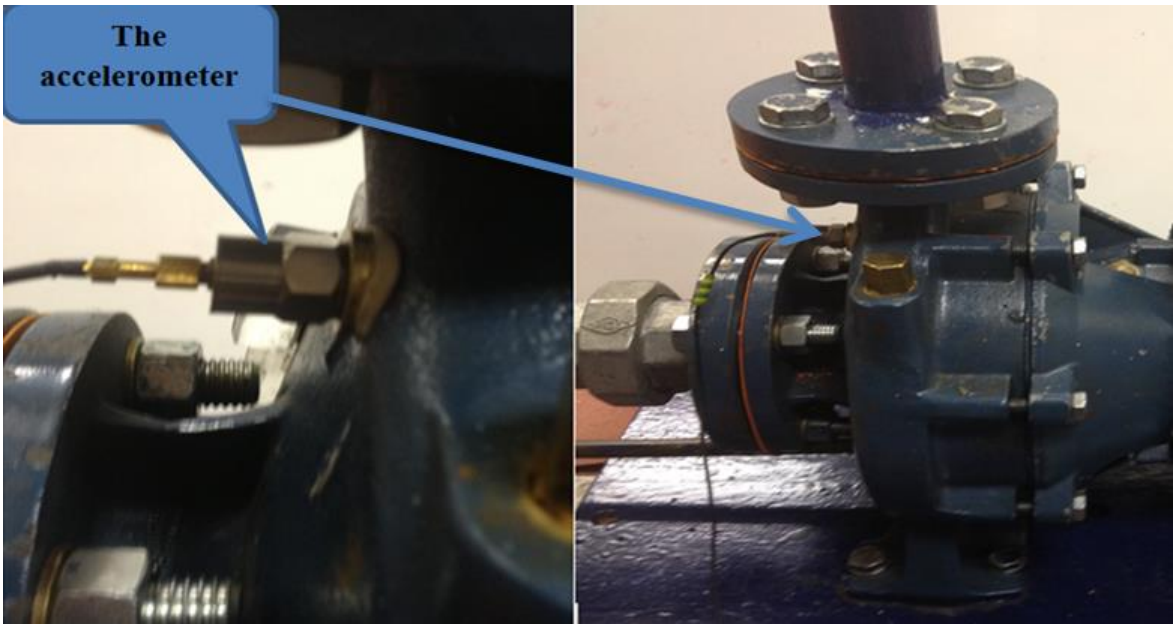

Figure 5-11 Position of the accelerometer

The piezoelectric accelerometers are the most common type of sensors which are used for fault detection and condition monitoring processes. There are several advantages for using piezoelectric accelerometers. They are easy to install, have a wide range of frequency response and are relatively low cost. The output of these devices is directly proportional to the magnitude of acceleration. The devices can be modified in order to record measurements for velocity and displacement readings [123].

Figure 5-11 shows a picture that was taken of the accelerometer which was used at the outlet of the pump. The accelerometer was attached to a screw-threaded brass stud which was attached to the casing of the pump by first tapping and then screwing processes to avoid the cap between the casing and the accelerometer to achieved good respond. The vibration transducer was connected to a charge amplifier (Sinocera YD3 131). The charge amplifier was connected to the data acquisition system and the recorded data was then sent to a computer system ready to be analysis by Matlab. A sample of the online raw data can be seen in Figure 5-12 which was collected with the accelerometer in the pump outlet.

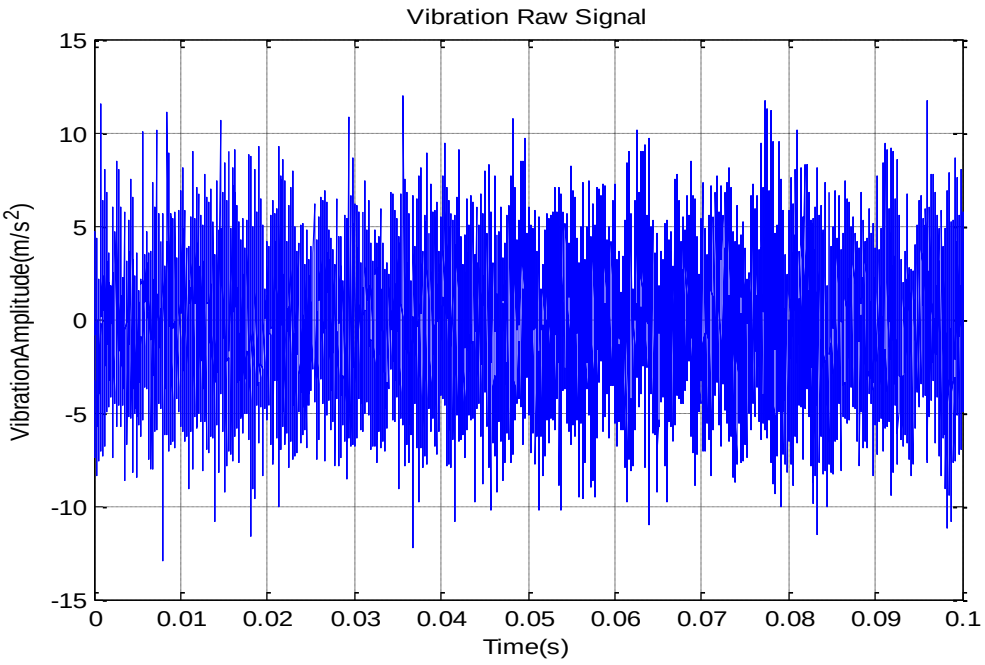

Figure 5-12 Raw vibration signals recorded from the accelerometer on the pump outlet

5.2.4 Acoustic

Acoustic devices are main parts in this field now being used for condition monitoring. Acoustic analysis is now a recognised method for carrying out non-destructive examination due to the developments in acoustic technology field. This approach focuses on the analysis of noise waveforms which are produced by the machinery (hydrophones and microphones). Microphones are usually used to pick up acoustic signals to be used for comparison against vibration-monitored waveforms. There are several advantages for using microphones, which are sensitive also easy to mount and possess a wide range of frequency response. This would allow microphones to gather appropriate and comprehensive information [16].

5.2.5 Microphone

The microphone used to measure the microphone signal generated radiated by the pump was the Sinocera type, which is a half-inch precision microphone as presented in Figure 5-13. Furthermore, the Table 5-7 shows the specifications of the microphone and pre-amplifier which were used on this investigation. The microphone was placed away from the pump outlet around 50 mm due to the high vibration noise and it was connected to a pre-amplifier as filter then to the data acquisition system finally the PC system [123] .

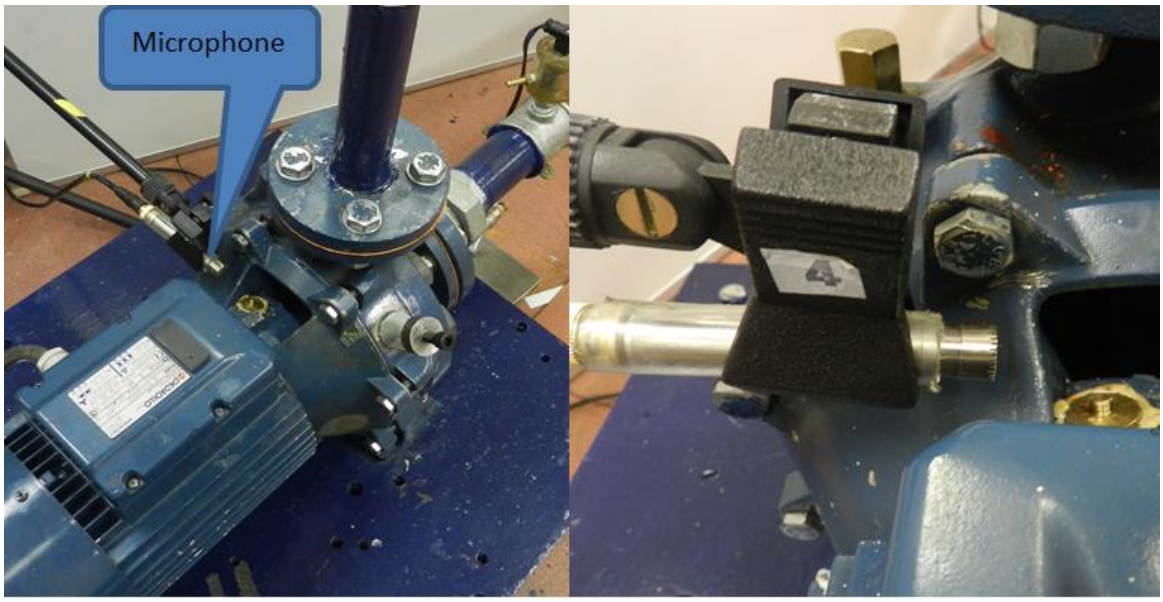

Figure 5-13 Microphone and position of microphone

Table 5-7 Specifications of the microphone and pre-amplifier

Manufacturer	**Sinocera**
Microphone	Electret condenser microphone
Linear frequency range	20 Hz – 20kHz (free field)
Sensitivity	40 mv/Pa
Microphone preamplifier	YG201
Linear frequency range	20Hz – 100 KHz ± 0.2dB
Sensitivity	50 mV/Pa
Dimensions	Ø 12.7 mm x 70 mm (including connector)
Max output voltage	5.0 V_{rms}
Operating temperature range	40 ºC to +80 ºC

The acoustic signals are used as support for the measurements from the accelerometer, due to the presence of high background noise levels which is generated from two contents the discrete content from mechanical components and hydraulic pulsations is more deterministic whereas the wideband content from flow turbulences and cavitation is more random in nature. Moreover, the use of special conditioning techniques is often required before the signal can be used for condition monitoring. Figure 5-14 shows the online data which was collected using the microphone.

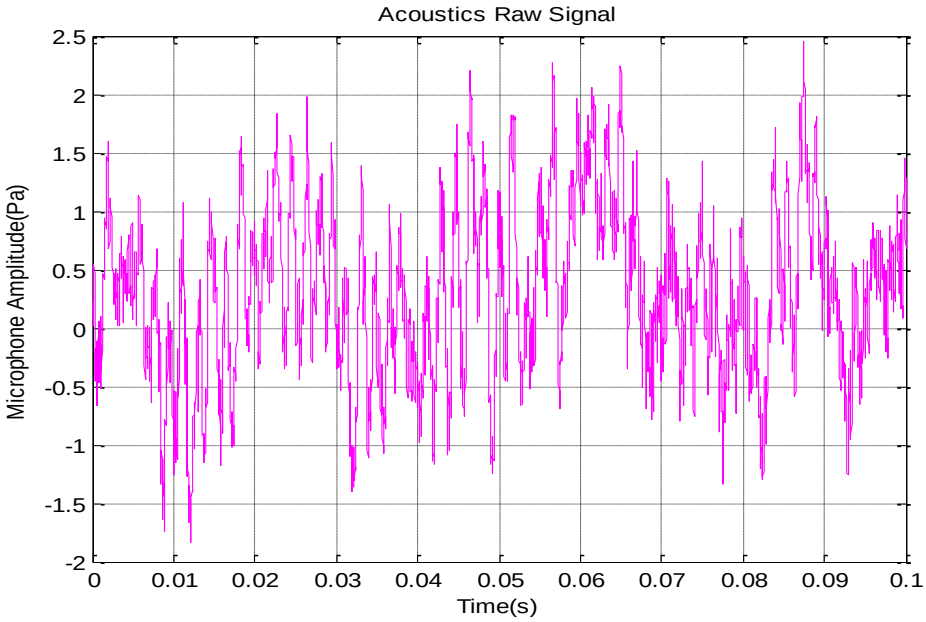

Figure 5-14 Raw data for the pump noise that is measured by a microphone

5.2.6 Shaft Encoder

The pump's instantaneous angular speeds were captured using an incremental optical encoder (Model-RI 32) and data that were obtained from measurements. The shaft encoder which was attached to a spindle adaptor on the non-drive end of the pump rotor shaft by meaning of rigid rubber coupling as can be seen in Figure 5-15 and the specifications of the encoder that was used are listed in Table 5-8. In addition, the encoder which was used was an optical type encoder which contained a glass disk with opaque and transparent areas. The source of light as well as the photo detector array, recorded the optical patterns that defined the shaft's position at any given time. The codes were read using a controlling device, like a microprocessor so as to define the angle and speed of the shaft [123].

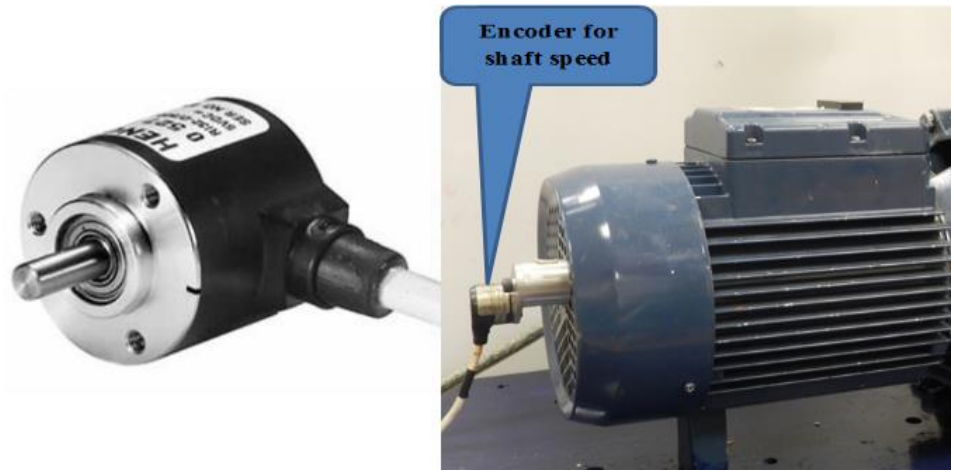

Figure 5-15 The shaft encoder and position of encoder for shaft speed

Table 5-8 Specifications of encoder

Manufacturer of encoder	Hengstler
Type	R1 32
Out put	High 2.5 V ,low 0.5 V
Power supply	5 V d.c
Max pulses per revolution	360
Mounting round	Flange
Shaft diameter	5 mm, 6 mm
Maximum speed	6,000 RPM
Torque	≤ 0,05 Ncm
Protection class housing/ball bearing	IP 50/40
Operating temperature	–10 … +60 °C
Pulse shape	Rectangular
Vibration performance	(IEC 68-2-6) 100 m/s^2 (10 … 2000 Hz)
Shock resistance	(IEC 68-2-27) 1000 m/s^2 (6 ms)
Connection	cable axial/radial
Material	flange: aluminum, cover: plastics
Weight	50 g approx.
Bearing life	In excess of 107 revolutions

An encoder is connected directly to a data acquisition system (CED) that is connected to the PC as well. Thus device generated a square pulse for each angular degree (therefore the name 360-line encoder) for each complete revolution. This enabled the determination of the shaft speed. The online raw data which was obtained by the encoder can be seen in Figure 5-16.

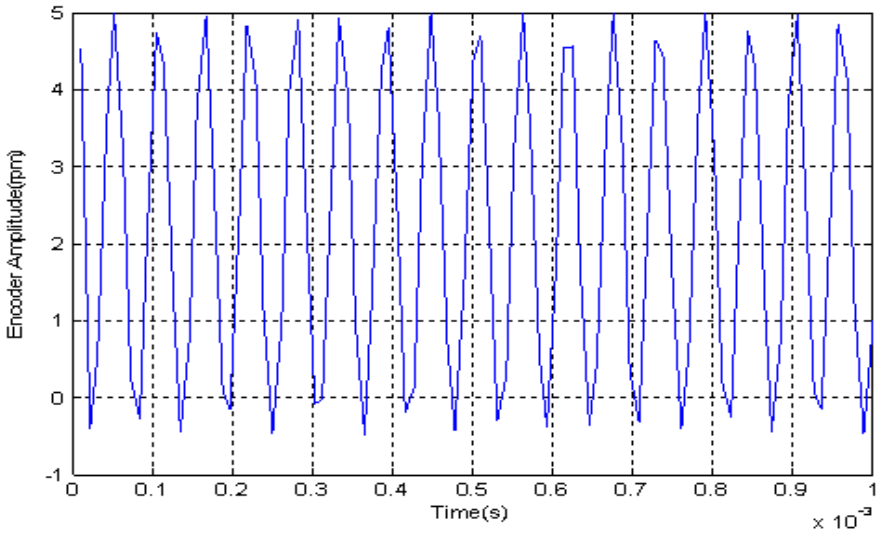

Figure 5-16 The outlet signal of encoder

5.2.7 Speed Controller

Many speed applications of centrifugal pumps require employing a control interface which would allow the speed of the motor to respond to the system requirements, i.e. speed changes to complement the pumping system requirements. This is often accomplished by variable frequency speed control for AC. Induction motors are and will continue to be a viable high technology product.

In order to control the pump output and avoid the negative downsides of the aforementioned methods, a speed controller was used instead. The speed controller matches the output to the head requirements of the system and this eliminates the need of having a control valve in the pump. Due to the ability of the speed controller to regulate the pump's speed so as to match the system's head requirements, a single impeller diameter is required. The pump's speed should change to match the system's new conditions. However, this approach has two major limitations. First, a pump impeller is often rigid and designed for a particular running speed and flow rate. Also, as the speed changes the efficiency of the device is significantly reduced [125].

An inverter-type speed controller was used in the test-rig. There was completely different reason as to why the students mounted a speed controller on the test-rig. It meant that the forthcoming researchers (students) would manage to simulate various potential faults of the centrifugal pump at various speeds and also explore the effects of altering pumps speeds on the energy costs. The operation principles of an inverter are based on rectifying the mains AC supply to DC and then inverting it back to AC, this would provide the frequency which is required to match pump demand. This method controls the pump speed and saves energy [126].

The Omron speed controller was easy to use and could deliver high-torque control at low speeds. The 3G3MV inverter was a three-phase type which was compatible with the given power supply. The inverter-type speed controller can be seen in Figure 5-17. The maximum pump speed with the Omron speed controller was at 3000 rpm which could gradually get reduced to zero. The specifications of the speed controller can be seen in Table 5-9.

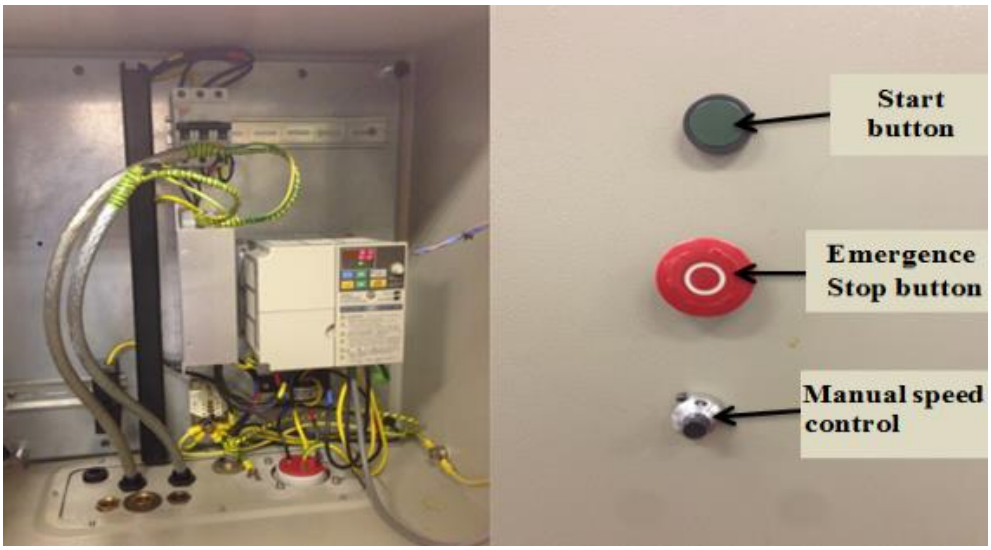

Figure 5-17 Omron speed controller

Table 5-9 Specifications of the speed controller

Speed controller manufacturer	Omron
Model	3G3MV
Allowable voltage fluctuation	±15% to 10%
Allowable frequency fluctuation	± 5%
Power supply	380 to 460 V AC at 50/60 Hz
Max output frequency	400 Hz
Heat radiation	20.1 W
Frequency control range	0.1 to 400 Hz
Output frequency resolution	0.01 Hz
Location	indoor
Control method	Sine wave PWM
Ambient temperatures	Operating ± 10 to 600C

5.2.8 Data Acquisition (Sinocera YE6232B)

In order to achieve the goal, it was necessary to improve the previous Data Acquisition that was available in the lab; it was old and has 8CH channels only. With this test-rig, one is required to get the values of various variables simultaneously; vibration levels, flow rates, pressures, airborne noise, shaft speeds, hydro acoustic noise, as well as the impedance for capacitive measurements as presented in Figure 5-18. Figure 5-19 shows the data acquisition (DAQ), Sinocera YE6232B (with 16CH channel 16bit), and the interface panel. Data will be recorded

and collected using an analogue type device, in this case a chart recorder. A chart recorder can physically plot the signal on a paper or display it on an oscilloscope.

With this test rig it will be required to obtain the values of several variables simultaneously;

Figure 5-18 Sinocera YE6232B data acquisition system

The sampling rate was at 96,000Hz. As demonstrated in Table 5-10, nine channels were used for collection of data from the test-rig, all the channels were connected to other data acquisition CED 1401:1992 except one channel was connected directed to the accelerometer which was mounted on the pump housing in the horizontal direction.

Table 5-10 Connection orders for the channels

Chanel No	**Remarks**
1	Encoder
2	Suction pressure
3	Discharge pressure
4	Vibration
5	Microphone
6	Hydrophone
7	Flow rate

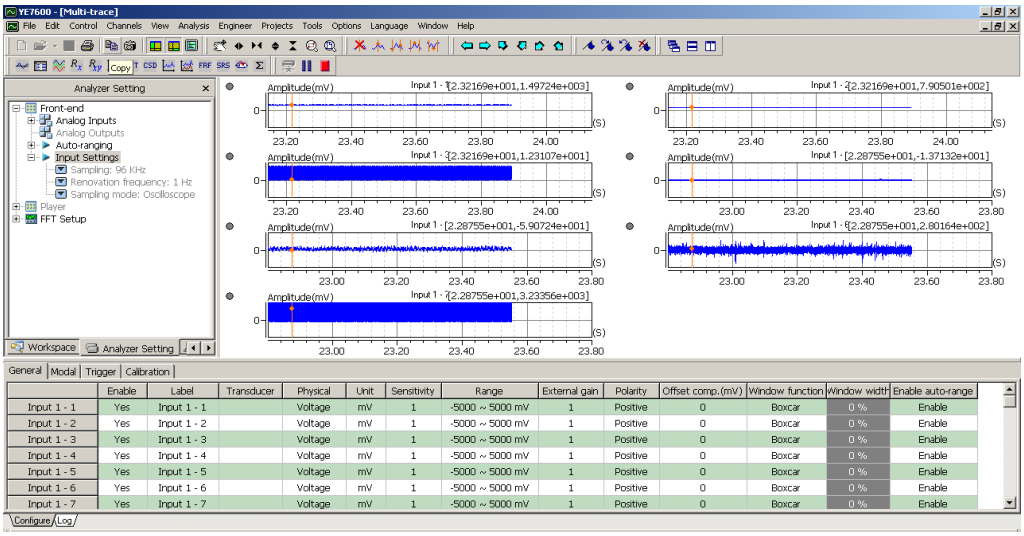

Figure 5-19 Interface panel for YE6232B

Efforts were made in adjusting the conversion and amplification of the output of each sensor so that they share common signal conditions, typically ± 5 V the generated voltage signal. This was used as input for the multiplexer which was regulated using a microprocessor system. A microprocessor captures signals and transmits them through a sample and holding unit. Then, they are passed to an A/D converter to produce a parallel input to that of PC and they get processed after which they can be displayed or stored [123]. In the PC system, an A/D converter and a multiplexer were attached on one expansion slot. This unit had signal conditioning elements that could be used together with sensors (like thermocouples) and transducers. There were 16 A/D channels having a 16 bits resolution in the card as shown in Table 5-11.

Table 5-11 The specifications of the Sinocera YE6232B

DAQ system manufacturer	**Sinocera**
Type	YE6232B
Number of channels	16 channels selectable voltage/IPE input, multiplexing is used to sample each channel in turn.
A/D conversion resolution	16 bit
Sampling rate (maximum)	100 kHz per channel parallel sampling
Input range	±5 V
Gain	Selectable, either 1, 10 or 100
Filter	Anti-aliasing filter
Interface	USB 2.0

5.2.9 Data Acquisition (CED 1401 1992)

The CED 1401:1992 is presented in Figure 5-20 and Figure 5-21. This DAQ is capable of recording and storing data as well as maker information for simultaneous, real-time and multitasking systems, under control of a host PC. In this case, it was used to analyse data recorded for shaft speed, flow rate and pump outlet and inlet pressures. A number of projects conducted previously had used DAQ.

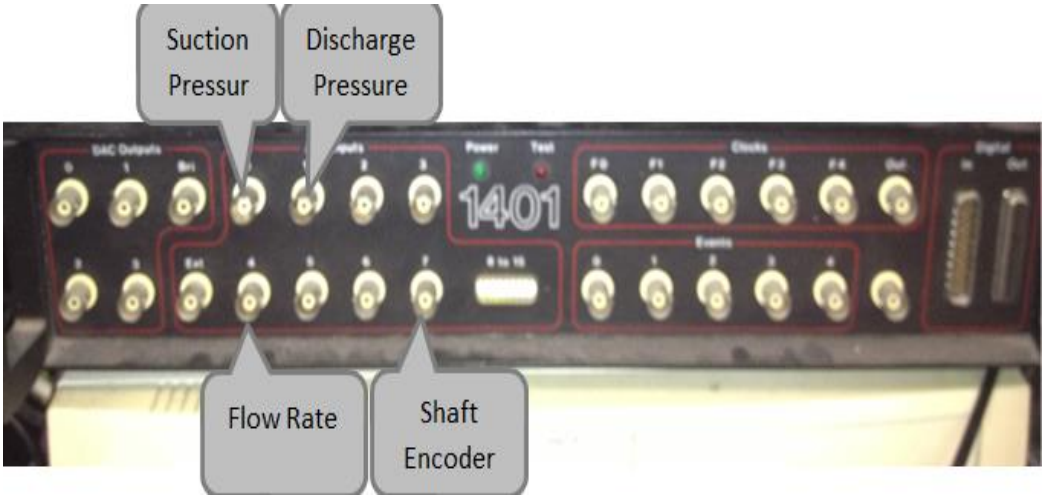

Figure 5-20 The CED 1401 plus data acquisition system

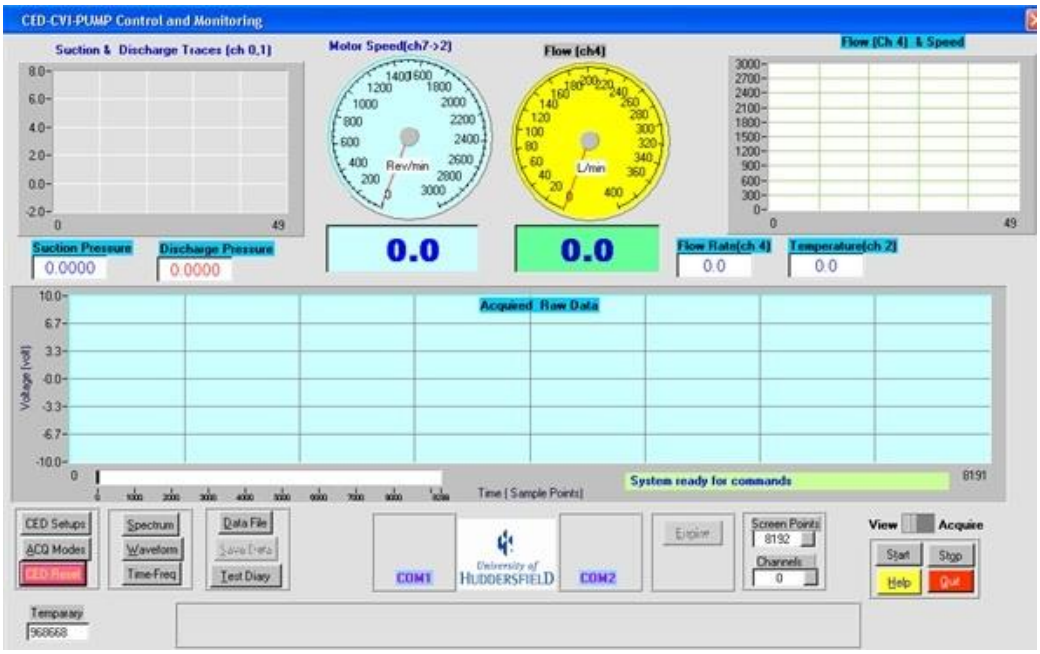

Figure 5-21 The interface panel for CED 1401

5.3 Centrifugal Pump

The centrifugal pump type is a Pedrollo standard horizontal inlet, closed impeller, single-stage content of Pump and motor, moreover the general purpose of centrifugal pump can be seen in Figure 5-22. This pump was designed for civil, industrial and agricultural applications. In addition, this pump can deliver water at a rate of up to 30 m^3h^{-1} (500 lit/min) at a head of up to 57m. The pump is driven by a three-phase electric motor which can running speed up to 2900 rpm on 8.9 A at 380-400 V (nominal 4 kW/5.5hp). The centrifugal pump specifications are presented in Table 5-12. Appendix A

Figure 5-22 The pedrollo F32/200AH centrifugal pump

Table 5-12 The specifications of pedrollo F32/200AH pump

Pump Manufacturer	Pedrollo
Type	Centrifugal pump F32 / 200AH
Head	46 – 57 (m)
Capacity	10 – 30 (m^3/h)
Speed	2900 (rpm)
Maximum pressure	10 (bar)
Impeller type	Closed, brass
Number of stages	Single
Power	4 kW
HP	5.5
Frequency	50 Hz
Rated current	8.9 A
Rated voltage	380-400 V

Connection	Closed

5.4 Pump Performance Test

ISO 3555 asserts that the predicted features between NPSHR (Net positive Suction Head Required) and NEPSHA (Net positive Suction Head Available) for this system can be acquired by throttling the discharge line valve progressively while maintaining the speed of the pump at 2000 revolution/minute and the valve mounted at the suction line open (100%), as presented in Figure 5-23. Appendix A

The experiments were carried out on healthy and full opened valve on discharge line by using test rig which discussed in Figure 5-2. Also Figure 5-1presented the Schematic Diagram of the Pumping System. All tests with different flow rates signals were measured, namely, zero, 50, 100, and 150, up to 450, to know the system behaviour under these healthy conditions. The test repeated three times with the fixed speed of 2900 rpm and different flow rates the signals were measured.

The rate of flow was controlled by adjusting the discharge line valve. At least nine data sets were recorded for each test and they covered the required flow range. Every test is repeated thrice to ensure reliable results were obtained. Also, there were time breaks between the successive tests to ensure that there are no high temperatures and also ensure the temperature of water remains the same for each test. Data records from all tests were processed in the Matlab in order to analyse signals as well as identify various parameters for the detection and diagnosis of faults at this stage depending on the signal vibration data with the health case as the standard measurement.

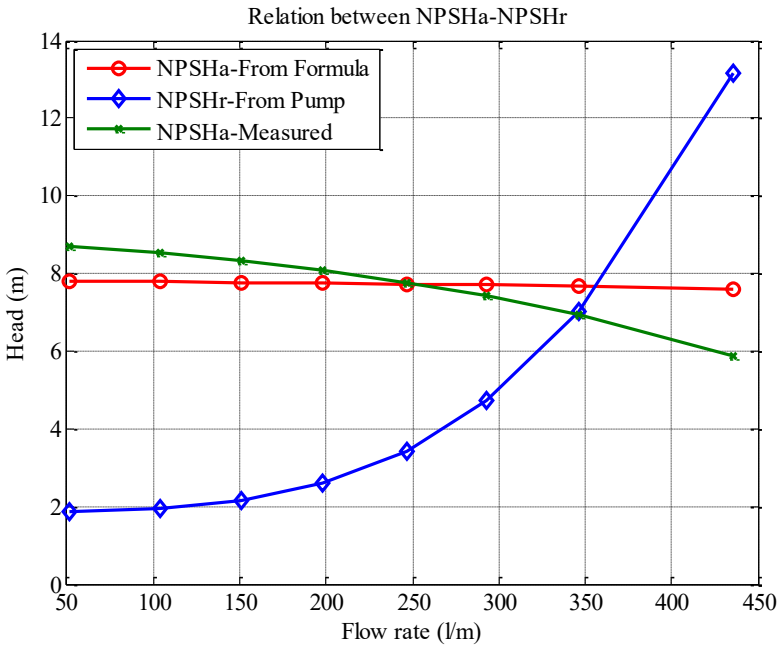

Figure 5-23 Pump performance at 100% open valve. Appendix A

5.5 Relation between the Pump Flow Rate and Pump Head

The Figure 5-24 below presents the curve of pump flow rate with the pump head as well as its corresponding flow rates ranging between 0 l/min and 450 l/min and the baseline (BL). An increase in the rate of pump flow decreases the developed head. When the flow rate exceeds 300 l/min, reducing the resistance to flow (developed head) generates small increase in the flow.

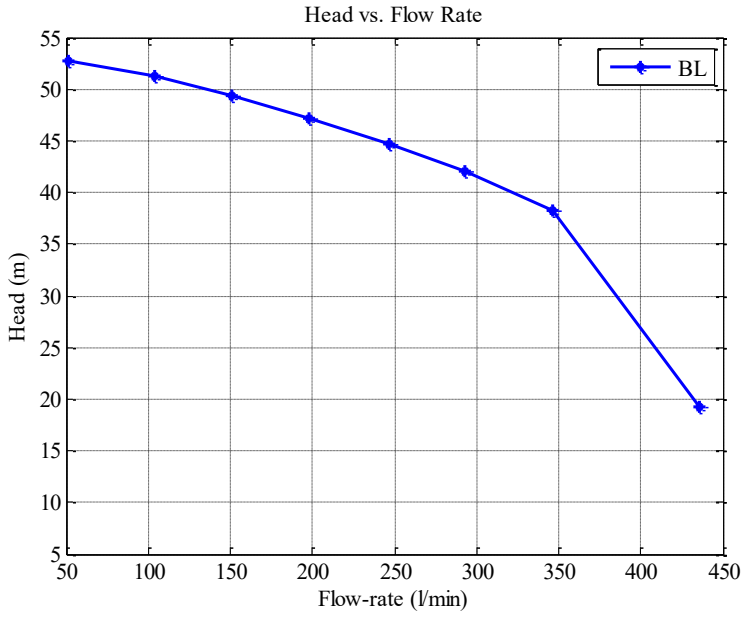

Figure 5-24 Head– flow rate pump curve. Appendix A

5.6 Simulated (seeded) Faults

5.6.1 Impeller Inlet faults (Blockages)

In the Figure 5-25 it shows the location of the blockage on the inlet vane which is created by blockage the inlet between two vanes, one is small blockage whereas the second is large blockage. After a baseline test, two tests were selected from various fault severities respectively. The first test was experiencing only small blockage defect and the second a larger blockage. This enables two degrees of the inlet-vane blockages to undergo accuracy evaluation of vibration-based diagnosis.

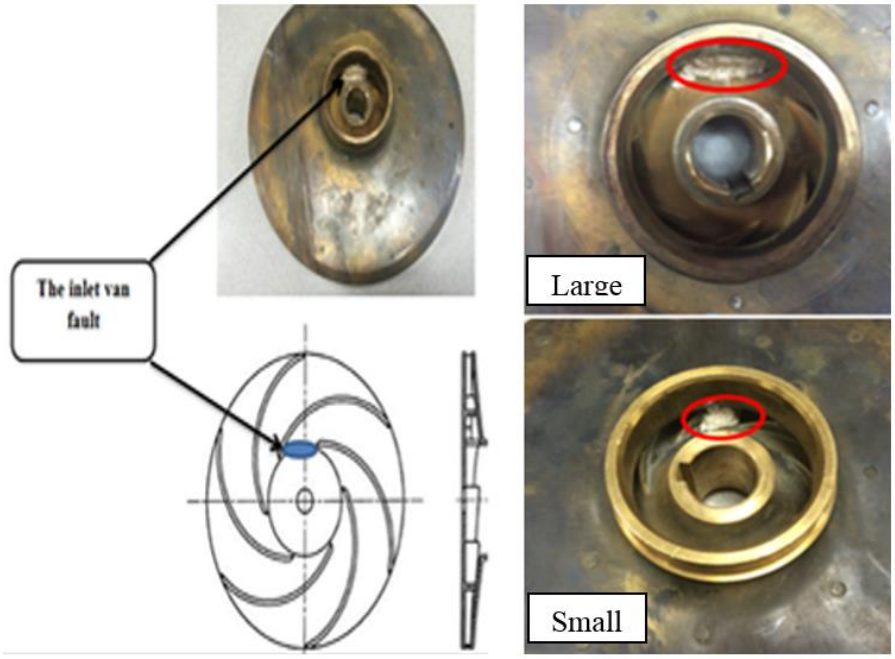

Figure 5-25 The impeller inlet van blockages (small & large)

5.6.2 Impeller Outlet Vans Fault (by Cutting Vans)

Figure 5-26 demonstrates the location of faults on the vane's outlet tip. This defects are created by extracting a part of the vane about 3 mm away along the vane's length direction one by one during this test. After a baseline test, the five tests were selected from various defect severities respectively. The first test was under a fault on a single tip. Also, the second test was under the fault of two tips and the other tests replicated the same sequence.

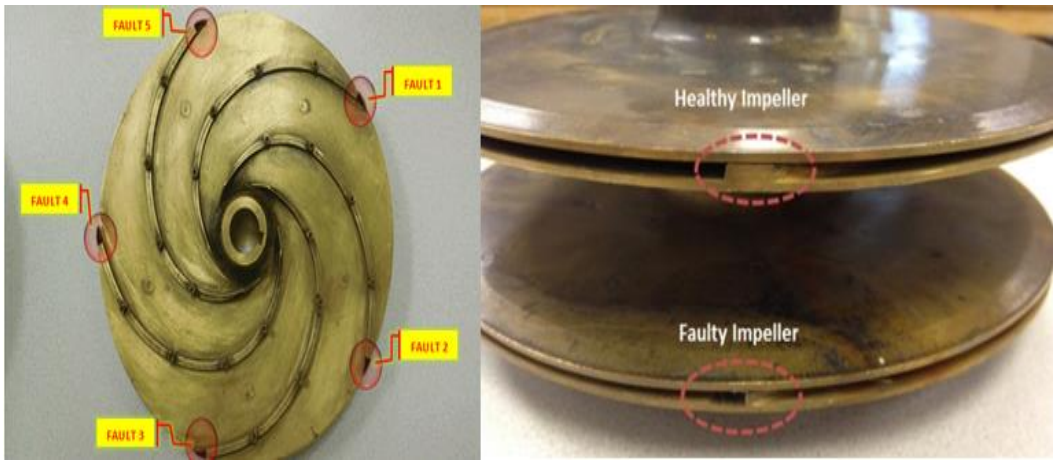

Figure 5-26 Types and location of faults created on exist impeller blades

5.6.3 Impeller Inlet Vans Fault (by Cutting Vans)

As illustrated in Figure 5-27, the fault of inlet defects was induced to the second impeller as the first impeller was health one, and the fault on each vane's inlet tip were generated by eliminating a small portion of the vane tips 3mm away on the edges near the inlet, and along each vane's direction during the test.

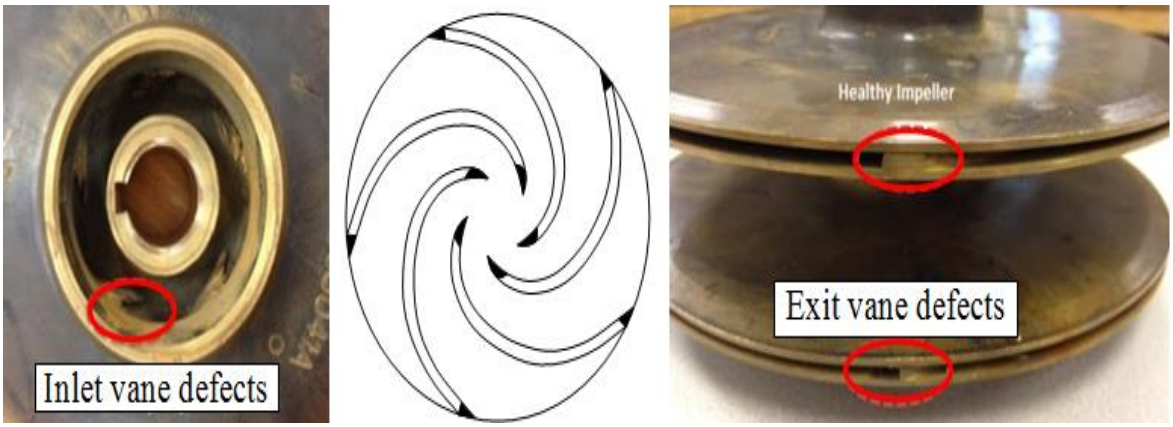

Figure 5-27 The healthy and faulty impellers

5.6.4 Bearings faults (Out-Race, Inner-Race)

The faults for two bearings inner and outer-race faults. The first bearing is induced Inner- race fault (A), in the same way was Outer-race fault (B). Figure 5-28 presented the photo of defects on the bearing outer and inner race faults.

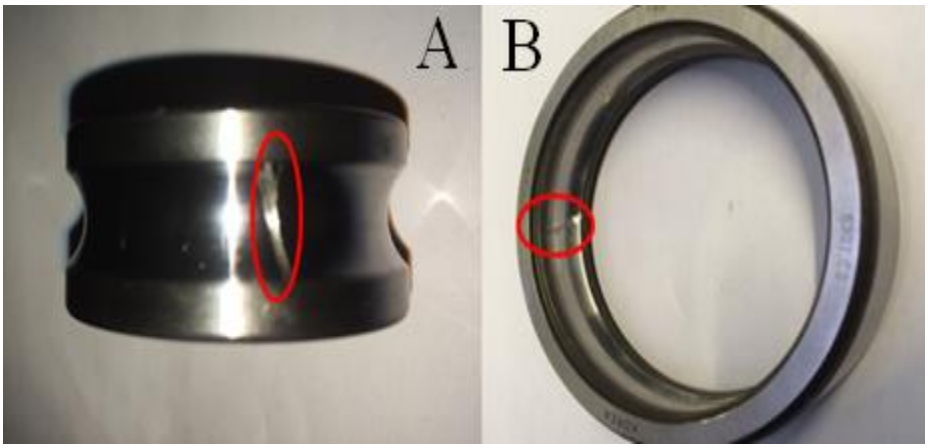

Figure 5-28 Defects on the both bearings which are (A) inner-race, (B) on outer-race

5.6.5 Combined faults as (Bearing Outer-Race +Impeller small and large blockages)

The experiment was carried out based on two different cases, first one healthy (BL), where's the second have bearing outer-race defect + small impeller blockage fault (ORD+SIB), where's the third have outer-race defect + large impeller blockage fault (ORD+LIB). One bearing and impeller are healthy and taken as the baseline form comparison. Figure 5-29 presented the photo of defect on the inlet van fault and Figure 5-30 shows the bearing outer race fault. Were tested under full constant speed (2900) rpm and nine different flow rates (0, 50,100,150,200, up to 450) each test acquired data at fourthly seconds record.

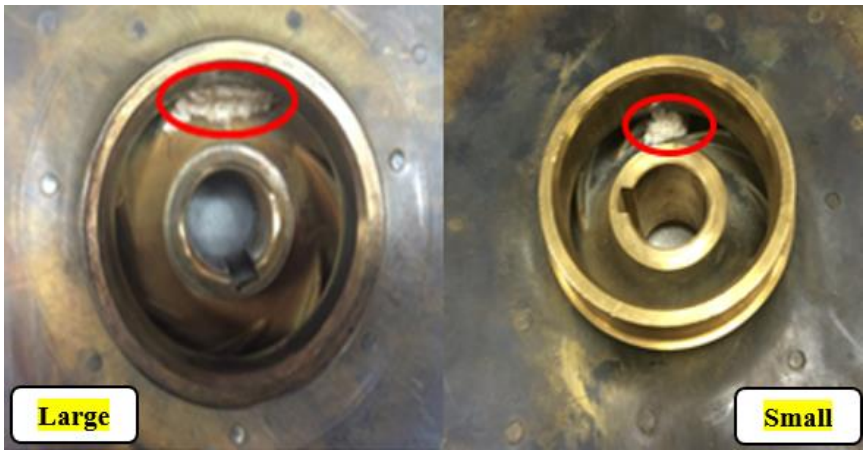

Figure 5-29 The impeller inlet blockage (Large, Small)

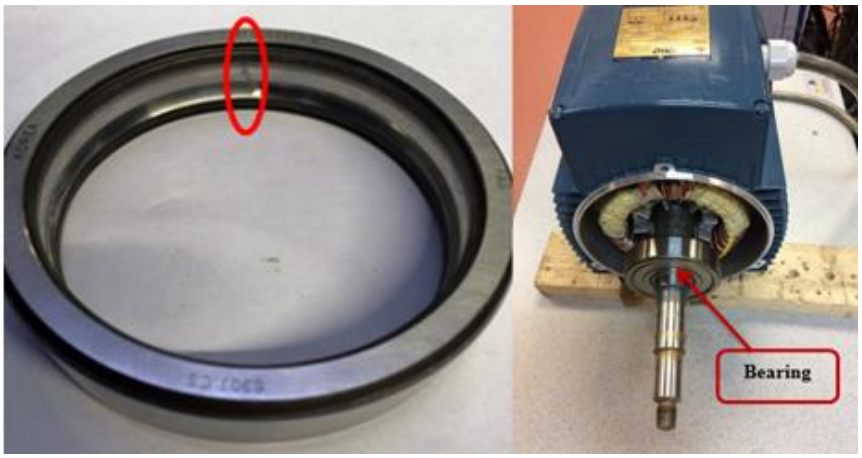

Figure 5-30 Defects subjected to the bearing outer-race and it's position

5.7 Test Procedure

There are three different cases that will be used for the experimental purpose. The first case is healthy. Both the second as well as the third have bearing faults and impeller faults. Tests are for different of simulated defects on bearings and impeller. In each test, vibrations are measured at a constant motor speeds of 2000 revolutions/minute but with seven flow rate increments of 50 l/min, 100 l/min, 150 l/min, 200 l/min, 250 l/min, 350 l/min as well as 450 l/min.

Nine channels were used to collect the data from the test rig as given in Table 5-10 with sampling rate of 96000Hz were adapted to collect the data using all channels as well as by maximum rate). The rotational speed of the pump is measured by a shaft encoder which is mounted on the motor and the accelerometer located on the pump casing to measure the vibration of the pump. Also, two pressure sensors were mounted on the discharge and suction line. The Hydrophone is mounted on discharge line and the Microphone was installed 50mm away from the Pump to measure the pump vibration, where the flow sensor was mounted along the discharge to measure the flow rate.

5.8 Summary

This chapter has explained in detail about the design and construction test rigs, for the experiments to detect centrifugal pump faults. In addition, all the mechanical and electrical components, instrumentation and data acquisition software. The centrifugal pump was introduced and specifications given, also the design optimization is necessary to balance the conflicting requirements of these parameters. Lastly, the test procedures and fault simulation applied in this research were elaborated in detail.

Based on the general knowledge regarding the vibration characteristic of the pumps, various experimental studies were conducted on the centrifugal pump in order to establish appropriate diagnostic features for the impeller and bearing faults. This research has been established a condition monitoring system for centrifugal pump based on vibration measurements, in order to analyse the performance of the pump with the healthy condition and to detect faults of pump components. Particularly, amplitudes at the vane passing frequency as well as the high order harmonics in the shaft frequency would be suitable features to detect and diagnose the severity of a fault.

The initial test has been conducted and results are presented in the healthy condition case, the relationship between flow rate and the pump head was obtained. The pump flow rate curve shows the pump head and corresponding flow rates over the range from 0 l/min to 450 l/min. It can be noted that, as the pump flow rate increases the developed head decrease, and the pump head above flow rate of 350 l/min was dramatically decreased.

CHAPTER SIX

DIAGNOSIS OF CENTRIFUGAL PUMP IMPELLER FAULTS USING SPECTRUM OF VIBRATION SIGNALS

This chapter explores the effects of various seeded impeller defects on vibration characteristics and overall performance of the centrifugal pump. Moreover, the chapter describes how the centrifugal pump's vibration levels and performance is affected by the defective impeller faults. Also, the chapter introduces the application of vibration spectra in both high and low frequency detect various impeller faults. Finally, experimental outcomes are presented and discussed.

6.1 Introduction

Depending on the nature of the source that generates vibrations, the vibration signal's content will comprise of various discrete frequency peaks as well as broadband noise. As mentioned above, in a centrifugal pump, broadband content is generated as a result of pressure fluctuations that are caused by fluid turbulence, viscous forces, boundary layers vortex shedding, the lower velocities of process fluid and boundary layers interactions between lower and high velocity zones of the nearby static components of a pump casing. These sources may only be reduced if the pump functions at a design operation [37].

On the other hand, the pumps discrete part vibration characteristics experienced across the spectra are as a results of the interactions between impeller vanes and the adjacent stationary parts, like the volute tongue as well as the periodicities in fluid flow because of the discrete nature of impeller blades of the centrifugal pump. Both mechanisms present discrete parts as a rotational frequency with the shift frequency f_r as well as vane passing frequency f_{vp}.

In addition, impeller defects generate vibrations, which are dispersed over a wide-band of frequency. During the early fault development stages, the impulse generated has low energy levels with a very strong background noise. This resulting impulse stimulates natural frequency for the housing structures and the impeller, which is distinct from the impulse generated by the other components of the machine like bearing. In this case, various types of the impeller faults have been explored in various flow rates in order to understand characteristics of vibrations and define the effective diagnostic features for different fault incidents. Both normal spectrum and bispectrum patterns are used to analyse the vibration signals. The general quantitative understanding concerning pump vibration responses aforementioned, such as the one explored analytically in section three allows one to conduct a detailed examination regarding certain components like vane passing vibrations in order to make accurate diagnostics. Moreover, to established a condition monitoring system for centrifugal pump, in order to analysis the performance of the pump conditions and detect faults of pump components.

6.2 Healthy Impeller

The experiment was carried out on healthy and full opened valve on discharge line by using test rig, which discussed in Figure 5-24. With Different flow rates signals were measured, namely, 50, 100, and 150, up to 450, to know the system behaviour under these conditions. The

test repeated three times with the fixed speed of 2900 rpm and different flow rates the signals were measured. An adjusting valve in the discharge line adjusted the flow rate stage by stage. Each test run had at least 8 data sets recorded which covered the necessary flow range. To achieve reliable results, every test conducted was repeated thrice with time breaks between the tests, to avoid high temperatures and keep the water temperatures almost the same for every test. Each test's data records were then processed in the Matlab in order to analyse signals and to identify various consistent parameters that could enable fault diagnosis in this stage depending on the vibration signal data generated with the healthy case.

6.3 Faulty Impeller with Inlet Vanes (blockage)

A closed type impeller's internal construction is demonstrated in the photograph in Figure 5-25. The point of blockage on the pump's inlet vane is shown in the figure and it is created by blocking the inlet between two vanes; one is small blockage whereas the second is large blockage between the in-let of vanes. After a baseline test was conducted, two other tests were performed from two different defect severities respectively. The first test was under the fault of a small blockage, the second for large blockage. This then allows two degrees of inlet vane blockages to be explored for evaluation of accuracy of vibration based diagnosis.

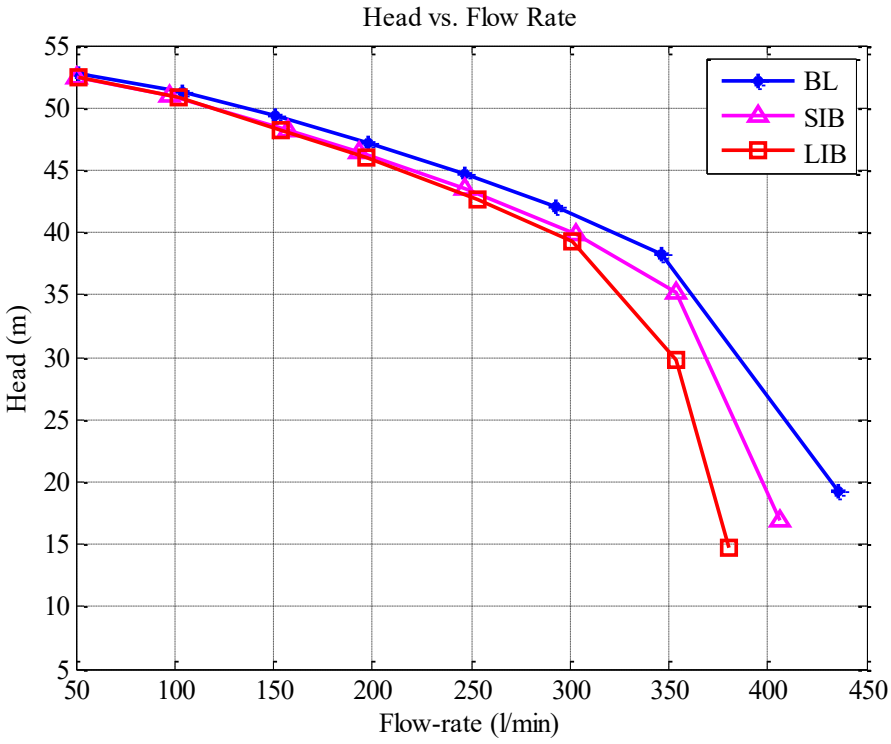

Figure 6-1 Changes of the pump performance

Figure 6-1 presents the differences recorded from the main performance curves of each case, the first impeller is a healthy as baseline one (BL), whereas the second is small impeller blockage (SIB), and third is large impeller blockage (LIB). As Figure 6-1 Figure 6-1 presents the differences recorded from the main performance curves of each case. From the figure, it is evident that the smallest and the large blockages on the inlet vane has led to decreases the performance curves compared with healthy one. It can be understood that the faults have changed the optimal operation. It is expected that this change can be diagnosed from vibration signals measured externally.

6.4 Faulty Impeller with Exit Vanes Effect

A closed type impeller's internal construction is presented in the photograph in Figure 5-26. In this figure, the defect is located at each vane's exit, which is made by removing away 3mm along a lengthwise direction. The cut is done for each vane one by one during the test. After a baseline test was conducted, five other tests were performed from two different defect severities respectively. The first test taken was under defect of a single tip and the second was under defect of two tips and so on. Thus, this allows the fiver vane damage degrees to be explored in order to measure the vibration accuracy based on diagnosis. Moreover, these test cases are represented as BL, F1, F2, F3, F4 as well as F5 respectively so as to ease their discussion.

Five tests were performed on the closed loop centrifugal pump test rig to study the impellers fault detection and diagnosis, each test was performed maintaining same/fixed speed but with various flow rates of 50 l/m, 100 l/m, 150 l/m, 200 l/m, 250 l/m ,300 l/m as well as 340 l/m. The rate of sampling was at 96,000HZ. Seven different signal channels were collected. One of them was from the accelerometer that was placed on the pump's housing. The accelerometer was positioned in a horizontal direction. Each test was performed when the pump was operating at its full speed.

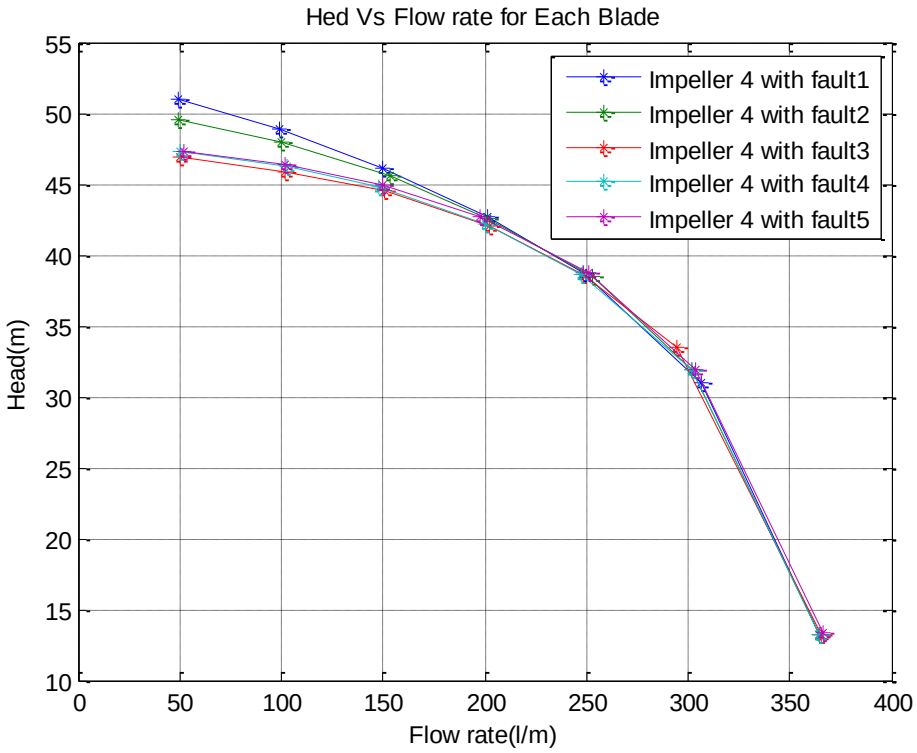

Figure 6-2 Collected data at different flow rates (impeller 4)

The graphical representation of the output shows on Figure 6-2 that the simulated Fault-1 started with the highest head at around 52 m. In Fault-2, where another blade has been treated with a flaw, the head was consequently reduced to approximately 49 m. As the faults was further increased with three blades, the decrease in head becomes more evident, declining to 47 m. Close to this rate, the pressure was further reduced as more blades were subjected to faults as implied in the condition of Fault-4 and Fault-5. The bottom line measure of head acquired the reading of around 46 m. Through all the increased amount of faults for the impeller blades, the flow rate has started at 50 l/m. As observed through the graphical presented in Figure 6-2, the more the number of faults placed on an impeller blade, the higher deterioration of performance is obtained in terms of head and flow rate.

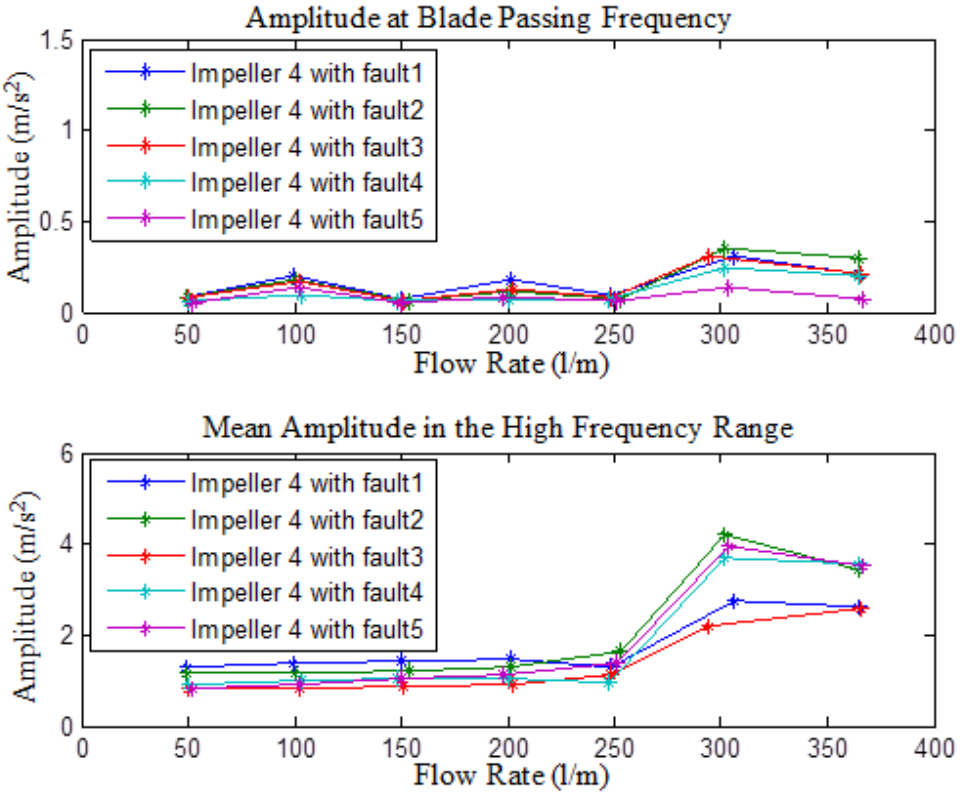

Figure 6-3 Collected vibration data at different flow rates (impeller 4)

Reference to amplitude at blade pass frequency in Figure 6-3, it is observed that the impeller with fault 1 is having moderate amplitude at different frequency range due to the fact that possibly the residual unbalance component has got neutralized, however the flow separation condition is generating the higher amplitude at high frequency. It can further be seen that the vibration amplitude increases with Fault 2 condition as the resultant unbalance components has increased significantly and also the flow separation condition. The condition is same for Fault 3 but with Fault 4 and 5 the amplitude reduces because of the fact that the unbalance components are getting balanced as the mass removal is in approximately from 180-degree location, thus balancing the unbalanced components.

6.5 Healthy and Faulty Impeller with Exit Vanes Effect

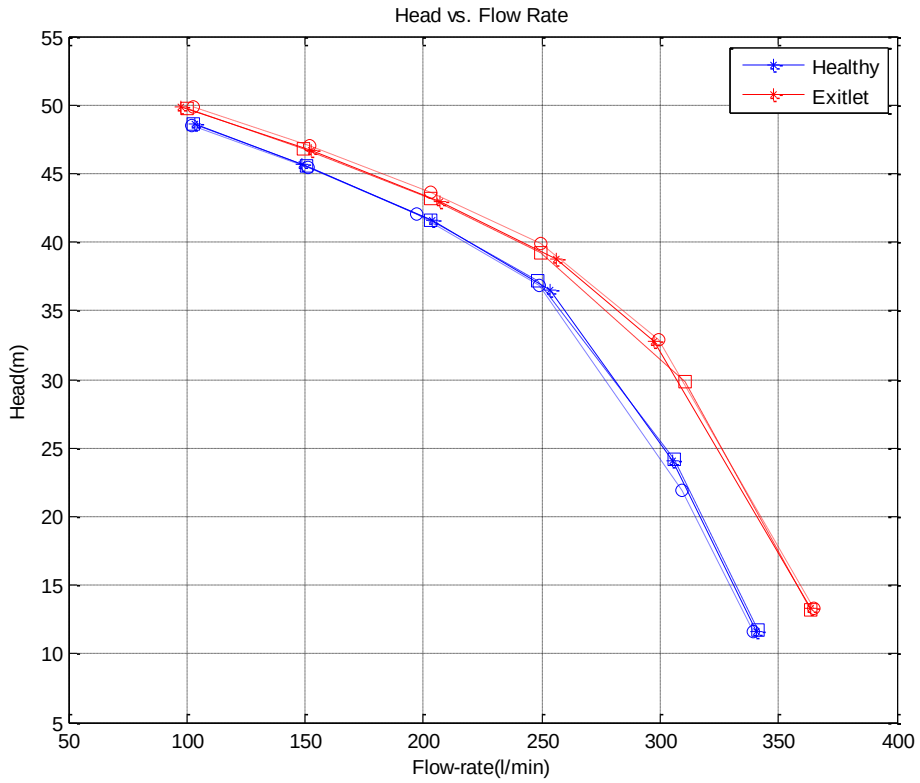

Figure 6-4 Change of pump performance with exit vane defects

The first impeller was a healthy case and the second impeller has an exit vane fault. Figure 6-4 presents the differences between the key performance curves for the two cases and it is evident that an exit vane defect enhances performance. It is understandable that an original design may never be optimal and the main performance may be improved by removing the vane tip. It is anticipated that such a change can easily be diagnosed from vibrations signals that are measure externally.

Both bispectrum patterns and normal spectrum techniques are used to analyze vibration signals in order to understand the characteristics of vibrations and define the appropriate signal features based on various fault cases.

6.5.1 Spectrum Characterises in the Low Frequency Range

As explained in chapter 3, a pump's vibration signals can be distributed over wide frequency ranges. To evaluate the details of various responses, their spectra are explored in frequency of flow ranges between 1 kHz and 10 kHz.

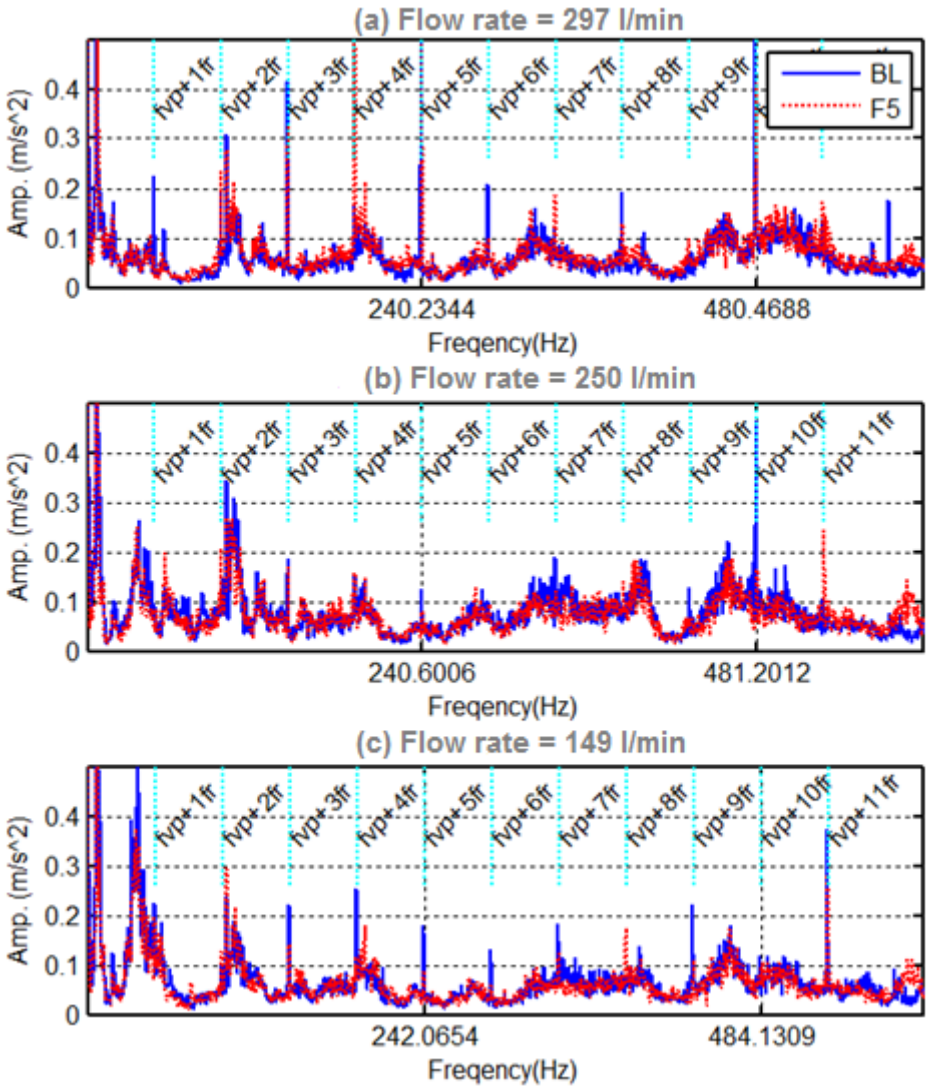

Figure 6-5 Vibration spectrum in the low frequency range

Figure 6-5 presents the low frequency vibration spectrum under three flow rates: below the BEP flow, the BEP flow as well as BEP flow for defect and baseline on the five vanes. It is evident that the vibration spectrum demonstrates a clear broadband because of the flow of turbulence as well as the visible discrete elements as a result of interactions between flow and vane. The broadband amplitudes demonstrated higher amplitudes on BEP operations. These discrete components are typically more distinctive for off BEP operations, demonstrating that increased pressure pulsations are as a result of interaction effects such as the more turbulent

interactions experienced at the BEP. Moreover, discrete components do appear at vane frequencies, f_{VP}= 240.6 Hz as well as 481.2Hz and at shaft frequency of f_r = 48.1Hz as well as its harmonics. The shaft-based commoners, particularly its harmonics attempt to show the symmetry between the vanes. As a result, this could assist to detect the faults. The various frequency values assist in the detection of faults.

However, the distinction between the baseline and the defect case in both discrete components and wideband components is not very clear. Moreover, considering the fact that it is very difficult to have an accurate value of wideband components, it is only discrete components that are recorded at every shaft frequency and evaluated in detail. Figure 6-6 the three typical component against various impeller cases and flow rate are presented. Also, Figure 6-6 [a], 1Xfr presents the same amplitude in all the various flow rates, showing that is more related to misalignments and unbalance problems. Moreover, it does not have any relation with the anticipated behaviour generated by defects.

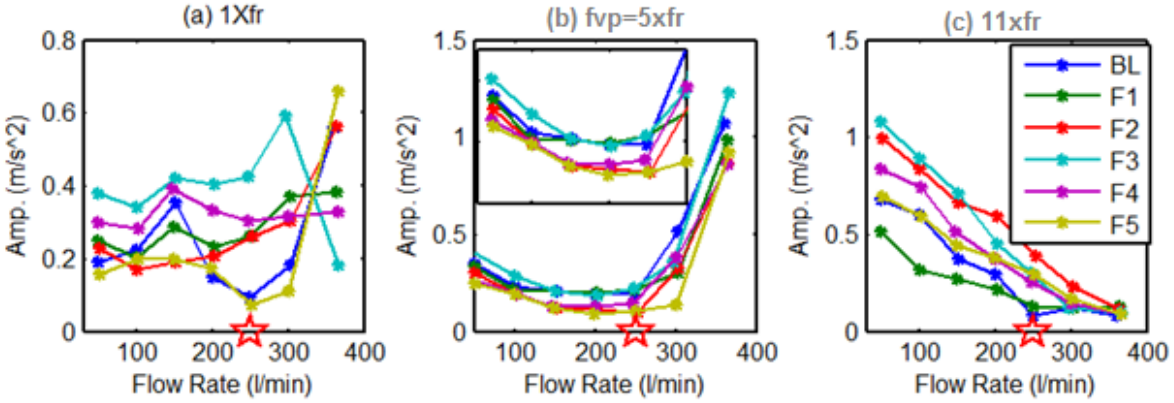

Figure 6-6 Spectral amplitudes of discrete components for different fault cases

Conversely, the component in the vane-passing frequency displays a good match with the vibration at its lowest BEP. Moreover, amplitudes for F3, F4 as well as F5 are lower as compared to the baseline. Also, F1 and F2 were closer to the baseline, indicating that interactions were lower because of the higher recirculation generated by faults. Thus, this component is more related to the fault cased induced. However, it is impossible to separate F3 and F1 from the baseline. Also, it may generate inaccurate diagnosis for F2.

Meanwhile, amplitude behaviours exhibit more consistency with fault cases in flow range, which is lower compared to that of the BEP. This demonstrates that defects generate more vibrations. Particularly, F3 is one of the most asymmetrical defect. Thus, it produces the highest vibrations. F2 as well as F4 the second one and their vibration amplitudes are high. On the other hand, F5 and F1 have the minimal asymmetrical defects and therefore their amplitudes are the lowest and very close to that of the baseline. However, all defect cases' amplitudes near BEP, especially in applications are not very consistent. Especially, the amplitudes of F3, F4 as well as F5 are lower than that of F2.

Generally, discrete components of $11\times f_r$ and f_{vp} can generate large quantities of data for diagnosing vane defects, however they are not very accurate due to influence of the wideband random components.

6.5.2 The Spectrum Characterises of High Frequency Range

Figure 6-7 presents the high frequency range vibration spectrum under three flow rates: below the BEP flow, the BEP flow as well as BEP flow for defect and baseline on the five vanes. It is evident that the vibration spectrum displays a wide broadband. Moreover, amplitude in frequency ranges between 3.5 kHz and 5.5 kHz and it is typically high for higher flow beyond the BEP, demonstrating crucial effects of cavitation.

When comparing spectral difference between F5 and the baseline, it is reported that the amplitude of frequency range decrease or increase with defect degrees. In addition, these two ranges are selected since they have less influence from any noise including the components from variable frequency that come as a result of turbulence effects. Figure 6-8 below presents the average spectral amplitudes of the two ranges. The amplitude exhibits an increasing tendency with flow rates, which match with the anticipated turbulence-based vibrations. The difference between various fault cases cannot be easily differentiated to match with the introduced fault severity. This may be because of changes to defects, which are caused by strong inherent flow turbulence vibration. Thus, it becomes so difficult to utilise high frequency data in diagnosing faults.

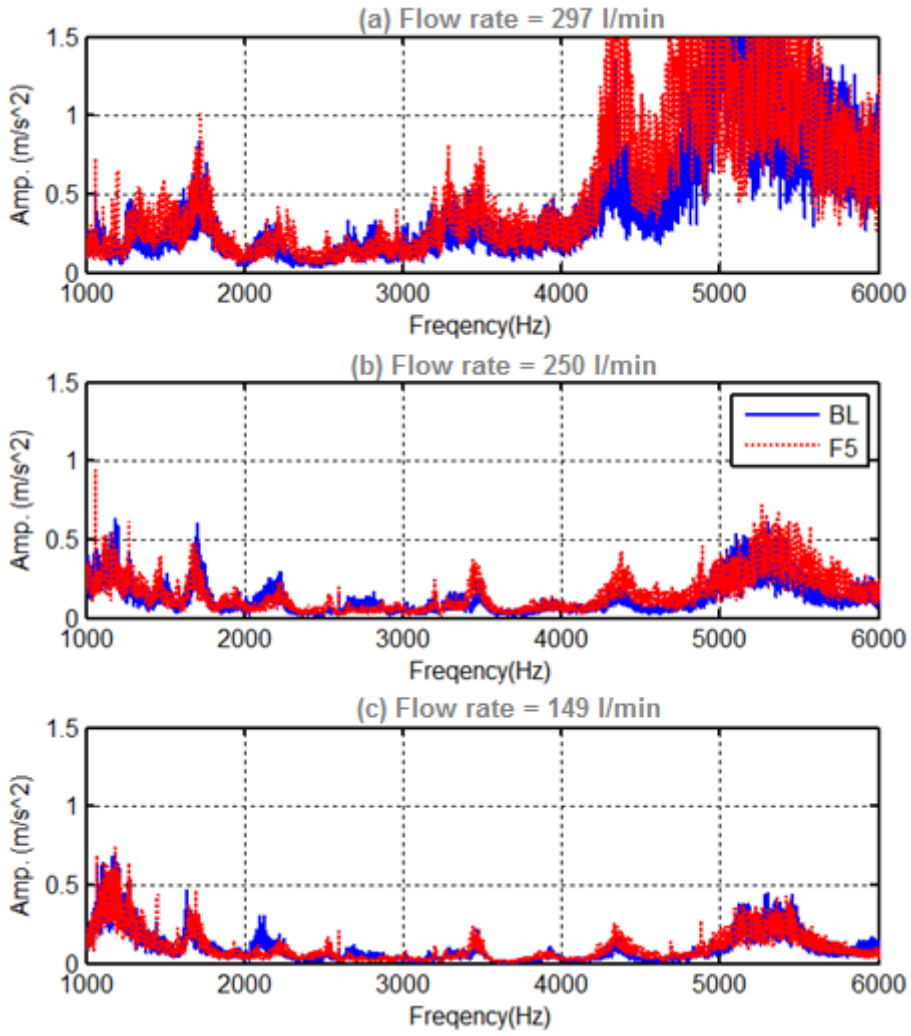

Figure 6-7 Vibration spectrum in the high frequency range

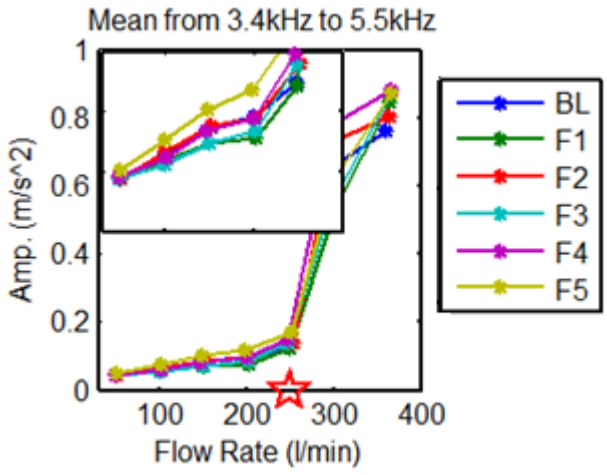

Figure 6-8 Mean amplitude

6.6 Summary

Based on a broad understanding on the pump's vibration characteristics, various experimental studies have been conducted on the centrifugal pump in order to develop effective diagnosis features for the emerging impeller defects. Also, the results for all tests have shown that the trimming of the outer blades of pump impeller at discharge side has changed the operating points completely from its design point and pump head found to be less than expected while flow rate was larger. This is due to a mismatched impeller and casing. As the blade diameter of the impeller decreases, added clearance between the impeller blade and the pump casing increases internal flow recirculation, causes reduction in head, and degrades pump performance.

Moreover, it has been reported that spectral components from a flow turbulence are very predominant in high frequencies exceeding 1 kHz and it shows little changes because of the defects at the impeller's exit tip. On the other hand, discrete components generated by interactions of flow, casing and impeller exhibit more definitive changes because of the defects. In particular, the high-order harmonics at the shaft frequency and amplitudes at the vane passing frequency could be effective aspects for detection as well as diagnosis of fault severities.

The results have shown that at each defective impeller blade, the performance curve is degraded from the baseline curve. The vibration responses are examined to show corresponding changes. By eliminating vibration from other sources, key detection features are extracted to represent the pump conditions with impeller faults. Test results show that features are effective in detecting these types of faults, providing a more reliable way for pump monitoring and diagnosis.

CHAPTER SEVEN

FAULT DETECTION AND DIAGNOSIS OF THE IMPELLER USING THE MSB ANALYSIS OF VIBRATION SIGNALS

This chapter explores a new technique of monitoring centrifugal pump impellers' conditions using surface vibrations with more advanced signal analysis: modulation signal bispectrum. Moreover, this chapter explains how the pump's level of vibration and performance is affected due to the presence of a defective impeller. The chapter also introduces the application of a vibration spectrum in order to detect faults. Finally, various experimental findings are presented and extensively discussed.

7.1 Introduction

In this chapter, the pump diagnosing as well as signal processing methods reviewed in the chapter four are explored. These techniques are frequency-domain, time-domain, as well as envelope spectrum analysis. This chapter aims to provide a detailed insight on these techniques of signal processing when used to diagnose impeller faults, and to identify the effect of different outlet and inlet impeller on the faulted impeller's vibration signals generated. '

In addition, there are three types of impeller conditions tested for the clearance of each impeller; the healthy impeller, which was the reference baseline; the outlet impeller fault; the inlet impeller fault. The particular fault size is selected in order to understand and quantify the effect of vane tips on an impeller vibration signature. In addition, the results are applied to explore the centrifugal pumps performance, which is comprehensively discovered in chapter six.

Conversely, there are component characteristics across the spectra that are as a result of interactions between the impeller vanes and the adjacent stationary objects, like volute tongue as well as periodicities in flow because of the discrete nature of impeller blades of the pump. These two approaches produce discrete components as vane passage frequency f_{vp} and/or rotational frequency f_r .

Also, the vane passing frequency will be modulated by the shaft frequency to produce nonlinear vibration responses. One of the most suitable techniques of diagnosing faults in a centrifugal pump is through examination of the various harmonics as well as sub-harmonics of the rotational speed of the machine in a vibration spectrum. These modulation effects change when various impeller changes occur because of the changes in interactions between the pump's vane tips and the pump's stationary casing. With this understanding, a diagnosis technique based on deterministic information can be developed through characterization of the modulation process.

7.2 Faulty Impeller with Inlet and Exit Vanes Effect

The impeller is one of the common faults in the centrifugal pump in the industry applications. Over its operating life, the impeller spins at several speeds for lengthy periods. Moreover, it's becomes corrupted with grooves and corrugations after operation for age of time. These can lead to both inefficient operation and increased noise levels. Moreover, the reflected load variations from the pump would allow the fault to be detected in the vibration signal.

This experiment is conducted using the same pump casing but with three different pump impellers. The first impeller used is a healthy one. The second impeller has a faulty inlet vane and the third impeller a faulty exit vane. As presented in Figure 5-27, the inlet defect fault was induced on the second impeller by extracting a small part of the vane tip on an edge close to an inlet vane. Similarly, an exit fault was formed at the edges of the exit vane. The previous studies have reported these faults as typical erosion modes.

During the tests, vibration signals from the accelerometer mounted on the pump casings were collected at 24-bit rate and 96 kHz sampling rate. Moreover, performance parameters of the pump including the flow rate discharge rate as well as motor speed were measured. Then, each impeller was mounted on the pump casing in turns and tested for six consecutive flow rates: 100 l/min, 150 l/min, 200 l/min, 250 l/min, 300 l/min, as well as 350 l/min.

Figure 7-1 illustrates the differences of the main performance curves of these three cases. It is evident that inlet defects reduce the anticipated performance. On the other hand, the exit vane faults enhance the performance. It is understood that an original design is not likely the optimal and eliminating the vane tip enhances the main performance. However, both faults change the optimal operation. It is likely that these changes can be diagnosed by measuring the vibration signals externally.

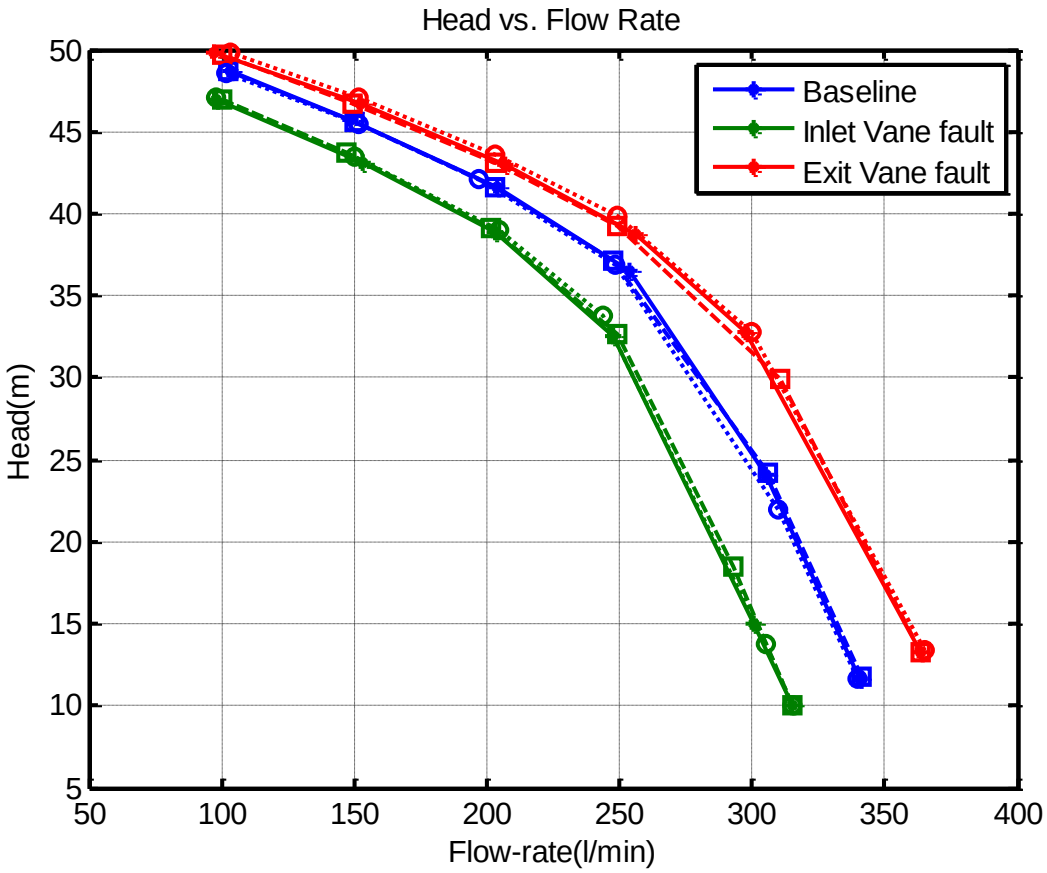

Figure 7-1 The change of pump performance

In order to evaluate the performance of vibration-induced impeller diagnosis, all the signals collected are analysed using the MSB technique to identify effective diagnostic features. Moreover, the findings from the power spectrum are computed using the Equation

(4-19) in order to benchmark the various topics explored in both chapter 2 and 3.

7.2.1 Diagnosis by Spectrum

Figure 7-2 below presents the vibration spectra of three typical flow rates as well as that of the various tested impeller cases. It is evident that the spectrum has both distinctive components as it was expected. They include the continuous components, which have a wideband over the entire frequency range and the discrete tone elements, which are distinctive in a low frequency range. The discrete tone components come as a result of mechanical excitations as well as propeller based flow pulsations. On the other hand, continuous components occur as a result of random excitations such as turbulence and cavitation effects. These demonstrate that vibration signals have information of various sources.

Moreover, the discrete components' spectral amplitudes, such as shaft-rotating frequency, (*fr* =49Hz); van-passing frequency, (*fvp*=245Hz), as well as their harmonics rises with the flow rates, demonstrating that flow pulsating and mechanical sources are highly influenced by the flow velocity or reduced by an increase of the head. Whereas, wideband continuous components show adverse changes with the flow velocity or with increase in pressure.

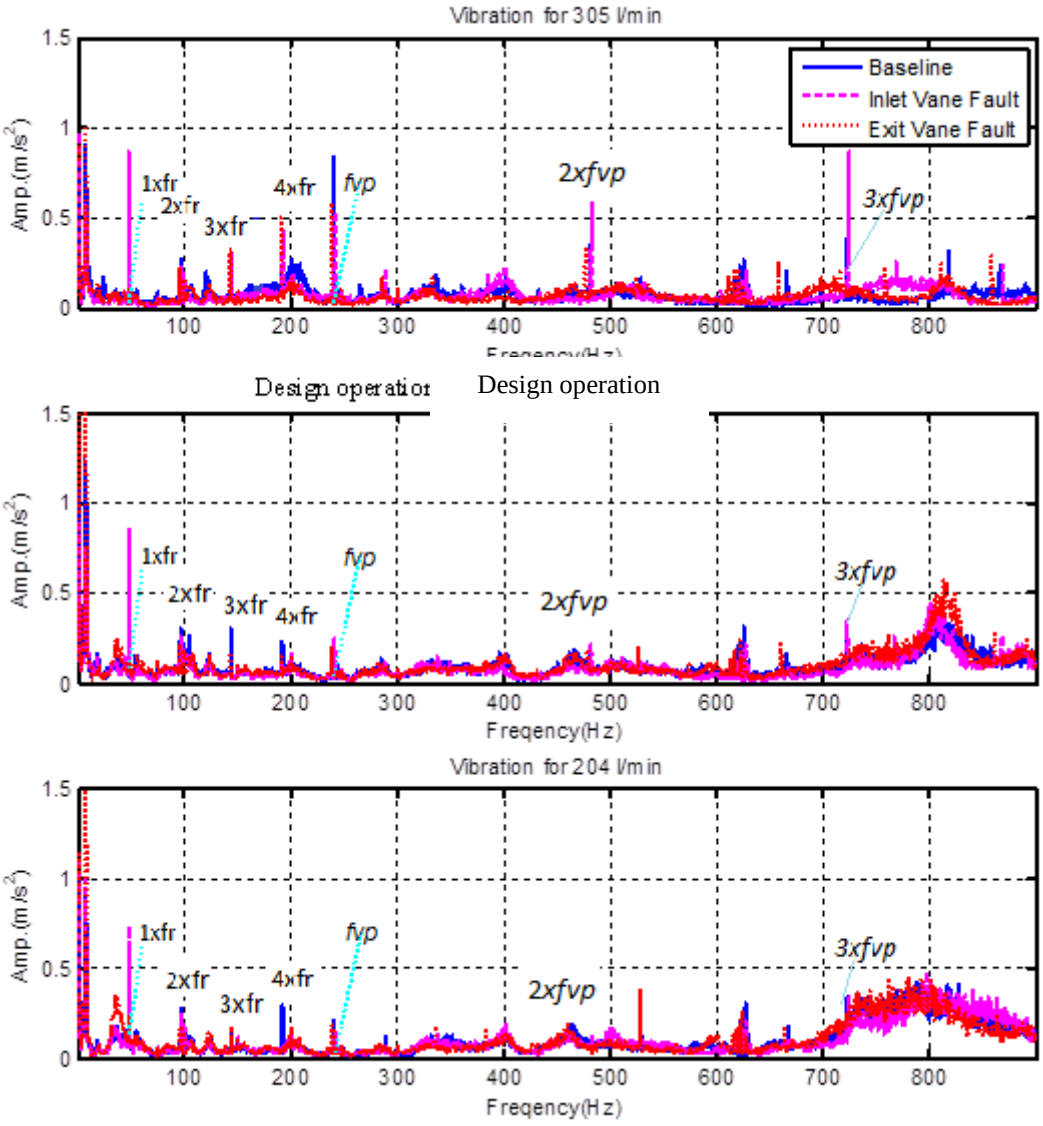

Figure 7-2 Vibration signals in the frequency domain

Also, discrete components exhibit clear differences among the three pump impeller cases. On the other hand, continuous contents exhibit morel less differences. The pattern of the continuous contents in frequency ranges between 600 Hz and 1000Hz and they are similar for all the three cases. Thus, there is more focus on low discrete components to build a diagnostic feature.

The spectral amplitudes presented on Figure 7-3 are averaged over the first four harmonics of the shaft-rotating frequency as well as the first four vane passing frequency with the highest amplitudes as recorded with the Green colure. This demonstrates that amplitudes experience little changes with the flow rates but they allow inlet vane defect to be differentiated fully. However, due to the influence of wideband noise, various exit vane defects can be diagnosed easily when there is a high flow rate.

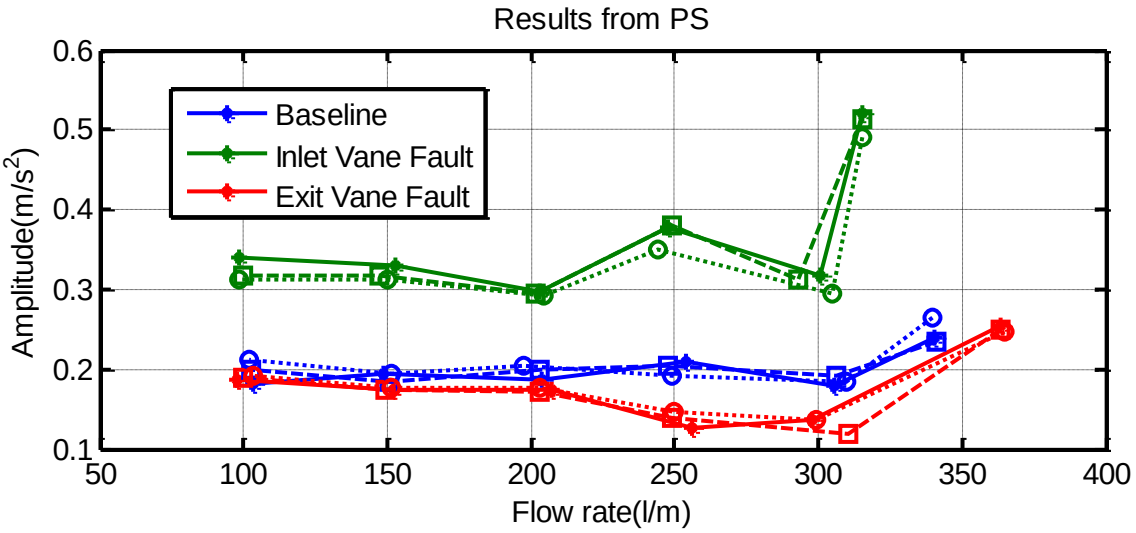

Figure 7-3 The average amplitudes of discreet components

7.2.2 Diagnosis by MSB

In order to enhance diagnosis performance, MSB is used for wideband noise suppression and these improves the discrete components. A representation of MSB at low frequency range is shown in Figure 7-4 The magnitude results of MSB for three graphs of the top row indicate less noise contamination for each of the three cases. Also, their non-linear coupling can be identified further by the consistent MSB coherences recorded in three graphs at the bottom. Moreover, the two results display a distinctive difference among the three cases. The inlet vane peak defect have higher peaks due to higher hydraulic and mechanical pulses. The exit vane fault produces smaller pulses resulting to lower MSB peaks compared to those of inlet vane fault.

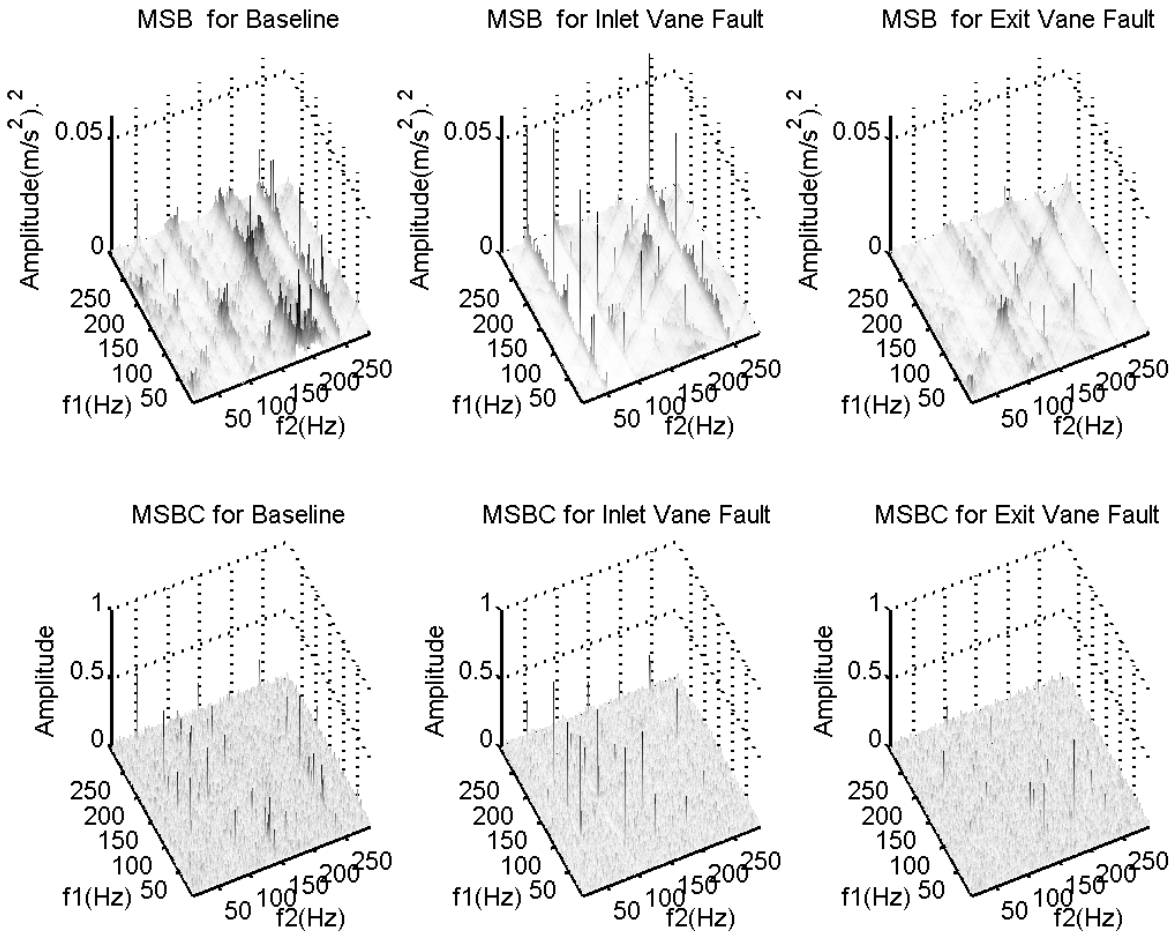

Figure 7-4 MSBc and MSB of the vibration signals for various impeller cases at a flow rate of 305 l/min

The MSB peaks in low frequency ranges are extracted and averaged based on the Equation (4-19).

$$A_B = \frac{1}{4k^2} \sum_{j=m-k}^{m+k} \sum_{i=n-k}^{n+k} A_{ij} \qquad (7\text{-}1)$$

In this equation, (m, n) represents the MSB peak position's index, k=2 denotes the number of spectral lines around the peak (m, n). Figure 7-5. shows the diagnostic features extracted. It demonstrates that a healthy case can be separated from an exit vane fault more distinctively than with the results obtained from a power spectrum. Also, it is very consistent with performance characteristics changes. When the flow pressure is low, the vibration of the inlet vane defect goes higher and vice versa for the case of exit vane defect.

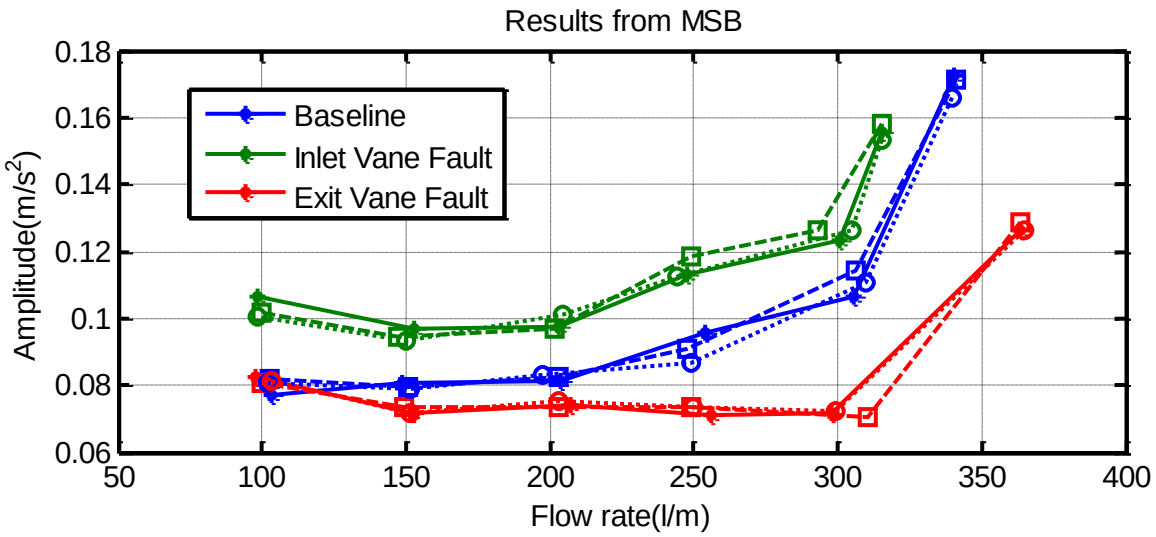

Figure 7-5 Fault diagnosis based on MSB analysis

7.2.3 Summary

The vibration signals are used as the conventional method modulation signal bispectrum in the faults detection for the impeller. However, the third and second impellers have exit vane fault and inlet vane faults respectively. The first impeller is considered a health case. The faults simulated in the pump impeller were compared with the baseline condition. Besides, both a dynamic and static characteristic parameters are involved as features for impeller fault diagnosis. Eventually, the concluded results show a remarkable difference between the three simulated faults of impeller conditions.

Results from power spectrum demonstrates that there is less changes in the amplitudes with flow rates, however it permits inlet vane faults to be differentiated fully. Whereas the results of MSB demonstrates that a healthy case can be separated from an exit vane fault more distinctively than with power spectrum results.

Using the MSB, the spectral amplitudes as a result of pulsations can be estimated accurately. This due to the fact that MSB has the ability to suppress wideband noise. Based on the experimental results, it is evident that the diagnostic feature proposed, which is acquired my averaging the MSB peaks in the low frequency ranges, is an excellent differentiation for exit vane defect and inlet vane fault from an healthy case impeller. This shows that this approach is very effective.

CHAPTER EIGHT

FAULT DETECTION AND DIAGNOSIS OF THE ROLLING ELEMENT BEARING IN CENTRIFUGAL PUMP USING ENVELOPE ANALYSIS

This chapter investigates and monitors the conditions of centrifugal pump, bearings using surface vibration signal analysis, with advanced envelope analysis based on fast Kurtogram. In addition, the chapter explores how defective bearings affect the performance of the centrifugal pump. Which introduces the use of envelope spectrum techniques to obtain the fundamental characteristics of the fault signatures under such conditions.

8.1 Introduction

In this chapter, the signal processing as well as pump diagnosis methods that were previously reviewed in chapter 4 are explored further. These approaches include frequency domain, time-domain, as well as envelope spectrum analysis. This chapter aims to present an extensive insight regarding signal processing approaches and how they are used to diagnose bearing faults and clarify the effects of different inner-race and outer-race on the resulting vibration signals for faulted bearing.

Centrifugal pumps are widely used in different industrial processes, such as power generation plants, the chemistry and petroleum industries. The problem of bearing failures in the centrifugal pumps is a large concern due to its significant influence over industrial production. Particularly, the bearing as the core parts of the pump is subject to different corrosions and theirs faults can cause major degradation of pump performances and lead to breakdown of production. Therefore, an early detection of such faults would provide information to take timely preventive actions.

The bearing is one of the common faults in the centrifugal pump in the industry applications. Over its operating life, the bearing spins at several speeds for lengthy periods. Moreover, it has becomes corrupted with grooves and corrugations after operation for age of time. These can lead to both inefficient operation and increased noise levels. Moreover, the reflected load variations from the pump would allow the fault be detected in the vibration signal.

The aforementioned works are mainly based on the statistical characteristics of the vibration signals and how they are used to detect and diagnose faults. These techniques may lack generalization because the statistical characteristics highly depend on design features as well as the various applications of the pumps. Moreover, the results obtained cannot be explained from an engineering perspective and this makes it very difficult to be convinced of fault presence at the early stages. To address the shortcomings of these technique, this research aims to develop detection and diagnostic approaches with more deterministic features like the pump’s vibration components. Also, the study focuses on approaches to diagnose early defects on a pump, which are as a result of corrosion such as inevitable cavitation turbulence as well as bearing. A good number of the bearings become faulty at early stages due to wear, static load, corrosion, contamination, overheating, or lubricant failure.

8.2 Test Specification and Procedures

In this experimental study, the same test-rig used as the test-rig, which used in the 5-post-test experiments, for more details and specifications (see Chapter 5). To investigate further enhancement for the effects of the bearings on the performance of the centrifugal pump, the experimental data collected from the bearing of the pump test rig illustrated in Figure 5-2. It is composed of motor, shaft, bearings, and pump pipes, tank. The pump bearing type is FAG Type 6307 Ball Bearing and its geometric dimensions presented in Table 8-1. In addition, the accelerometer, and (sensor) measurement system is installed vertically on the bearing pump case in order to offer a complete measurement for vibration data.

Table 8-1 Specification of FAG type 6307 ball bearing

Parameter	Measurement
Number of Balls	8
Ball Diameter	13.49mm
Pitch Diameter	58.42mm
Contact Angle	0

This work characterises vibration signals from a centrifugal pump to determine an effective and reliable feature sets for detecting and diagnosing bearing faults. As the signals contain high-level background noises due to inevitable flow cavitation and turbulences, noise reduction and feature extraction are critical procedures in vibration signal analysis. This work presents an improved envelope analysis parameters including the filtering band frequency to investigated and suppress the noise and optimise band filter parameters. Vibration signals under three different conditions (baseline, inner-race fault, outer-race fault) are based on to evaluate the method. It has shown that the improved envelope analysis produces correct detection for each type of the faults and their compounds.

There are three different cases will be used for the experimental purpose. The first is a healthy one whereas the second and third have bearing faults. Tests are for different of simulated defects on bearings, for each test the vibration is measured at the fixed motor speed of 2900 rpm but with nine increments of flow rates of 50, 100, 150, 200, 250 350 and 450 l/min.

Seven channels were used to collect the data from the test rig as given in Table 5-10, with sampling rate of 96000Hz. A shaft encoder that is mounted on the motor measures the rotational speed of the pump, and the accelerometer located on the pump casing to measure the vibration

of the pump. In addition, two pressure sensors installed in the suction and discharge lines respectively, also Hydrophone mounted on discharge line and the Microphone installed 50mm away from the Pump to measure the pump vibration, where flow sensor installed in the discharge line for flow rate measurement.

The experiment was carried out based on three different cases one healthy and two bearings inner and outer-race faults. The healthy one taken as the baseline form comparison for both two bearings are induced (A) inner-race fault and the same way (B) outer- race fault. Figure 5-28 shows the bearing inner and outer race faults. Were tested under full constant speed (2900) rpm and nine different flow rates (0, 50,100,150,200, up to 450) each test acquired data for forty seconds duration time.

8.3 Rolling Element Bearing Fault Frequencies Calculations

Pumps are very demanding applications for bearings. Many factors such as flow, temperature, pressure and others have to be considered prior to the selection of the right bearing for specific applications [82]. Two main causes of the failure of centrifugal pumps are excessive leakage and bearing problems. There are many reasons for the failure of the bearing balling element these include excessive heating of the bearing due to improper dissipation of heat, excessive radial load caused by low flow operation, misalignment of the unit, bent shaft or severe vibration within the installation [127]. Bearing problems can be best corrected by replacing the defected bearing and by correcting the problem behind the fault.

The rolling-bearing parts are considered some of the most significant components of rotating machinery systems. They are components that easily wear out due to interactions with the stationary parts. Therefore, most of the system failures occur due to faulty bearing operations with the machinery. In order to find the balling element bearing faults, as the bearing consists of outer-race and inner-race, the cage, and balling elements as shown in the Figure 8-1, balling element bearings can frailer in different ways such as spalls, due to fatigue in the manner spalls appear on the outer race, inner race or balling components. Provided that race has a spall, then it will affect the balling elements periodically. A fault signature is signified by consecutive pulses with repetitive rates depending on a faulty element, rotational speed and geometric dimensions. The period between various impacts is distinct for the various elements listed and it depends on the bearing's geometry, load angle and rotational speeds. Theoretical fault

frequencies of the fixed outer race bearings can be computed using these equations are presented below [84].

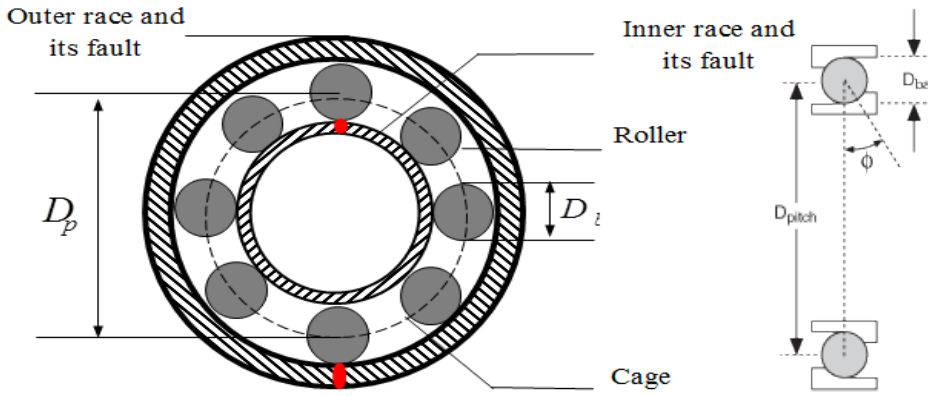

Figure 8-1 Balling element bearing components and fault location

Table 8-2 Fault characteristic frequency and equation [128]

Fault type	**Equation Calculation**		**Defect Frequency (Hz)**
Inner Race	$BPFI = \frac{nf_r}{2}\left(1+\frac{d}{D}\cos\phi\right)$	(8-1)	241.5
Outer Race	$BPFO = \frac{nf_r}{2}\left(1-\frac{d}{D}\cos\phi\right)$	(8-2)	150.9
Fundamental train frequency	$FTF = \frac{f_r}{2}\left(1-\frac{d}{D}\cos\phi\right)$	(8-3)	18.7
Ball Spin	$BDF = \frac{D}{2d}\left(1-\left(\frac{d}{D}\cos\phi\right)^2\right)$	(8-4)	100.5

where, d represents the ball diameter; D denotes the pitch diameter; n represents the number of balls, ϕ denotes the contact angle as well f_r represents the shaft-rotational frequency (Hertz). Moreover, there is often a slippage and slight sliding, especially when the bearings are under

dynamic loads as well as severe loads. Thus, these frequencies may show slight differences form the one calculated as listed in Table 8-2.

8.4 Signal Processing Techniques Results and Discussion

The vibration is greatly influenced by the water flow; therefore, the characteristics of these behaviours are quite different which results in the change of the optimal bands. To achieve a reliable bearing fault detection, the selection of the optimal band is quite important. In this work, an automatic band selection technique, Fast Kurtogram is used to select the optimal sub-bands for further envelop analysis.

Figure 8-2. presents the procedure for signal processing procedure. Firstly, the demodulated signal's quality depends on the selected frequency band for demodulation, which needs two parameters; central frequency and bandwidth. In this case, Kutorgram optimization will be employed because of the different central frequencies and bandwidths. It is an SK cascade derived from various values of STFT (Short Time Frequency Transform) window length. Once the fast Kurtogram selects the frequency band, it the computes the envelope of the vibration signal analysis conducted to improve the non-linear elements of the signal. The following step is to extract these features at different bearing characteristics frequencies form the power spectra results.

Envelope analysis is considered one of the appropriate techniques for diagnosis of machinery faults whose amplitude modulation affects the machinery's characteristic frequencies [104]. Based on this algorithm, the modulating signal's power spectrum is computed and the various steps for its application are presented below.

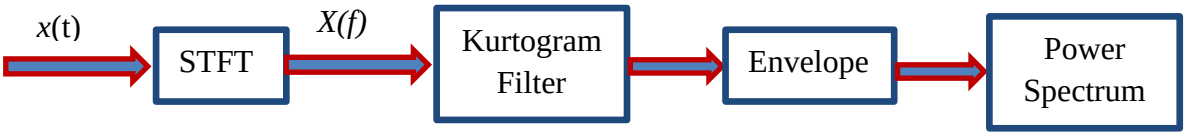

Figure 8-2 Procedures of envelope analysis

On the first step, the band pass filter is used to eradicate low frequency contents that have high amplitude signals as a result of misalignment or imbalance as well as high-frequency noise from measurement system. This enables the system to achieve a good signal to noise ratio. [104]. Figure 8-3 shows the raw data vibration signals; for baseline presented and two faulty signals for inner race defect and outer race defect. It can be seen that the amplitude of the faulty signals, Figure 8-3 (b) and (c), a little higher compared to that of baseline signal as presented in, Figure

8-3 (a). Based on the central frequency obtained and the Kurtogram's window length values, an 80 order FIR (finite impulse response) band pass filter with a pass-rand ranging between 2000Hz and 5000Hz is used to filter various vibration signals as presented in Figure 8-4.

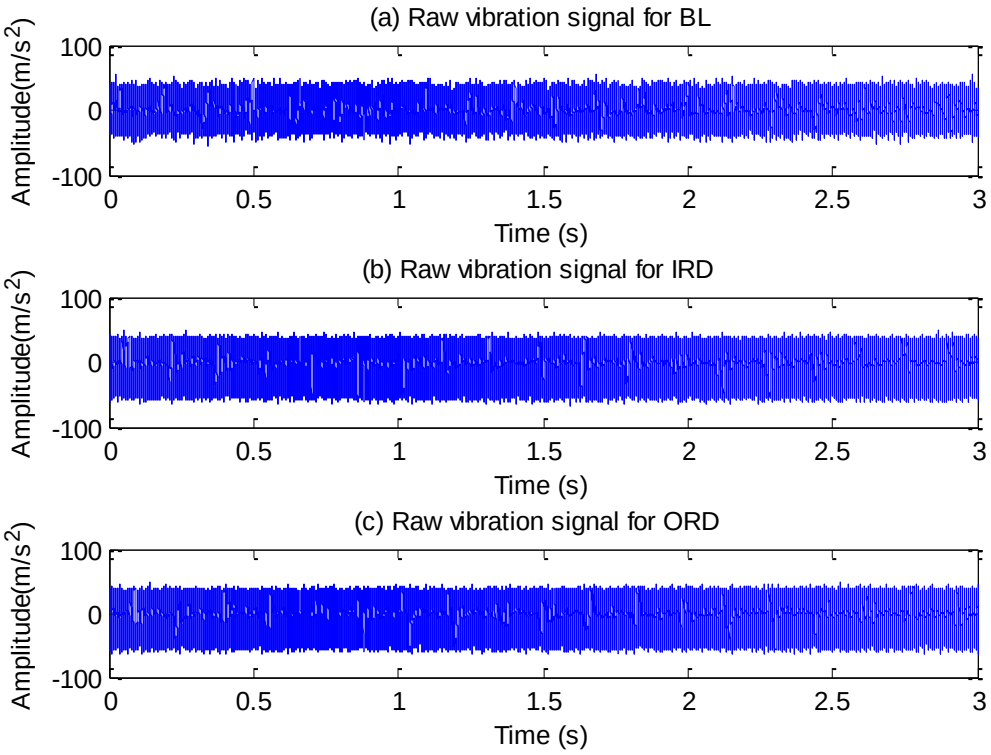

Figure 8-3 Raw data of vibration signal

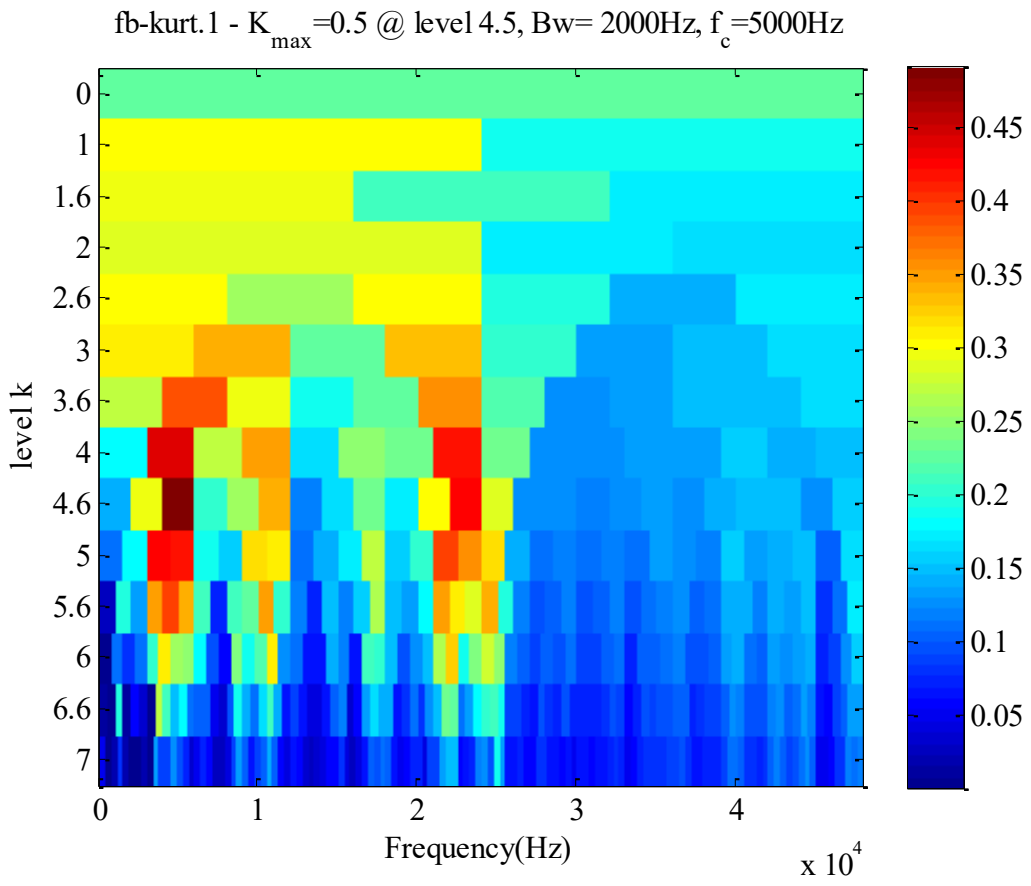

Figure 8-4 Fast Kurtogram optimised filter results

Second step, signal's envelope is calculated by using the FFT. The signal measured is considered a complex signal with the real part only [105]. The Equations (4-5), (4-6) and (4-7) illustrates the procedures followed when calculating FFT. The analytical signal's real part represents the original data. Also, equation (4-8) presnts the envelope of a vibration signal.

The third step, the envelope's power spectrum is presented in equation (4-9). Moreover, by applying this technique, the computing buffer may be reused and this is a very significant fora processor with little storage.

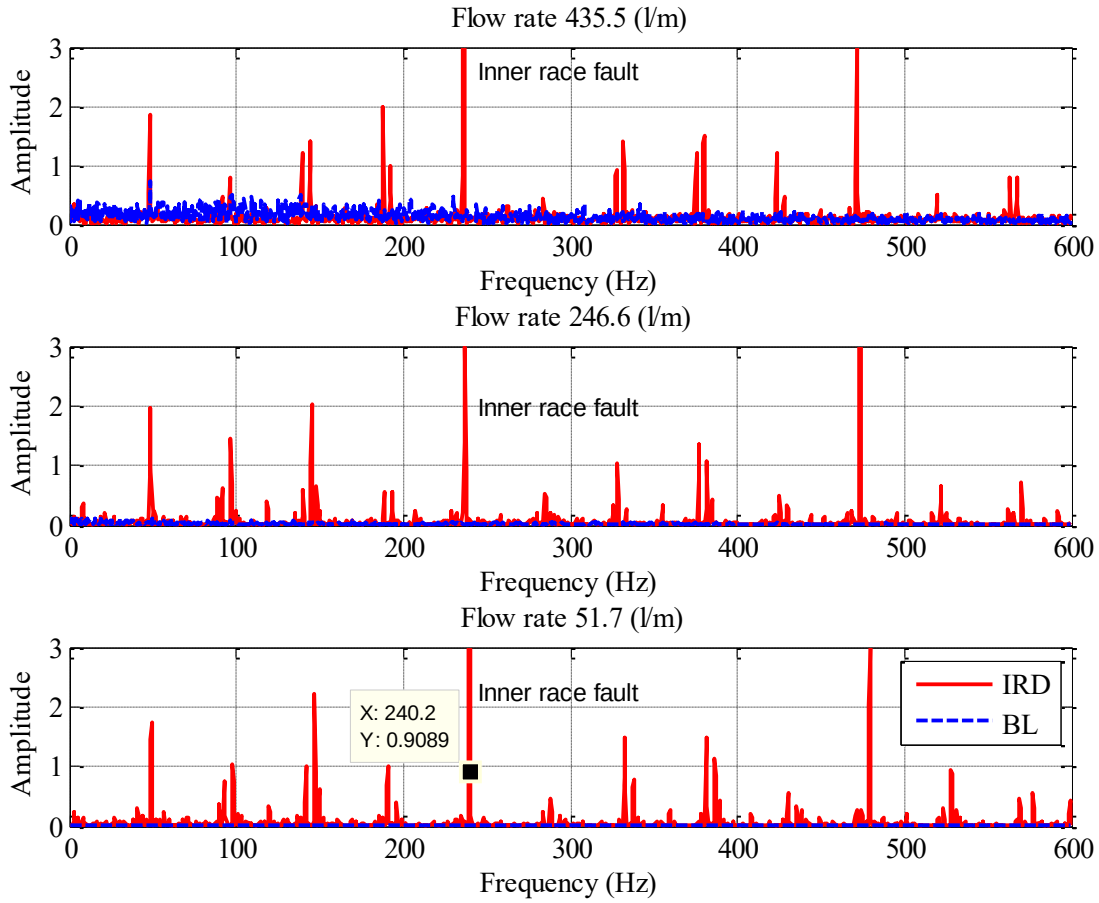

Figure 8-5 Envelope analysis results for inner-race defect

Figure 8-5 gives envelope analysis results of inner-race fault and baseline under three typical different flow rates. From the figures, it is obvious that characteristic frequencies and their harmonics are significant, the amplitude of inner race defect frequency around 241Hz appear on the three cases almost the same peaks respectively in comparing with the baseline case. The dominant peaks in the spectrum can easily identified by the difference between the baseline and the faulty cases. Moreover, the shaft frequency and high order harmonics can easily have identified. The results from envelope analysis indicate that the approach can be used for detection of faults. It can also be used to reveal the specific fault type using the fault characteristics frequencies.

In addition, the discrete components' spectral amplitudes, such as the inner-race defect frequency (241Hz), shaft rotating frequency (49Hz) and their harmonics increases with flow rates, showing that flow pulsation and mechanical sources are significantly influenced higher flow velocity or limited dumbness due to increased fluid pressure.

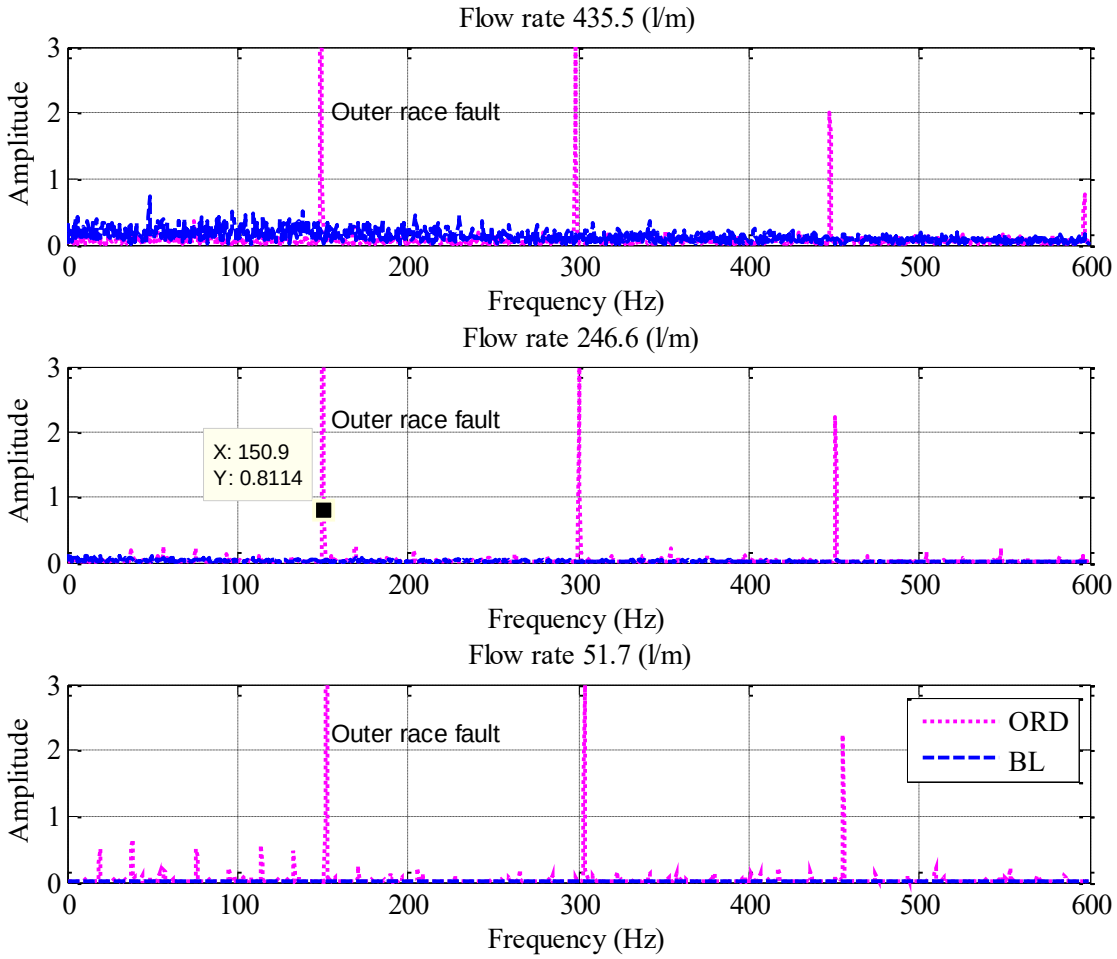

Figure 8-6 Envelope analysis results for outer-race defect

Figure 8-6 gives the envelope spectrum of the baseline and outer-race fault under the three typical different flow rates. It can be obvious that the characteristic frequencies and their harmonics are clearly visible compared with inner-race. The amplitude of outer-race defect frequency around 150Hz appear on the three cases almost the same peaks respectively when comparing with the baseline case. Furthermore, the dominant peaks in the spectrum can easily identified by the difference between the baseline and the faulty ones. Therefore, it can conclude that the optimized envelope analysis can be implemented on the ball element bearing outer-race defect detection and diagnosis. Moreover, discrete components appear both in the outer race fault frequency of 150 Hz and shaft-frequency of 48Hz as well as in its harmonics. All shaft-related commoners, particularly its harmonics van show the asymmetry between the vanes. This could be so crucial in detecting the faults.

8.5 Summary

This chapter examines the optimized envelope-based fast Kurtogram analysis approach for detection as well as diagnosis of the roller element bearings. Based on the general understanding of the pump's vibration characteristics, experimental studies have been conducted on the centrifugal pump in order to develop suitable diagnosis feature for bearing faults. A detection of balling bearing faults diagnosis on the STFT based on fast Kurtogram has a strong ability to optimize the parameters with minimal constraints on centre frequency and bandwidth for further envelop analysis. The results for both simulated as well as actual bearing vibration signals show the effectiveness of the proposed approach to extract the balling bearing fault impulses buried in the noisy vibration signal. In the meantime, can be effective features for the detection and diagnosis bearing conditions.

Moreover, the fast kurtogram has noise suppression capability. Also has shown that the improved envelope analysis produces correct detection for each type of the bearing outer and inner race defects and their compounds.

CHAPTER NINE

DETECTION AND DIAGNOSIS OF COMBINED FAULTS

This chapter details the investigation into monitoring the conditions of centrifugal pump with combined faults on both the bearings and impellers. Vibration signals were collected when the pump were induced with small and large impeller blockages (shorten as SIB and LIB respectively thereafter) alongside with an outer race defect on the bearing (ORD). Based on these signals, both conventional methods such as spectrum analysis and the advanced analysis such as Kurtogram based envelope spectrum and MSB analyses are evaluated in detecting and diagnosing these faults under different flow rates.

9.1 Introduction

Centrifugal pumps are widely used in different industrial processes, such as power generation plants, the chemistry and petroleum industries. The problem of failures in centrifugal pumps is a large concern due to its significant influence over industrial production. Particularly, as the core, parts of the pump, bearings and the impellers are subject to different corrosions and their faults can cause major degradation of pump performances and lead to breakdown of production. Therefore, an early detection of such faults would provide information to take timely preventive actions.

A centrifugal pump contains the rotating part and the stationary part. The rotating part is composed of a shaft and a pump impeller while the stationary part includes the casing, bearing, electric motor and an associated cooling fan. Based on the working process, the pump vibration sources can be categorized into two types as mechanical and hydraulic sources. Mechanical sources caused by vibration of unbalanced rotating masses and friction in bearing and seals. The hydraulic sources are due to fluid flow perturbation in the pump and interaction between the rotor blades and stationary component such as the volute tongue or guide vanes [129].

This work characterises vibration signals from a centrifugal pump to determine an effective and reliable feature sets for detecting and diagnosing pump faults from the bearings and impellers. As the vibration signals contain high-level background noises due to inevitable flow cavitation and turbulences, noise reduction and feature extraction are critical procedures in vibration signal analysis. Therefore, power spectrum analysis alone does not produce correct detection for both bearing and impeller faults.

However, considering the modulation effect between rotating shaft and vane passing components in the low frequency band, a modulation signal bispectrum (MSB) method employed to extract these deterministic characteristics of modulations, which is different from previous researches in that broadband random sources are often used. Experimental results show that the diagnostic features developed by MSB allow impellers with inlet impeller blockage and bearing outer-race defect to be identify under different operating conditions.

9.2 Test Specification and Procedures

To investigate further enhancement for the effects of the bearings on the diagnostic performance of the centrifugal pump, the experimental data analysed in this work are collected

from the bearing of the pump test rig illustrated in Figure 5-2. In this experimental study, the test-rig used is the same as that detailed in Section 0.

This works mainly based on statistical characteristics of vibration signals for detection and diagnosis. As these statistical characteristics are highly depending on the design features and applications of different pumps, these approaches may be lack of generalisation. In addition, the results often cannot explain by engineering sense, making it difficult to convince the presence of faults at early stage. To overcome the shortcomings of the methods, this study focuses on developing detection and diagnostics using more deterministic features such as the vibration components from the pump. In addition, it focuses on the diagnosis of early faults on the pump, which are subject to different erosions including inevitable cavitation turbulence and bearing.

There are three different cases will be used for the experimental purpose. The first test is a healthy one whereas the second have bearing and impeller faults, Tests are for different of simulated defects on bearings and impeller, for each test the vibration is measured at the fixed motor speed of 2900 rpm but with seven increments of flow rates of 50, 100, 150, 200, 250 350 and 450 l/min.

The data acquisition was connected to seven channels were used to collect the data from the test rig as given in Table 5-10 with sampling rate of 96000Hz. A shaft encoder that is mounted on the motor measures the rotational speed of the pump and the accelerometer located on the pump casing, measures the vibration of the pump. In addition, two pressure sensors installed in the suction and discharge lines respectively, also Hydrophone mounted on discharge line and the Microphone installed 50mm away from the Pump to measure the pump vibration, where flow sensor installed in the discharge line for flow rate measurement.

The experiment was carried out based on three different cases healthy one where’s the second the third have bearing outer-race defect + small and large impeller blockage faults. One bearing and impeller are healthy and taken as the baseline form comparison. Figure 5-29 out the photo of defect on the inlet impeller blockage faults and Figure 5-30 shows the bearing outer race fault and its position on the pump shift. Were tested under full constant speed (2900) rpm and nine different flow rates (0, 50,100,150,200, up to 450) each test acquired data at fourthly seconds record.

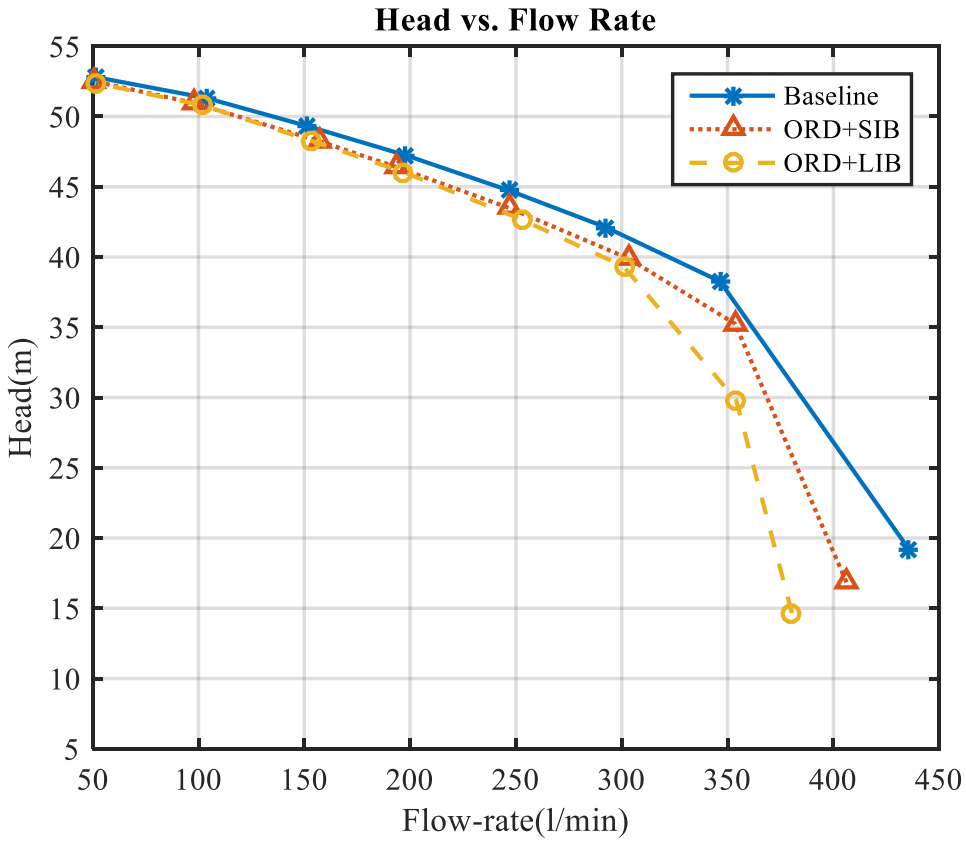

Figure 9-1 Change of performance curve. Appendix C

Figure 9-1 shows the differences of main performance curves for three cases, the first is a healthy as baseline one (BL), whereas the second has bearing outer-race plus a small impeller blockage (ORD+SIB), and third has bearing outer-race plus a large impeller blockage (ORD+LIB) have inlet vanes fault (blockage). As Figure 9-1 shows the differences of performance curves for three cases, it can be seen that the ORD+SIB and the ORD+LIB which are blockages on the inlet vane has led to decreases the performance curves compared with healthy one. It can be understood that the impellers fault has changed the optimal operation, whereas the bearing fault has not changed the performance curves. It is expected that this change can be diagnosed from vibration signals measured externally.

9.3 Spectrum Analysis based Diagnostics

This section aims to study the spectrum analysis based diagnostics of the bearings and impellers under different fault conditions and flow rates.

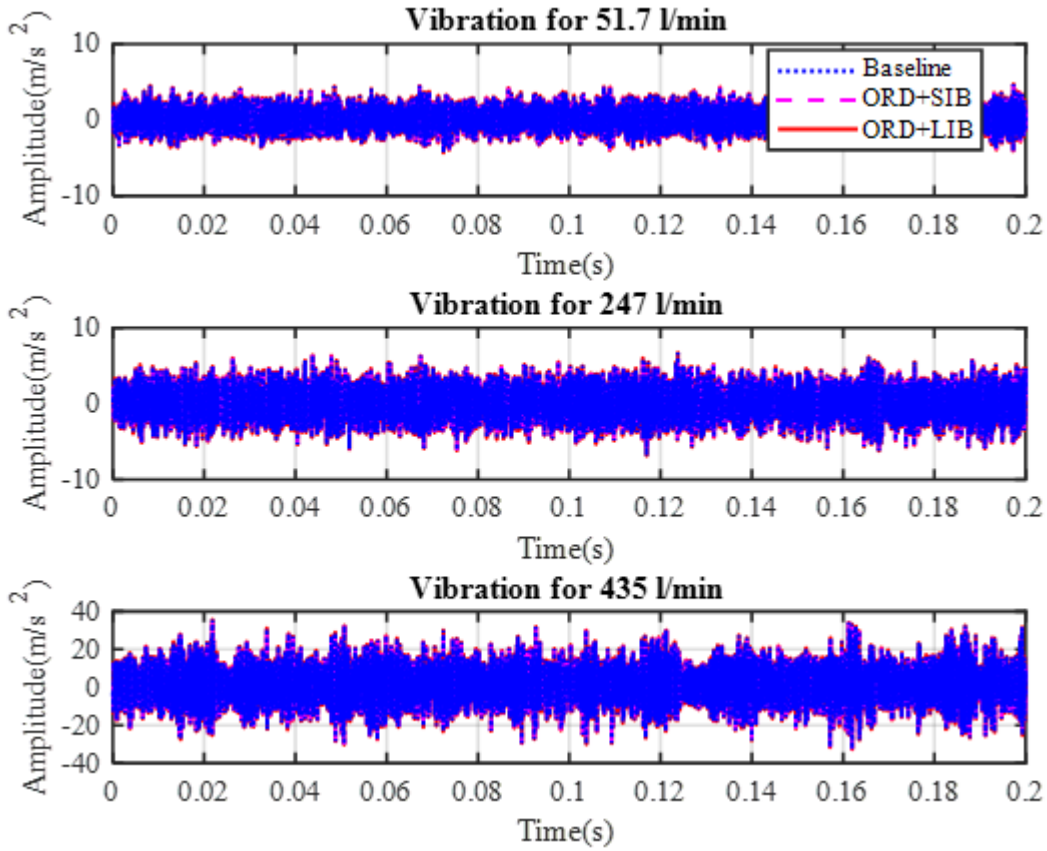

Figure 9-2 Vibration signal in time domain. Appendix C

Figure 9-2 shows the vibration signals; for three different cases stated as (BL, ORD+SIB, ORD+LIB) under different flow rates from 51 l/m, 247 l/m and 400 l/m. It can be observed that the results of the three cases baseline and two faulty signals for inner race defect and outer race defect that the amplitude of the faulty signals are slightly higher than that of the baseline signal.

9.3.1 Spectrum comparison

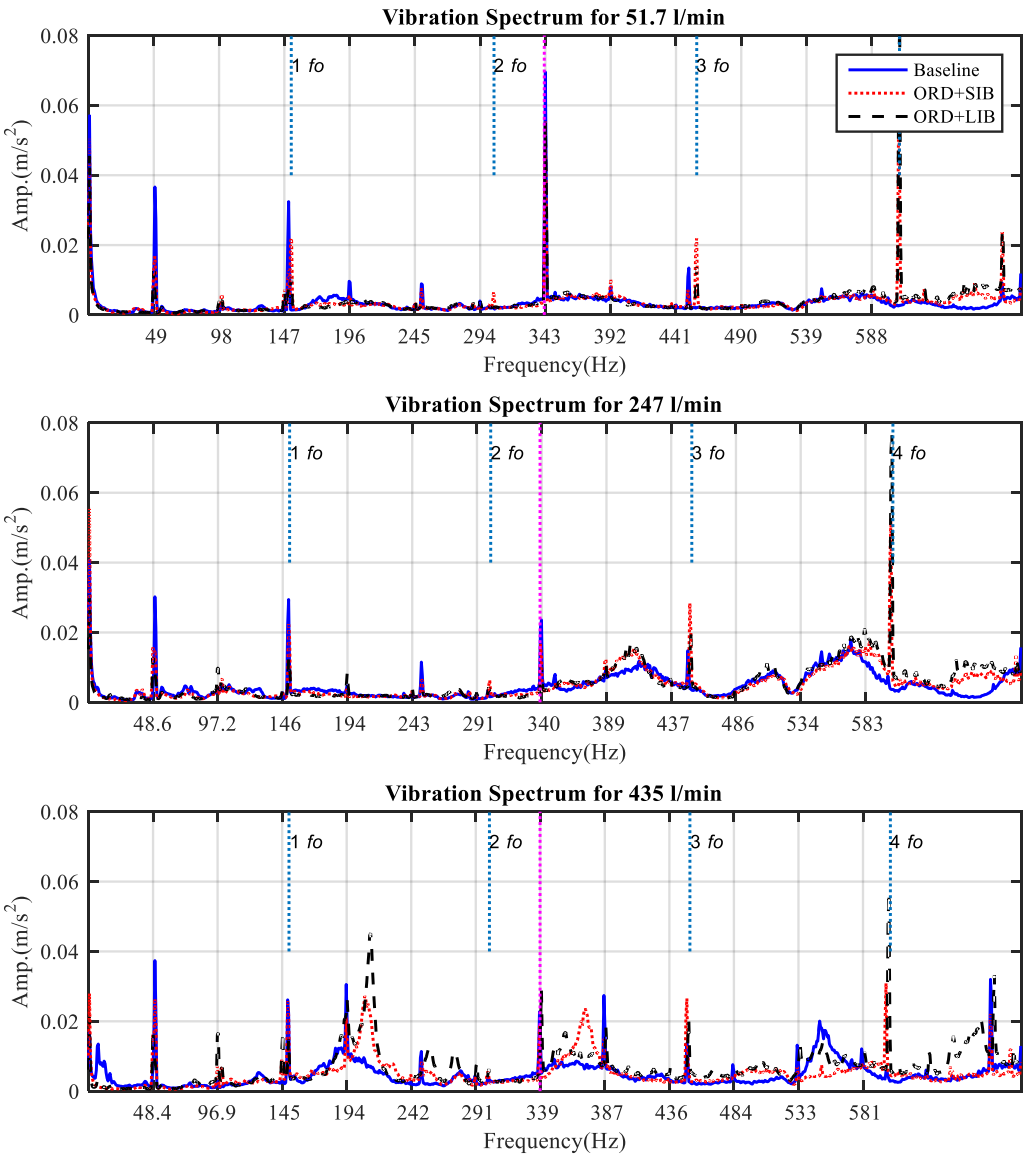

Figure 9-3 Vibration spectrum in the low frequency range

Figure 9-3 shows the vibration spectrum in a low frequency under three typical flow rates: above 400 l/m flow rate, around 250 l/m flow rate and low flow 50 l/m for the baseline and the defects on bearings and impeller. It can be observed that the vibration spectrum exhibits clear broadband due to flow turbulence and visible discrete components due to the interactions between vane and flow. In addition, the discrete components appear at the frequencies of 147 Hz and second harmonics 292 Hz but also at the shaft frequency 48.4.1Hz and its harmonics. Moreover, the $4f_O$ it's the 4 harmonics of bearing outer-race which have both fault appear at the same harmonics. The shaft related commoners all most for three different flow rates,

especially at its harmonics may indicate the asymmetry between vanes and hence could be useful for reveal the faults. It is difficult to find the characteristic frequencies for making diagnostics. However, these mechanisms of generating vibration cause the structure of the pump to vibrate. Moreover, general vibration responses to faults characteristic frequency Small differences and usually masked by random noises due to unsteady flows.

9.3.2 Detection and Diagnosis of Impeller Faults

The diagnostic features extracted are shown in Figure 9-4. For three different cases stated as (BL, ORD+SIB, ORD+LIB) under different flow rates from 50 l/m to 400 l/m. It can be observed that the results of the three cases at graphs from f_r to $7f_r$ cannot which cannot be separated. In addition, when marriage the middle row $5f_r$ + $3f_r$ it can shows that the both impeller faults can be separated from the healthy case with more distinctively less noise contamination for all three cases. Especially, their nonlinear coupling can be further identified. Which is spirited over the large impeller blockage fault at the first 4 harmonics of shaft rotating frequency and the first vane passing frequency. It shows that the amplitudes show less change with low flow rates under 300 for (SIB) but allows the (LIB) faulty to be differentiated fully, because of the influences of the wideband noise. Moreover, it is consistent with the changes of the performance characteristics.

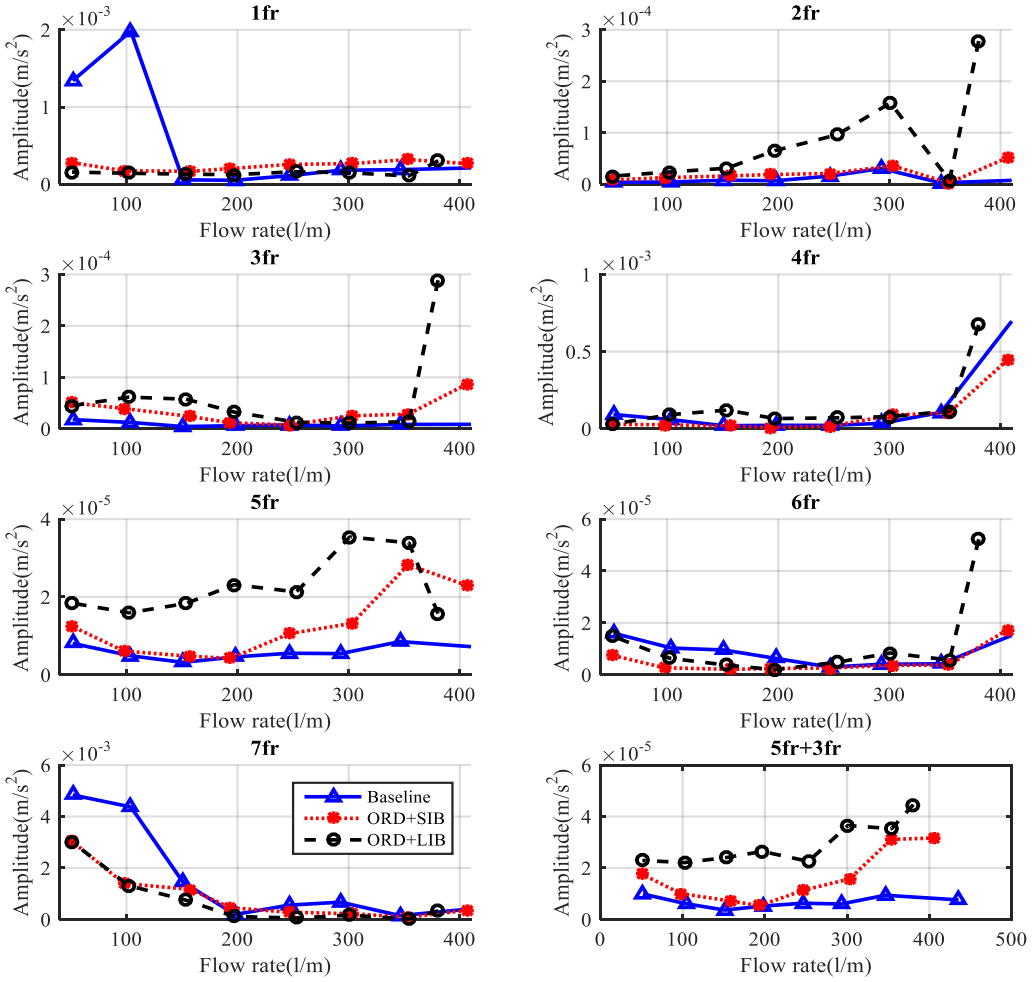

Figure 9-4 Comparison of diagnostic results for impeller faults

9.3.3 Detection and Diagnosis of Bearing Faults

Figure 9-5 shows the spectrum of vibration data collected on pump bearing for three different cases stated as (BL, ORD+SIB, ORD+LIB), under different flow rates from 50 l/m up to 400 l/m. It can be observed that the results of the three cases at graphs from $1f_o$ to $4f_o$ which can observed that from the two bottom graphs $3f_o$ and $4f_o$ shows that the both bearing faults can be separated from the healthy case with more distinctively less noise contamination for all three cases as shown in Figure 9-5. which is spirited over the bearings with large impeller blockage fault at all flow rates range. It shows that the amplitudes show the change with high flow rates above 300 for (SIB) but allows the (LIB) faulty to be differentiated fully, because of the influences of the wideband noise. Moreover, it is consistent with the changes of the performance characteristics.

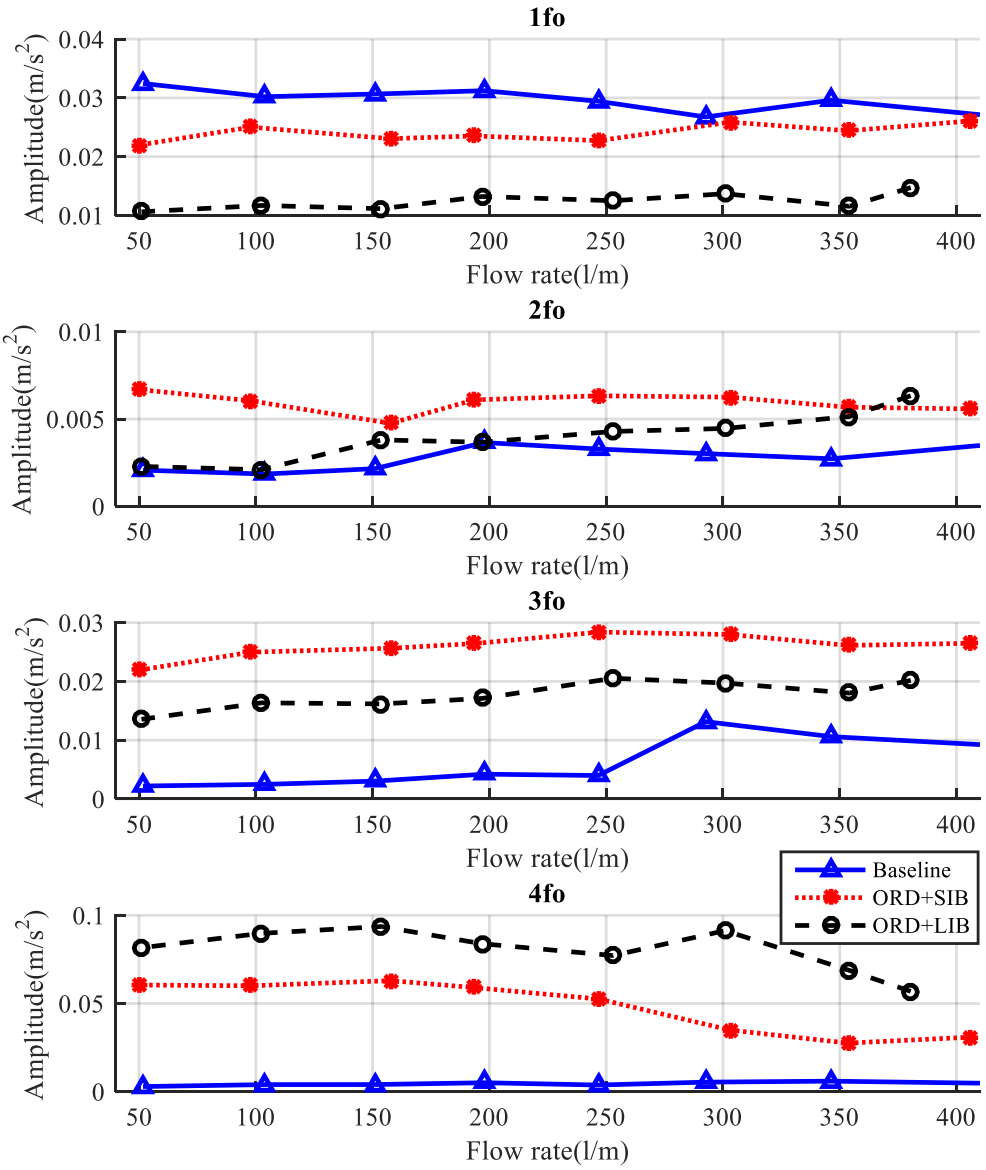

Figure 9-5 Comparison of diagnostic results for bearing faults using spectrum

9.4 Envelope Analysis based Diagnostics

The envelope spectrum has been applied to remove the resonance frequency by using a band-pass filter, which to extract these small changes, Kurtogram based envelope spectrum can easily identify the bearing fault.

9.4.1 Optimal Bands based on Fast Kurtogram

The vibration is greatly influenced by the water flow; therefore, the characteristics of these behaviours are quite different which results in the change of the optimal bands. Moreover, the centre frequency will be around several kHz. This means that a measurement system needs

such a wide band and data size is large. To achieve a reliable bearing faults detection, the selection of the optimal band is quite important. In this work, an automatic band selection technique, based on Fast Kurtogram, used to select the optimal sub-band for further envelop analysis, and hence it allows resonance regions to be identified and envelope filter edges to be selected as shown in Figure 9-6.

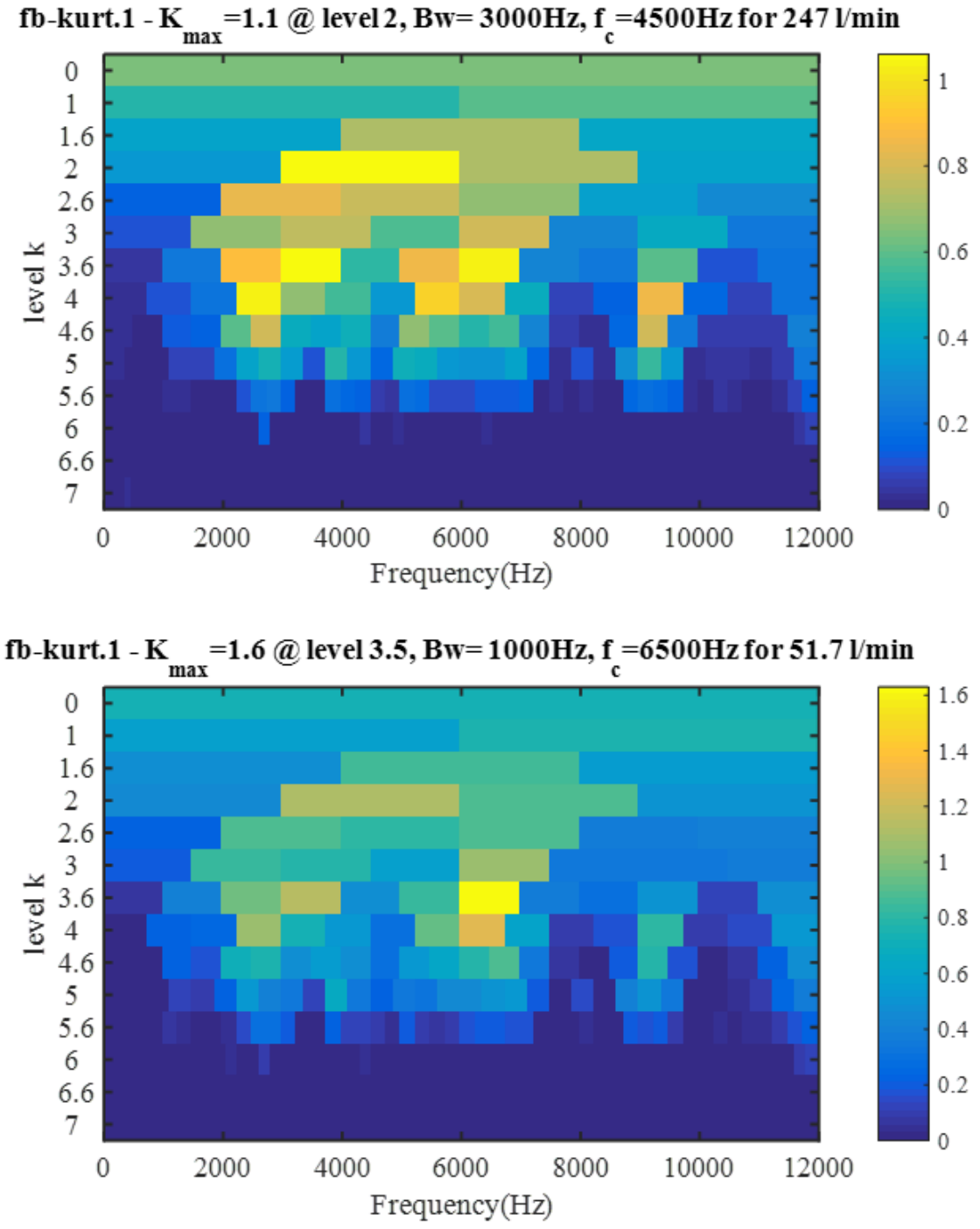

Figure 9-6 Fast Kurtogram optimised filter results. Appendix C

9.4.2 Bearing Fault Detection and Diagnosis

Generally, vibration responses to faults periodic with bearing characteristic frequency small differences and usually masked by random noises due to unsteady flows. By applying the fast Kurtogram to the vibration signal collected from (ORD+SIB, ORD+LIB), it results in an optimal filter as presented in the Figure 9-6. illustrates the fast Kurtogram (filter bank) for the collected signal contains irregular pulses along with white background noise. The maximum kurtosis value with the filter bandwidth is 4500 Hz and the central frequency is 6500 Hz.

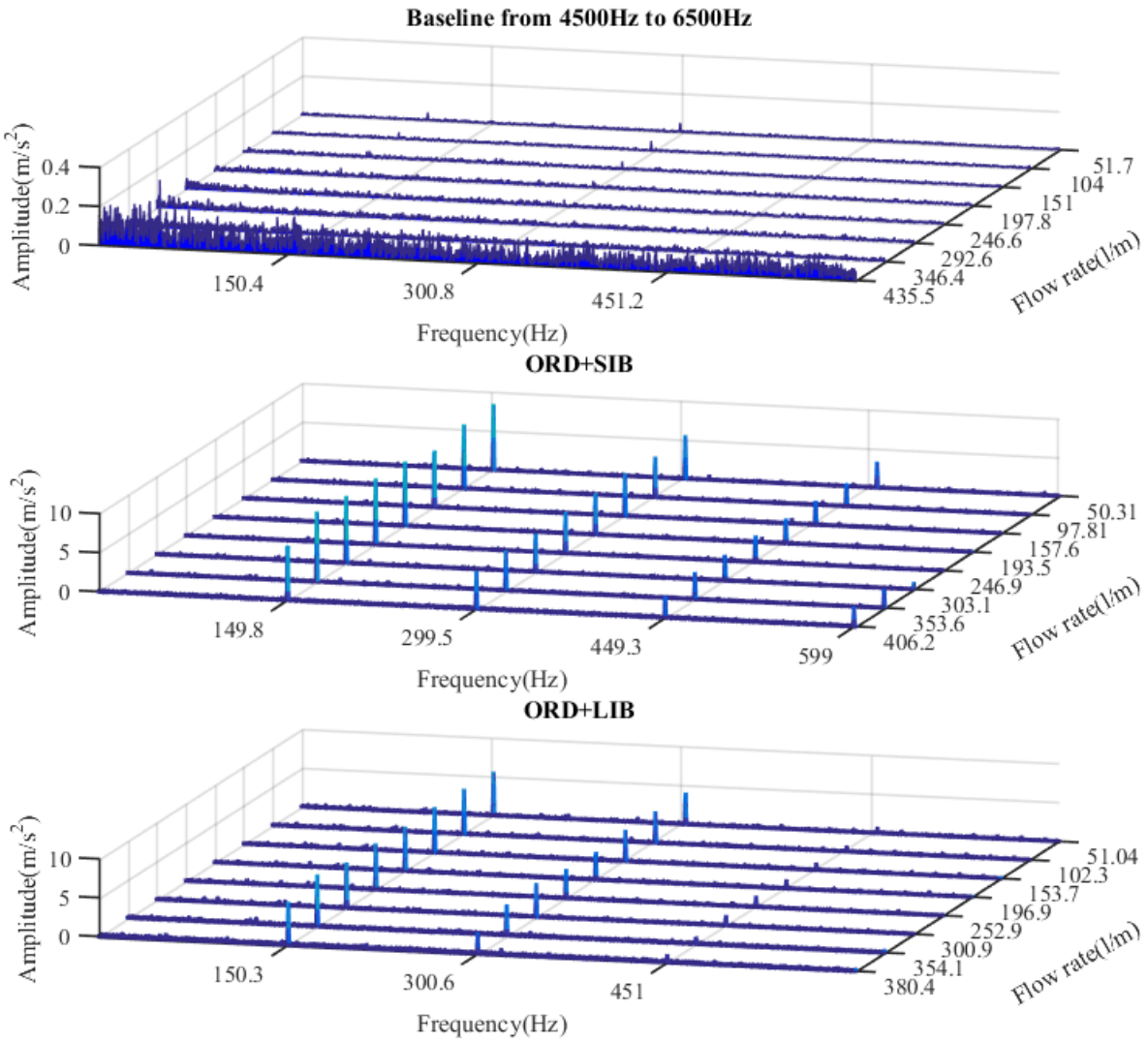

Figure 9-7 Envelope spectrum of filtered signal (BL), and (ORD+SIB, ORD+LIB)

Figure 9-7 illustrates the envelope spectrum of the baseline and the outer-race defect + small impeller blockage, outer-race defect + large impeller blockage. A clear indication for the presence of a fault can be seen. Moreover, the characteristic of the outer-race defect frequency and its harmonics clearly indicated, as well as the pair of modulation sidebands. It can be obvious that the characteristic frequencies and their harmonics are clearly visible compared to spectrum. The amplitude of ORD frequency around 150 Hz appear, when compared with the baseline case, which has no fault induced to. Furthermore, the dominant peaks in the envelope spectrum can easily identified by the difference between the baseline and the faulty ones as shown in Figure 9-7. In addition, envelope spectrum has very high-level background noise and no distinctive peaks appear at the fault frequency only for bearings defect. To extract these small changes, Kurtogram based envelope spectrum can easily identify the bearing fault. Therefore, it shows that the envelope spectrum detector is much more accurate and reliable than spectrum.

9.4.3 Impeller Fault Detection and Diagnosis

Not able to find any features for impellers, which in turn clarify that the envelope based on fast kurtogram is not sufficiently robust for impellers blockage because it is very sensitive to random noise and large aperiodic impulses, which normally exist the wideband content from flow turbulences and cavitation is more random in nature.

Moreover, it can be concluded that the optimized envelope analysis can be implemented on the ball element bearing outer-race defect only, which not be able to identify the impeller faults. In addition, envelope spectrum has very high-level background noise and no distinctive peaks appear at the fault frequency only for bearings defect.

9.5 MSB Analysis based Diagnostics

This section aims to study the Modulation signal bispectrum analysis based diagnostics of the bearings and impeller faults under different conditions and flow rates.

9.5.1 Bearing Fault Detection and Diagnosis

9.5.1.1 Characteristics of MSB

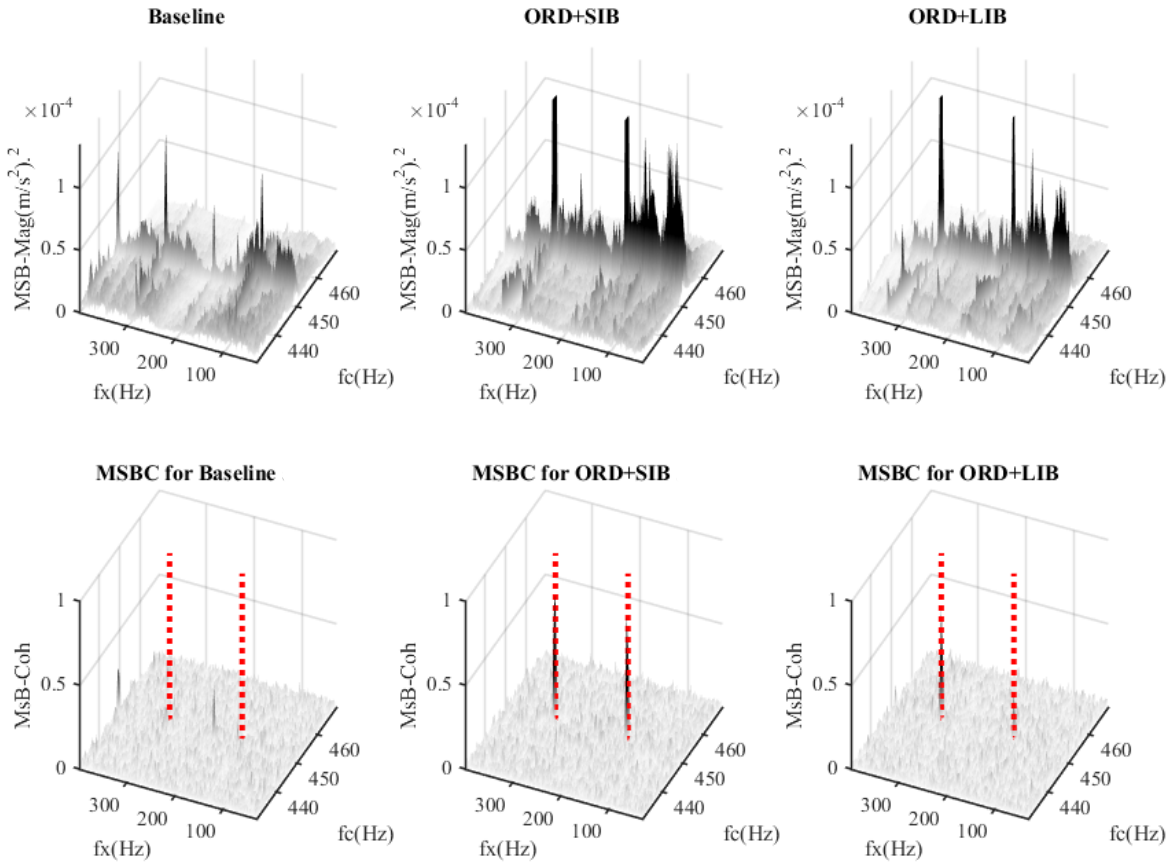

Figure 9-8 MSB magnitude and MSB coherence of vibration signals for bearing different cases at flow rate 250 l/min. Appendix B

Figure 9-8 shows the MSB magnitude and MSB coherence of vibration data collected on pump bearing for three different cases stated as (BL, ORD+SIB, ORD+LIB). The MSB magnitude results of the three graphs on top row show less noise contamination for all three cases. Especially, their nonlinear coupling can be further identified by corresponding MSB coherences in the three graphs of the bottom row. Subsequently, the average of the two components obtains the results from MSB coherence detector as shown on the three graphs of bottom row, which are coloured, red. In addition, the results show clear peaks at outer race fault frequency and its second harmonic, when compared with the baseline case, which has no fault induced to. In the meantime, both results show distinctive differences between three cases in that the outer race faults causes higher peaks because of higher mechanical pulses during to the defects whereas the baseline induces very smaller pulses and hence lower MSB coherence peaks.

9.5.1.2 Diagnostics of Bearings Based on MSB

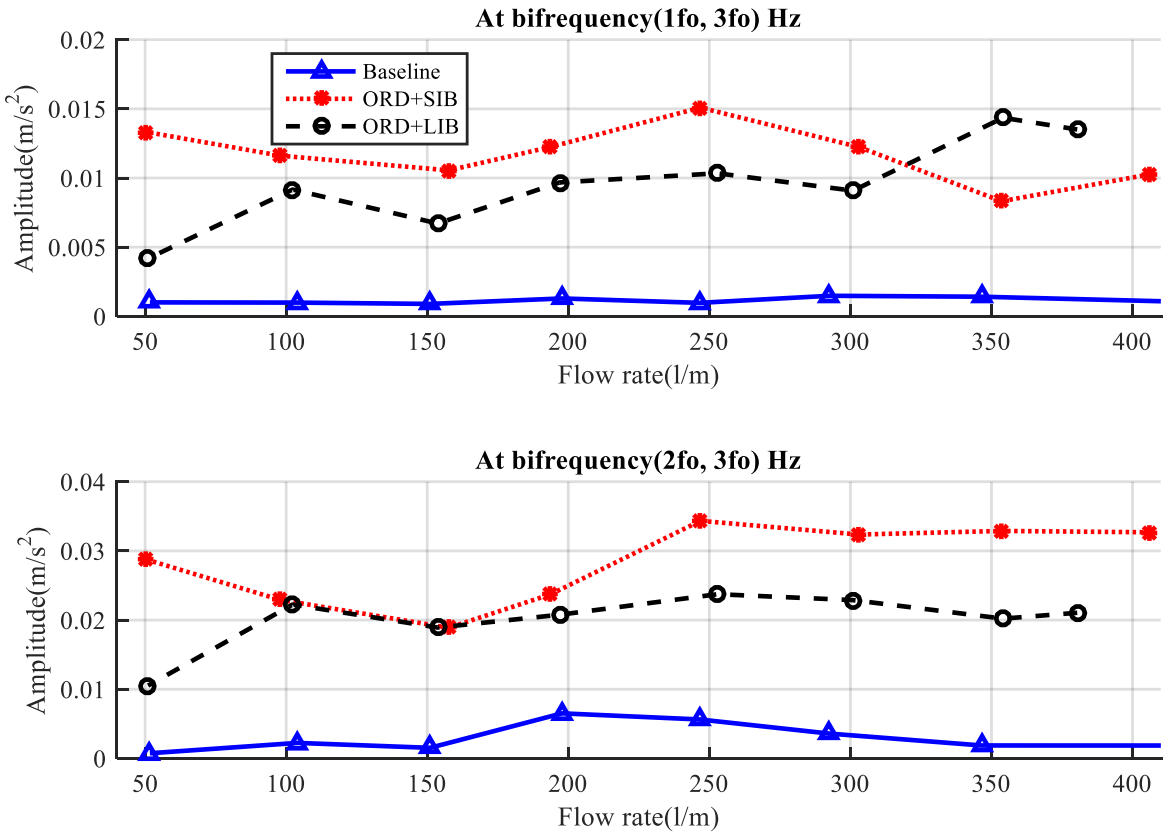

Figure 9-9 Comparison of diagnostic results for bearing faults. Appendix B

The diagnostic features extracted as shown in Figure 9-9 for three different cases stated as (BL, ORD+SIB, ORD+LIB) under different flow rates from 50 l/m up to 450 l/m. It can be observed that MSB magnitudes at the bifrequency pairs of $1f_o$- $3f_o$ and $2f_o$ - $3f_o$ allow both bearing faults to be separated from the healthy case due to the effect of MSB noise reduction.

By combining the results between the two pairs, the two fault cases can be also separated completely. In particular, MSB magnitudes at$1f_o$- $3f_o$ gives better separation at lower flow rates (<300l/m) while MSB magnitudes at$2f_o$- $3f_o$ produces good separating under high flow rates (>200/m).

Moreover, these separation behaviours are consistent with the changes of dynamic characteristics. As the flow pressure is lower or flow rate is higher, the vibration goes higher for the (ORD+LIB) fault and vice versa for the (ORD+SIB).

9.5.2 Impeller Fault Detection and Diagnosis

9.5.2.1 Characteristics of MSB

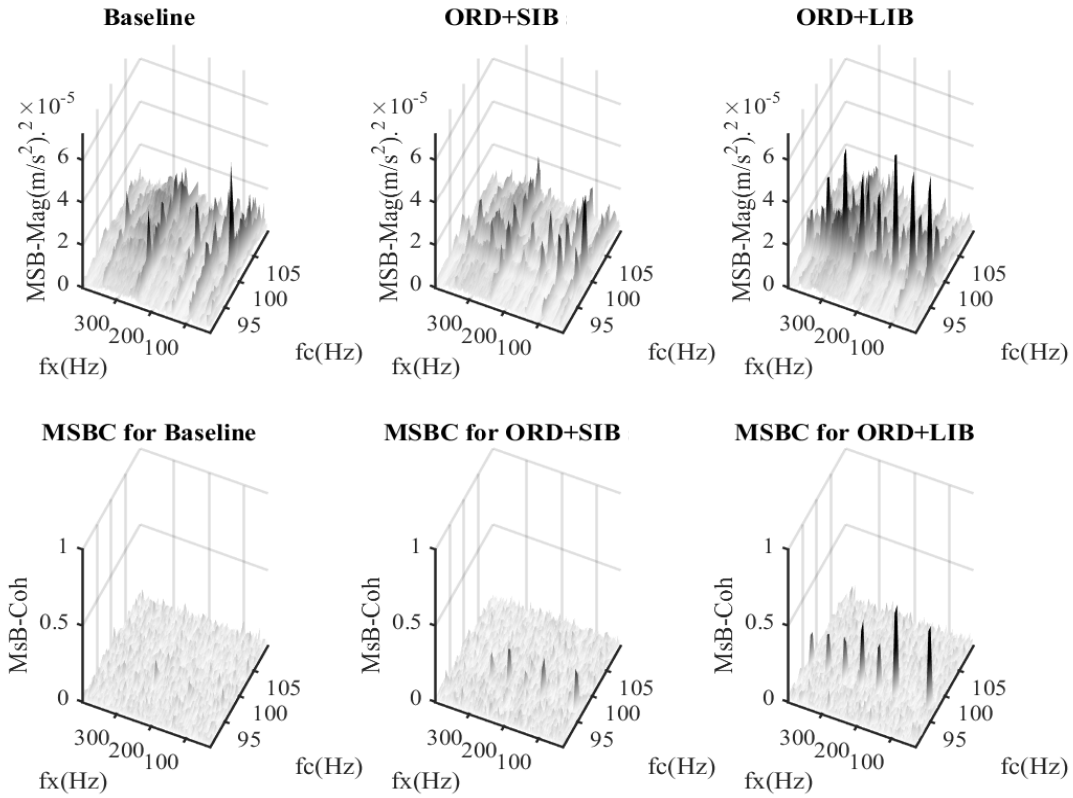

Figure 9-10 MSB magnitude and MSB coherence of vibration signals for impeller different cases at flow rate 250 l/min. Appendix B

To improve the diagnosis performance, the MSB is applied to suppress the wideband noise and hence to enhance the discrete components. Figure 9-10 represents MSB in the low frequency range. The MSB magnitude results of the three graphs of top row show less noise contamination for all three cases. Especially, their nonlinear coupling can further have identified by the corresponding MSB coherences in the three graphs of bottom. Subsequently, the average of the two components obtains the results from MSB coherence detector as shown on the three graphs of bottom row in Figure 9-10. The results show clear peaks at small impellers blockage fault frequency and its second harmonic, when comparing with the baseline case, which has no fault induced to. In addition, both results show distinctive differences between three cases in that the large impeller fault causes higher peaks because of higher mechanical and hydraulic asymmetric pulses whereas the small impeller fault induces smaller pulses and hence lower MSB coherence peaks.

9.5.2.2 Diagnosis of Impellers Based on MSB

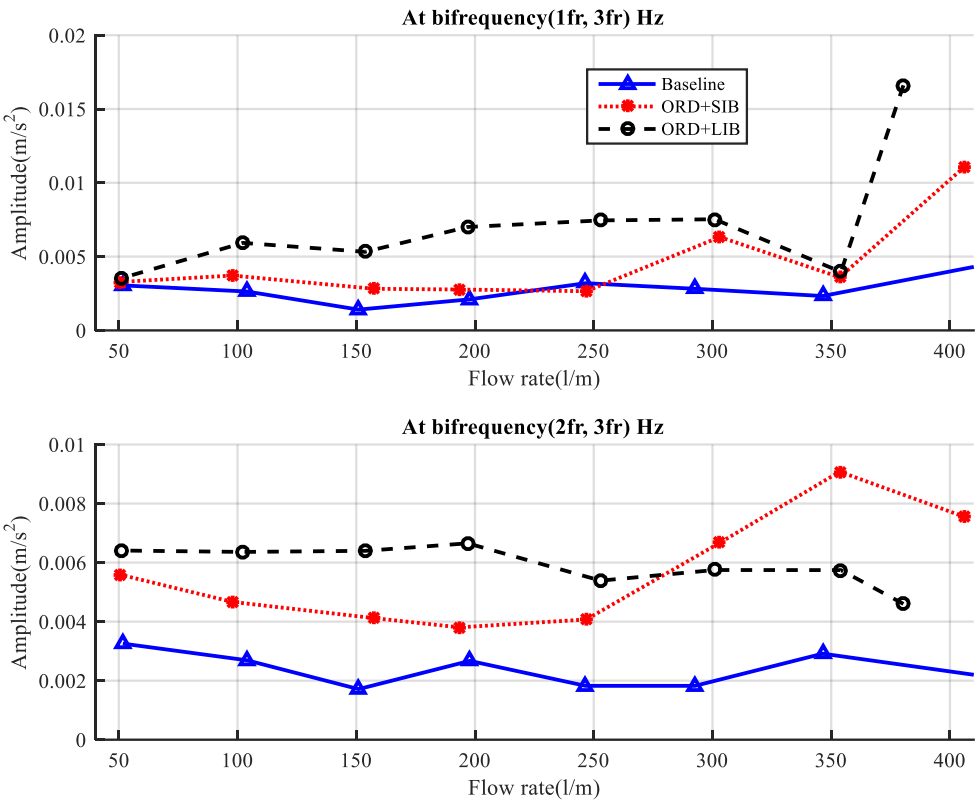

Figure 9-11 Comparison of diagnostic results for impeller faults. Appendix B

The diagnostic features extracted as shown in Figure 9-11 for three different cases stated as (BL, ORD+SIB, ORD+LIB) under different flow rates from 50 l/m up to 450 l/m. It can be observed that MSB magnitudes at the bifrequency pairs of $1f_r$- $3f_r$ and $2f_r$ - $3f_r$ allow both impeller faults to be separated from the healthy case due to the effect of MSB noise reduction.

By combining the results between the two pairs, the two fault cases can be also separated completely. In particular, MSB magnitudes at$1f_r$- $3f_r$ gives better separation at lower flow rates (<300l/m) while MSB magnitudes at$2f_r$- $3f_r$ produces good separating under high flow rates (>250/m). Which is separated over the impellers blockage at the high flow rates of shaft rotating frequency

Moreover, these separation behaviours are consistent with the changes of dynamic characteristics. As the flow pressure is lower or flow rate is higher, the vibration goes higher for the (ORD+LIB) fault and vice versa for the (ORD+SIB).

9.6 Summary of Main Findings

It starts with an in-depth examination of the vibration excitation mechanisms associated with each type of common pump faults including impeller small and large blockages, bearing inner race defects and bearing outrace defects. Subsequently, fault diagnosis was carried out using popular spectrum and envelope analysis, and more advanced kurtogram and MSB analysis. These methods all can provide correct detection and diagnosis of the faults, which are induced manually to the test pump.

Envelope analysis in a bands optimised with Kurtogram produces outstanding detection results for bearing faults but not the impeller faults in a frequency range as high as several thousand hertz (about 7.5kHz). In addition, it cannot provide satisfactory diagnostic results in separating the faults across different flow rates, especially when the compound faults were evaluated. This deficiency is because they do not have the capability of suppressing the random noises.

On the other hand, it has found that the MSB analysis allows both impeller and bearing faults to be detected and diagnosed. Especially, when the pump operated with combined faults both the fault types and severity can be attained by the analysis with acceptable accuracy for different flow rates. This high performance of diagnosis is due to that MSB has the unique capability of noise reduction and nonlinearity demodulation. Moreover, MSB diagnosis can be a frequency range lower than 2 times of the blade pass frequency (<1kHz), meaning that it can be more cost-effective as it demands lower performance measurement systems. which is obtained by averaging MSB peaks in low frequency range, can make good differentiation of the impeller defects and the bearing defect from the healthy ones because of its capability of wideband noise suppression, demonstrating that the proposed method is effective. Moreover, the discrete components caused by the interaction of flow, impeller and bearing show more definitive change due to the defects. In particular, the amplitudes at vane passing frequency and the higher order harmonics at shaft frequency can be effective features for the detection and diagnosis of the fault severity.

CHAPTER TEN

CONCLUSION AND FUTURE WORK

This chapter highlights a key of the research achievements in respect to the original objectives. The chapter begins by giving a summary of each key project achievement in relation to the various objectives introduced in chapter one. Then, the key conclusions drawn from this research made for the detection and diagnosis of centrifugal pump faults based on advanced analysis of vibration signals. A summary of the novel elements is presented with the aid of the knowledge obtained from this comprehensive study. Lastly, recommendations for future work on the pump condition have been presented.

10.1 Review of the Aim, Objectives and Achievements

The main aim of this research was to determine and discover the diagnostic information from data collected at the accelerometer sensor of centrifugal pump system. It additionally pursues to identify the prospective of developing a novel cost effective and reliable approach for condition monitoring of centrifugal pump systems by using information and vibration signals obtainable for fault detection and diagnosis. The work carried out based on experimental studies and satisfied successfully by focusing on development of hybrid detection as well as diagnosis techniques to monitoring several characteristic faults arising on a centrifugal pump system, by a typical vibration signals.

The main aim of this research was:

To achieve this study mainly involves the condition monitoring of centrifugal pump test system and fault detection by vibration measurements and also develop more advanced measurement and analysis systems for pump condition monitoring.

The thesis's principal aim was achieved by the experimental work study has been carried out based on detection and diagnosis of the pump's defects. Also, the study explores and monitors centrifugal pumps defect since it is a relatively known fault in these pumps that can cause high vibrations, low performance, damage to the components of the pump and severe failure. This conventional method for fault detection based on vibration analysis also has discovered for comparison and benchmarking purposes.

In the following, the study's summary of main objectives and achievements are presented as follows:

Objective 1:

To review different condition monitoring techniques and especially vibration data analysis methods in developing effective vibration features for monitoring pump conditions. This is to include fault detection methods for pumps system.

Achievement 1:

The definitions of condition monitoring (CM) as well as its relationship with predictive and preventive maintenance is clearly define in the Sections 1.1, 0, and **Error! Reference source not found.** along with the advantages of condition monitoring techniques. Moreover, Chapter

one describes the process of vibration based on condition monitoring measurement, as this is one of the most suitable techniques for condition monitoring, detection as well as diagnosis. Also, it has been applied in the industry and the same approach is employed for centrifugal pumps in this study project. An extensive literature review regarding the related literature was conducted to establish both theoretical and historical developments in the field Section 1.3 of chapter 1 entails a critical discussion of the significant studies in this field. A discussion for condition monitoring (CM) as well as its benefits is presented. Then, it goes further to investigate the various conventional monitoring approaches and their disadvantages as well as limitations. This allows the researchers to identify alternative techniques which are reliable as well as cost effective.

Objective 2:

To review the centrifugal pump fundamentals: operating process, types, pump selection, an overview of various applications where centrifugal pumps can be used, mechanical construction, mechanical and hydraulic faults including impellers and bearings.

Achievement 2:

Fundamental theory of the centrifugal pump was expansively described in chapter Two Sections 2.1, 2.2, 2.3, and 2.8, 2.9, 2.11, and 2.12. These Sections discovered the pump theory, various applications where the centrifugal pumps can be used, mechanical construction also mechanical and hydraulic faults, including impeller and bearing.

Objective 3:

To re-examine the influences of the centrifugal pump faults on the mechanical and hydraulic vibrations, this includes general assessments of vibration analysis methods that can be applied to the detection and diagnosis of pump faults.

Achievement 3:

The general vibration sources in the centrifugal pump are explained in Section 3.3, 3.4. This encompasses the mechanical sources that come as a result of vibration of bearings, seals, impeller and unbalanced rotating masses. Hydraulic sources are as a result of fluid flow perpetuation as well as interactions between rotor blades and the stationary parts. They caused by flow turbulent and cavitation. Moreover, Chapter three describes the vibration method review based on fluid dynamics in Sections 3.4, 3.5 and 3.6 also provided the Vibration, Noise

and Pressure Pulsation Spectra. Moreover, chapter four introduces and comprehensively discusses other relevant methods of condition monitoring (CM) of the centrifugal pump faults in order to promote the understanding of the outcomes presented in the successive chapters. The vibration signals generated from the centrifugal pump were anticipated to be non-linear as well as non-linear stationary. Furthermore, traditional signal processing techniques such as frequency-domain, time-domain as well as envelope analysis were used to process the signals. Also, Kurtogram-based STFT (Short Time Fourier Transform), and advanced signal processing approaches like HOSA (Higher Order Spectra Analysis) measures (spectrum), an extension of the second-order measures (such as power spectrum) to higher-order measures. Also frequency and time domain techniques were presented.

Objective 4:

To refine the existing pump test rig to be suitable for monitoring the centrifugal pump conditions by inducing different fault parts into the system and hence allowing a full evaluation of the vibration based condition monitoring techniques developed. In addition, right sensors and measurement systems are specified for adequately measuring vibrations along with speed encoder, suction and discharge pressures, flow rate hydraulic sound and airborne sound.

Achievement 4:

The required test rig was designed and configured in Chapter Five Sections 5.1, 0 and 0. In addition to centrifugal pump monitoring, the constructed test-rig is suitable for experimental on the entire range of faults in centrifugal pump. These faults include mechanical and hydraulic faults. The test-rig was also equipped with speed controller that enabled the pump to operate at different speeds if necessary. In order to achieve this objective, it was necessary to improve the previous test-rig that was available in the lab. It includes some improvements in both design and configuration. In addition, the all measurements unit were identified and installed including the sensors for vibration, speed encoder, suction and discharge pressure and flow rate. In addition, the specifications of these sensors are presented in Chapter Five the pressure and flow rate sensors were selected based on the pump specifications, while the vibration and sensors were chosen w.r.t the characteristics of vibration and signal in frequency domain. The speed encoder sensor was selected according to the pump and motor shaft speed. All the sensors and equipment's are used in this research were of good value and introduced from recognised manufacturers.

Objective 5:

To collect and analyse vibration signals under healthy/baseline pump conditions, and then perform experiments that reproduce common mechanical faults such as impellers and bearings with different degrees of severity at constant speed and under different flow rate/discharge conditions.

Achievement 5:

The vibrations signals for pumps healthy condition (baseline) as well as were examined under nine different flow rate also the pump performance test obtained as presented in Sections 5.4 and 5.5 this including the relation between the pump flow rate and pump head was obtained. According to ISO 3555, the predicted characteristics between the Net Positive Suction Head Available (NPSHA) and Net Positive Suction Head Required (NPSHR) for this system are obtained by throttling the valve in the discharge line progressively while the pump speed is at 2900rpm and the valve in the suction line is fully open (100%). As shown in Figure 5-23, three different common faults were studied including impellers inlet and outlet faults, bearings outer and inner race defects and the combination of both faults which are (bearing outer race + Impeller small and large blockages) as explained in Section 5.6. In addition, for more details see Chapter Five. All faults were seeded with different degree of severities.

Objective 6:

To analyse vibration signal data recorded from faulty and healthy condition using vibration spectrum for detecting and diagnosing the faults under different flow rates.

Achievement 6:

When the tests were conducted, the vibrations from the accelerometer attached on the pump's casing was recorded as 96 kHz sampling rate as well as 24-bit rate. Furthermore, the pump's performance parameters such as the motor speed and discharge flow rate were measured as well. Each impeller was mounted on the pump casing in turns and eight consecutive flow rates were tested: 50, 100, 150, 200, 250, 300, 350 and 450 (l/min). Moreover, the vibration signals for different impeller faults condition were obtained. It was found that various differences were observed among the main performance curves of the three cases. It is evident that the smaller and the large blockages on the inlet vane has led to decreases the performance curves compared with healthy one, which is expected. Surprisingly, it can be seen that the fault at the exit vane enhances the performance of the machine. Also, it is understandable that an original design is not likely optimal and removing the pump vane tip is likely to enhance the main performance.

However, these defects have altered the optimal pump operations discussed in Sections 6.3, 6.4, 6.5. This counting the use of vibration spectrum to detect the faults for different flow rates range.

Objective 7:

To apply higher order spectrum analysis techniques to the vibration signals for detecting and diagnosing impeller faults under different flow rates.

Achievement 7:

The spectrum signals for three different impeller conditions (baseline, inlet van fault, exit van fault). In chapter seven, experiments were conducted on vibration signal and analysed using the MSB technique in order to enhance the diagnosis performances by collecting significant information from a wideband noise. This approach enhances discrete components as well as allowing spectral amplitudes caused by pulsations to be determined more accurately. Also, the signals were studied using a combination of spectrum analysis, modulation signal analysis as well as conventional bispectrum as illustrated Section 7.2.

Objective 8:

To analyse vibration signals recorded using the time domain, frequency domain and envelope analysis based on fast Kurtogram for bearing fault diagnosis under different flow rates.

Achievement 8:

Experimental studies were conducted on the centrifugal pump to develop suitable diagnostic features for the three different bearing conditions (baseline, inner race defect, outer race defect) as were examined under nine different flow rates and constant speed as described in Sections 8.3, and 8.4. Compared to the time-waveform analysis, frequency-domain analysis is considered more reliable for the detection as well as diagnosis of rotating machinery faults. However, this approach cannot be applied for the bearing vibration signals since such signals are masked by extremely high background noises due to flow turbulence and cavitation. Moreover, to achieve reliable bearing faults detection, the selection of the optimal band is quite important. In this work, an automatic band selection technique, Fast kurtogram, used to select the optimal sub-band for further envelop analysis. It has shown that the improved envelope analysis produces correct detection for each type of the bearing outer and inner race defects and their compounds as detailed in 8.4.

Objective 9:

To analyse vibration signals for developing methods are being capable of the detection and diagnosis of combined faults using advanced signal processing methods.

Achievement 9:

The most popular condition monitoring approaches for detection as well as diagnosis of the impeller and rolling bearing faults were comprehensively discussed in Sections 9.3, 9.4 and 9.5. These include comparison of vibration spectrum analysis, envelope analysis and modulation signal bispectrum respectively Furthermore, various experimental studies were performed on the centrifugal pump to develop suitable diagnosis features for the three different conditions (baseline, outer race defect + small impeller blockage, outer race defect + large impeller blockage). As were examined under nine different flow rates and constant speed as described in Section 9.2 The vibration signals comprise of two elements. The wideband contents resulting from cavitation and flow turbulences is random in nature whereas discrete content resulting from hydraulic and mechanical pulsations is highly deterministic. However, MSB analysis technique is considered very effective in random noise suppression and in the decomposition of the non-linear modulation contents in the vibration signals measured. From the results, it is evident that MSB exhibits better noise suppression performance than the power spectrum and envelope results for detection and diagnosis of the combined faults. Chapter Nine debated the obtained result.

10.2 Conclusions on Pump Monitoring Based on Advanced Analysis of Vibration Signals

This research investigated and monitor the centrifugal pump faults. It has enabled a number of key conclusions from this study to be drawn. The main conclusions under each of these areas will be described and summarised as follows

10.2.1 Pump Performance Test

1. According to ISO 3555, the predicted characteristics between the Net Positive Suction Head Available (NPSHA) and Net Positive Suction Head Required (NPSHR) for this system are obtained, by throttling the valve in the discharge line progressively while the pump speed is at 2900rpm and the valve in the suction line is fully open (100%).

2. The experiments were carried out on healthy and full opened valve on discharge line by using test rig that discussed in Figure 5-2. In addition, Figure 5-1presented the Schematic Diagram of the Pumping System. All tests with different flow rates signals were measured, namely, zero, 50, 100, and 150, up to 450, to know the system behaviour under these conditions as healthy. The test repeated three times with the fixed speed of 2900 rpm and different flow rates the signals were measured.
3. This research has been established a condition monitoring system for centrifugal pump based on vibration measurements, in order to examine the performance of the pump with the healthy condition and to detect faults of pump components. In particular, the amplitudes at vane passing frequency and the higher order harmonics at shaft frequency can be effective features for the detection and diagnosis of the fault severity.
4. The initial result has been conducted and presented in the healthy condition case, the performance test of the pump with the healthy condition was achieved also the relationship between flow rate and the pump head was obtained. The pump flow rate curve shows the pump head and corresponding flow rates over the range from 0 l/min to 450 l/min. It can be noted that as the pump flow rate increases the developed head decrease, and the pump head above flow rate of 350 l/min was dramatically depressed.

10.2.2 Detection and Diagnosis of Impeller Faults Using Spectrum Analysis

10.2.2.1 Faulty impeller with inlet vanes (blockages)

1. Three impeller conditions (baseline/ healthy impeller, small impeller blockage, large impeller blockage,) which is created by blockage the inlet between two vanes one is small blockage whereas the second is large blockage along the length direction of vane during the test. This then allows two degrees of inlet vane blockages to be explored for evaluation of accuracy of vibration based diagnosis.
2. The result shows the differences of main performance curves for three cases, it can be seen that the smallest and the large blockages on the inlet vane has led to decreases the performance curves compared with healthy one. It can be understood that the faults have changed the optimal operation. It is expected that this change can be diagnosed from vibration signals measured the externally.
3. The results have shown that at each defective impeller blade, the performance curve is degraded from the baseline curve. The vibration responses are examined to show corresponding changes. By eliminating vibration from other sources key detection

features are extracted to represent the pump conditions with impeller faults. Test results show that these features are effective in detecting these types of faults, providing a more reliable way for pump monitoring and diagnosis.

10.2.2.2 Faulty impeller with exit vanes effect

1. Five impeller conditions (baseline/ healthy impeller, F1/fault1, F2/fault2, F£/fault3, F4/fault, F5/fault5) which are made by removing away 3 millimetres along the length-wise direction starting from one vane to another during the test. After the baseline test, five tests were taken for five various defect severities respectively. In the first test, it was under the fault of a single tip. The second was under the fault of two tips and so on. Therefore, this permits the five digressions of the pump vane damages to be studied in order to evaluate accuracy of the vibrations based on diagnosis. Furthermore, in order to discuss these tests easily, they will be represented as BL, F1, F2, F3, F4 as well as F5 respectively.
2. In this set of experiments, five tests were conducted. The first one entails the baseline test which is performed using a healthy impeller. The other remaining experiments are performed using impellers of different vane tip defect degrees. As previously mentioned, the level of vibration (acceleration) for each test was measured at fixed motor speeds of about 2900revolutions/minutes but with seven different flow rates including 50 l/min, 100 l/min, 150 l/min, 200 l/min, 250 l/min, 300 l/min as well as 340 l/min acquired by closing or opening the throttle valve for the fluid line.
3. The result shows the differences of main performance curves for five cases, which the simulated Fault-1 started with the highest head at around 52 m. In Fault-2, where another blade has been treated with a flaw, the head was consequently reduced to approximately 49 m. As the faults was further increased with three blades, the decrease in head becomes more evident, declining to 47 m. Close to this rate, the pressure was further reduced as more blades were subjected to faults as implied in the condition of Fault-4 and Fault-5.
4. The bottom line measure of head acquired the reading of around 46 m. Through all the increased amount of faults for the impeller blades, the flow rate has started at 50 l/m. As observed through the graphical representation in Section 6.4, the more the number of faults placed on an impeller blade, the higher deterioration of performance is obtained in terms of head and flow rate.

5. Reference to amplitude at blade pass frequency, it is observed that the impeller with fault-1 is having moderate amplitude at different frequency range due to the fact that possibly the residual unbalance component has got neutralized, however the flow separation condition is generating the higher amplitude at high frequency. It can further be seen that the vibration amplitude increases with fault-2 condition as the resultant unbalance components has increased significantly and also the flow separation condition. The condition is same for fault-3 but with fault-4 and 5 the amplitude reduces because of the fact that the unbalance components are getting balanced as the mass removal is in approximately from 180-degree location, thus balancing the unbalanced components.

10.2.2.3 Healthy and Faulty Impeller with Exit Vanes Effect

1. Two impeller conditions (baseline/healthy, exit vanes effect) The first impeller is a healthy one whereas the second impeller have exit vans fault, which explained in the last test as we used the fault-5/F5 as one effects and it is created by removing about 3 millimeters away along the vane's length direction, on each of the vanes during the test.

2. Based on the results from the differences from the main performance curves of the two cases, it is evident that exit vane defects enhance the performance of the machine. Furthermore, it is well understood that an original design is not likely to be optimal as well as removal of vane tips enhance the main performance as illustrated in Section 6.5. Nevertheless, the fault has changed the optimal operation. It is expected that this change can be diagnosed from vibration signals measured externally.

3. In addition, the results for all tests have shown that the trimming of the outer blades of pump impeller at discharge side has changed the operating points completely from its design point and pump head found to be less than expected while flow rate was greater, this is due to a mismatched impeller and casing. As the blade diameter of the impeller decreases, added clearance between the impeller blade and the pump casing increases internal flow recirculation, causes reduction in head, and degrades pump performance.

4. It can be observed that the the vibration spectrum in a low frequency range response from pumps can spread over a wide frequency range. To examine the details of the responses its spectrum is studied in a flow frequency range from zero to 1 kHz and 1 kHz to 10 kHz. In addition, it can be observed that the vibration spectrum exhibits clear

broadband due to flow turbulence and visible discrete components due to the interactions between vane and flow.

5. Vibration spectrum has a high frequency range under these three flow rates: below BEP flow, the BEP flow and above BEP flow for a baseline as well as the fault on the five vanes. It is evident that a spectrum demonstrates a typical wideband feature. Furthermore, there are various frequency ranges exhibiting higher amplitudes because of the resonance effects in casing structures or in the flow.

10.2.3 Detection and Diagnosis of Impeller Faults Using MSB Methods

1. The experiment was conducted based on the same pump casing with three different impellers. In the first case, the impeller used was healthy. The second impeller had an inlet vane defect and the third impeller had an exit vane fault. The inlet vane fault was induced to the impeller in the second case by eliminating part of the vane tip along the edge near the inlet as presented in in Section 7.2, Similarly, the exit vane fault was made on the edges of the vane at the exit. These defects are typical erosion faults presented in the previous studies.

2. To assess the performance of vibrations-based impeller fault diagnosis, the signals collected were analysed using thee power spectrum. Based on the power spectrum results, it was reported that the spectrum has two different components as anticipated. First, the discrete tone contents. They are highly distinctive in a low frequency range. Second, the continuous components, they demonstrate wide-band over a full frequency range. Discrete contents are as a result of propeller-based flow pulsations and mechanical excitations. On the other hand, continuous contents are as a result of random excitations like cavitation as well as turbulence effects. Thus, these exhibit that vibration signals have information of each source.

3. Furthermore, spectral amplitudes of discrete contents such as vane-passing frequency at 245Hz, the shaft-rotating frequency at 49 Hz as well as their harmonics often increase with the flow rates, demonstrating that flow pulsation and mechanical sources are highly influenced by the flow velocity or they are less dampened with increase in fluid pressure (head). Conversely, wideband continuous components demonstrate a rapid change with the flow velocity or increase with fluid pressure.

4. Also, discrete contents exhibit more clear differences among these three impeller cases. On the other hand, continuous components exhibit less difference. Especially continuous contents' patterns in frequency range between 600Hz and 1000Hz are almost equal for the three cases. Thus, the low discrete contents are high focused on in order to develop diagnostic features.
5. To enhance diagnostic performance, MSB is used to facilitate wideband noise suppression and thus improve discrete contents. The MSB in low frequency range is illustrated in Section 7.2 The MSB magnitude outcomes of all the three graphs in the top low exhibit less noise contamination in the three cases. Particularly, their non-linear coupling may be identified further by same MSB coherences among the three graphs at the bottom. Furthermore, both results exhibit various differences among the three cases. The inlet vane defect causes high peaks due to hydraulic and mechanical pulses. On the other hand, exit vane faults causes smaller pulses, thus causing lower MSB peaks.
6. The vibration signals are used as the conventional method modulation signal bispectrum in the faults detection for the impeller. However, the faults have been simulated in the pump impeller were compared with the baseline condition. Besides that, both a dynamic and static characteristic parameters are involved as features for impeller fault diagnosis.
7. MSB permits the spectral amplitude as a result of pulsations to be examined more accurately since it effectively supresses wideband noise. Various results exhibit that proposed diagnostic feature obtained by averaging the MSB peaks under low frequency range, promote good differentiation of the exit vane defect and inlet vane fault from a healthy impeller and this shows that the proposed technique is effective.
8. A new method has been approached to monitoring the conditions of centrifugal pump impellers to allow significant suppression of noise content in the signals, leading to more accurate diagnostic features, by using surface vibration with advanced signal analysis: the modulation signal bispectrum (MSB).

10.2.4 Detection and Diagnosis of Bearing Faults Using Envelope Analysis

1. Three bearings conditions (baseline/healthy bearing, inner-race defect, and outer-race defect) were used to detect and diagnose the bearing faults. Vibration signals obtained from the centrifugal pump bearings were processed and analysed via time domain, frequency domain and fast kurtogram based on envelope analysis approaches. The time

domain provided limited information about the vibration signals. The frequency domain highlights significant frequency content that may be associated with the characteristic frequencies of specific bearing defects. The envelope spectrum based on kurtogram of the filtered data presents a clear indication of the bearing faults.

2. The optimal filter is used to select signal frequency bands with high SNR. The filter parameters (band width and central frequency) are optimised by an automatic band selection technique, Fast kurtogram, used to select the optimal sub-band for further envelop analysis. The experimental studies have been carried out on a centrifugal pump for developing effective diagnosis features for the bearing defects. A detection of balling bearing faults diagnosis on the STFT based on fast kurtogram has a strong ability to optimize the parameters with minimal constraints on centre frequency and bandwidth for further envelop analysis.
3. The results for both simulated bearings defect are obtained, as well as actual bearing vibration signals show the effectiveness of the proposed approach to extract the balling bearing fault impulses buried in the noisy vibration signal. In the meantime, can be effective features for the detection and diagnosis of the bearing conditions. It has shown that the improved envelope analysis produces correct detection for each type of the bearing outer and inner race defects and their compounds.

10.2.5 Detection and Diagnosis of Combined Faults on the Pump

In this research, an optimal band pass filter fast kurtogram based on envelope has been examined by combining spectrum with envelope and MSB analysis for combined faults of centrifugal pump bearings and impeller.

1. The experiment was carried out on a centrifugal pump test rig for developing effective diagnosis features from three different conditions (baseline, outer race defect + small impeller blockage, outer race defect + large impeller blockage) when pump operated under nine different flow rates or pressure heads at a constant speed as described in Sections 9.2.
2. It can be observed that the vibration spectrum exhibits clear broadband due to flow turbulence and visible discrete components due to the interactions between vane and flow. In addition, it is difficult to find the characteristic frequencies for making diagnostics. However, these mechanisms of generating vibration cause the structure of the pump to vibrate. Moreover, a general vibration response to faults of impeller and

bearing characteristic frequency is small differences and usually masked by random noises due to unsteady flows.

3. The result on the Kurtogram based envelope spectrum has little noise reduction effect. In addition, it is quite difficult to find the characteristic frequencies for making diagnostics for impeller. However, these mechanisms of generating vibration cause the structure of the pump to vibrate. Consequently, envelope has the capability to identify only bearing faults whereas the envelop fails to identify the impeller faults only.
4. The vibration characteristics of the pumps vibration signals has two contents. First, he discrete contents that are generated from hydraulic and mechanical pulsations which is more deterministic. Second, the wide-band contents resulting from cavitation and flow turbulences and it is random in nature. However, MSB analysis technique is suitable for suppressing the random noise as well as decomposing the non-linear modulation contents in the vibration signals measured.
5. Based on the experimental results, it is evident that the proposed diagnosis features obtained by getting the average of the MSB peaks in low-frequency range, makes good differentiation of impeller faults as well as bearing defects from the healthy cases since it is able to suppress wideband noise. This indicates that this approach is effective. Furthermore, discrete components resulting from interactions of flow, bearings and impeller demonstrate more definitive changes because of the faults. In particular, amplitudes of the vane passing frequency as well as the high-order harmonics at the shaft frequency are considered effective features to detect and diagnose the severity of faults.

6. The results from experimental data analysis demonstrate that MSB analysis has a better noise suppression performance as compared to the results of power spectrum. Furthermore, both the types of defects and their severity can be identified and estimated more accurately.
7. Whereas, the Kurtogram-based envelope spectra have limited noise reduction effects, as well as consequently (MSB) has the capability to identify both impeller and bearing faults whereas the envelop fails to identify the impeller faults only.
8. The modulation signal bispectrum (MSB) method suggested in this thesis is able to include the pump effects of discrete components and hence to suppress noise influences to obtain an accurate estimation of the discrete components.

10.3 Novelties and Contribution to Knowledge

This section summarizes the key aspects of novelty created during this study projects as well as its report. They are focused mainly on the researched phenomena, the methodologies applied as well as results obtained.

Novelty One:

The writer believes that this methodical research has been conducted to detect incipient impeller defects (at exit vanes) of centrifugal pump using the state of the art MSB analysis. It can be seen that the exit vane defect has led to an increase the performance, which this clearly indicate in Figure 7-1, this a clarify for long-term benefit to the system stability. Moreover, it can be understood that the original design may not optimal and the removal of the vanes tip may improve the main performance.

Novelty Two:

The author never found papers in literature applying modulated signal spectrum for the detection of combining faults bearing and impeller and so believes that HOSA (particularly MSB) is considered a novel technique for analysis of the centrifugal pump's surface vibrations for condition monitoring(CM) and noise and interference suppression of the bearing and impeller defects.

Novelty Three:

The author found that the methodical research has been carried out to detect the impeller and bearing faults simultaneously. It observed that the impeller faults have led to change the main performance curve of the centrifugal pump. In addition, a literature review study has been conducted was quite challenging since little papers are published in this field. This work has a ground-breaking element as well as contributes to the body of knowledge by offering significant information as a basis for studies in the future against which researchers can evaluate relative merits.

Novelty Four:

A new method has been developed to monitor the condition of the centrifugal pump impellers in order to allow more suppression of the noise content inherent in signals, resulting to more accurate and reliable diagnostic features by using surface vibration with advanced signal analysis: the modulation signal bispectrum (MSB).

10.4 Recommendations for Future Work on Pump Condition Monitoring

Recommendation One:

It is recommended to carry out experiments to introduce more specific faults into a centrifugal pump component, such as seals.

Recommendation Two:

Introduce another signal processing technique such as acoustic and compare with the vibration technique.

Recommendation Three:

Establish theoretical understanding of the experimental behaviour by develop a mathematical model to study the vibration signal for both healthy and faulty condition.

Recommendation Four:

Fatigue tests should be conducted to quantify the typical wear ratio and normal changes in internal clearance.

Recommendation Five:

To replace the impeller of the test-rig centrifugal pump with ones made of different materials, e.g. a replacement made of a material with high internal damping and to compare results.

Recommendation Six:

It is recommending for further improvement of signal processing MSB method to apply at high range a good result will be obtain.

Recommendation Seven:

It is recommended to carry out experiments to introduce more specific advanced signal processing such as continues wavelet transformer will be more useful to differentiate the simulate faults.

REFERENCES

1. Ciocoiu, L., E.-M. Hubbard, and C.E. Siemieniuch, *Implementation of remote condition monitoring system for predictive maintenance: An organisational challenge.* 2015.
2. Patton, J.D., *Preventive maintenance*. 2004, Research Triangle Park, Car. du N.: ISA-The Instrumentation, Systems, and Automation Society.
3. Mobley, R.K., *An introduction to predictive maintenance*. 2002: Butterworth-Heinemann.
4. Davies, A., *Handbook of condition monitoring: techniques and methodology*. 1998: Springer.
5. Devore, J.L., *Probability and statistics for engineering and the sciences*. 2012, Boston, MA: Brooks/Cole, Cengage Learning.
6. Collacott, R.A., *Mechanical fault diagnosis and condition monitoring*. 1977, London: Chapman & Hall [usw.].
7. Kryter, R.C. and H.D. Haynes, *Condition monitoring of machinery using motor current signature analysis*. 1989, Oak Ridge National Lab., TN (USA).
8. Mba, D. and R.B.K.N. Rao, *Development of Acoustic Emission Technology for Condition Monitoring and Diagnosis of Rotating Machines; Bearings, Pumps, Gearboxes, Engines and Rotating Structures.* 2006.
9. Randall, R.B., *Vibration-based condition monitoring: industrial, aerospace and automotive applications*. 2011: Wiley.
10. Swansson, N.S. *Application of Vibration Signal Analysis Techniques to Condition Monitoring*. in *Conference on Lubrication, Friction and Wear in Engineering 1980, Melbourne: Preprints of Papers*. 1980. Institution of Engineers, Australia.
11. Sohn, H. and C.R. Farrar, *Damage diagnosis using time series analysis of vibration signals.* Smart materials and structures, 2001. **10**(3): p. 446.
12. Lin, J., M.J. Zuo, and K.R. Fyfe, *Mechanical fault detection based on the wavelet de-noising technique.* Journal of vibration and acoustics, 2004. **126**(1): p. 9-16.
13. Pandian, R. and B. Rao, *Predictive maintenance programme for GEN sets and reciprocating MUD pumps of oil fields*, in *Condition Monitoring and Diagnostic Engineering Management*. 1990, Springer. p. 197-202.
14. Deutsch, E., M. Macklin, and B. Kuttel, *Redundant seal apparatus and method*. 2015, Google Patents.
15. Batchelor, B., D.A. Hill, and D.C. Hodgson, *Automated Visual Inspection*. 1985, Kempston: IFS.
16. Jiang, J., *Acoustic condition monitoring in industrial environments : a book renewing your understanding of traditional condition monitoring*. 2011, Saarbrucken (Germany): LAP Lambert.
17. Sachse, W., et al. *Acoustic emission : current practice and future directions*. Philadelphia, PA: ASTM.
18. Anagnostopoulos, J.S., *A fast numerical method for flow analysis and blade design in centrifugal pump impellers.* Computers & Fluids, 2009. **38**(2): p. 284-289.
19. Moore, J., *A Wake and an Eddy in a Rotating, Radial-Flow Passageâ€"Part 1: Experimental Observations.* Journal of Engineering for Power, 1973. **95**: p. 205.

20. Visser, F., J. Brouwers, and J. Jonker, *Fluid flow in a rotating low-specific-speed centrifugal impeller passage.* Fluid dynamics research, 1999. **24**(5): p. 275-292.
21. Acosta, A.J., *An experimental and theoretical investigation of two dimensional centrifugal pump impellers*. 1952, California Institute of Technology.
22. Hodkiewicz, M.R. and M.P. Norton, *The effect of change in flow rate on the vibration of double-suction centrifugal pumps.* Proceedings of the Institution of Mechanical Engineers, Part E: Journal of Process Mechanical Engineering, 2002. **216**(1): p. 47-58.
23. Koo, I.S. and W.W. Kim, *The development of reactor coolant pump vibration monitoring and a diagnostic system in the nuclear power plant.* ISA transactions, 2000. **39**(3): p. 309-316.
24. Benaroya, H., *Mechanical vibration : analysis, uncertainties, and control*. 2004, New York, NY: Dekker.
25. Lobanoff, V.S. and R.R. Ross, *Centrifugal pumps design and application.* 1992.
26. Zhengjia, H., et al. *Wavelet transform and multiresolution signal decomposition for machinery monitoring and diagnosis*. in *Industrial Technology, 1996.(ICIT'96), Proceedings of The IEEE International Conference on*. 1996. IEEE.
27. McGarry, K. and J. MacIntyre. *Data mining in a vibration analysis domain by extracting symbolic rules from RBF neural networks*. in *Proceedings of 14th International Congress on Condition Monitoring and Engineering Management*. 2001.
28. Wang, K., *Intelligent condition monitoring and diagnosis system: a computational intelligent approach*. Vol. 93. 2003: IOS Press.
29. Sharif, M.A. and R.I. Grosvenor, *Process plant condition monitoring and fault diagnosis.* Proceedings of the Institution of Mechanical Engineers, Part E: Journal of Process Mechanical Engineering, 1998. **212**(1): p. 13-30.
30. Rao, B.K.N., *Handbook of condition monitoring*. 1996, Oxford: Elsevier.
31. ZHOU, Y.-l., et al., *Fault Diagnosis Methods for Centrifugal Pump Based on Autoregressive and Continuous Hidden Markov Model [J].* Proceedings of the CSEE, 2008. **20**: p. 018.
32. Yunlong, Z. and Z. Peng, *Vibration fault diagnosis method of centrifugal pump based on EMD complexity feature and least square support vector machine.* Energy Procedia, 2012. **17**: p. 939-945.
33. Zheng, J., J. Cheng, and Y. Yang, *A rolling bearing fault diagnosis approach based on LCD and fuzzy entropy.* Mechanism and Machine Theory, 2013. **70**: p. 441-453.
34. Farokhzad, S., *Vibration Based Fault Detection of Centrifugal Pump by Fast Fourier Transform and Adaptive Neuro-Fuzzy Inference System.* Journal of Mechanical Engineering and Technology.
35. Zhang, L., et al., *Bearing fault diagnosis using multi-scale entropy and adaptive neuro-fuzzy inference.* Expert Systems with Applications, 2010. **37**(8): p. 6077-6085.
36. Nasiri, M., M. Mahjoob, and H. Vahid-Alizadeh. *Vibration signature analysis for detecting cavitation in centrifugal pumps using neural networks*. in *Mechatronics (ICM), 2011 IEEE International Conference on*. 2011. IEEE.
37. Al Thobiani, F., F. Gu, and A. Ball, *The monitoring of cavitation in centrifugal pumps based on the analysis of vibro-acoustic measurements.* 2010.
38. Wang, H. and P. Chen, *Intelligent diagnosis method for a centrifugal pump using features of vibration signals.* Neural Computing and Applications, 2009. **18**(4): p. 397-405.
39. Muralidharan, V. and V. Sugumaran, *Feature extraction using wavelets and classification through decision tree algorithm for fault diagnosis of mono-block centrifugal pump.* Measurement, 2013. **46**(1): p. 353-359.
40. Li, P., Q. Cai, and B. Wei, *Failure analysis of the impeller of slurry pump used in zinc hydrometallurgy process.* Engineering Failure Analysis, 2006. **13**(6): p. 876-885.
41. Perovic, S., P.J. Unsworth, and E.H. Higham. *Fuzzy logic system to detect pump faults from motor current spectra*. in *Industry Applications Conference, 2001. Thirty-Sixth IAS Annual Meeting. Conference Record of the 2001 IEEE*. 2001. IEEE.

42. Farokhzad, S., N. Bakhtyari, and H. Ahmadi, *Vibration Signals Analysis and Condition Monitoring of Centrifugal Pump.* 2013.
43. Siegler, J.A., *Motor current signal analysis for diagnosis of fault conditions in shipboard equipment*. 1994, DTIC Document.
44. Schmalz, S.C. and R.P. Schuchmann, *Method and apparatus of detecting low flow/cavitation in a centrifugal pump*. 2004, Google Patents.
45. Zouari, R., S. Sieg-Zieba, and M. Sidahmed, *Fault detection system for centrifugal pumps using neural networks and neuro-fuzzy techniques.* Surveillance, 2004. **5**: p. 11-13.
46. Lei, Y., et al., *Application of an improved kurtogram method for fault diagnosis of rolling element bearings.* Mechanical Systems and Signal Processing, 2011. **25**(5): p. 1738-1749.
47. Mike Petrashko, N.C. *Extending the Life of Pump Bearings* Pumps and Systems [cited 2016 15/12]; Available from: http://www.pumpsandsystems.com/topics/bearings/extending-life-pump-bearings.
48. Podugu, R. and J.S. Kumar, *A modal approach for vibration analysis and condition monitoring of a centrifugal pump.* International Journal of Engineering Science and Technology (IJEST), 2011.
49. Birajdar, R., R. Patil, and K. Khanzode. *Vibration and Noise in Centrifugal Pumps-Sources and Diagnosis Methods*. in *3rd International Conference on Integrity, Reliability and Failure, Porto/Portugal*. 2009.
50. Albraik, A., et al. *Diagnosis of centrifugal pump faults using vibration methods*. in *Journal of Physics: Conference Series*. 2012. IOP Publishing.
51. Kaiser, T., R.H. Osman, and R.O. Dickan. *Analysis Guide for Variable Frequency Drive Operated Centrifugal Pumps*. in *Proceedings of the 24th International Pump Userâ€™s Symposium, Texas: Texas A&M University, USA*. 2008.
52. Eti, M.C., S.O.T. Ogaji, and S.D. Probert, *Implementing total productive maintenance in Nigerian manufacturing industries.* Applied Energy, 2004. **79**(4): p. 385-401.
53. Juneja, B.L., G.S. Sekhon, and N. Seth, *Fundamentals of metal cutting and machine tools*. 2003, New Delhi: New Age International Ltd. Publishers.
54. Nishith. *Centrifugal pump: characterisitcs, efficiency, NPSH*. Energy conservation 2012 [cited 2013.
55. Dorota Z. Haman, F.S.Z., Forrest T. Izuno2, *Selection of centrifugal pumping equipment*. 1994.
56. Karassik, I.J. and T. McGuire, *Centrifugal pumps*. 1998, New York, N.Y.: Chapman and Hall.
57. Program, I.T. *Select an Energy-Efficient Centrifugal Pump*. 2005 [cited 2013.
58. Kutbi, II, *Evaluation of centrifugal pump performance in nuclear power plants.* Annals of Nuclear Energy, 1991. **18**(11): p. 629-654.
59. Yates, M.A., *Pump performance monitoring. in Profitable condition monitoring*, in *BHR Group conference series*. 1996: Harrogate UK.
60. Bloch, H.P. and A.R. Budris, *Pump user's handbook: life extension*. 2004: The Fairmont Press, Inc.
61. *WATER TREATMENT PLANT*. 1998 [cited 2016 15/12/2016]; Available from: http://www.gdbcjt.com/UpFile/201608/2016080410486119.jpg.
62. *Pumping equipment*. Commissioning Technical Services 2006 [cited 2016 15/12/2016]; Available from: http://quarus.ru/en/portfolio/pumping-equipment/.
63. Nelik, L., *Centrifugal and rotary pumps: fundamentals with applications*. 1999: CRC PressI Llc.
64. Karassik, I.J., et al., *Pump handbook*. Vol. 3. 2001: McGraw-Hill New York.
65. Spraker, W., *The effects of fluid properties on cavitation in centrifugal pumps.* Journal of Engineering for Power, 1965. **87**(3): p. 309-318.
66. Cooper, P. and G. Tchobanoglous, *Performance of Centrifugal Pumps.* Pumpin Station Design, 2006.

67. Al-Hashmi, S., et al. *Cavitation Detection of a Centrifugal Pump Using Instantanous Angular Speed*. in *ASME 7th Biennial Conference on Engineering Systems Design and Analysis*. 2004. American Society of Mechanical Engineers.
68. Antoni, J., *Fast computation of the kurtogram for the detection of transient faults.* Mechanical Systems and Signal Processing, 2007. **21**(1): p. 108-124.
69. Sahu, G.K., *Pumps : rotodynamic and positive displacement types : theory, design and applications*. 2000, New Delhi: New Age International (P) Ltd. Publishers.
70. Karassik, I.J. *Pump handbook*. 2006; Available from: http://libaccess.mcmaster.ca/login?url=http://www.digitalengineeringlibrary.com/html/TitleWiseChapterList.asp?catid=&contentid=2000b14e&contenttype=book.
71. Griffin, S. *Clogged Pool Pump Impellers.* 2010 [cited 2017 12/02/2017]; Available from: http://blog.poolcenter.com/article.aspx?articleid=6090.
72. Godbole, V., R. Patil, and S. Gavade. *Axial thrust in Centrifugal Pumps–Experimental analysis*. in *15th International Conference on Experimental Mechanics, Porto/Portugal*. 2012.
73. Barnard, P. *The way forward*. in *Meeting of the British Institute of Mechanical Engineers*. 1991.
74. Schöb, R., *Centrifugal pump without bearings or seals.* World Pumps, 2002. **2002**(430): p. 34-37.
75. Wolfram, A., et al. *Component-based multi-model approach for fault detection and diagnosis of a centrifugal pump*. in *American Control Conference, 2001. Proceedings of the 2001*. 2001. IEEE.
76. Shiels, S., *Troubleshooting centrifugal pumps: rolling element bearing failures.* World Pumps, 2001. **2001**(423): p. 28-30.
77. Mc Nally, W., *Troubleshooting the ball bearings in a centrifugal pump.* World Pumps, 2004. **2004**(454): p. 28-29.
78. Shiels, S., *Failure of mechanical seals in centrifugal pumpsâ€"part two.* World Pumps, 2002. **2002**(432): p. 34-37.
79. Marscher, W.D. *Avoiding Failures in Centrifugal Pumps*. in *PROCEEDINGS OF THE INTERNATIONAL PUMP USERS SYMPOSIUM*. 2002.
80. Brennen, C.E., *Hydrodynamics of pumps*. 2011: Cambridge University Press.
81. Florjancic, S. and A. Frei. *Dynamic Loading on Pumps—Causes for Vibrations*. in *10"'International Pump Symposium*. 1993.
82. Black, H., *Effects of hydraulic forces in annular pressure seals on the vibrations of centrifugal pump rotors.* Journal of Mechanical Engineering Science, 1969. **11**(2): p. 206-213.
83. Budris, B.A.R. *Centrifugal Pump Bearings: Tips for Improving Reliability and Reducing Failure*. 2010 [cited 2016 18-12-2016]; Available from: http://www.waterworld.com/articles/print/volume-30/issue-9/inside-every-issue/pump-tips-techniques/centrifugal-pump-bearings-tips-for-improving-reliability-and-reducing-failure.html.
84. Barszcz, T. and N. Sawalhi, *Fault detection enhancement in rolling element bearings using the minimum entropy deconvolution.* Archives of acoustics, 2012. **37**(2): p. 131-141.
85. Chenxiao, N. and Z. Xushe. *Study on Vibration and Noise For the Hydraulic System of Hydraulic hoist*. in *Proceedings of the 1st International Conference on Mechanical Engineering and Material Science*. 2012. Atlantis Press.
86. McKee, K., et al., *A Review of Machinery Diagnostics and Prognostics Implemented on a Centrifugal Pump*, in *Engineering Asset Management 2011*. 2014, Springer. p. 593-614.
87. Majidi, K., *Numerical study of unsteady flow in a centrifugal pump.* Journal of Turbomachinery, 2005. **127**(2): p. 363-371.
88. Blake, W.K., *Mechanics of Flow-Induced Sound and Vibration V2: Complex Flow-Structure Interactions*. Vol. 2. 2012: Elsevier.

89. Timouchev, S. and J. Tourret. *Numerical simulation of BPF pressure pulsation field in centrifugal pumps*. in *PROCEEDINGS OF THE INTERNATIONAL PUMP USERS SYMPOSIUM*. 2002.
90. Birajdar, R., R. Patil, and K. Khanzode, *VIBRATION AND NOISE IN CENTRIFUGAL PUMPS-SOURCES AND DIAGNOSIS METHODS.*
91. Florjancic, S. and A. Frei. *Dynamic Loading on Pumps—Causes for Vibrations*. in *Proceedings of the Tenth International Pump Users Symposium, Turbomachinery Laboratory, Texas A&M University, College Station, Texas*. 1993.
92. Frazer, H. *Flow Recirculation in Centrifugal Pumps*. in *ASME meeting*. 1981.
93. Davies, A., *Handbook of condition monitoring: techniques and methodology*. 2012: Springer Science & Business Media.
94. Jayaswal, P., A. Wadhwani, and K. Mulchandani, *Machine fault signature analysis.* International Journal of Rotating Machinery, 2008. **2008**.
95. Yang, H., J. Mathew, and L. Ma, *Vibration feature extraction techniques for fault diagnosis of rotating machinery: a literature survey.* 2003.
96. DeDad, J. *A Key Troubleshooting Parameter. Retrieved from EC&M*. 2008 [cited 2016 07/09/2016]; Available from: http://ecmweb.com/power-quality/crest-factor-key-troubleshooting-parameter.
97. DeCarlo, L.T., *On the meaning and use of kurtosis.* Psychological methods, 1997. **2**(3): p. 292.
98. Randall, R.B. and J. Antoni, *Rolling element bearing diagnostics—a tutorial.* Mechanical Systems and Signal Processing, 2011. **25**(2): p. 485-520.
99. Programs, M. *Skewness/Kurtosis*. 2014 07/09/2016]; Available from: http://mvpprograms.com/help/mvpstats/distributions/SkewnessKurtosis.
100. Assaad, B., M. Eltabach, and J. Antoni, *Vibration based condition monitoring of a multistage epicyclic gearbox in lifting cranes.* Mechanical Systems and Signal Processing, 2014. **42**(1): p. 351-367.
101. Transform, T.F. *Introduction to the Fourier Transform.* . 06/09/2016]; Available from: http://www.thefouriertransform.com/transform/fourier.php#introduction.
102. He, S., et al., *Modeling and Dynamic Analysis of Planetary Gear Transmission Joints With Backlash.* Int. J. Control Autom, 2015. **8**(2): p. 153-162.
103. BLOG, X.B. *Gearboxes: Gear Mesh Frequency*. 05/09/2016]; Available from: http://www.xyobalancer.com/xyo-balancer-blog/sidebands.
104. Feng, G., et al. *The real-time implementation of envelope analysis for bearing fault diagnosis based on wireless sensor network*. in *Automation and Computing (ICAC), 2013 19th International Conference on*. 2013. IEEE.
105. Holm, S., *FFT pruning applied to time domain interpolation and peak localization.* IEEE Transactions on Acoustics, Speech, and Signal Processing, 1987. **35**(12): p. 1776-1778.
106. Lavanya. M, D.S.U., *Analysis of Vibrational Signal of Industrial Equipment Through Short Time Fourier Transform* International Journal of Emerging Technology and Advanced Engineering, 2008: p. 160-162.
107. Lab, O., *Short-Time Fourier Transform (STFT)*, in *Origin Lab*. 2014.
108. Prof. Mario Oliveira, A.S.B., *Application of Discrete Wavelet Transform for Differential Protection of Power Transformers*, in *Discreter wavelet transforms biomedical applications*. 2011, InTech: Rio Grande do Sul. p. 2.
109. Gao, R.X. and R. Yan, *From Fourier Transform to Wavelet Transform: A Historical Perspective*, in *Theory and Applications for Manufacturing*. 2011, Springer. p. 27-30.
110. Gao, R.X. and R. Yan, *From fourier transform to wavelet transform: A historical perspective*, in *Wavelets*. 2011, Springer. p. 17-32.
111. Tandon, N. and A. Choudhury, *An analytical model for the prediction of the vibration response of rolling element bearings due to a localized defect.* Journal of sound and vibration, 1997. **205**(3): p. 275-292.

112. Antoni, J., *The spectral kurtosis: a useful tool for characterising non-stationary signals.* Mechanical Systems and Signal Processing, 2006. **20**(2): p. 282-307.
113. Choudhury, A. and N. Tandon, *Vibration response of rolling element bearings in a rotor bearing system to a local defect under radial load.* Journal of Tribology, 2006. **128**(2): p. 252-261.
114. Choudhury, M., S.L. Shah, and N.F. Thornhill, *Detection and diagnosis of system nonlinearities using higher order statistics.* IFAC Proceedings Volumes, 2002. **35**(1): p. 337-342.
115. Rivola, A. *Comparison between second and higher order spectral analysis in detecting structural damages*. in *Proceedings of Seventh International Conference on Recent Advances in Structural Dynamics, University of Southampton, Southampton, UK*. 2000. Citeseer.
116. Vaseghi, S.V., *Power Spectrum and Correlation.* Advanced Digital Signal Processing and Noise Reduction, Saeed V. Vaseghi Copyright© 2000 John Wiley & Sons Ltd ISBNs: 0-471-62692-9 (Hardback): 0-470-84162-1 (Electronic), 2000: p. 263.
117. Zhixiong Li, X.Y., Chengqing Yuan, Jiangbin Zhao and Zhongxiao Peng, *Fault Detection and Diagnosis of a Gearbox in Marine Propulsion Systems Using Bispectrum Analysis and Artificial Neural Networks.* J. Marine Sci. Appl, 2011: p. 17-24.
118. Ahmed Alwodai, T.W., Zhi Chen, Fengshou Gu, Robert Cattley, Andrew Ball, *A Study of Motor Bearing Fault Diagnosis using Modulation Signal Bispectrum Analysis of Motor Current Signals* Journal of Signal and Information Processing, 2013, 4, 2013: p. 72-79
119. Jouny, II and R.L. Moses, *Bispectra of modulated stationary signals.* Electronics Letters, 1994. **30**(18): p. 1465-1466.
120. Stack, J.R., R.G. Harley, and T.G. Habetler, *An amplitude modulation detector for fault diagnosis in rolling element bearings.* IEEE Transactions on Industrial Electronics, 2004. **51**(5): p. 1097-1102.
121. Hamomd, O., et al., *A new method of vibration analysis for the diagnosis of impeller in a centrifugal pump.* 2014.
122. Gu, F., et al., *Electrical motor current signal analysis using a modified bispectrum for fault diagnosis of downstream mechanical equipment.* Mechanical Systems and Signal Processing, 2011. **25**(1): p. 360-372.
123. Thobiani, F.A., *The Non-intrusive Detection of Incipient Cavitation in Centrifugal Pumps*. November 2011, The University of Huddersfield.
124. *RotorFlow® Operating Principle*. 2015 [cited 2016 18-12-2016]; Available from: http://www.gemssensors.com/CustomerSupport/Literature-pdfs/Operating-Principle-Installation-and-Maintenance/RotorFlow-Operating-Principle.
125. Stavale, A.E., J.A. Lorenc, and E.P. Sabini. *Development of a Smart Pumping System*. in *PROCEEDINGS OF THE INTERNATIONAL PUMP USERS SYMPOSIUM*. 2001.
126. Chapman, S.J., *Electric machinery and power system fundamentals*. 2002: McGraw-Hill New York.
127. Williams, T., et al., *Rolling element bearing diagnostics in run-to-failure lifetime testing.* Mechanical Systems and Signal Processing, 2001. **15**(5): p. 979-993.
128. Rai, V. and A. Mohanty, *Bearing fault diagnosis using FFT of intrinsic mode functions in Hilbert–Huang transform.* Mechanical Systems and Signal Processing, 2007. **21**(6): p. 2607-2615.
129. Albraik, A., et al. *Diagnosis of centrifugal pump faults using vibration methods*. in *Journal of Physics: Conference Series*. 2012. IOP Publishing.

APPENDICES

The following section contains the appendices of the additional results.

APPENDIX A

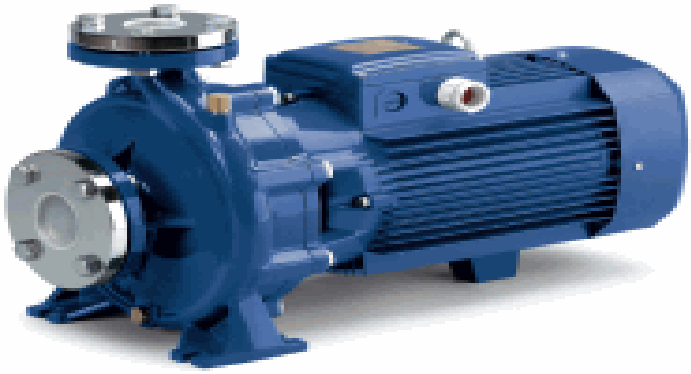

The Pedrollo F32/200AH Centrifugal Pump

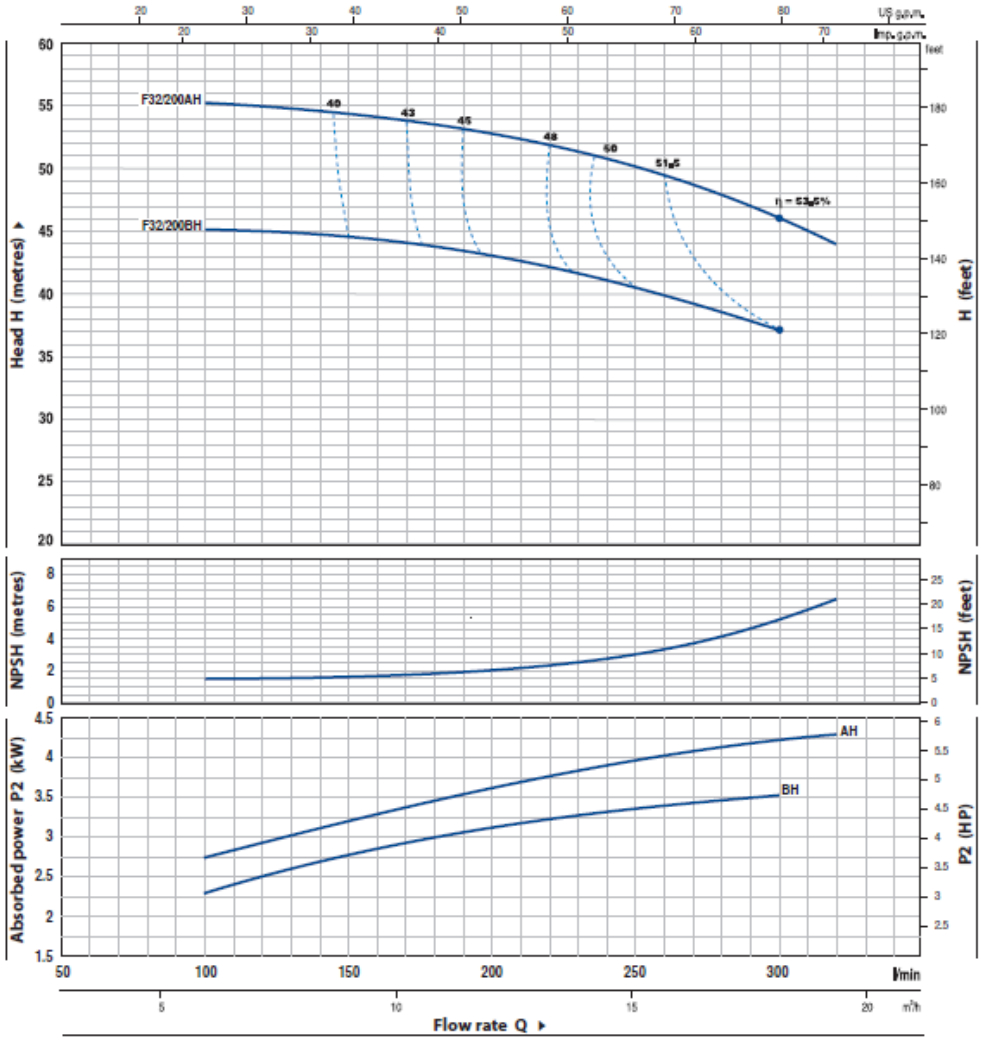

Pump Performance Curve

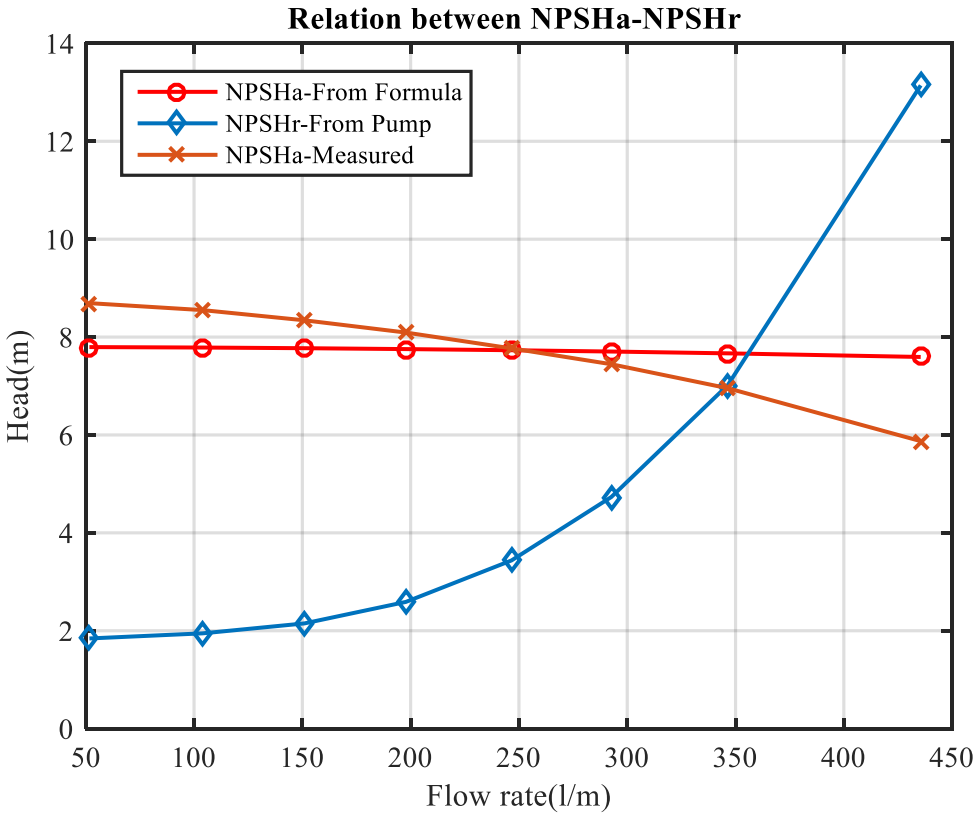

Pump Performance at 100% Open Valve.

According to ISO 3555, the predicted characteristics between the Net Positive Suction Head Available (NPSHA) and Net Positive Suction Head Required (NPSHR) for this system are obtained by throttling the valve in the discharge line progressively while the pump speed is at 2900rpm and the valve in the suction line is fully open (100%).

APPENDIX B

MSB results bearing detection and diagnose

Characteristics of MSB

Figures below shows the MSB magnitude and MSB coherence of vibration data collected on pump bearing for three different cases stated as (BL, ORD+SIB, ORD+LIB). The MSB magnitude results of the three graphs of top row show less noise contamination for all three cases. Especially, their nonlinear coupling can be further identified by the corresponding MSBC in the three graphs of bottom. Subsequently, the average of the two components obtains the results from MSB coherence detector as shown on the three graphs of bottom row, which are coloured, red. In additional, the results show clear peaks at outer race fault frequency and its 2nd harmonic, when comparing with the baseline case, which has no fault induced to. In the meantime, both results show distinctive differences between three cases in that the outer race faults causes higher peaks because of higher mechanical pulses during to the defect whereas the baseline induces very smaller pulses and hence lower MSB coherence peaks.

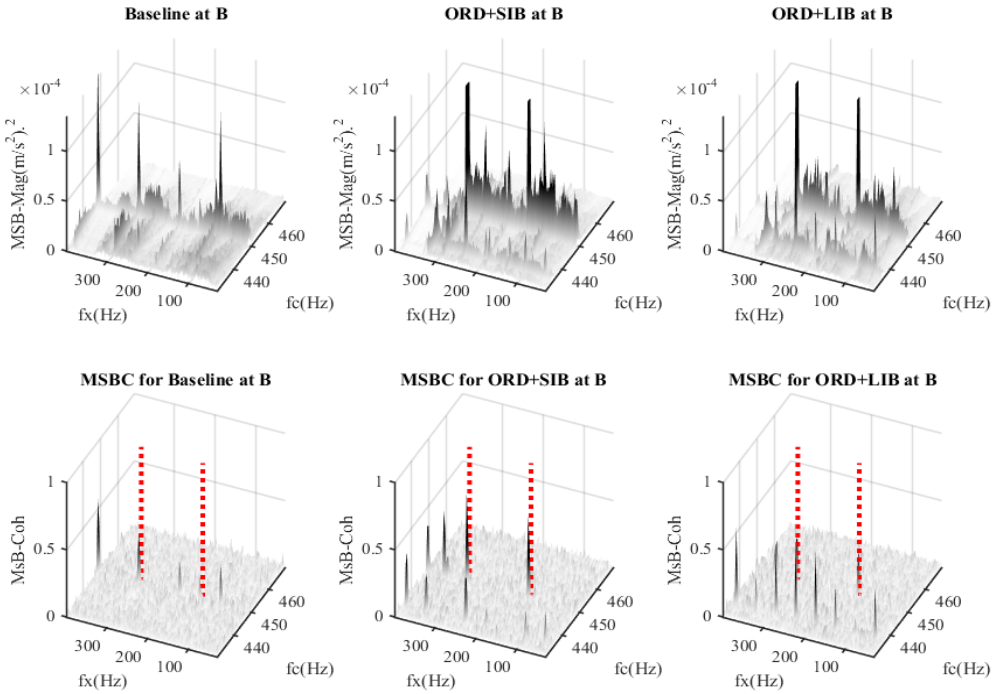

MSB magnitude and MSB coherence of vibration signals for bearing different cases at flow rate **450** l/min

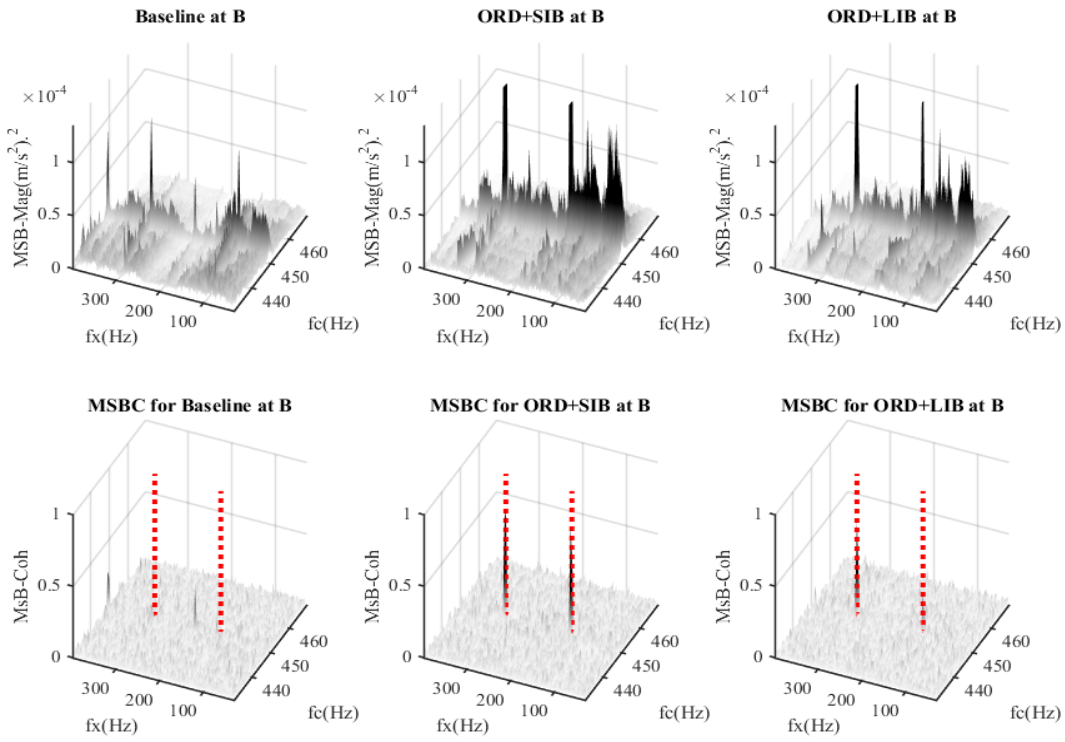

MSB magnitude and MSB coherence of vibration signals for bearing different cases at flow rate **250** l/min

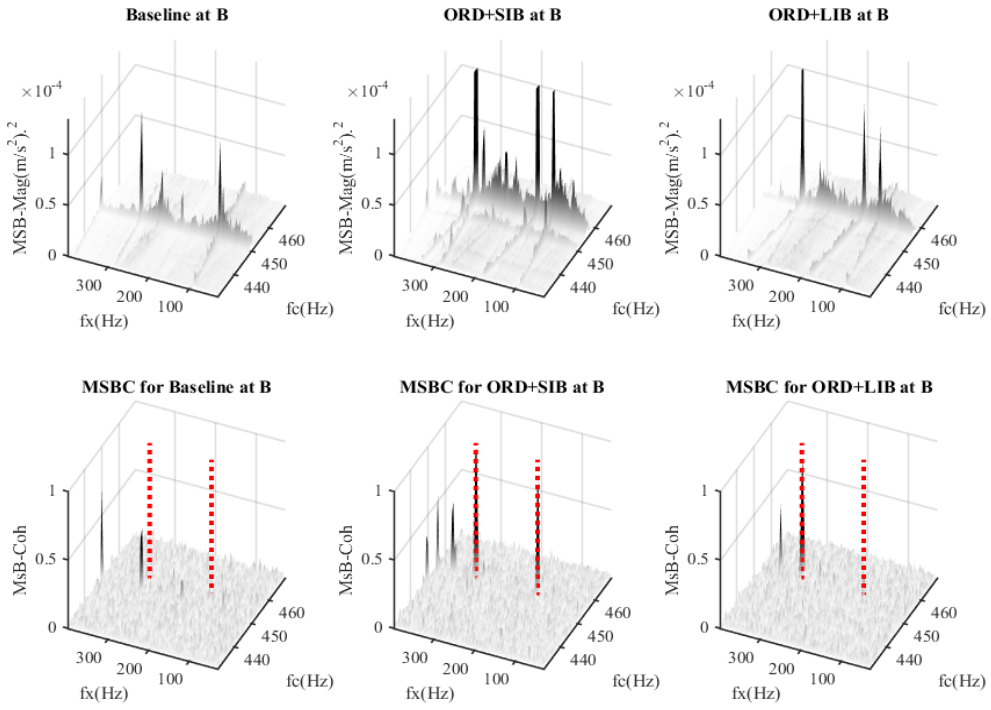

MSB magnitude and MSB coherence of vibration signals for bearing different cases at flow rate **50** l/min

Diagnostics of Bearing based on MSB

The diagnostic features are extracted as shown in the Figures below. For three different cases stated as (BL, ORD+SIB, ORD+LIB). It can be observed that the MSB Magnitude Entropy results of the three cases at graphs of the top row, which shows that the both bearing faults can be separated from the healthy case with more distinctively less noise contamination for all three cases. Especially, their nonlinear coupling can be further identified by the corresponding MSBC entropy in the raw graph of bottom, compared with the results from MSB magnitude entropy in the raw graph of middle which is spirited over the large bearing fault at the first 5 harmonics of shaft rotating frequency. It shows that the amplitudes show less change with high flow rates above 350 but allows the (ORD) faulty to be differentiated fully at the first 5 harmonics, because of the influences of the wideband noise. Moreover, it is consistent with the changes of the performance characteristics. As the flow pressure is lower, the vibration goes higher for the (ORD+LIB) fault and vice versa for the (ORD+SIB).

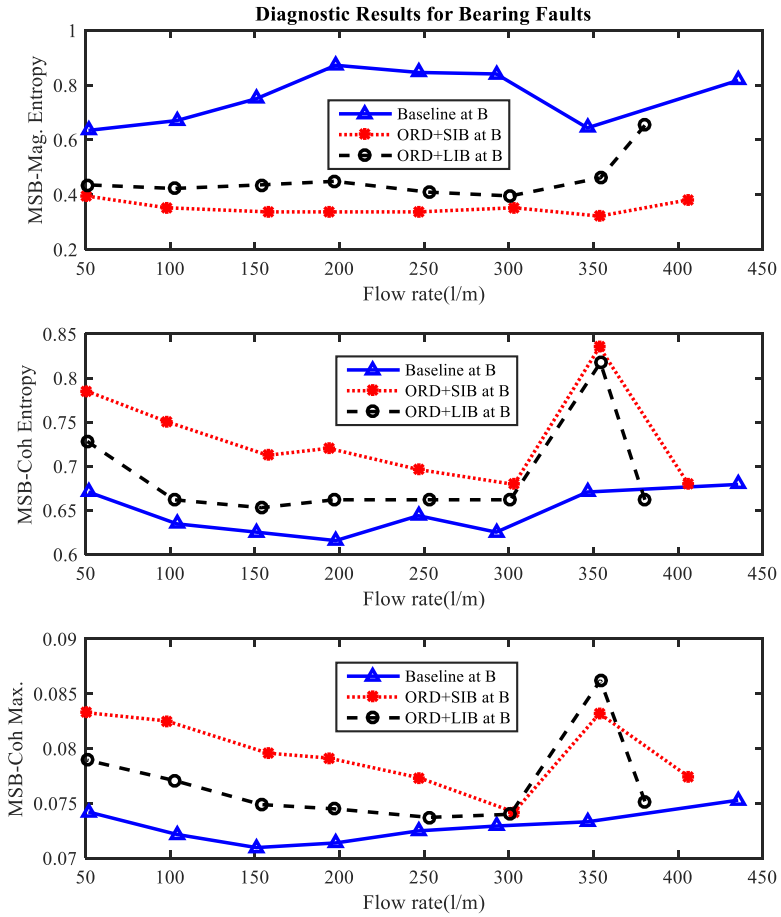

Compared of diagnostic results for bearing faults.

MSB results impeller detection and diagnose

Characteristics of MSB

To improve the diagnosis performance, the MSB is applied to suppress the wideband noise and hence to enhance the discrete components. Figures below representative of MSB magnitude in the low frequency range. The MSB magnitude results of the three graphs of top row show less noise contamination for all three cases. Especially, their nonlinear coupling can be further identified by the corresponding MSB coherences in the three graphs of bottom. Subsequently, the average of the two components obtains the results from MSB coherence detector as shown on the three graphs of bottom row. The results show clear peaks at small impeller blockage fault frequency and its 2nd harmonic, when comparing with the baseline case, which has no fault induced to. In addition, both results show distinctive differences between three cases in that the large impeller fault causes higher peaks because of higher mechanical and hydraulic pulses whereas the small impeller fault induces smaller pulses and hence lower MSB peaks.

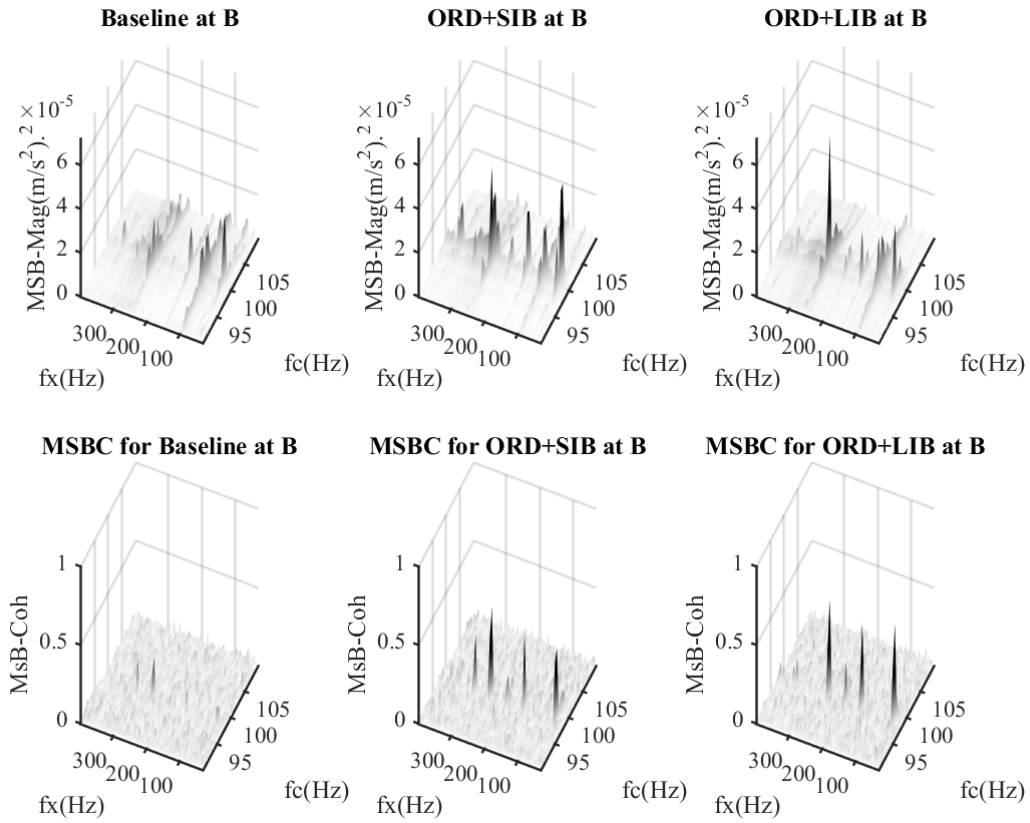

MSB magnitude and MSB coherence of vibration signals for impeller different cases at flow rate **50** l/min

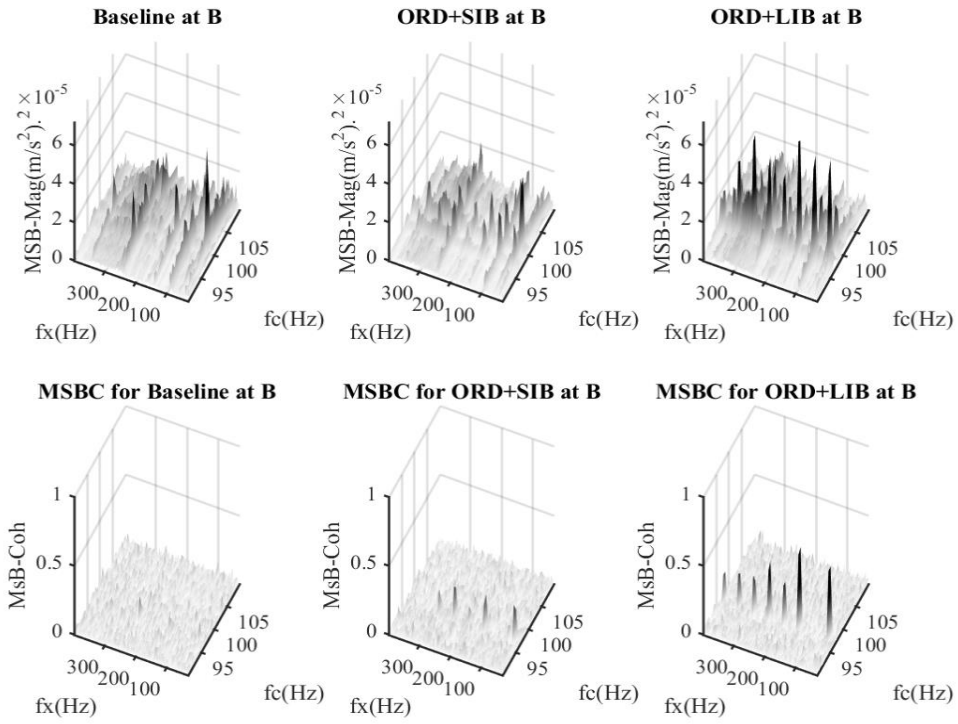

MSB magnitude and MSB coherence of vibration signals for impeller different cases at flow rate **250** l/min

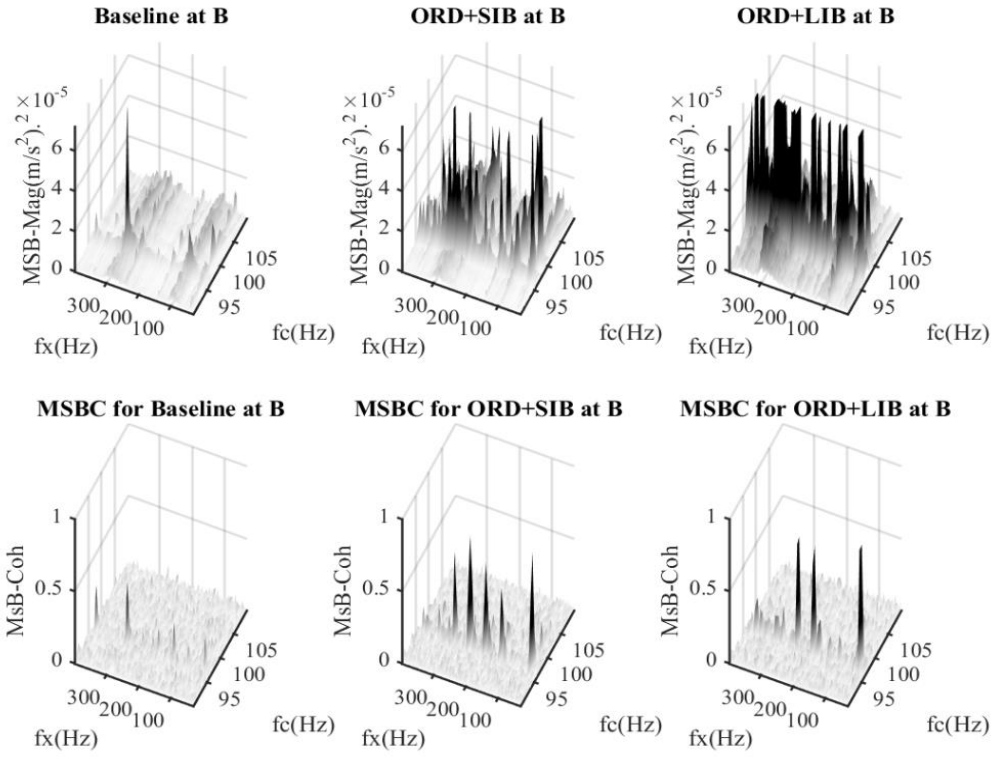

MSB magnitude and MSB coherence of vibration signals for impeller different cases at flow rate **250** l/min

Diagnostics of impellers

The diagnostic features are extracted as shown in Figures below. For three different cases stated as (BL, ORD+SIB, ORD+LIB). It can be observing that the MSBC Entropy results of the three cases at graphs of middle row shows that the both impeller faults can be separated from the healthy case with more distinctively less noise contamination for all three cases. Especially, their nonlinear coupling can be further identified by the corresponding MSBC entropy in the raw graph of bottom, compared with the results from MSB magnitude entropy in the raw graph of top which is spirited over the large impeller blockage fault at the first 4 harmonics of shaft rotating frequency and the first vane passing frequency. It shows that the amplitudes show less change with high flow rates above 250 but allows the (LIB) faulty to be differentiated fully at the first 4 harmonics, because of the influences of the wideband noise. Moreover, it is consistent with the changes of the performance characteristics. As the flow pressure is lower, the vibration goes higher for the large impeller blockage fault and vice versa for the small blockage fault.

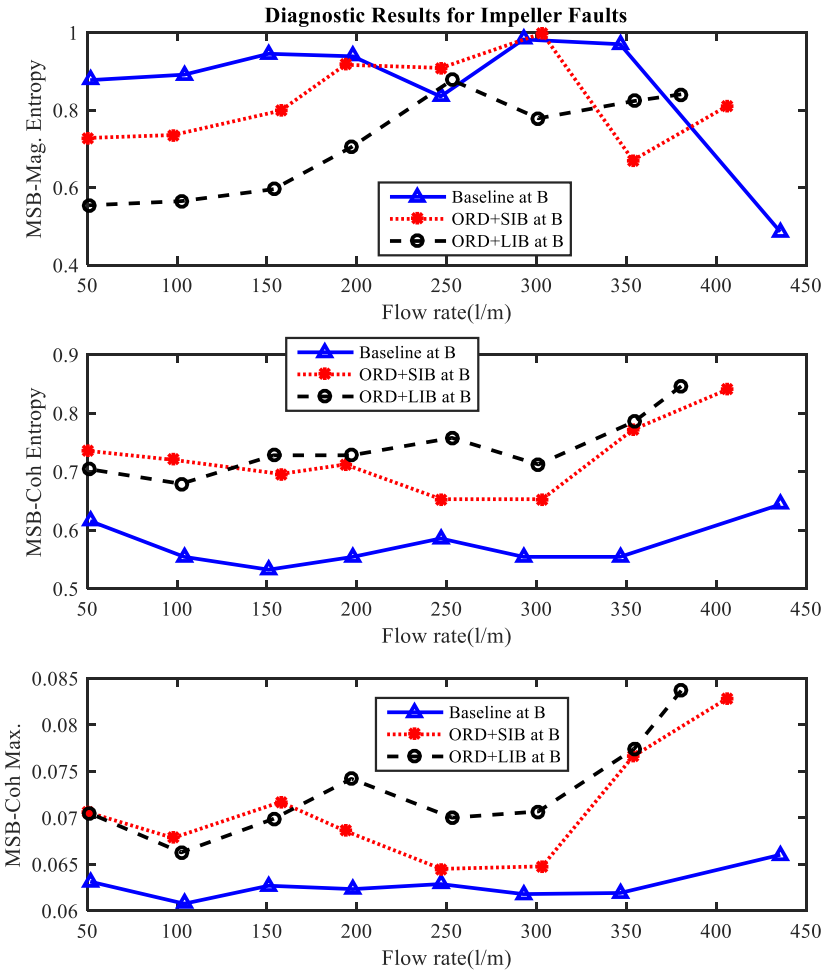

Compared of Diagnostic Results for Impeller Faults

APPENDIX C

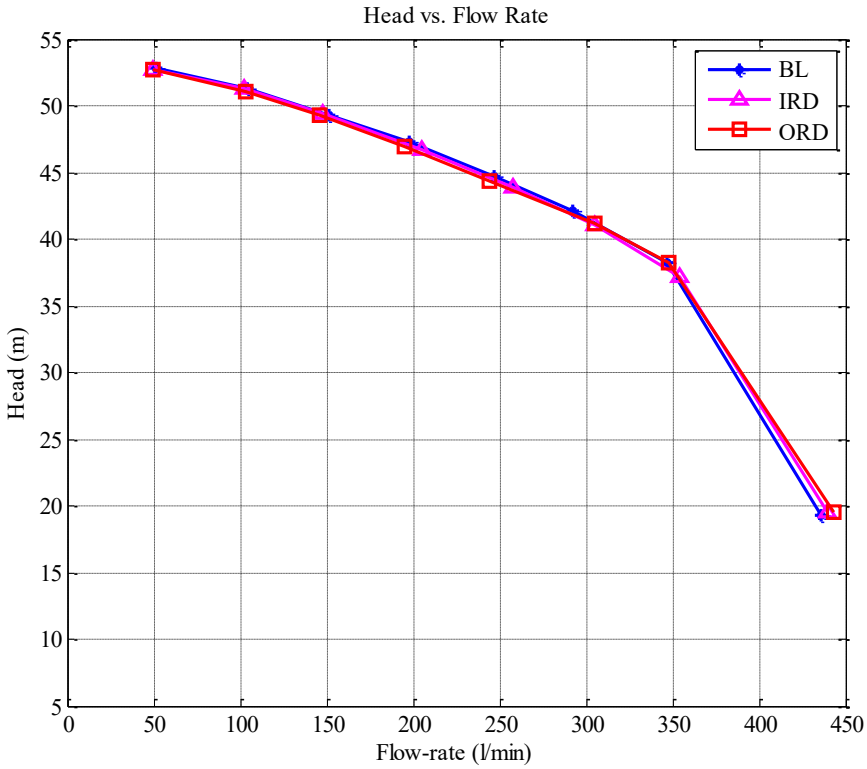

The performance carve with bearing defects

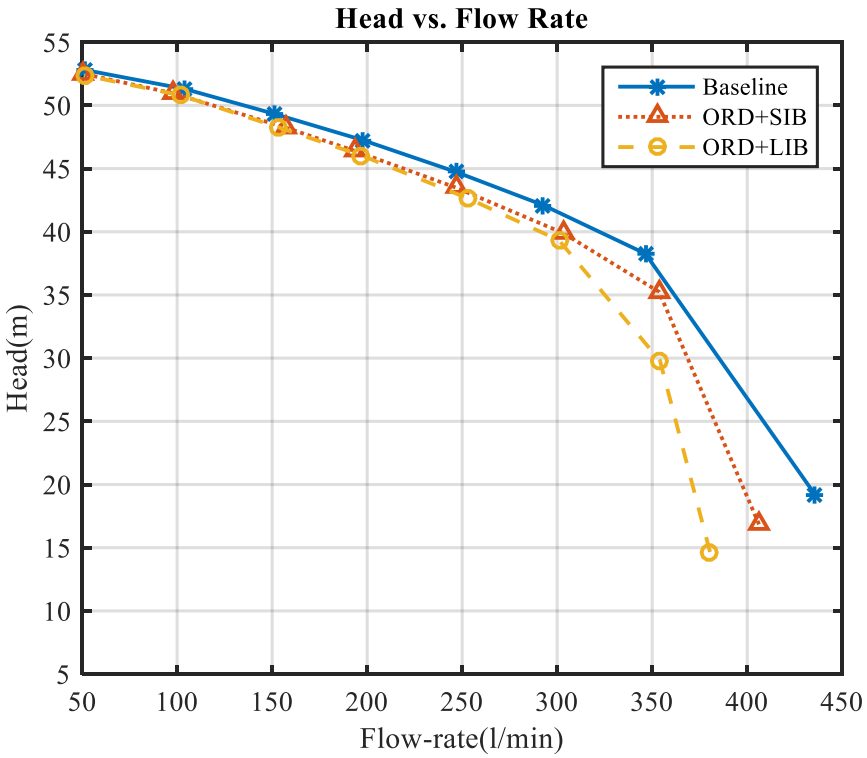

The performance carve with bearing + impeller defects

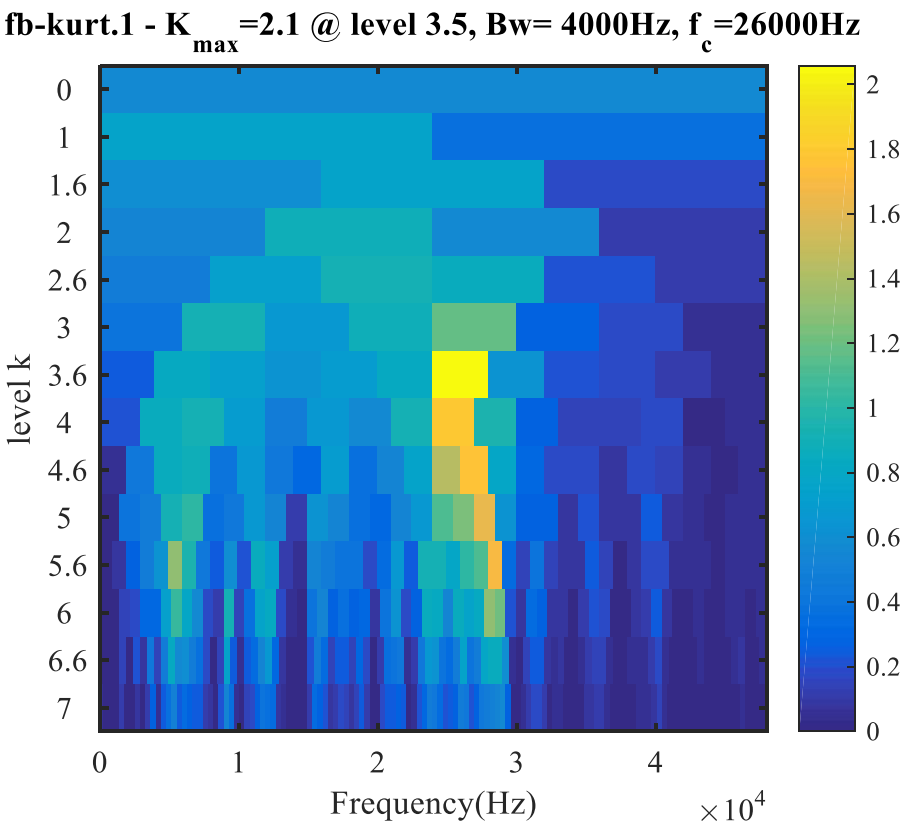

Fast Kurtogram optimised filter results for (ORD+SIB)

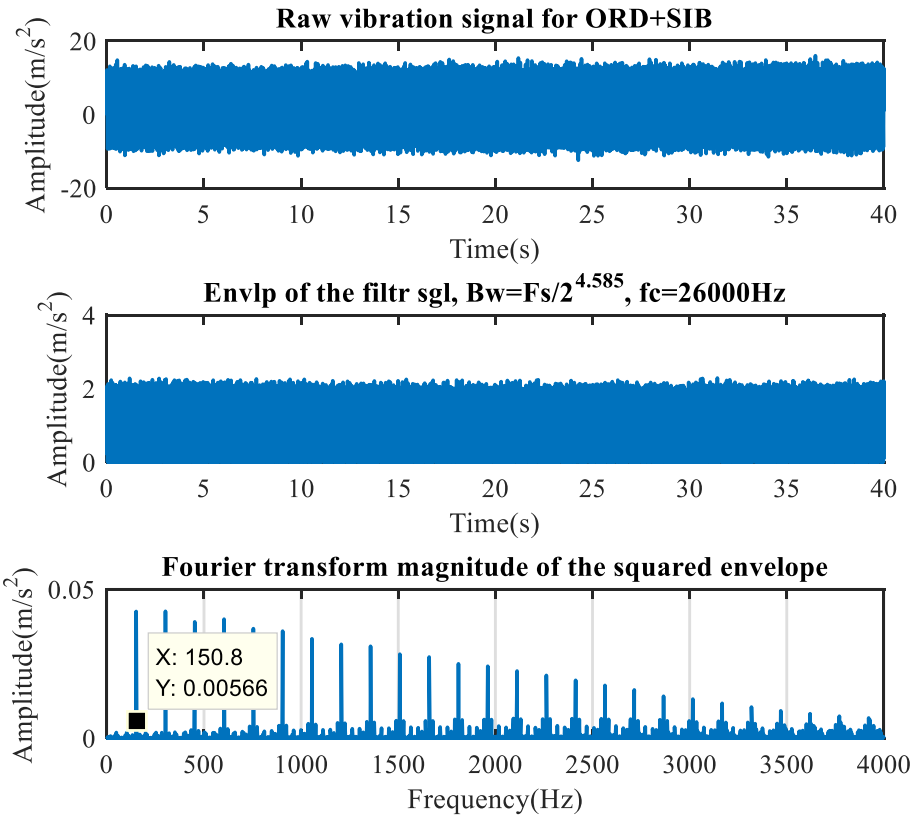

Raw vibration signal for (ORD+SIB), envelope of filtered signal, Fourier transform magnitude of the squared envelope

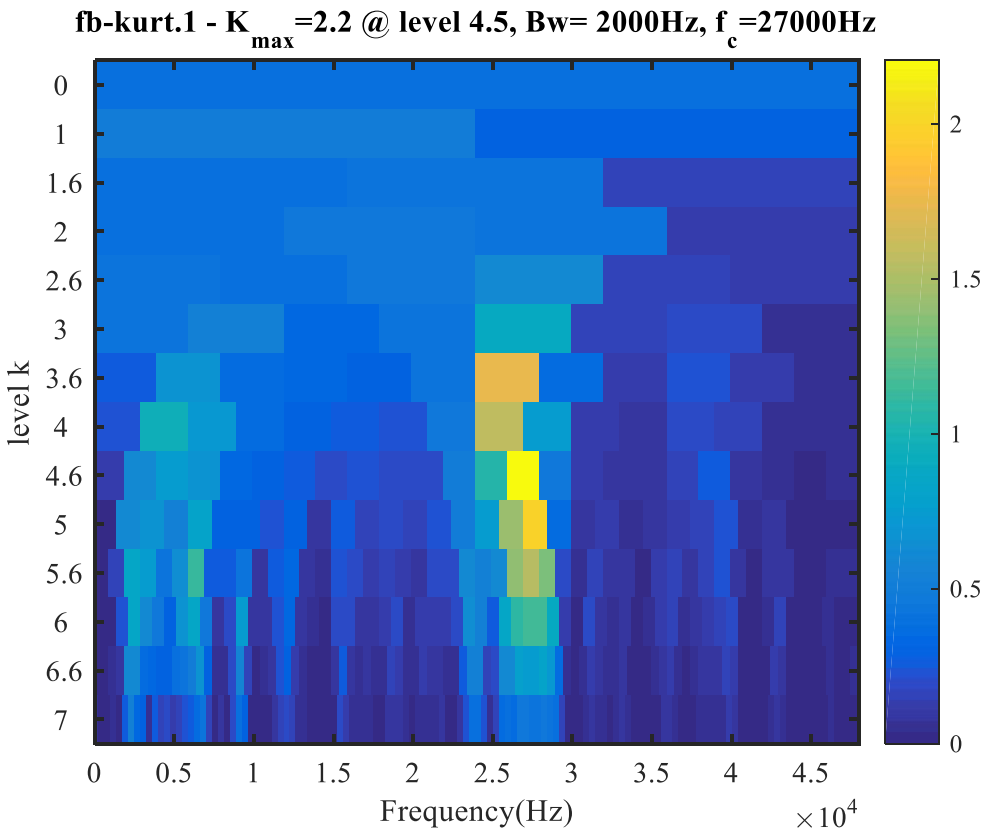

Fast Kurtogram optimised filter results for (ORD+LIB)

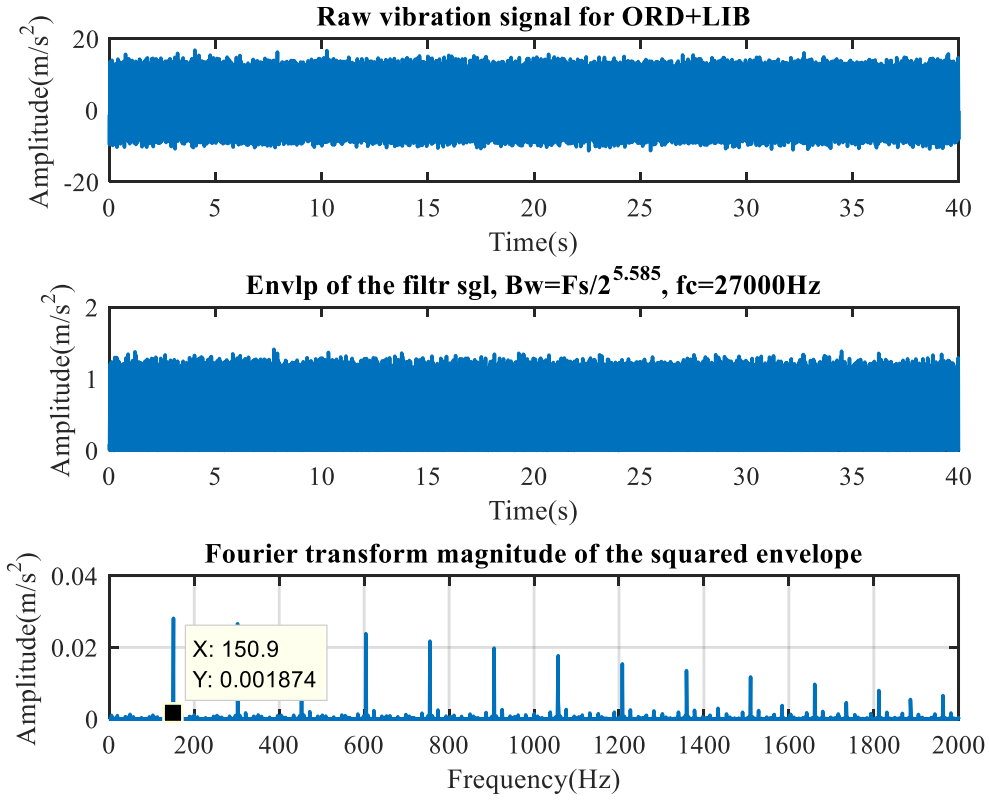

Raw vibration signal for (ORD+LIB), envelope of filtered signal, Fourier transform magnitude of the squared envelope